# Toward the Synthesis of Complex Bacterial Deoxy-Amino Sugars: A Diastereoselective Late-Stage Cyclization Approach

A dissertation submitted by

**Olivea M. Vasquez**

in partial fulfillment of the requirement for the degree of

Doctor of Philosophy

in

Chemistry

Tufts University

May 2025

Research Advisor: Clay S. Bennett

## Abstract

The synthesis of bacterial deoxy-amino sugars has been recognized as a significant challenge in carbohydrate chemistry. These sugars are integral to the structure and function of various bacterial species but, despite their biological relevance, efficient synthetic methods for accessing them remain underdeveloped. Existing methods often rely on the stereochemical manipulation of sugar building blocks, while others start with commercially available amino acids that undergo late-stage cyclization after installation of various chiral centers. Each of these methods rely on synthetic routes that are limited in scope and frequently suffer from poor diastereoselectivity in the construction of key intermediates.

In this thesis, we present a more efficient, diastereoselective, and versatile protocol for the construction of 2,4-diamino-2,4,6-trideoxyhexoses (DATDHs). This novel approach is characterized by its ability to generate these complex monosaccharides in high stereochemical control, facilitating the synthesis of biologically relevant compounds that are otherwise difficult to access. We also develop protecting group manipulations to these molecules, which enables subsequent enzymatic and biologic testing on glycosylation-ready sugar donors and/or acceptors. In addition, various improved *de novo* synthetic routes toward complex bacterial 8-*epi*-legionaminic acid are proposed, inspired by the diastereoselective methods developed toward DATDHs in this thesis.

**Chapter 1** introduces the significance of carbohydrates, with a particular focus on deoxy-amino bacterial sugars in the context of glycobiology and the development of novel therapeutics. Existing methods toward the synthesis of similarly derived deoxy-amino sugars are also highlighted as background for further method development. **Chapter 2**

delves into the importance of Krische allylation chemistry in facilitating highly diastereoselective C-C bond-forming reactions. The extension and optimization of this chemistry to more sterically encumbering and stereochemically complex substrates by our lab is then described. Additionally described is the complete *de novo* synthesis of four bacterial DATDH sugars via a long-chain, chemical elongation followed by late-stage cyclization strategy. By this approach, four 2,4-diamino-2,4,6-trideoxypyranosides arise from threoninol starting materials in moderate overall yield and excellent diastereoselectivity. The stereochemical characterization and purity of these compounds is confirmed through extensive analytical techniques, including variable temperature (VT) NMR, 1-D NOE NMR, and $^{13}C$ NMR of acetonide protected compounds.

Building on the methodology developed in Chapter 2, **Chapter 3** demonstrates the scalability of this chemistry and extends it to the synthesis of derivatized 2,4-diacetamido- and 2-amino-4-acetamido-2,4,6-trideoxyhexoses. These compounds, synthesized in larger quantities, are valuable for exploring the enzymatic promiscuity of various glycosyltransferases and other enzymes. Through collaborative efforts, these derivatized sugars are exposed to said enzymes to assess their ability to recognize and process different stereoisomers of deprotected DATDHs. Such studies are crucial for understanding the enzymatic pathways that these sugars may undergo once activated, providing a deeper understanding of their potential biological roles. We also explore the use of aldolase enzymes in the transformation of 2-amino-4-acetamido-2,4,6-trideoxyhexoeses into 9-carbon nonulosonic acids, a promising direction for the biosynthesis of novel sugar-based therapeutics. This work is an ongoing and collaborative

effort, which promises to shed light on biochemical transformations involving these bacterial sugars.

**Chapter 4** presents the ongoing efforts toward the *de novo* synthesis of 8-*epi*-legionaminic acid (8epiLeg), a complex bacterial sugar with significant bioactivity. This chapter discusses several synthetic routes that have been explored toward constructing 8epiLeg in a more diastereoselective and efficient manner than previously reported. Building on the principles developed in earlier chapters, we propose a strategy that employs long-chain chemical elongation followed by late-stage cyclization, which may lead to the formation of 8epiLeg. The development of this method could have far-reaching implications for the synthesis of novel therapeutic agents derived from bacterial sugars.

## Acknowledgements

First and foremost, I would like to acknowledge my advisor, Clay Bennett. Without his guidance, inspiration, and mentorship, none of this work would have been possible. Dr. Bennett, I will always value our brainstorming sessions and your imparted scientific expertise, which helped me navigate through the tougher moments of research and taught me the importance of perspective and collaboration.

I also want to extend thanks to the additional members of my committee, Sam Thomas and Luke Davis, who were always pushing me to the next level, showing support, and giving advice (both scientifically and personally) when needed. Sam, I will always think of you as a role model in terms of mentorship— you exhibit patience, active listening, and act as a soundboard just as frequently as you lend advice. You taught me that often, scientists do not need to hear solutions, but rather need someone to inspire them to find the answers for tough problems by looking inward.

I would also like to thank my past and current lab members. Dr. Caleb Wehrmann, Dr. Joseph Romeo, Dr. Colin Mizia, Dr. Brian Gareffi, Dr. Vanessa Jones, Jack Florek, Katie Maiello, Claire Thomas, Morgan Brutus, Megan Sargent, *et al*. Thank you each for your mentorship throughout my time at Tufts and Lehigh University. Each of you has your own unique skillset that I mirrored to mold myself into the scientist I am today. I owe many of my accomplishments to your influence.

To my partner, Will Allen, no “thank you” is big enough to account for the level of support and unwavering faith you have shown me throughout the past five years. I think your jokes and laugh could have single-handedly gotten me through the trials of graduate

school. But, beyond that, you inspire me daily to be mentally stronger, love harder, and dig deeper in all facets of my life. WE did this. Together.

And finally, to my family, friends, and roommates: I love you with all my heart! Thank you for the warm meals, hugs, and words of support when I needed them most. I recognize most of you had no idea what I was doing on a day-to-day basis, but you bore with me as I explained carbohydrate synthesis and looked to you for encouragement, anyway. For that, I am so grateful. And to my late grandpa, Anibal Vasquez, and late grandma, Arlene Marian (both of whom were scientists in their own respects), I know you were with me every step of this journey.

## Table of Contents

## List of Tables

### Chapter 1

### Chapter 2



### Chapter 3



### Chapter 4

## List of Schemes

### Chapter 1

**Chapter 4**

## List of Figures

### Chapter 1



### Chapter 2

## Abbreviations

CPS: capsular polysaccharide

LPS: lipopolysaccharide

KDO: 3-Deoxy-D-manno-octulosonic acid

DATDH: 2,4-diamino-2,4,6-trideoxyhexose

NulO: nonulosonic acid

Neu5Ac: *N*-acetylneuraminic acid, sialic acid

Pse: pseudaminic acid

Leg: legionaminic acid

4eLeg: 4-*epi*-legionaminic acid

8eLeg: 8-*epi*-legionaminic acid

Aci: acinetaminic acid

8eAci: 8-*epi*-acinetaminic acid

AMR: antimicrobial resistance

UDP-diNAcBac: urine diphosphate N,N'-Diacetylbacillosamine

UDP-GlcNAc: uridine diphosphate N-acetylglucosamine

TCAI: trichloroacetimidate

$Et_3B$: triethylborane

$Et_2Zn$: diethylzinc

RPKA: reaction progress kinetic analysis

DFT: density functional theory

TBS: tert-Butyldimethylsilane

Boc: tert-butyloxycarbonyl

$K_2CO_3$: potassium carbonate

$PPh_3$: triphenylphosphine

$Me_2S$: dimethyl sulfide

TES: triethylsilane

NOE: nuclear Overhauser effect

TBSCl: tert-Butyldimethylsilyl chloride

$OsO_4$: osmium tetraoxide

$NaIO_4$: sodium periodate

VT NMR: variable temperature NMR

$CH_2Cl_2$: dichloromethane

THF: tetrahydrofuran

PTFE: polytetrafluoroethylene

$KH_2PO_4$: potassium dihydrogen phosphate

EtOAc: ethyl acetate

Hex: hexanes

TBAF: tetra-n-butylammonium fluoride

$NH_4Cl$: ammonium chloride

$NaHCO_3$: sodium bicarbonate

$Na_2SO_4$: sodium sulfate

MeOH: methanol

$SOCl_2$: thionyl chloride

$(Boc)_2O$: di-tert-butyl carbonate

HCl: hydrochloric acid

TBSOTf: tert-Butyldimethylsilyl trifluoromethanesulfonate

EtOH: ethanol

$LiBH_4$: lithium borohydride

DMF: dimethylformamide

LiCl: lithium chloride

$NaBH_4$: sodium borohydride

NaOH: sodium hydroxide

$KHSO_4$: potassium bisulfate

MeI: methyl iodide

Tol: toluene

$Et_3N$: triethylamine

TsOH: *p*-toluenesulfonic acid

$Na_2S_2O_3$: sodium thiosulfate

NDP: nucleoside diphosphate

TFA: trifluoroacetic acid

TLC: thin layer chromatography

DMAP: 4-dimethylaminopyridine

$Cu(II)SO_4$ x $5H_2O$: copper sulfate pentahydrate

NaOMe: sodium methoxide

NHC-ligand: N-heterocyclic carbene ligand

GC: gas chromatography

MVG: methyl vinyl glycolate, methyl 2-hydroxybut-3-enoate

OCM: olefin cross metathesis

TTIP: titanium (IV) isopropoxide

$BF_3OEt_2$: boron trifluoride diethyletherate

$Pt(dba)_3$: tris(dibenzylideneacetone) platinum(0)

$B_2(pin)_2$: Bis(pinacolato)diboron

ESI: electrospray ionization

# Toward the Synthesis of Complex Bacterial Deoxy-Amino Sugars: A Diastereoselective Late-Stage Cyclization Approach

# Chapter 1: The Significance and Challenges of Diamino Sugars as it Relates to Bacterial Pathogenicity

## 1.1. The Significance of Bacterial Polysaccharides

All cells and many macromolecules contain an array of carbohydrates, making carbohydrates among the most abundant and essential biomolecules on earth.[1] Located on the outer surface of cellular and secreted molecules, carbohydrates are crucial components in the mediation and modulation of cell-cell and cell-matrix interactions. This includes the assembly of complex multicellular organs and organisms by assisting in protein folding[1–3] and structural stability.[4]

In addition to their presence on mammalian cells, the cellular wall of bacteria contains polysaccharides and glycoconjugates with so-called “unusual” or “rare” sugars not found in eukaryotes, which serve both structural and functional roles.[5] Notably, the capsular polysaccharide (CPS) and lipopolysaccharide (LPS) of bacteria serve as the first line of defense against complement proteins and bacteriophages.[1,5] Additionally, the carbohydrate moieties present in these structures contain major antigenic determinants that define bacterial serotypes, which are crucial for the immune system’s ability to recognize and respond to different bacterial strains.[5–8]

The LPS consists of a lipid A domain, core domain (consisting of KDO (K), heptoses (H), and neutral sugars such as galactose (G)), and the outer *O*-Antigen (consisting of sugar fragments 2-8 units long) (**Figure 1.1**). Sugars on the *O*-Antigen range from free and amidated uronic acids, amino sugars, methylated and deoxygenated derivatives, acetylated sugars, and others containing covalently bound amino acids and phosphates.[5] Due to the location of prokaryote-specific sugars on the outermost portion of the LPS, it is thought that these bacterial sugars play an essential role in bacterial fitness and pathogenicity.[9,10] To support this, it has been observed that bacteria produce

glycoconjugates closely related to those found in mammals. This assembly of eukaryotic-like glycans by bacteria is thought to be a form of “molecular mimicry,” allowing bacteria to evade host immunity or otherwise compromise the immune system of the host.[5] However, the fundamental questions of why bacteria utilize such structurally complex sugar moieties and what specific roles they play in pathogenicity are still not fully understood.[7,11] The variability in these sugars allows bacterial to evade immune surveillance and adapt to different host environments, making them prime targets for therapeutic intervention.

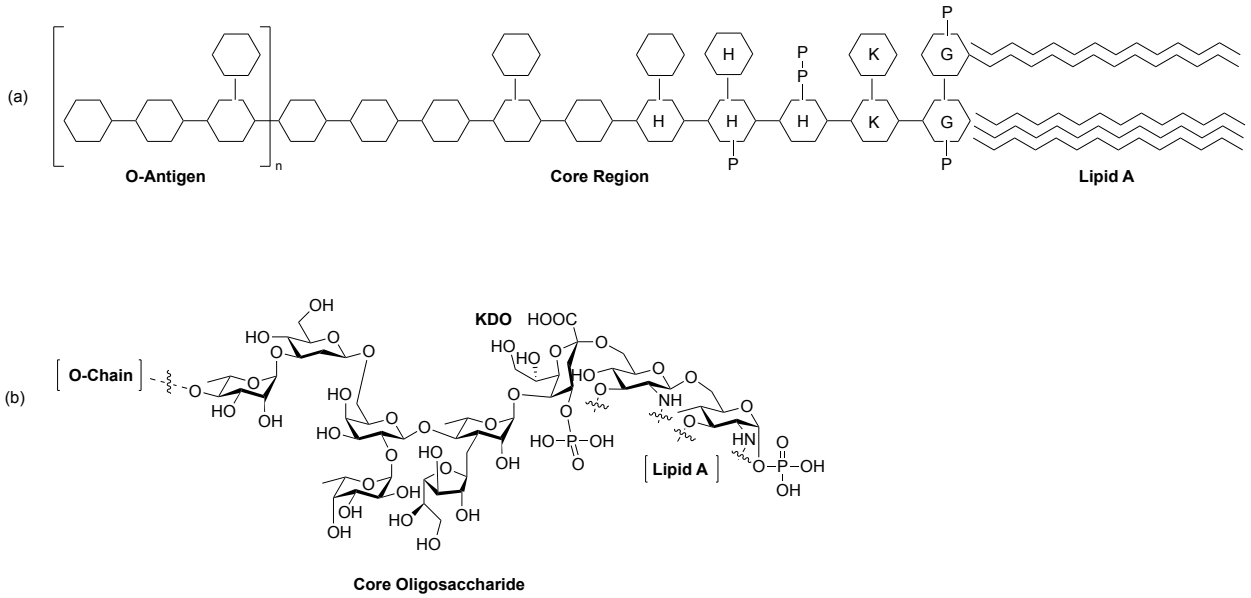


**Figure 1.1.** (a) Representative structure of the lipopolysaccharide (LPS) of *E. coli.* (b) Example of a core oligosaccharide structure from *B. vulgatus*.

### 1.1.1. Deoxy-amino Sugar Prevalence on Pathogenic Bacteria

Modified prokaryote-specific sugars such as 2,4-diamino-2,4,6-trideoxyhexoses (DATDHs) and their derived nonulosonic acids (NulOs) are among those sugars found on bacterial glycans.[12] These deoxy-amino sugars are found at the reducing end of oligosaccharides of *N*- and *O*-linked bacterial protein glycosylation pathways of Gram-negative pathogens.[11] In many cases, the presence of these sugars has been related to pathogenicity and virulence.[6,12,13]

Structurally speaking, NulOs are highly modified monosaccharides consisting of a 9-carbon backbone, 3-carbon exocyclic side chain, and C5 acetamide substituent. The most widely known of these α-keto acidic sugars is sialic acid (*N*-acetylneuraminic acid, Neu5Ac) **1.1**, which was first discovered as a product released by acid hydrolysis of brain glycolipids or salivary mucins[14,15] and later found to be a recognition target by the influenza virus.[16] Over 90 variants of 3-deoxy sialic acids have subsequently been found on mammalian and bacterial cells. A subset of 3,9-dideoxy "sialic acid-like" formed NulOs were later discovered, which only present themselves on bacteria and archaea.[17] Of this class of NulOs, there are six stereoisomer subclasses: pseudaminic acid (Pse) **1.9**, legionaminic acid (Leg) **1.4**, 4-*epi*-legionaminic acid (4eLeg) **1.5**, 8-*epi*-legionaminic acid (8eLeg) **1.6**, acinetaminic acid (Aci) **1.7**, and 8-*epi*-acinetaminic acid (8eAci) **1.8**.[17] Compounds 1.1-1.9 in **Figure 1.2** represent relevant, characterized nonulosonic acids present in nature, including various 3-deoxy and all 3,9-dideoxy derivatives.

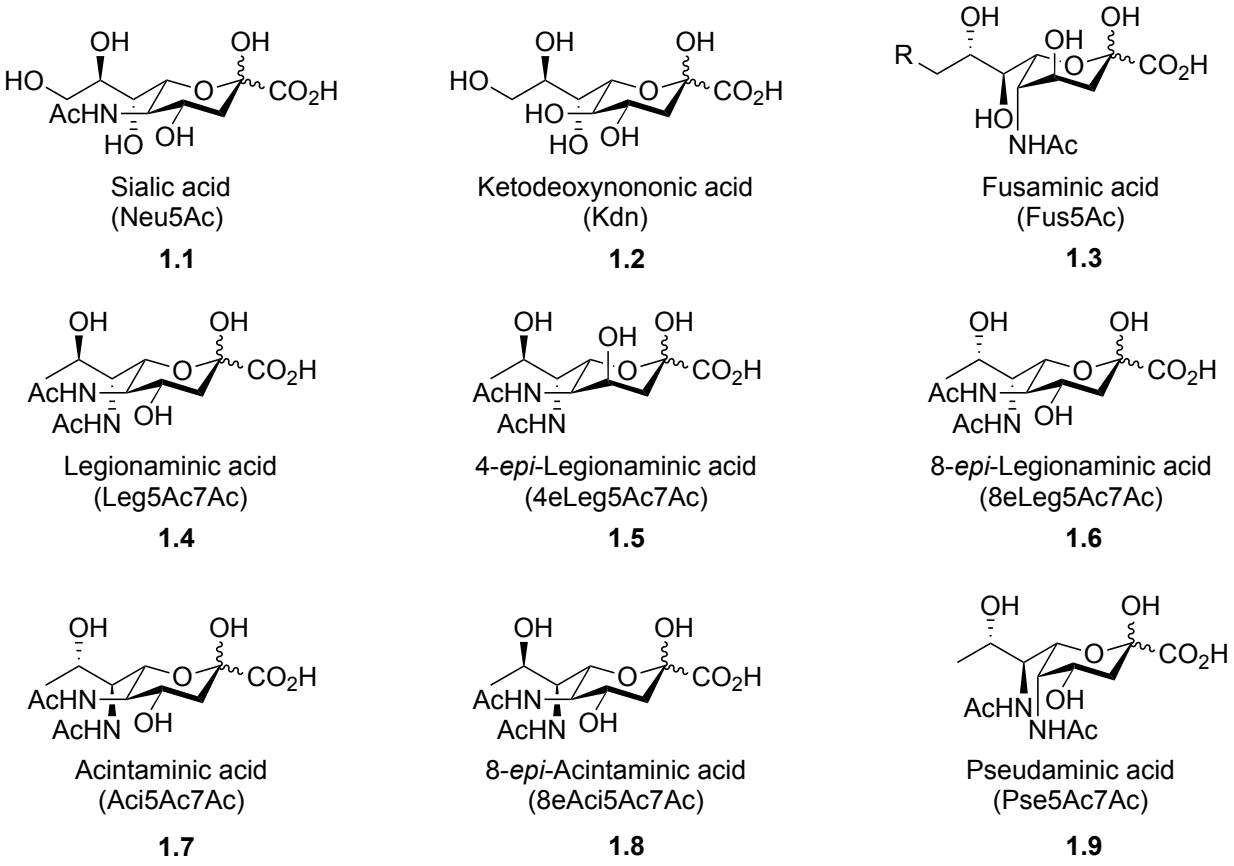


**Figure 1.2.** Sialic acid in its most common form, *N*-Acetylneuraminic acid (Neu5Ac), as well as structural depictions of relevant 3-deoxy and 3,9-dideoxy nonulosonic acids (NulOs).

Regarding 8-*epi*-legionaminic acid **1.6** specifically, derivatives of this 9-carbon sugar are found on various strains of pathogenic bacteria. Compounds 1.10 - 1.14 in **Figure 1.3** depict five different 8epiLeg derivatives and the respective bacterial strain(s) they are found on. Modifications are most commonly observed on the C5 and C7 amine substituents. While this NulO sugar, in a variety of forms, is present on upwards of nine different bacterial serotypes, it has yet to be sufficiently synthesized in any appreciable quantity. **Section 1.2.3** delves into past attempts at synthesis of this compound, while Chapters 3 and 4 discusses future improvements on the literature envisioned for either a *de novo* or chemoenzymatic synthesis of 8epiLeg **1.6**.

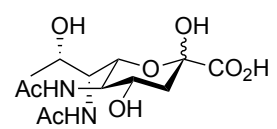

*A. baumannii* LAC-4 (LPS)
*E. coli* O108 (LPS)
*P. stuartii* O20 (LPS)
*P. aeruginosa* O12 (LPS)
*V. fisheri* ES114 (LPS)

**1.10**

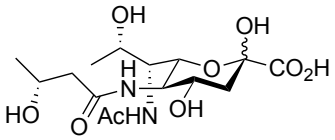

*S. arizonae* O61 (LPS)

**1.11**

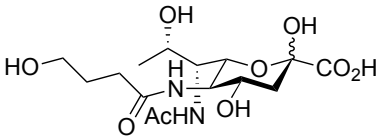

*Y. ruckeri* O1 (LPS)

**1.12**

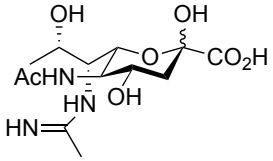

*S. putrefaciens* A6 (LPS)

**1.13**

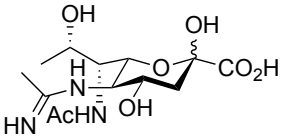

*M. morganii* KF 1676 (RK 4222) (LPS)

**1.14**

**Figure 1.3.** Derivatives of 8epiLeg found on the LPS of various pathogenic bacterial strains.

## 1.1.2. Antimicrobial Resistance and The Glycoconjugate Vaccine

Antimicrobial resistance (AMR) is among the leading causes of death around the world,[18] and it is projected that an estimated 10 million people *per annum* will die from AMR by the year 2050.[19] Reports from the Center for Disease Control (CDC) and European Antimicrobial Resistance Surveillance Network (EARS-Net) have identified *A. baumannii, C. difficile, E. coli, E. faecium, K. pneumoniae, N. gonorrhoeae, P. aerunginosa,* and *S. aureus* among the human pathogenic bacteria that possess AMR.[20,21] As a result of this growing epidemic, there is a need for alternative prevention methods for bacterial infection. One alternative consideration for treatment of bacterial infection can be found in the development of carbohydrate-based vaccination.[22] Benefits to vaccination include a lowered chance of genetic evolution of bacteria, which in turn leads to a lower possibility for further AMR mechanisms.[23,24] Additionally, and with high vaccination rates, resulting herd immunity can result from vaccine treatment.[23,25]

Carbohydrate-based vaccines were first explored as a possible treatment to bacterial infection as early as 1929.[26,27] The 1930s and 1940s were a period of further CPS-based vaccine development, but this momentum was halted by the development of penicillin and other antibiotics in the 1950-1970s.[28,29] The emergence of antibiotic resistant bacteria that followed these discoveries, however, called for a renewal in the development of carbohydrate-based vaccines.[30] In the 1980s, CPS-based vaccines were reintroduced as treatments for tetravalent meningococcal, *H. influenza type b*, and *Salmonella typhi* Vi. Advancements to immunogenicity were made by coupling the CPS to a carrier protein via a linker (glycoconjugate vaccine), which showed generation of a more heighted T-cell dependent immune response and long-lasting immunological memory in patients.[31,32] **Figure 1.4** lends a visual depiction to the mechanism of action for this heightened immune response.

More recently, Prevnar™ (PCV7 and later PCV13) became the first licensed pneumococcal CPS-based glycoconjugate vaccine, significantly reducing infection rates of various strains of *S. pneumoniae*, notably in children under the age of two and immunodeficient patients.[33,34] Many countries that routinely include carbohydrate-based vaccination in their immunizations have near eliminated strains of *S. pneumoniae, N. Meningitidis, and H. influenzae* based on the aforementioned scientific developments.[35]

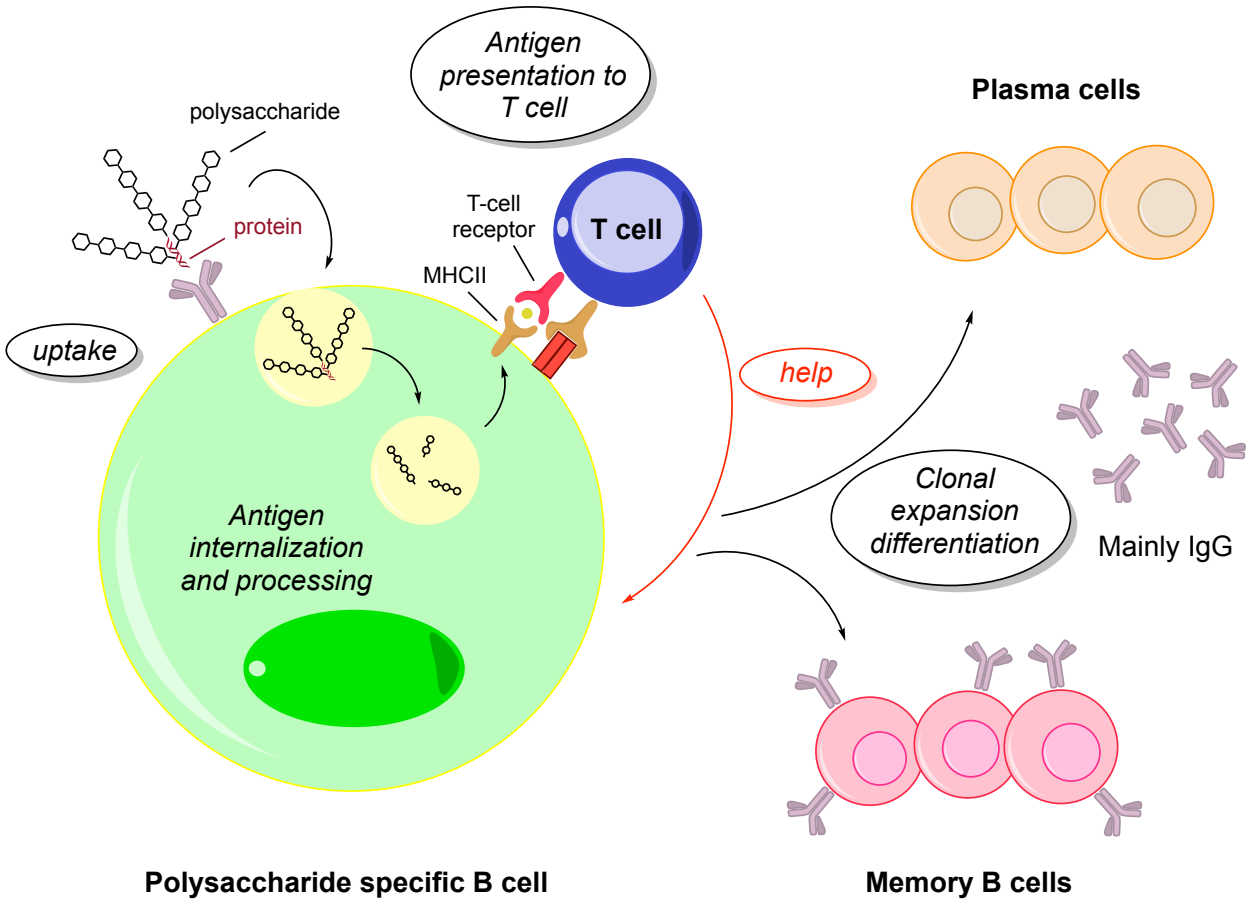


**Figure 1.4.** Schematic for the mechanism of action of glycoconjugate vaccines. Conjugation of polysaccharides to protein carriers result in carrier specific T-cell recognition that induce polysaccharide-specific B-cell differentiation. This leads to long lasting immunological memory in patients.

There are notable downsides to carbohydrate-based vaccine technology, however. These downsides lie mainly in the natural isolation methods of the vaccine's polysaccharide moiety.[35,36] Traditional carbohydrate-based vaccines rely on the extraction of polysaccharides from bacterial cultures, which are then purified and coupled to a carrier protein. Commonly, the carrier protein-conjugate coupling involves random cross-linkages along the sugar chain.[18] The result is an ambiguously defined glycoconjugate. Not only does this limit our understanding of what specific sugars on the CPS/LPS are most important for recognition and virulence, but also results in

considerable batch-to-batch variability in developed vaccines.[32,37,38] This type of cross-linked lattice vaccine also displays artificial epitopes (and, therefore, production of non-protective antibodies), which diminishes vaccine quality and may result in a lessened host immune response.[39] Additionally, the capability to increase the amount of bacterial serotypes one vaccine can fight against is heavily limited by the sheer size of the extracted polysaccharide(s).

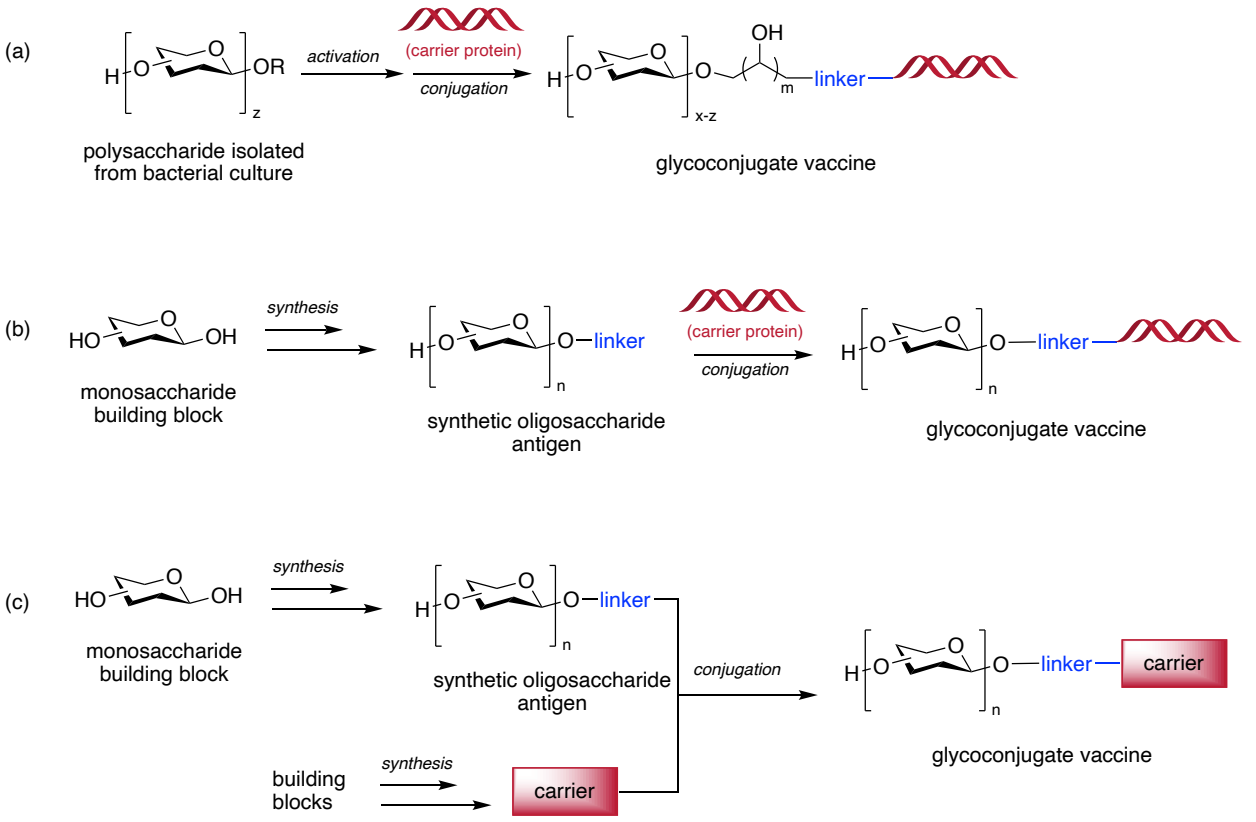


**Figure 1.5.** (a) Traditional polysaccharide-based glycoconjugate vaccine (b) Semisynthetic glycoconjugate vaccine, where the oligosaccharide antigen is synthetic and has defined structure, while the carrier protein does not (c) Synthetic glycoconjugate vaccine, where both the oligosaccharide antigen and carrier molecule are synthetic.

A more rational design approach therefore lies in semi-synthetic or totally synthetic approaches to generate more well-defined glycoconjugates. **Figure 1.5** compares makeup of the (a) traditional polysaccharide-based glycoconjugate vaccines, (b) semi-synthetic glycoconjugate vaccines, and (c) totally synthetic glycoconjugate vaccines. Through the utilization of synthetic alternatives, quality control, vaccine efficacy, and serotype coverage can potentially all be increased. This will provide a more prudent alternative to the current carbohydrate-based vaccines on market.[38] **Figure 1.6** is an example of two recently developed semisynthetic glycoconjugate vaccines, both of which have been shown to elicit effective immune responses against *N. meningitidis* serogroups B and C (**Figure 1.6a**)[40] and *A. baumannii* (**Figure 1.6b**)[41] during conducted *in vivo* studies in mice. In **Figure 1.6a**, the synthesized species is conjugated to CRM 197, while in **Figure 1.6b** the synthesized sugar is conjugated to both CRM 197 and PorA.[40,41] Work in 2024, performed by Seeberger and co-workers, showed additional promise for the future of glycoconjugates in the clinic.[42] Limitations to the translation of these vaccines to clinic often still lies in the lack of efficient methodology for synthesis of the bacterial sugars present on the potential vaccine candidates, unfortunately. As a result, there is a push to further develop routes toward bacterial sugars that may be linked to bacterial virulence and pathogenicity.

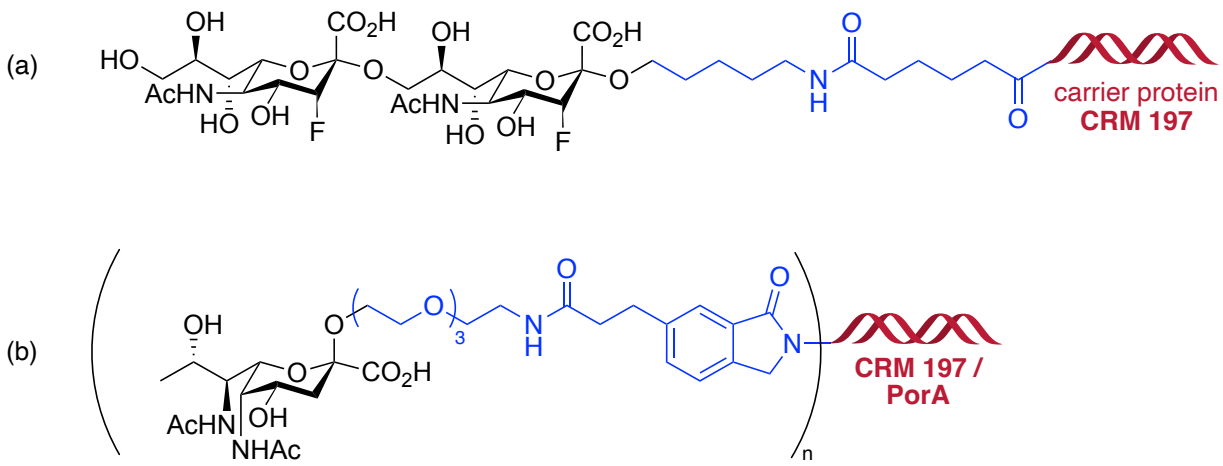


**Figure 1.6.** (a) Fluorinated sialic acid-based glycoconjugate vaccine shown to elicit an immune response against *N. meningitidis* (b) Pseudaminic acid-based glycoconjugate vaccine shown to elicit an immune response against *A. baumannii* infection.

## 1.2. Approaches Toward Accessing Deoxy-amino Sugars

### 1.2.1. Biosynthesis of DATDHs and NulOs

While the aforementioned deoxy-amino sugars (both DATDHs and NulOs) are abundant in nature, their isolation has been difficult. Depending on the sugar in question, the natural product may be labile to acid hydrolysis or enzymatic transformations.[43] Semisynthetic pathways have been explored to circumvent these issues, but they are often limited by the number of configurational changes that can be made to the molecule. Therefore, there is need for a simple, selective, and widely applicable *de novo* synthetic pathway to access these rare bacterial monosaccharides.

When attempting to synthesize complex sugar moieties, scientists frequently look to biology for inspiration. Biosynthetically, it has been shown that various nonulosonic acids (NulOs) are derived from diamino-trideoxyhexoses (DATDHs), which are further derived from UDP-activated 2-deoxyaminohexoses.[11] **Scheme 1.1** illustrates the bacterial strains *C. jejuni, N. gonorrheoeae,* and *A. baumannii* deriving activated urine

diphosphate 2-acetamido-4-amino-2,4,6-trideoxyhexose (UDP-diNAcBac) **1.18** from UDP-GlcNAc **1.15**, which is observed to then be further enzymatically transformed into the nonulosonic acid, legionaminic acid (Leg).[11] The biosynthesis of nonulosonic acids (such as the one shown in **Scheme 1.1b**) has inspired synthetic chemists to synthesize DATDHs (such as 2,4-diacetamido-2,4,6-trideoxymannose **1.19**) as relevant therapeutic targets. Furthermore, biology inspires glycoscientists to view these DATDHs as relevant precursors for further chemical/chemoenzymatic elongations to create isolated nonulosonic acid products or other glycosylated natural products.[44–47]

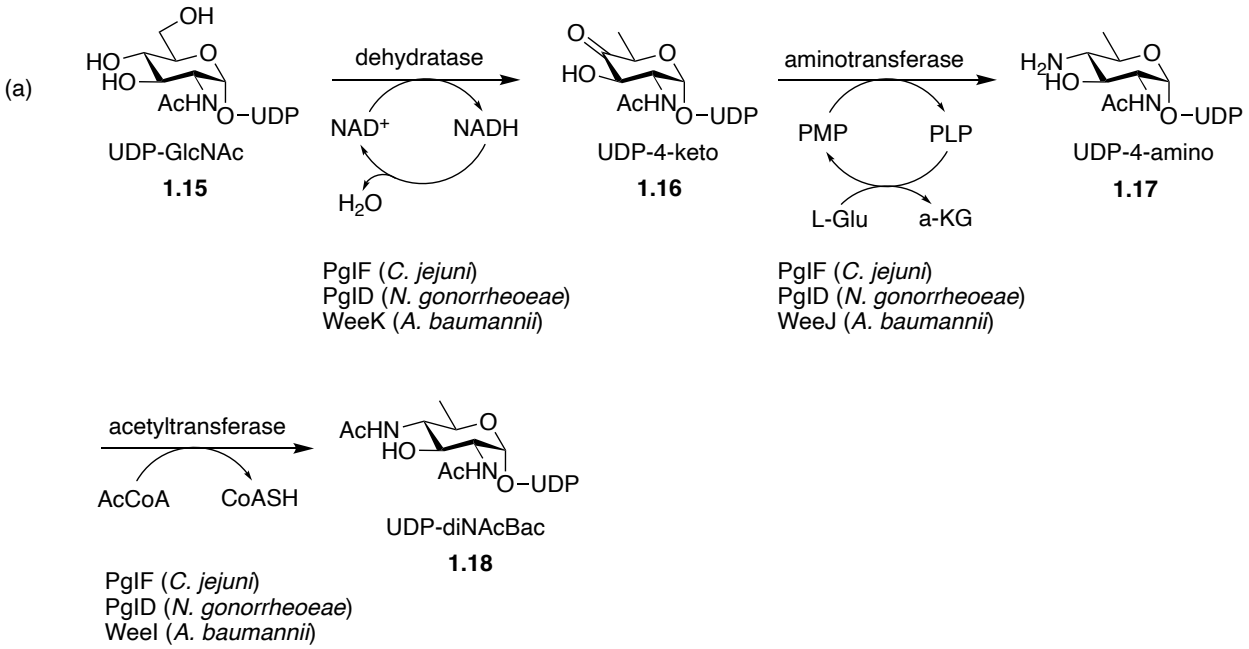

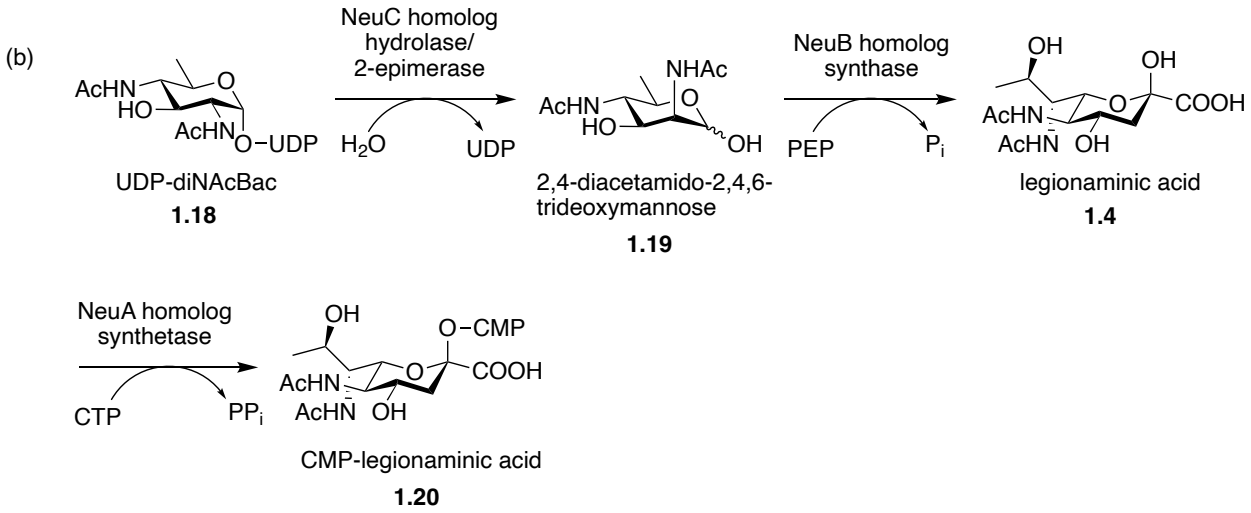


**Scheme 1.1.** (a) The biosynthetic conversion of UDP-GlcNAc into UDP-diNAcBac as seen in *C. jejuni, N. gonorrhoeae,* and *A. baumannii* (AYE strain). (b) The biosynthetic conversion of UDP-diNAcBac into CMP-legionaminic acid in *L. pneumophila*.

## 1.2.2. Previous *De Novo* Syntheses of DATDHs

Due to the presence of DATDHs on bacterial pathogens, many groups have developed routes to synthesize them. These syntheses have been met with varying levels of success. In 2006, Imperiali and co-workers performed a pioneering synthesis of a bacillosamine glycosyl donor from D-fucal (**Scheme 1.2**).[48,49] Starting with commercially available peracetylated D-fucal **1.21**, an azidophenylselenylation resulted in the stereoselective synthesis of 2-azido-$\alpha$-selenoglycoside **1.22** in 74% yield. Deacetylation was then performed, followed by stannylidene-mediated benzylation to generate deoxy-amino sugar **1.23** in 75% yield over two steps. A C4 mesylate was then installed, followed by substitution with sodium azide to install additional amino functionality to generate protected target compound **1.25**. Imperiali and co-workers then nicely demonstrated the utility of DATDH **1.25** as a glycosyl donor to generate a biologically relevant disaccharide fragment after installation of a trifloroacetimidate (TFAI) at the anomeric position (compound **1.26**). While efficient in step count, this route did lack differentiation between

C2 and C4 amine substituents, as well as utilized what may be considered relatively expensive starting material. These developments did, however, set the stage well for future iterations of DATDH sugar synthesis. In 2020, Codeé and co-workers utilized a similar route to generate a selenoglycoside from D-fucal **1.21**, but with a few alternative steps.[50] These alterations provided the diamino sugar in a way that allowed for differentiation between C2 and C4 amine functionality and was performed in an improved 47% overall yield (**Scheme 1.3**).

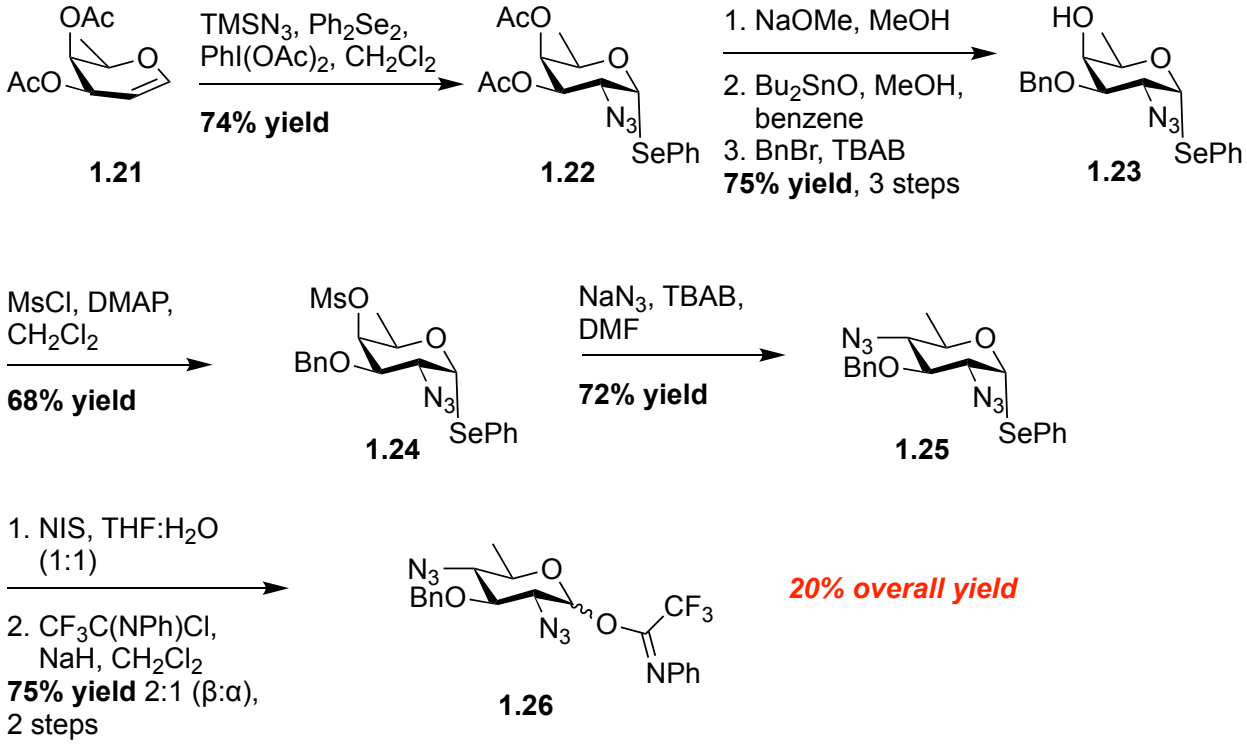


**Scheme 1.2.** Imperiali and co-workers' synthesis of TCAI bacillosamine donor from D-fucal.

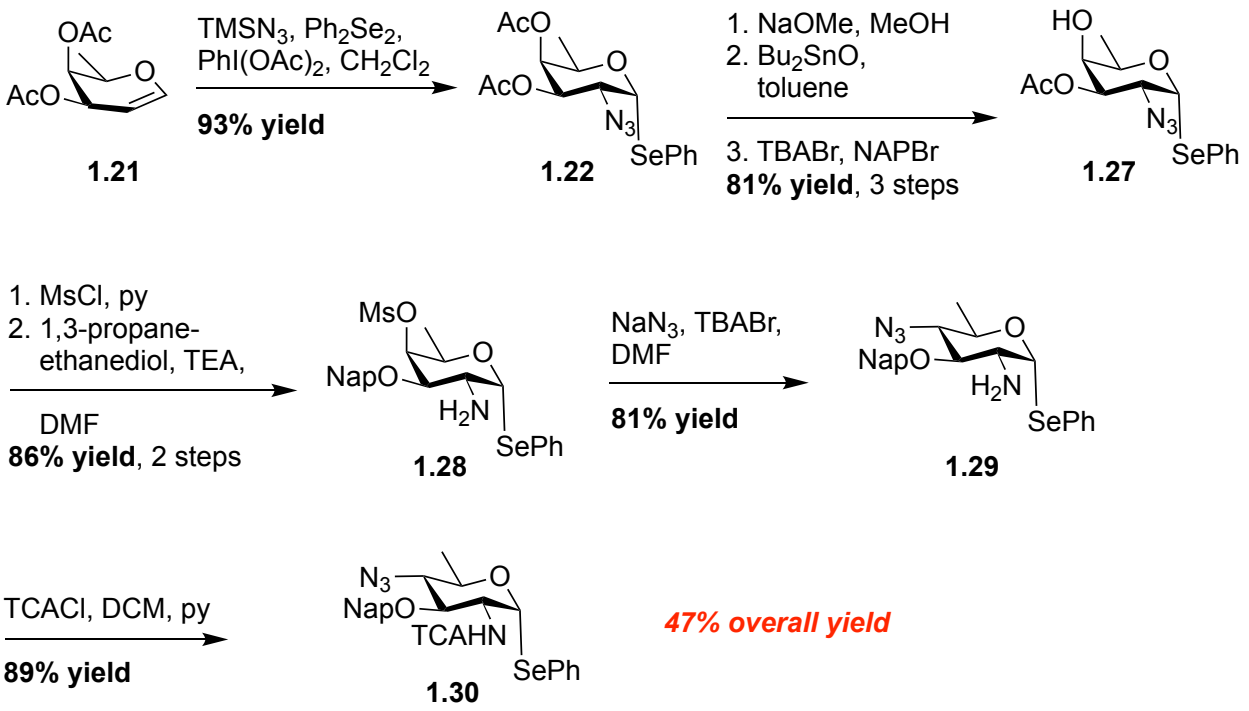


**Scheme 1.3.** Codeé and co-workers' synthesis of bacillosamine from D-fucal.

Following Imperiali's method, work by Kulkarni and co-workers was published in 2013 that developed a route toward various bacterial deoxy-amino sugar thioglycosides starting from D-rhamnosyl 2,4-diol **1.32**.[51] 2,4-diazido-2,4,6-trideoxy derivatives were synthesized via a double parallel $S_N2$ displacement of triflates by azide nucleophiles. Adaptations to this route allowed for different protecting groups (azide, phthalimide, acetate and $NO_2$ anions) to be selectively installed at the C2 and C4 position, resulting in a small array of D-galactosamine (AAT) configured deoxy-amino derivatives **1.34** and **1.33** (32% and 47% overall yield shown below, respectively). Additionally, double-serial inversion at C4 resulted in the D-bacillosamine derivative **1.36** in 27% overall yield and good selectivity. **Scheme 1.4** summarizes this work as well as shows synthesis of the D-rhamnosyl 2,4-diol **1.32** from commercially available thioglycoside **1.31**. Kulkarni's

method for C4 azide displacement has henceforth inspired other groups to generate deoxyamino derivatives in a similar fashion.[52,53]

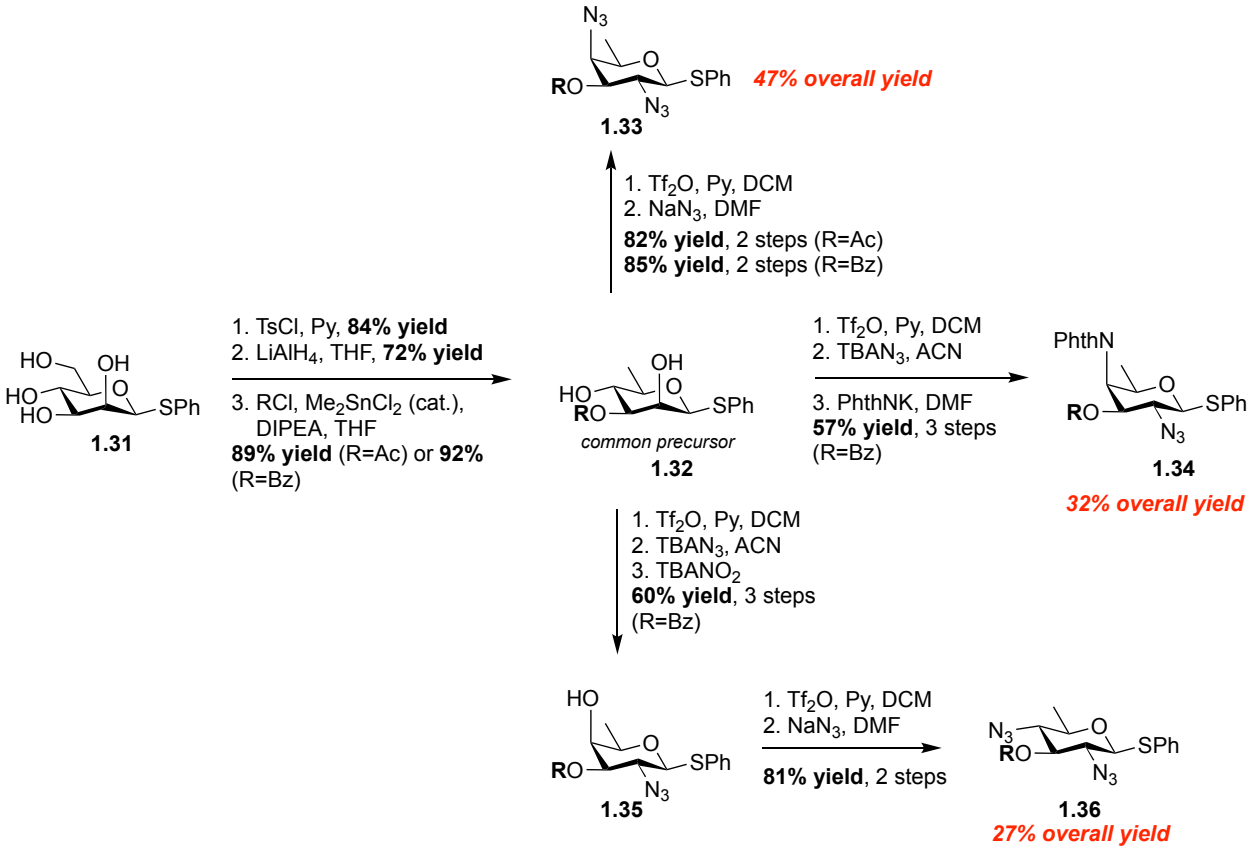


**Scheme 1.4.** Summary of Kulkarni and co-workers' synthesis of D-bacillosamine and AAT DATDH derivatives.

In 2010 Seeberger and co-workers developed a route toward deoxy-amino D-galactosamine (AAT) building blocks from *N*-Cbz-L-threonine (**Scheme 1.5**). [46,54] Key to this method was utilization of Dieckmann cyclization of acetate **1.38** to generate enone **1.39**.[55] Also notable was the Luche reduction of the conjugated enone to generate the glycal **1.40**.[56] Azido nitration (step 5) of the glycal under a variety of conditions was then explored, which was met with stereoselectivity issues about the C2 position of target **1.42**. At best, a 67% yielding (3.5:1 dr) azidoselenation was performed, resulting in 25% overall yield of the desired DATDH selenoglycoside **1.42** from commercially available threonine

**1.37**. Seeberger and co-workers then demonstrated the utility of this DATDH as a glycosyl donor to generate biologically relevant polysaccharide fragments after installation of a trichloroacetimidate (TCAI) at the anomeric position. [46,54]

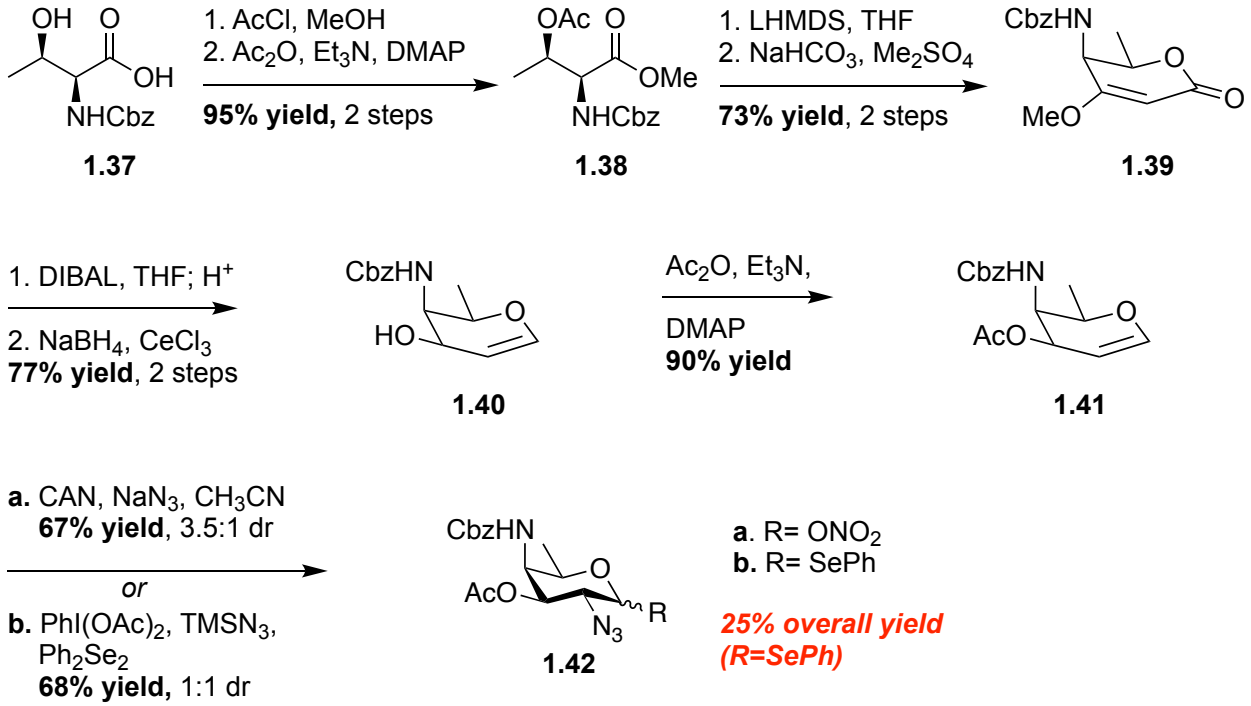


**Scheme 1.5.** Seeberger and co-workers' synthesis of D-galactosamine configured DATDH (AAT) from *N*-Cbz-threonine.

Additional work by Seeberger and co-workers in 2013 described a route toward D-bacillosamine starting from L-Garner's aldehyde **1.43** (**Scheme 1.6**).[53] Noteworthy was the chelate-controlled diastereoselective Grignard addition of propynylmagnesium bromide onto starting material **1.43** followed by *E*-selective alkyne reduction to generate compound **1.44** in a two-step, 66% overall yielding process. The penultimate step relied on Upjohn dihydroxylation of compound **1.45** followed by acetylation to generate the D-fucosamine building block **1.46** in 71% yield and 5:1 dr (when napthyl protected at C3).

Inspired by Kulkarni's work [57] (described above), a final $S_N2$ displacement of a C3 triflate intermediate by azide nucleophiles resulted in the desired D-bacillosamine derivative **1.47** in a 14% overall yield.

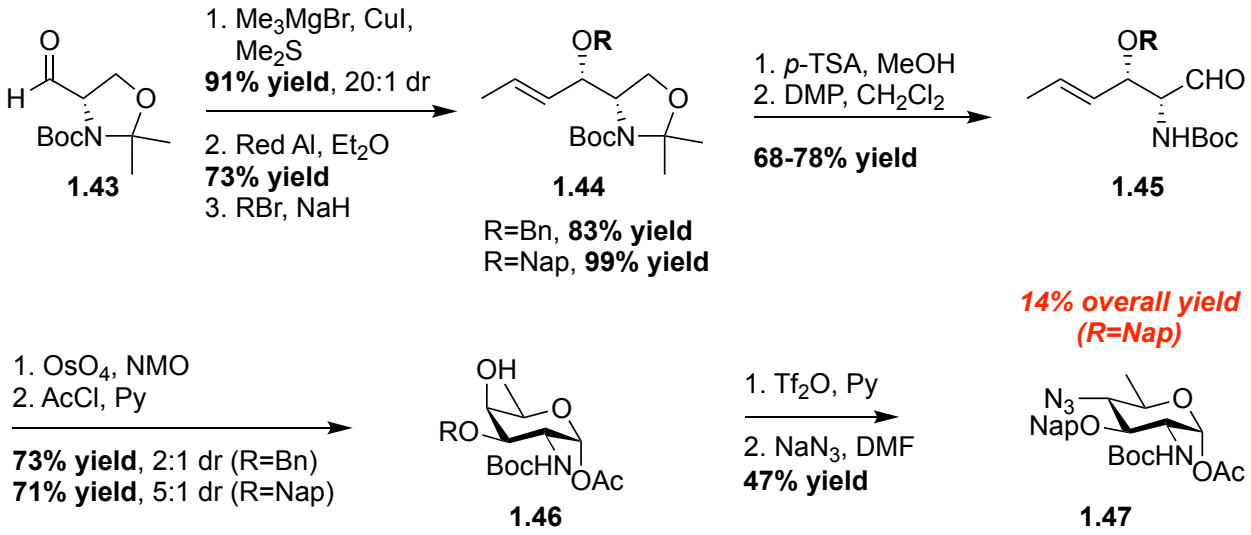


**Scheme 1.6.** Seeberger and co-workers' synthesis of D-bacillosamine from L-Garner's aldehyde.

In 2013, Schmid and co-workers developed an alternative route to the D-galactosamine (AAT) building block starting from L-threonine **1.48** (**Scheme 1.7**).[45] After a series of trivial steps to generate L-Garner's aldehyde **1.49**, a nitro aldol reaction with 2-nitroacetaldehyde diethylacetal served as the key step for diastereoselective insertion of two new chiral centers to generate intermediate **1.50**. After optimizing these reaction conditions, compound **1.50** was synthesized in 74% yield and 5:1 dr. The *galacto*-configuration of the product was favored, though *talo*- configured product was also observed. *Syn*-diastereoselectivity is justified between C2 and C3 via a Zimmermann-Traxler-like transition state. Between C3 and C4, Felkin-Ahn control can explain the *anti*-configurational preference. After nitro-reduction, acetylation, and exposure to water, the

target compound **1.53** was synthesized in 17% overall yield and moderate selectivity from commercially available amino acid **1.48**.

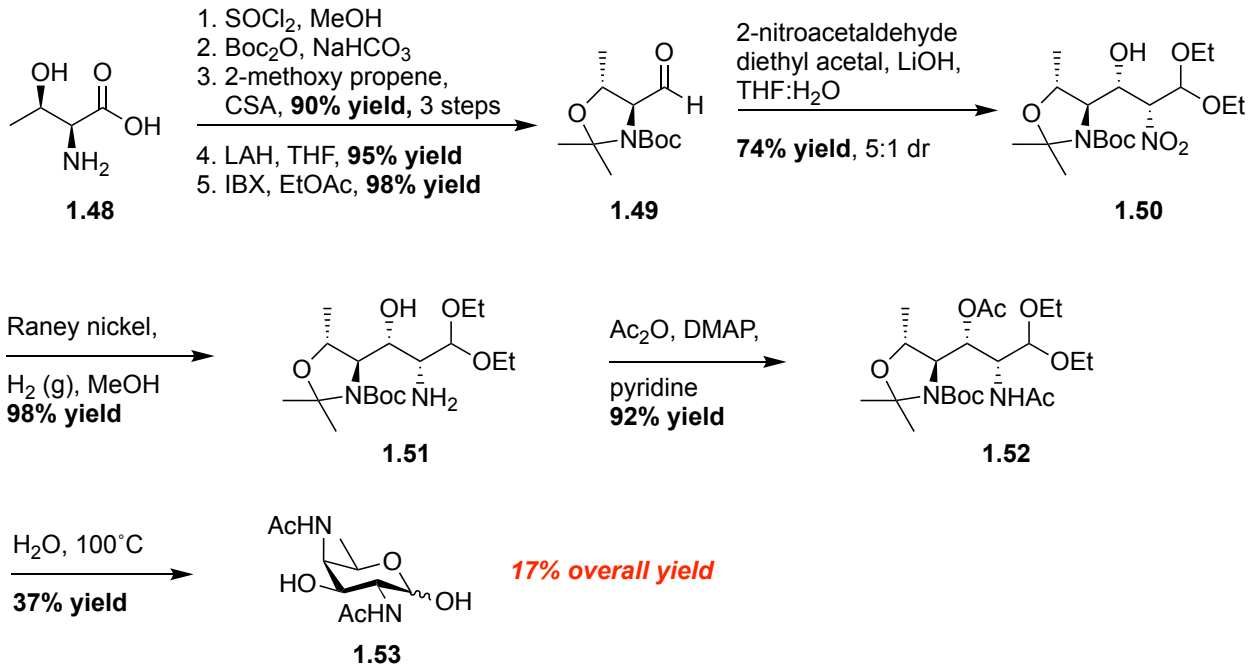


**Scheme 1.7.** Schmid and co-workers' synthesis of an AAT derivative from starting material L-threonine.

## 1.2.3. Previous *de novo* Syntheses of 8-*epi*-Legionaminic Acid (8epiLeg) and Other Nonulosonic Acids (NulOs)

As was previously mentioned, nonulosonic acids (NulOs), in their various isomeric forms, present on bacterial pathogens; Therefore, scientists have worked to develop routes to synthesize them. For the most part, these syntheses can be classified in one of three categories: (1) synthetic conversion from analogous NulOs (requires stereoinversion about various chiral centers), (2) *de novo* synthesis from chiral precursors, or (3) a biomimetic approach where synthesis of a DATDH intermediate is

performed and followed by an aldol-type condensation.[58] Due to their structural complexity, accessing these compounds has proven to be a significant challenge. Namely, work toward legionaminic acid, acinetaminic acid, pseudaminic acid and their C4 / C8 epimers has been met with low levels of success through both chemical and chemoenzymatic methodology. Some of the key developments toward *chemical* synthesis of 3,5,7,9-deoxy-5,7-diamino compounds are herein discussed as a point of reference for future developments. Chemoenzymatic [59–61] and Biosynthetic[62–66] attempts at synthesis of these compounds are not discussed in this chapter.

Much of the early work toward NulO synthesis was performed by Tsvetkov and co-workers in 2001.[67–69] Tsvetkov's strategy involved condensation of 2,4-diacetamido-2,4,6-trideoxyhexoses with oxalacetic acid in the presence of sodium tetraborate under basic conditions to generate desired NulOs in a non-stereoselective fashion. **Schemes 1.8** - **1.10** depict various iterations of this approach toward generation of pseudaminic acid, legionaminic acid, and acinetaminic acid. The generation of various stereoisomers during each NulO synthesis was a major downfall of this approach. In each case, the lack of stereocontrol resulted in a low yielding overall synthesis of the target sugar compound (3, 7, and 8 % overall yield of pseudaminic acid **1.9**, legionaminic acid **1.4**, and acinetaminic acid **1.7**). Additionally, complex separation methods to isolate each desired compound were necessary. As a first pass at the synthesis of NulOs, as well as the development of a route using DATDHs (during a time when these syntheses were also in their infancy), Tsvetkov's work was a tremendous feat.

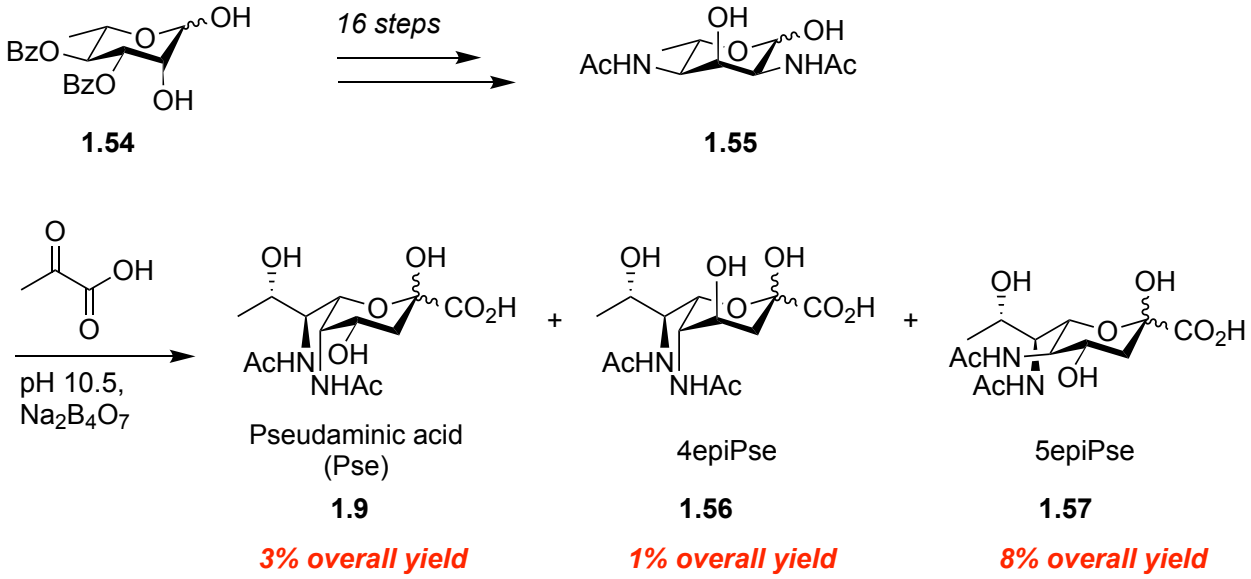


**Scheme 1.8.** Tsvetkov and co-workers' synthesis of pseudaminic acid and epimeric byproducts.

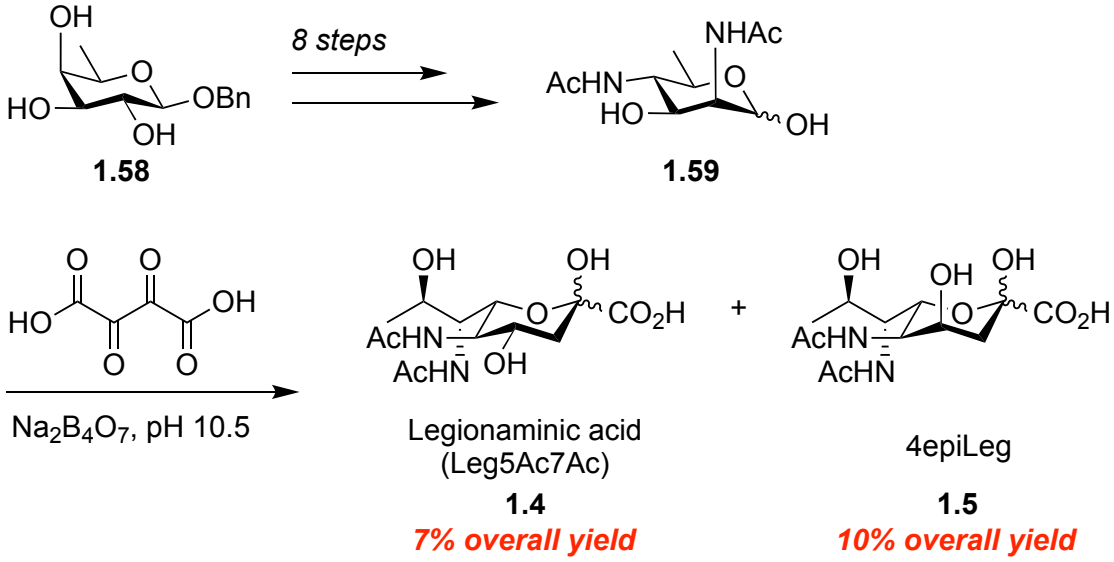


**Scheme 1.9.** Tsvetkov and co-workers' synthesis of legionaminic acid and epimeric byproduct.

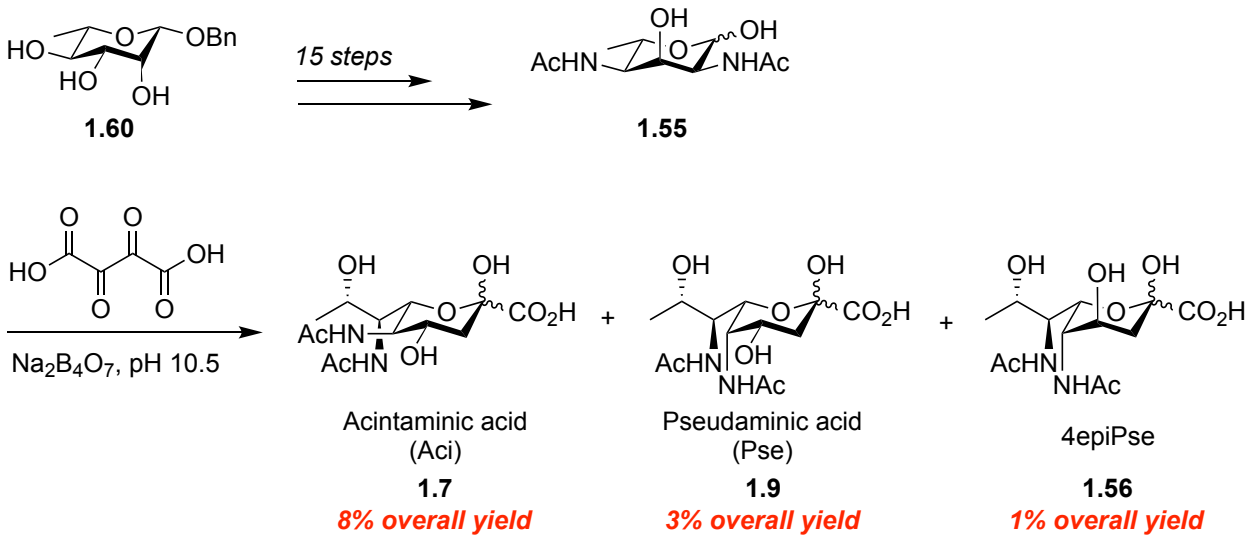


**Scheme 1.10.** Tsvetkov and co-workers' synthesis of acinetaminic acid and pseudaminic acid epimeric byproducts.

Another breakthrough in the chemical synthesis of NulOs arose with Ito and co-workers' report in 2011.[70] Key to this synthetic route was utilization of an indium mediated Barbier-type allylation with a bromomethylacrylate ester to chemically elongate DATDH **1.62** to alkene **1.63** / **1.64** (**Scheme 1.11**). This non-stereoselective allylation method resulted in generation of a 5:4 ratio of *anti*- (**1.63**) and *syn*- (**1.64**) allylation products. Following, ozonolysis and saponification resulted in synthesis of the desired pseudaminic acid derivatives **1.9** and **1.56**. Though this was an improvement on previous methods, low levels of stereocontrol in the key allylation step was a major limitation of this work. As a result, pseudaminic acid **1.9** was generated in only 12% overall yield and its 4-epimer **1.56** generated in 10% overall yield. Utilization of this non-stereoselective Barbier-type allylation for chemical elongation to NulOs was also utilized in later work by Li and co-workers to synthesis pseudaminic acid,[71] as well as Gintner and co-workers to synthesize legionaminic acid.[72] it is also noteworthy that this route was the first to display NulOs as

successful glycosyl donors (dibenzyl phosphate at the anomeric position) via a TMSOTf-mediated glycosylation with a methyl glycoside acceptor.

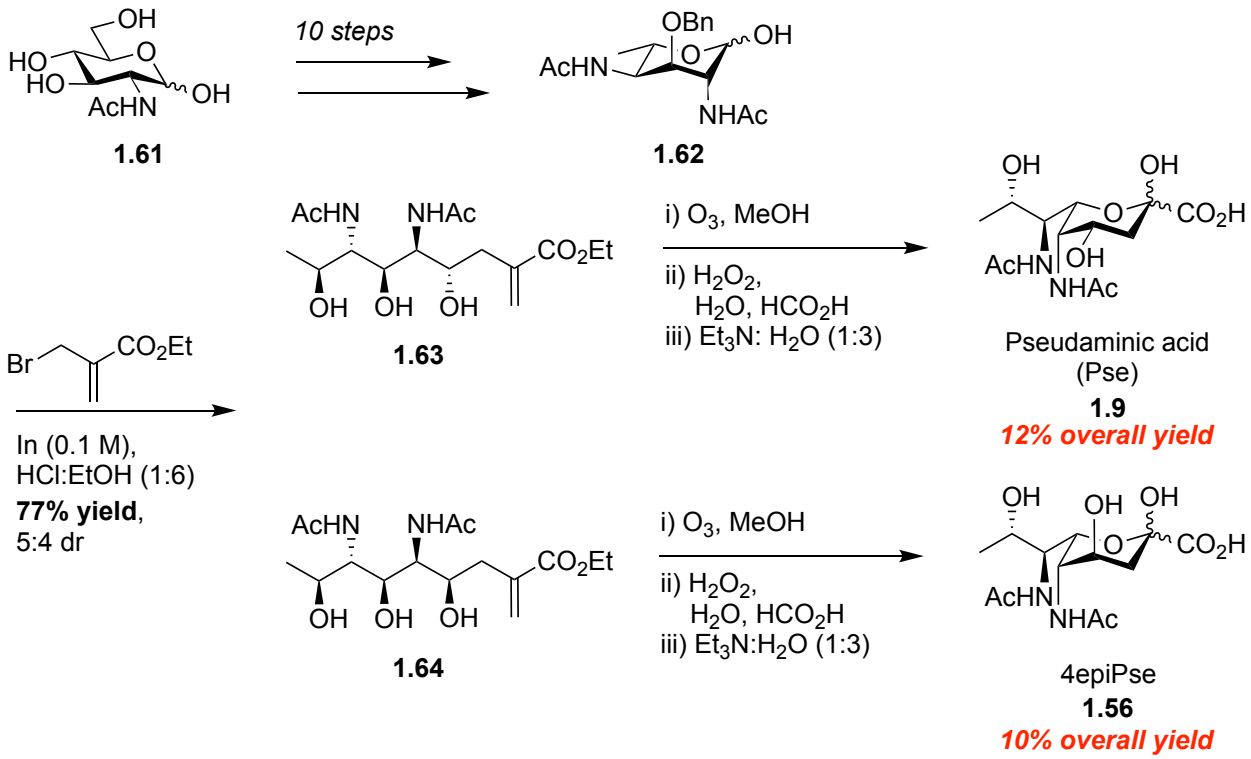


**Scheme 1.11.** Ito and co-workers' synthesis of pseudaminic acid and epimeric byproduct.

In 2014, Kiefel and co-workers introduced a new strategy toward NulO synthesis from protected 2-keto-3-deoxy-D-glycero-D-galacto-nonulosonic acid (KDN) to access 8-*epi*-pseudaminic acid **1.71** (**Scheme 1.12**).[73] Limited access to commercially available KDN **1.66** resulted in the species being synthesized from starting material **1.65** in 42% yield over two steps. Subsequent protecting group manipulations led to the formation of intermediate acetonide **1.67**. Parallel $S_N2$ displacement of this compound at C5 occurred after bis-triflate activation and treatment with sodium azide, stereoselectively generating compound **1.68** in 85% yield over two steps. Reduction followed by peracetylation of the

diazido compound **1.68** resulted in acetamide **1.69** generation in 80% yield over two steps. Final TBS deprotection, acetonide deprotection, and deoxygenation at C9 were performed to generate C9 iodinated compound **1.70**. Final hydrogenation of C9 generated 8-*epi*-pseudaminic acid **1.71** in 12% overall yield, over 11 steps.

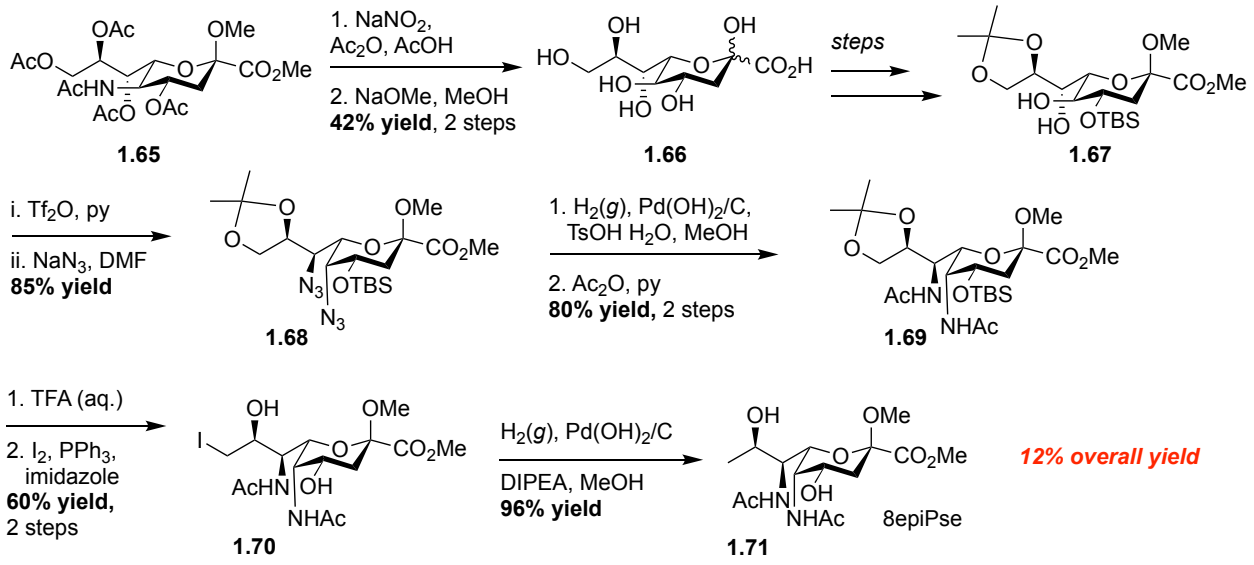


**Scheme 1.12.** Kiefel and co-workers' synthesis of 8-*epi*-pseudaminic acid.

After the authors' original synthetic strategy (**Scheme 1.12**), Kiefel and co-workers published a synthesis of pseudaminic acid from *N*-acetylneuraminic acid (sialic acid) **1.65** in 2016 (**Scheme 1.13**).[74] The desired product was stereoselectively synthesized in 12 steps and 1% overall yield from commercially available material. In 2018, Crich and Dhakal performed a similar synthesis to generate pseudaminic acid **1.9** in 5% yield over 20 steps from commercially available sialic acid **1.1** (**Scheme 1.14**). Notable improvements in stereoselectivity and yield occurred in Crich and Dhakal's method due to early-stage deamination followed by late-stage-employed double parallel inversion of C5 and C7 to generate the desired product.[75] Crich and co-workers also performed a

similar synthesis of protected legionaminic acid **1.90** from commercially available sialic acid **1.1** in 2017 (**Scheme 1.15**). This strategy took advantage of the inherent C5 amino chirality, allowing for synthesis of the protected product in 17% overall yield and 15 steps.[76]

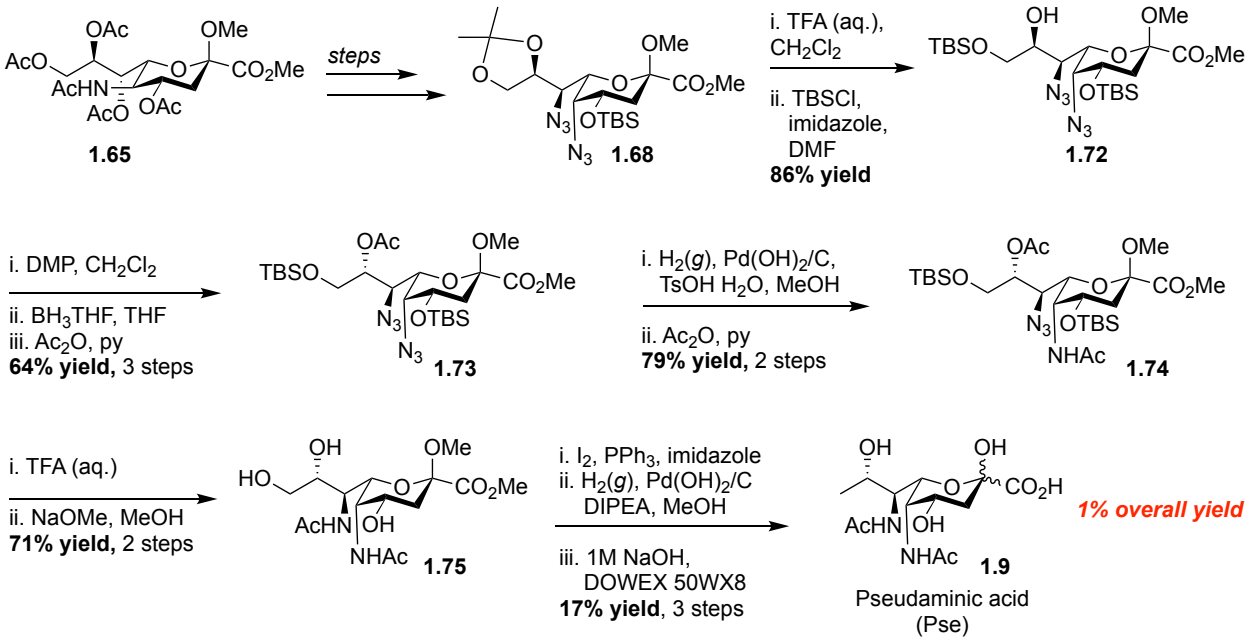


**Scheme 1.13.** Kiefel and co-workers' synthesis of pseudaminic acid.

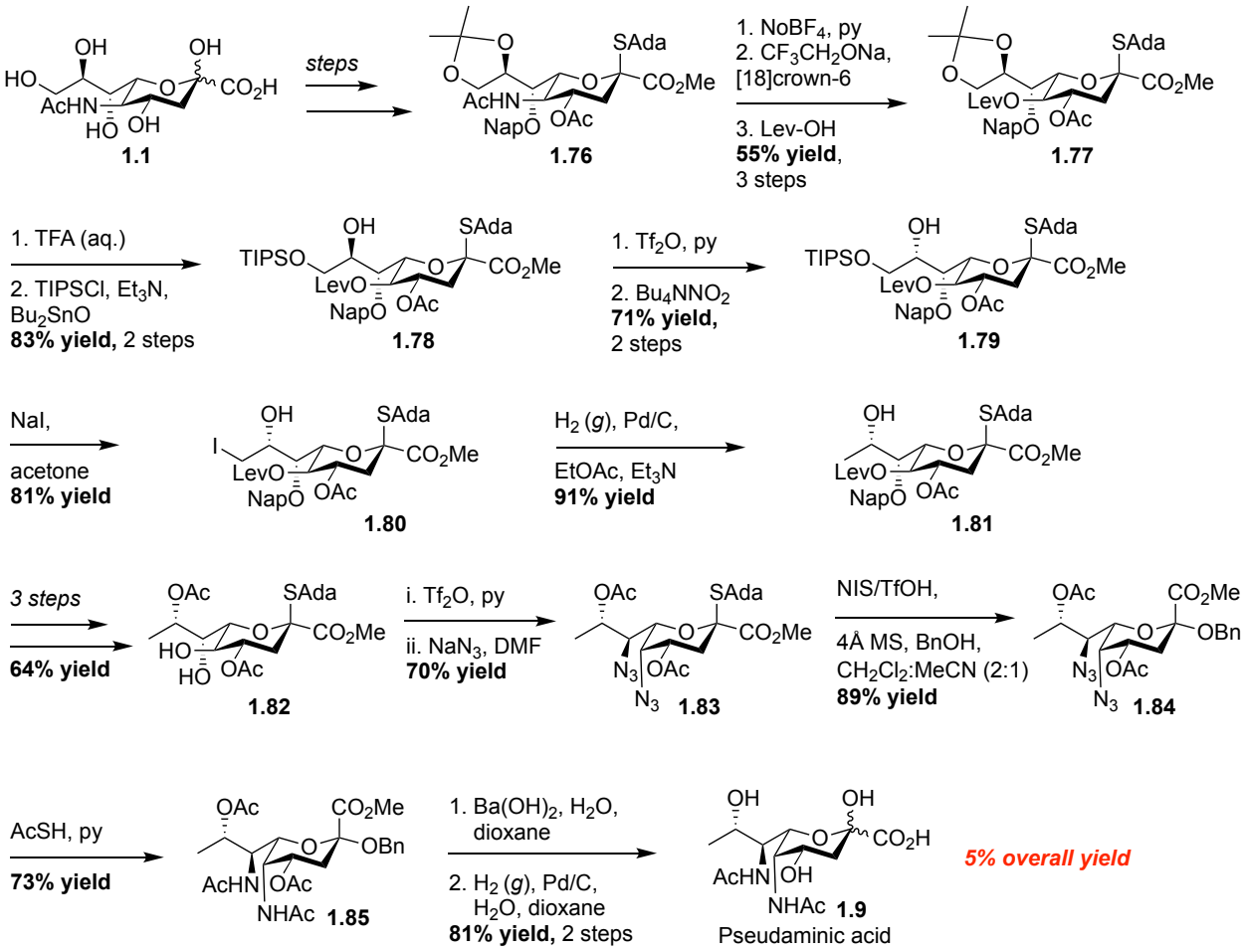


**Scheme 1.14.** Crich and Dhakal's synthesis of pseudaminic acid.

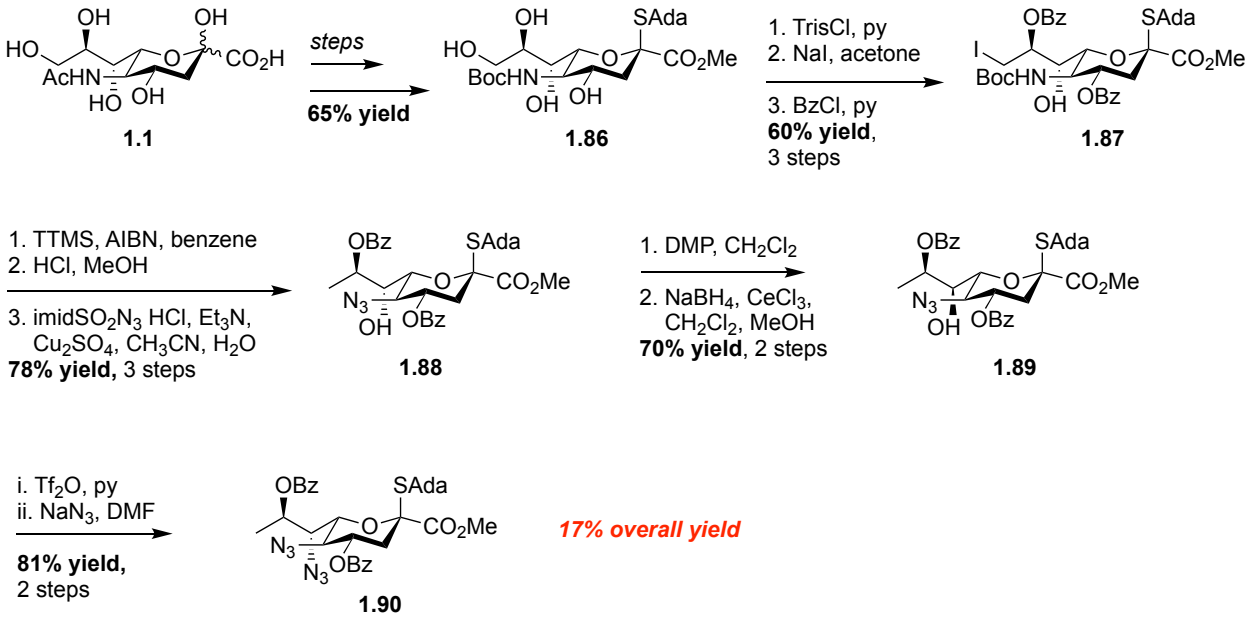


**Scheme 1.15.** Crich and co-workers' synthesis of a legionaminic acid derivative.

Other pivotal work toward the synthesis of NulOs was performed by Seeberger and co-workers in 2015.[77] At this time, it was shown that *de novo* synthesis of legionaminic acid **1.7** could be effectively performed starting from a commercially available amino acid **1.91** (**Scheme 1.16**). Key to this synthesis was employment of a Barbier-type allylation, which resulted chemical elongation of long-chain intermediate **1.95**. However, and as was shown in Ito's synthesis (above), a notable downside to this approach is low diastereoselectivity in the synthesis of key allylation intermediates. Overall, this 24-step reaction sequence went forward in 7% yield from commercially available D-threonine **1.91**. In 2018, Kiefel published a similar route to Leg and 7epiLeg, using a β-*O*-methylated Neu5Ac with a C5 acetamide as starting material.[78]

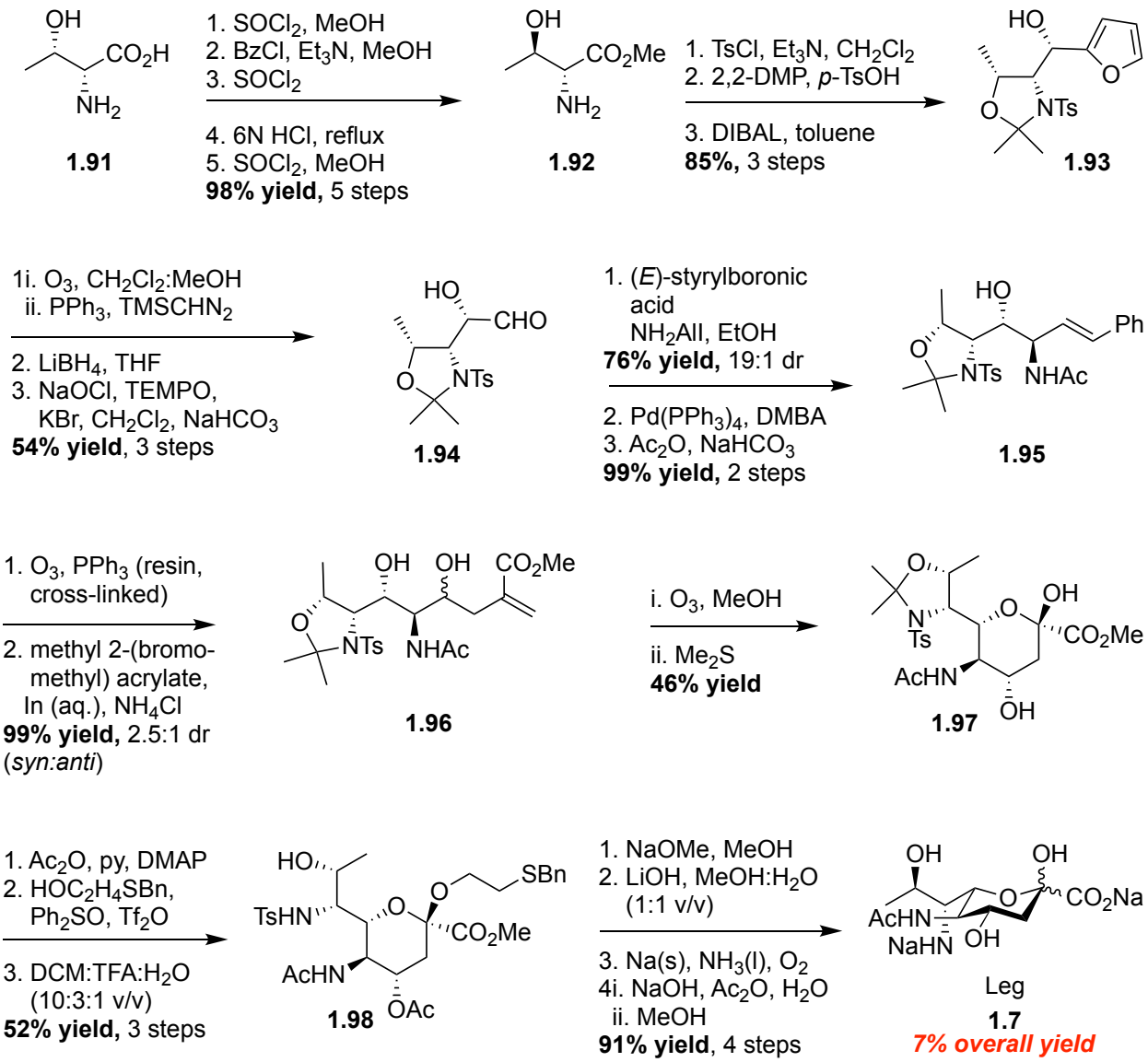


**Scheme 1.16.** Seeberger and co-workers' synthesis of legionaminic acid.

In 2022, Crich and co-workers developed the first and only reported total synthesis of 8-*epi*-legionaminic acid, in addition to synthesis of legionaminic acid, acinetaminic acid, 8-epi-acinetaminic acid, and pseudaminic acid from commercially available *N*-acetyl neuraminic acid **1.1** (**Scheme 1.17**).[79] This approach is by-and-large the most versatile synthesis of these NulO molecules. After a five-step transformation of sialic acid **1.1** into

the derived thioglycoside **1.99**, synthesis of the protected 8-*epi*-legionaminic acid derivative **1.102** proceeded by C7 *N*-sulfinyl imine generation (compound **1.100**). This occurred via condensation with an (*S*) / (*R*)-Ellman sulfinamide. The next step was a samarium iodide-mediated aza-pinacol reaction of intermediate **1.100** with acetaldehyde to generate compound **1.101**. In the case of the legionaminic acid targets, this reaction proceeded in 54% yield and 3:1 dr (Leg:8epiLeg) about the C8 stereocenter. Poor selectivity was attributed to a match-mismatch pair between the chiral auxiliary and chiral substrates.[80] The final thioglycoside donors were obtained after the acidic removal of the *N*-sulfinyl group, azide installation, and *O*-benzoylation. In the case of 8-*epi*-legionaminic acid **1.102**, the product was synthesized in 5% overall yield and in 13 steps. Analogous reactions were performed to synthesize acinetaminic acid **1.103**, 8-*epi*-acinetaminic acid **1.104**, and pseudaminic acid **1.105** in varying yield and step count (See **Scheme 1.17** for further details). Varying levels of diastereoselectivity and low overall yield of certain targets were the tradeoff to a more versatile pathway, in this instance.

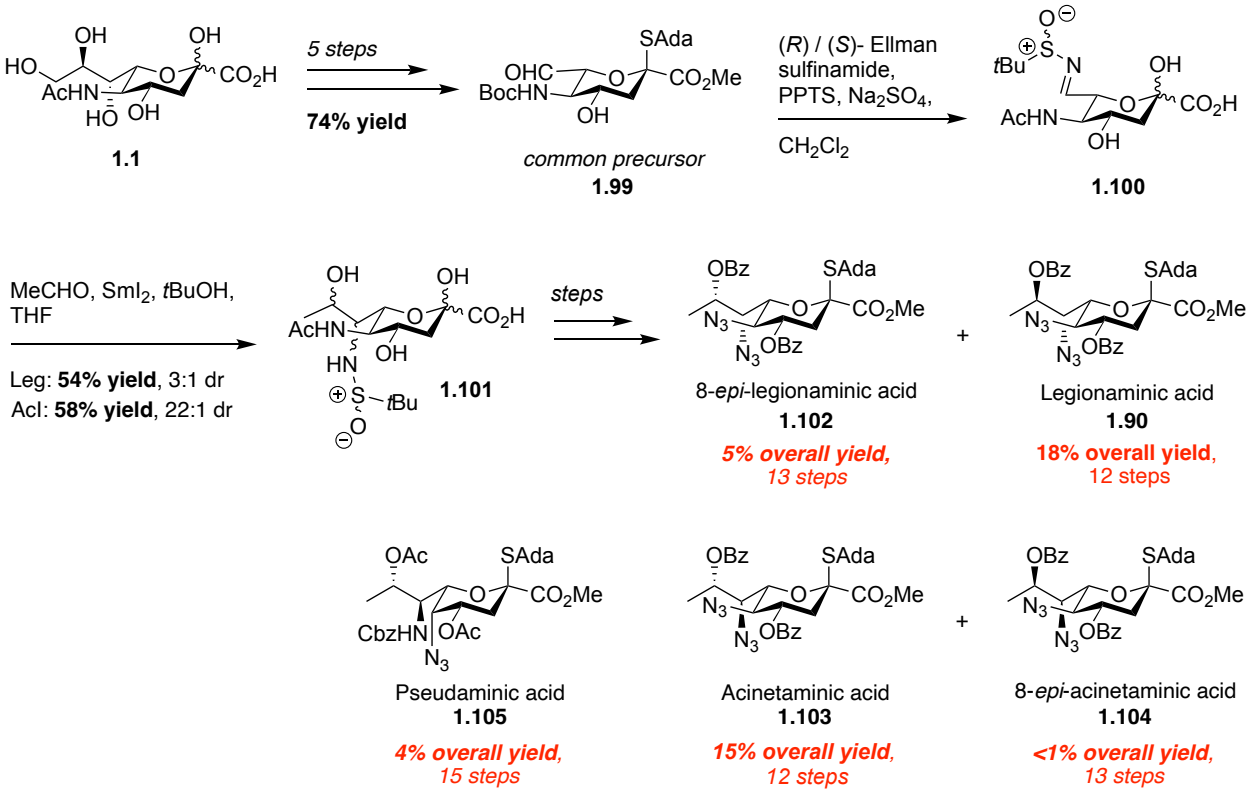


**Scheme 1.17.** Crich and co-workers' synthesis of various nonulosonic acid derivatives (including 8-epi-Leg) starting from *N*-acetylneuraminic acid (sialic acid).

## 1.4. Conclusions

Recent scientific advancements have significantly enhanced our ability to synthesize bacterial deoxy-amino sugars, particularly 2,4-diamino-2,4,6-trideoxyhexoses (DATDHs) and nonulosonic acids (NulOs). These developments provide a promising landscape for further refinement of *de novo* synthetic methods, with the potential to improve access to these important sugars. In the following chapters, we describe the synthesis of a select group of DATDHs, as well initial progress toward the synthesis of 8-epi-legionaminic acid, a complex bacterial sugar that holds significant therapeutic promise.

The successful development of an efficient, diastereoselective synthetic route toward these sugars marks a critical step forward in the field of therapeutics aimed at combating bacterial infection. These sugars are not only integral to bacterial cell wall structures and virulence factors, but also are key players in pathogen-host interactions. By providing better access to these complex sugars, our work will facilitate deeper insights into how they influence the interaction between bacteria and human cells. With this improved understanding, there is further capability of developing novel therapeutic strategies to combatting bacterial infection**.** Ultimately, the continued advancement of synthetic strategies for bacterial deoxy-amino sugar generation offers a promising future for the development of innovative treatments to fight bacterial infections and improve human health.

## 1.5. References


(1) Varki, A.; Cummings, R.; Esko, J.; Freeze, H.; Hart, G.; Marth, J. *Essentials of Glycobiology*; Varki, A., Ed.; Cold Spring Harbor Laboratory Press: Cold Spring Harbor, New York, 1999.

(2) Prates, E. T.; Guan, X.; Li, Y.; Wang, X.; Chaffey, P. K.; Skaf, M. S.; Crowley, M. F.; Tan, Z.; Beckham, G. T. The Impact of O-Glycan Chemistry on the Stability of Intrinsically Disordered Proteins. *Chem. Sci.* **2018**, *9* (15), 3710–3715.

(3) Jayaprakash, N. G.; Surolia, A. Role of Glycosylation in Nucleating Protein Folding and Stability. *Biochem. J.* **2017**, *474* (14), 2333–2347.

(4) Bertozzi, C. R.; Kiessling, L. L. Chemical Glycobiology. *Science (1979)* **2001**, *291* (5512), 2357–2364.

(5) Esko, J. D. Bacterial Polysaccharides. In *Essentials of Glycobiology*; Varki, A., Cummings, R., Esko, J., Hudson, F., Hart, G., Marth, J., Eds.; Cold Spring Harbor Laboratory Press: Cold Spring Harbor, New York, 1999; pp 321–331.

(6) Harnagel, A. P.; Sheshova, M.; Zheng, M.; Zheng, M.; Skorupinska-Tudek, K.; Swiezewska, E.; Lupoli, T. J. Preference of Bacterial Rhamnosyltransferases for 6-Deoxysugars Reveals a Strategy To Deplete O-Antigens. *J. Am. Chem. Soc.* **2023**, *145* (29), 15639–15646.

(7) Liu, B.; Furevi, A.; Perepelov, A. V; Guo, X.; Cao, H.; Wang, Q.; Reeves, P. R.; Knirel, Y. A.; Wang, L.; Widmalm, G. Structure and Genetics of *Escherichia Coli* O Antigens. *FEMS Microbiol. Rev.* **2020**, *44* (6), 655–683.

(8) Valvano, M. A. Export of O-Specific Lipopolysaccharide. *Front. Biosci.* **2003**, *8* (6), 1079.

(9) Van Deun, K.; Pasmans, F.; Ducatelle, R.; Flahou, B.; Vissenberg, K.; Martel, A.; Van den Broeck, W.; Van Immerseel, F.; Haesebrouck, F. Colonization Strategy of Campylobacter Jejuni Results in Persistent Infection of the Chicken Gut. *Vet. Microbiol.* **2008**, *130* (3–4), 285–297.

(10) Nothaft, H.; Szymanski, C. M. Bacterial Protein N-Glycosylation: New Perspectives and Applications. *J. Biol. Chem.* **2013**, *288* (10), 6912–6920.

(11) Morrison, M. J.; Imperiali, B. The Renaissance of Bacillosamine and Its Derivatives: Pathway Characterization and Implications in Pathogenicity. *Biochemistry* **2014**, *53* (4), 624–638.

(12) Schmidt, M. A.; Riley, L. W.; Benz, I. Sweet New World: Glycoproteins in Bacterial Pathogens. *Trends Microbiol.* **2003**, *11* (12), 554–561.

(13) Upreti, R. K.; Kumar, M.; Shankar, V. Bacterial Glycoproteins: Functions, Biosynthesis and Applications. *Proteomics* **2003**, *3* (4), 363–379.

(14) Blix, G. Über Die Kohlenhydratgruppen Des Submaxillarismucins. *Hoppe Seylers Z Physiol. Chem.* **1936**, *240* (1–2), 43–54.

(15) Blix, F. G.; Gottschalk, A.; Klenk, E. Proposed Nomenclature in the Field of Neuraminic and Sialic Acids. *Nature* **1957**, *179* (4569), 1088–1088.

(16) Faillard, H. The Early History of Sialic Acids. *Trends. Biochem. Sci.* **1989**, *14* (6), 237–241.

(17) Lewis, A. L.; Toukach, P.; Bolton, E.; Chen, X.; Frank, M.; Lütteke, T.; Knirel, Y.; Schoenhofen, I.; Varki, A.; Vinogradov, E.; Woods, R. J.; Zachara, N.; Zhang, J.; Kamerling, J. P.; Neelamegham, S.; Darvill, A.; Dell, A.; Henrissat, B.; Bertozzi, C.; Lisacek, F.; Hart, G.; Narimatsu, H.; Freeze, H.; Yamada, I.; Paulson, J.; Marth, J.; Vliegenthart, J. F. G.; et al. Cataloging Natural Sialic Acids and Other Nonulosonic Acids (NulOs), and Their Representation Using the Symbol Nomenclature for Glycans. *Glycobiology* **2023**, *33* (2), 99–103.

(18) Del Bino, L.; Østerlid, K. E.; Wu, D.-Y.; Nonne, F.; Romano, M. R.; Codée, J.; Adamo, R. Synthetic Glycans to Improve Current Glycoconjugate Vaccines and Fight Antimicrobial Resistance. *Chem. Rev.* **2022**, *122* (20), 15672–15716.

(19) de Kraker, M. E. A.; Stewardson, A. J.; Harbarth, S. Will 10 Million People Die a Year Due to Antimicrobial Resistance by 2050? *PLoS Med.* **2016**, *13* (11), e1002184.

(20) Arunachalam, P. S.; Walls, A. C.; Golden, N.; Atyeo, C.; Fischinger, S.; Li, C.; Aye, P.; Navarro, M. J.; Lai, L.; Edara, V. V.; Röltgen, K.; Rogers, K.; Shirreff, L.; Ferrell, D. E.; Wrenn, S.; Pettie, D.; Kraft, J. C.; Miranda, M. C.; Kepl, E.; Sydeman, C.; Brunette, N.; et al. Adjuvanting a Subunit COVID-19 Vaccine to Induce Protective Immunity. *Nature* **2021**, *594* (7862), 253–258.

(21) *Antibiotic Resistance Threats in the United States, 2019*; Atlanta, Georgia, 2019.

(22) García-Quintanilla, M.; Pulido, M. R.; Carretero-Ledesma, M.; McConnell, M. J. Vaccines for Antibiotic-Resistant Bacteria: Possibility or Pipe Dream? *Trends Pharmacol. Sci.* **2016**, *37* (2), 143–152.

(23) Micoli, F.; Bagnoli, F.; Rappuoli, R.; Serruto, D. The Role of Vaccines in Combatting Antimicrobial Resistance. *Nat. Rev. Microbiol.* **2021**, *19* (5), 287–302.

(24) Lipsitch, M.; Siber, G. R. How Can Vaccines Contribute to Solving the Antimicrobial Resistance Problem? *mBio* **2016**, *7* (3).

(25) Matsuoka, T.; Sato, T.; Akita, T.; Yanagida, J.; Ohge, H.; Kuwabara, M.; Tanaka, J. High Vaccination Coverage among Children during Influenza A(H1N1)Pdm09 as a Potential Factor of Herd Immunity. *Int. J. Environ. Res. Public Health* **2016**, *13* (10), 1017.

(26) Avery, O. T.; Heidelberger, M. Immunological Relationships of Cell Constituents of Pneumococcus. *J. Exp. Med.* **1923**, *38* (1), 81–85.

(27) Francis, T.; Tillett, W. S. Cutaneous Reactions in Pneumonia. The Development of Antibodies Following the Intradermal Injection of Type-specific Polysaccharide. *J. Exp. Med.* **1930**, *52* (4), 573–585.

(28) Kazanjian, P. Changing Interest among Physicians toward Pneumococcal Vaccination throughout the Twentieth Century. *J. Hist. Med. Allied Sci.* **2004**, *59* (4), 555–587.

(29) English, P. C. Therapeutic Strategies to Combat Pneumococcal Disease: Repeated Failure of Physicians to Adopt Pneumococcal Vaccine, 1900-1945. *Perspect. Biol. Med.* **1987**, *30* (2), 170–185.

(30) Jacobs, M. R.; Koornhof, H. J.; Robins-Browne, R. M.; Stevenson, C. M.; Vermaak, Z. A.; Freiman, I.; Miller, G. B.; Witcomb, M. A.; Isaäcson, M.; Ward, J. I.; Austrian, R. Emergence of Multiply Resistant Pneumococci. *N. Engl. J. Med.* **1978**, *299* (14), 735–740.

(31) Oosterhuis-Kafeja, F.; Beutels, P.; Van Damme, P. Immunogenicity, Efficacy, Safety and Effectiveness of Pneumococcal Conjugate Vaccines (1998–2006). *Vaccine* **2007**, *25* (12), 2194–2212.

(32) Costantino, P.; Rappuoli, R.; Berti, F. The Design of Semi-Synthetic and Synthetic Glycoconjugate Vaccines. *Expert Opin. Drug Discov.* **2011**, *6* (10), 1045–1066.

(33) Mettu, R.; Chen, C.-Y.; Wu, C.-Y. Synthetic Carbohydrate-Based Vaccines: Challenges and Opportunities. *J. Biomed. Sci.* **2020**, *27* (1), 9.

(34) Nunes, M. C.; Madhi, S. A. Review on the Immunogenicity and Safety of PCV-13 in Infants and Toddlers. *Expert Rev. Vaccines* **2011**, *10* (7), 951–980.

(35) Astronomo, R. D.; Burton, D. R. Carbohydrate Vaccines: Developing Sweet Solutions to Sticky Situations? *Nat. Rev. Drug Discov.* **2010**, *9* (4), 308–324.

(36) Rohokale, R.; Guo, Z. Development in the Concept of Bacterial Polysaccharide Repeating Unit-Based Antibacterial Conjugate Vaccines. *ACS Infect. Dis.* **2023**, *9* (2), 178–212.

(37) Khatun, F.; Stephenson, R. J.; Toth, I. An Overview of Structural Features of Antibacterial Glycoconjugate Vaccines That Influence Their Immunogenicity. *Chem. Eur. J.* **2017**, *23* (18), 4233–4254.

(38) Ravenscroft, N.; Costantino, P.; Talaga, P.; Rodriguez, R.; Egan, W. Glycoconjugate Vaccines. In *Vaccine Analysis: Strategies, Principles, and Control*; Springer Berlin Heidelberg: Berlin, Heidelberg, 2015; pp 301–381.

(39) Schumann, B.; Reppe, K.; Kaplonek, P.; Wahlbrink, A.; Anish, C.; Witzenrath, M.; Pereira, C. L.; Seeberger, P. H. Development of an Efficacious, Semisynthetic Glycoconjugate Vaccine Candidate against *Streptococcus Pneumoniae* Serotype 1. *ACS Cent. Sci.* **2018**, *4* (3), 357–361.

(40) Wei, R.; Yang, X.; Liu, H.; Wei, T.; Chen, S.; Li, X. Synthetic Pseudaminic-Acid-Based Antibacterial Vaccine Confers Effective Protection against *Acinetobacter Baumannii* Infection. *ACS Cent. Sci.* **2021**, *7* (9), 1535–1542.

(41) Jordan, C.; Siebold, K.; Priegue, P.; Seeberger, P. H.; Gilmour, R. A Fluorinated Sialic Acid Vaccine Lead Against Meningitis B and C. *J. Am. Chem. Soc.* **2024**, *146* (22), 15366–15375.

(42) Shen, D.; Seco, B. M. S.; Teixeira Alves, L. G.; Yao, L.; Bräutigam, M.; Opitz, B.; Witzenrath, M.; Fries, B. C.; Seeberger, P. H. Semisynthetic Glycoconjugate Vaccine Lead against *Klebsiella Pneumoniae* Serotype O2afg Induces Functional Antibodies and Reduces the Burden of Acute Pneumonia. *J. Am. Chem. Soc.* **2024**, *146* (51), 35356–35366.

(43) Schauer, R.; Corfield, A. P. Isolation and Purification of Sialic Acids; 1982; pp 51–57.

(44) Flack, E. K. P.; Chidwick, H. S.; Guchhait, G.; Keenan, T.; Budhadev, D.; Huang, K.; Both, P.; Mas Pons, J.; Ledru, H.; Rui, S.; Stafford, G. P.; Shaw, J. G.; Galan, M. C.; Flitsch, S.; Thomas, G. H.; Fascione, M. A. Biocatalytic Transfer of Pseudaminic Acid (Pse5Ac7Ac) Using Promiscuous Sialyltransferases in a Chemoenzymatic Approach to Pse5Ac7Ac-Containing Glycosides. *ACS Catal.* **2020**, *10* (17), 9986–9993.

(45) Schmölzer, C.; Nowikow, C.; Kählig, H.; Schmid, W. Gram Scale de Novo Synthesis of 2,4-Diacetamido-2,4,6-Trideoxy-D-Galactose. *Carbohydr. Res.* **2013**, *367*, 1–4.

(46) Pragani, R.; Stallforth, P.; Seeberger, P. H. De Novo Synthesis of a 2-Acetamido-4-Amino-2,4,6-Trideoxy-D-Galactose (AAT) Building Block for the Preparation of a *Bacteroides Fragilis* A1 Polysaccharide Fragment. *Org. Lett.* **2010**, *12* (7), 1624–1627.

(47) Emmadi, M.; Kulkarni, S. S. Orthogonally Protected D-Galactosamine Thioglycoside Building Blocks via Highly Regioselective, Double Serial and Double Parallel Inversions of β-D-Thiomannoside. *Org. Biomol. Chem.* **2013**, *11* (29), 4825.

(48) Bedini, E.; Esposito, D.; Parrilli, M. A Versatile Strategy for the Synthesis of N-Acetyl-Bacillosamine-Containing Disaccharide Building Blocks Related to Bacterial O-Antigens. *Synlett.* **2006**, *2006* (06), 825–830.

(49) Weerapana, E.; Glover, K. J.; Chen, M. M.; Imperiali, B. Investigating Bacterial N-Linked Glycosylation: Synthesis and Glycosyl Acceptor Activity of the Undecaprenyl Pyrophosphate-Linked Bacillosamine. *J. Am. Chem. Soc.* **2005**, *127* (40), 13766–13767.

(50) van Mechelen, J.; Voorneveld, J.; Overkleeft, H. S.; Filippov, D. V.; van der Marel, G. A.; Codée, J. D. C. Synthesis of Orthogonally Protected and Functionalized Bacillosamines. *Org. Biomol. Chem.* **2020**, *18* (15), 2834–2837.

(51) Emmadi, M.; Kulkarni, S. S. Synthesis of Orthogonally Protected Bacterial, Rare-Sugar and D-Glycosamine Building Blocks. *Nat. Protoc.* **2013**, *8* (10), 1870–1889.

(52) Dhara, D.; Bouchet, M.; Mulard, L. A. Scalable Synthesis of Versatile Rare Deoxyamino Sugar Building Blocks from D-Glucosamine. *J. Org. Chem.* **2023**, *88* (11), 6645–6663.

(53) Leonori, D.; Seeberger, P. H. De Novo Synthesis of D- and L-Fucosamine Containing Disaccharides. *Beilstein J. Org. Chem.* **2013**, *9*, 332–341.

(54) Pragani, R.; Seeberger, P. H. Total Synthesis of the Bacteroides Fragilis Zwitterionic Polysaccharide A1 Repeating Unit. *J. Am. Chem. Soc.* **2011**, *133* (1), 102–107.

(55) Ren, F.; Hogan, P. C.; Anderson, A. J.; Myers, A. G. Synthesis of L-Kedarosamine in Protected Form and Its Efficient Incorporation into an Advanced Intermediate to Kedarcidin Chromophore. *Org. Lett.* **2007**, *9* (10), 1923–1925.

(56) Luche, J. L. Lanthanides in Organic Chemistry. Selective 1,2 Reductions of Conjugated Ketones. *J. Am. Chem. Soc.* **1978**, *100* (7), 2226–2227.

(57) Emmadi, M.; Kulkarni, S. S. Total Synthesis of the Bacillosamine Containing α-L-Serine Linked Trisaccharide of Neisseria Meningitidis. *Carbohydr. Res.* **2014**, *399*, 57–63.

(58) Flack, E. K. P.; Chidwick, H. S.; Best, M.; Thomas, G. H.; Fascione, M. A. Synthetic Approaches for Accessing Pseudaminic Acid (Pse) Bacterial Glycans. *ChemBioChem* **2020**, *21* (10), 1397–1407.

(59) Liu, F.; Aubry, A. J.; Schoenhofen, I. C.; Logan, S. M.; Tanner, M. E. The Engineering of Bacteria Bearing Azido-Pseudaminic Acid-Modified Flagella. *ChemBioChem* **2009**, *10* (8), 1317–1320.

(60) Santra, A.; Xiao, A.; Yu, H.; Li, W.; Li, Y.; Ngo, L.; McArthur, J. B.; Chen, X. A Diazido Mannose Analogue as a Chemoenzymatic Synthon for Synthesizing Di-*N*-acetyllegionaminic Acid-Containing Glycosides. *Angew. Chem. Int. Ed.* **2018**, *57* (11), 2929–2933.

(61) McArthur, J. B.; Santra, A.; Li, W.; Kooner, A. S.; Liu, Z.; Yu, H.; Chen, X. *L. Pneumophila* CMP-5,7-Di-*N*-Acetyllegionaminic Acid Synthetase (LpCLS)-Involved Chemoenzymatic Synthesis of Sialosides and Analogues. *Org. Biomol. Chem.* **2020**, *18* (4), 738–744.

(62) Schoenhofen, I. C.; Young, N. M.; Gilbert, M. Biosynthesis of Legionaminic Acid and Its Incorporation Into Glycoconjugates; 2017; pp 187–207.

(63) Glaze, P. A.; Watson, D. C.; Young, N. M.; Tanner, M. E. Biosynthesis of CMP-*N*, *N'*-Diacetyllegionaminic Acid from UDP-*N*,*N'*-Diacetylbacillosamine in *Legionella Pneumophila*. *Biochemistry* **2008**, *47* (10), 3272–3282.

(64) Hassan, M. I.; Lundgren, B. R.; Chaumun, M.; Whitfield, D. M.; Clark, B.; Schoenhofen, I. C.; Boddy, C. N. Total Biosynthesis of Legionaminic Acid, a Bacterial Sialic Acid Analogue. *Angew. Chem. Int. Ed.* **2016**, *55* (39), 12018–12021.

(65) Schoenhofen, I. C.; Vinogradov, E.; Whitfield, D. M.; Brisson, J.-R.; Logan, S. M. The CMP-Legionaminic Acid Pathway in Campylobacter: Biosynthesis Involving Novel GDP-Linked Precursors. *Glycobiology* **2009**, *19* (7), 715–725.

(66) Kenyon, J. J.; Marzaioli, A. M.; De Castro, C.; Hall, R. M. 5,7-Di-N-Acetyl-Acinetaminic Acid: A Novel Non-2-Ulosonic Acid Found in the Capsule of an Acinetobacter Baumannii Isolate. *Glycobiology* **2015**, *25* (6), 644–654.

(67) Tsvetkov, Y. E.; Shashkov, A. S.; Knirel, Y. A.; Zähringer, U. Synthesis and NMR Spectroscopy of Nine Stereoisomeric 5,7-Diacetamido-3,5,7,9-Tetradeoxynon-2-Ulosonic Acids. *Carbohydr. Res.* **2001**, *335* (4), 221–243.

(68) Tsvetkov, Y. E.; Shashkov, A. S.; Knirel, Y. A.; Zähringer, U. Synthesis and Identification in Bacterial Lipopolysaccharides of 5,7-Diacetamido-3,5,7,9-Tetradeoxy-D-Glycero-D-Galacto- and -D-Glycero-D-Talo-Non-2-Ulosonic Acids. *Carbohydr. Res.* **2001**, *331* (3), 233–237.

(69) Tsvetkov, Y. E.; Shashkov, A. S.; Knirel, Y. A.; Backinowsky, L. V.; Zähringer, U. Synthesis of 5,7-Diacetamido-3,5,7,9-Tetradeoxy-L-Glycero-D-Galacto- and -L-Glycero-D-Talo-Nonulosonic Acids, Putative Components of Bacterial Lipopolysaccharides. *Mendeleev Commun.* **2000**, *10* (3), 90–91.

(70) Lee, Y. J.; Kubota, A.; Ishiwata, A.; Ito, Y. Synthesis of Pseudaminic Acid, a Unique Nonulopyranoside Derived from Pathogenic Bacteria through 6-Deoxy-AltdiNAc. *Tetrahedron Lett.* **2011**, *52* (3), 418–421.

(71) Liu, H.; Zhang, Y.; Wei, R.; Andolina, G.; Li, X. Total Synthesis of *Pseudomonas Aeruginosa* 1244 Pilin Glycan via *de Novo* Synthesis of Pseudaminic Acid. *J. Am. Chem. Soc.* **2017**, *139* (38), 13420–13428.

(72) Gintner, M.; Yoneda, Y.; Schmölzer, C.; Denner, C.; Kählig, H.; Schmid, W. A Versatile de Novo Synthesis of Legionaminic Acid and 4-Epi-Legionaminic Acid Starting from d-Serine. *Carbohydr. Res.* **2019**, *474*, 34–42.

(73) Zunk, M.; Williams, J.; Carter, J.; Kiefel, M. J. A New Approach towards the Synthesis of Pseudaminic Acid Analogues. *Org. Biomol. Chem.* **2014**, *12* (18), 2918.

(74) Williams, J. T.; Corcilius, L.; Kiefel, M. J.; Payne, R. J. Total Synthesis of Native 5,7-Diacetylpseudaminic Acid from *N* -Acetylneuraminic Acid. *J. Org. Chem.* **2016**, *81* (6), 2607–2611.

(75) Dhakal, B.; Crich, D. Synthesis and Stereocontrolled Equatorially Selective Glycosylation Reactions of a Pseudaminic Acid Donor: Importance of the Side-Chain Conformation and Regioselective Reduction of Azide Protecting Groups. *J. Am. Chem. Soc.* **2018**, *140* (44), 15008–15015.

(76) Popik, O.; Dhakal, B.; Crich, D. Stereoselective Synthesis of the Equatorial Glycosides of Legionaminic Acid. *J. Org. Chem.* **2017**, *82* (12), 6142–6152.

(77) Matthies, S.; Stallforth, P.; Seeberger, P. H. Total Synthesis of Legionaminic Acid as Basis for Serological Studies. *J. Am. Chem. Soc.* **2015**, *137* (8), 2848–2851.

(78) Carter, J. R.; Kiefel, M. J. A New Approach to the Synthesis of Legionaminic Acid Analogues. *RSC Adv.* **2018**, *8* (62), 35768–35775.

(79) Siyabalapitiya Arachchige, S.; Crich, D. Syntheses of Legionaminic Acid, Pseudaminic Acid, Acetaminic Acid, 8- *Epi* -Acetaminic Acid, and 8- *Epi* -Legionaminic Acid Glycosyl Donors from *N* -Acetylneuraminic Acid by Side Chain Exchange. *Org. Lett.* **2022**, *24* (16), 2998–3002.

(80) Masamune, S.; Choy, W.; Petersen, J. S.; Sita, L. R. Double Asymmetric Synthesis and a New Strategy for Stereochemical Control in Organic Synthesis. *Angew. Chem., Int. Ed. Engl.* **1985**, *24* (1), 1–30.

# Chapter 2: The Synthesis and Characterization of Four Derivatized 2,4-Diamino-2,4,6-Trideoxyhexoses (DATDHs)

## 2.1. Introduction

As was described in Chapter 1, with antibiotic resistance on the rise there is a need for alternative treatments and preventions of bacterial infection.[81] It is known that the lipopolysaccharide (LPS) and capsular polysaccharide (CPS) of bacteria are composed of so-called “rare” sugar chains that differ from those found in eukaryotes. The LPS and CPS are found on the extracellular matrix of bacteria and are known to play important roles in cellular recognition.[11,82,83] As a result, these glycans make attractive targets for carbohydrate-based vaccine development, providing an alternative to traditional antibiotics.[35,84–86] Among these bacterial sugars are various 2,4-diamino-2,4,6-trideoxyhexoses (DATDHs), which are found in repeating units on the *O*-Antigen of many Gram-negative pathogenic bacteria including *A. baumannii, C. jejuni*, *S. pneumoniae, P. alcaifaciens, N. gonorrheae*, *N. meningitidis, P. aeruginosa, etc*.[11,51,86–89] **Figure 2.1** illustrates some of these biologically relevant structures. Because such deoxy-amino sugars cannot be easily isolated from their natural sources, they have become attractive synthetic targets. Additionally, different stereoisomers of DATDH sugars are present on different bacterial serotypes, so there is a need for a widely applicable route to synthesize libraries of these compounds. This could allow for high-throughput screening and the development of therapeutics tailored to specific bacterial strains.

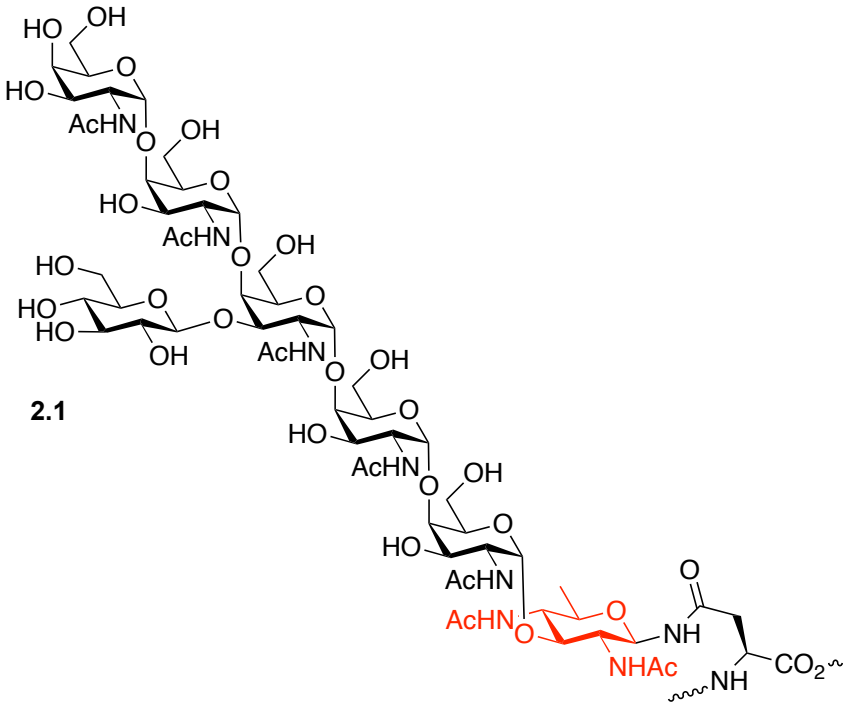


**2.1**

(a) *C. jejuni* N-linked glycan

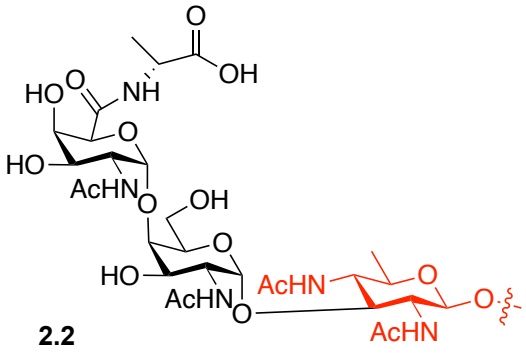


**2.2**

(b) *A. baumannii* K17 CPS

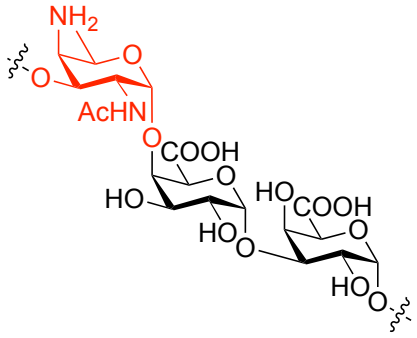


**2.3**

(c) *S. pneumoniae* ST1 CPS

**Figure 2.1.** (a) *C. jejuni* N-linked glycan (b) *A. baumannii* K17 capsular polysaccharide (c) *S. pneumoniae* ST1 capsular polysaccharide.

## 2.2. The Krische Allylation

### 2.2.1. History and Expansion of Krische Allylation Chemistry

In 2019, the first catalytic enantioselective carbonyl (α-amino) allylation was introduced by Krische and co-workers. This method involved a primary alcohol and phthalimido allene pronucleophile engaging in a hydrogen auto-transfer-mediated carbonyl reductive coupling, resulting in the formation of vicinal amino alcohols (**Scheme 2.1**).[90] This chemistry displayed high levels of regioselectivity, *anti*-diastereoselectivity and enantioselectivity for a range of aromatic and aliphatic primary alcohol substrates, notable examples of which are displayed in **Scheme 2.2**. In addition to high stereoselectivity, this chemistry neither required formation of a preformed carbanion, nor a terminal reductant (ex: Mn, Zn, $Et_3B$, $Et_2Zn$), which is standard for carbonyl additions or metal-catalyzed carbonyl reductive couplings.[91] This is made possible in the Krische allylation through the alcohol's dual role of reductant and carbonyl proelectrophile. Instead of the previously mentioned additives, the overall allylation reaction simply required catalytic amounts of iridium-$H_8$-BINAP to facilitate H-transfer catalysis, marking a significant advancement in the field of allylation chemistry.

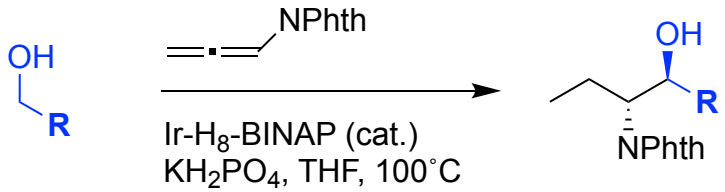


**Scheme 2.1.** General schematic for Krische allylation chemistry.

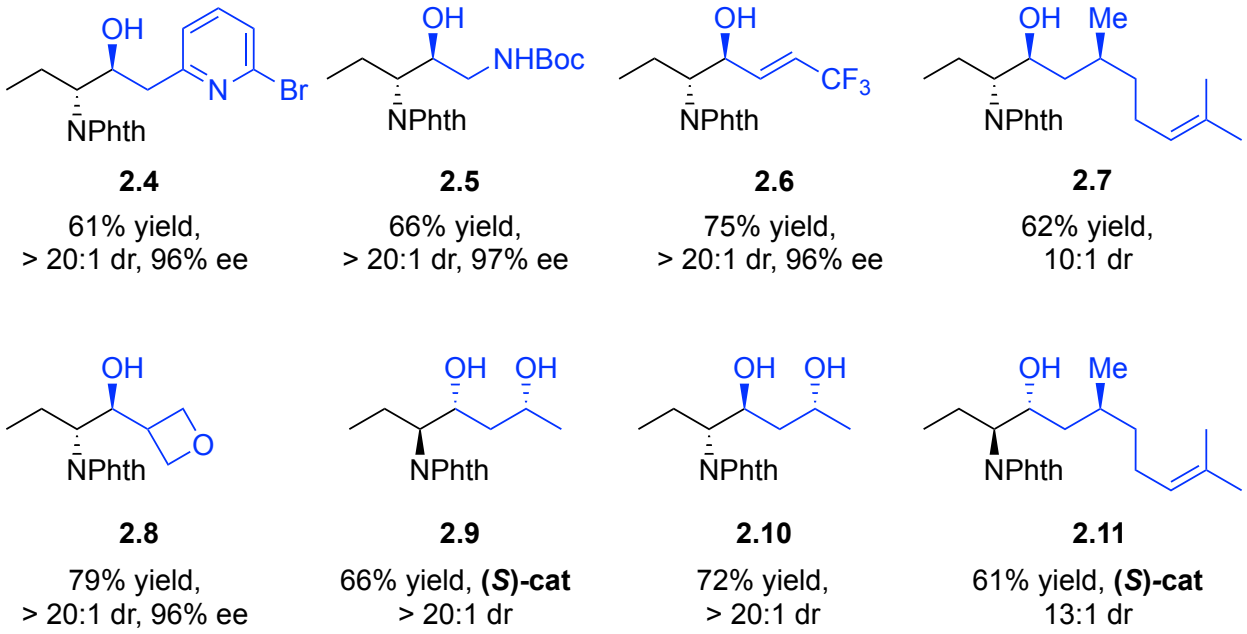


**Scheme 2.2.** Examples of original scope utilized in the iridium-catalyzed carbonyl reductive coupling, displaying various aliphatic and aromatic alcohol substrates (blue) and their generated *anti*-diastereoselective products (blue and black).[90]

Regarding scope, it was shown that vicinal alcohols and modified hetereoaryl-containing alcohols could be generated in good yield and excellent enantio- or diastereoselectivity through this method. Additionally, it was shown that free secondary alcohols were tolerated (see butane 1,3-*syn*- and 1,3-*anti*-diol adducts, **2.9** and **2.10**) and resulted in high *anti*-diastereoselectivity. Stereoselectivity could be tailored, in these instances, based on which chiral catalyst was utilized ((*R*) versus (*S*)). To this end, it was preliminarily indicated that the handedness of the catalyst has a direct effect on chirality generated at the primary alcohol. Additionally, and in the cases of an additional vicinal chiral center, the substrate alcohol-catalyst interaction still dictated *anti*-diastereoselectivity (see entries **2.7**, **2.9**-**2.11**).[90]

Regarding the reaction mechanism and transition state, initial studies utilizing reaction progress kinetic analysis (RPKA) via a “different excess” protocol along with DFT

labeling studies gave insight into the reaction mechanism (**Scheme 2.3**).[90] High levels of diastereoselectivity are thought to be generated through a "closed chair-like transition state," which forms an iridium (III) alkoxide and exchanges with the primary alcohol reactant to release the final product (squared off in **Scheme 2.3**).[90] More recent studies, however, supported the idea that stereochemistry at the iridium may be more important than the chiral phosphine ligand in directing enantiofacial selectivity.[92]

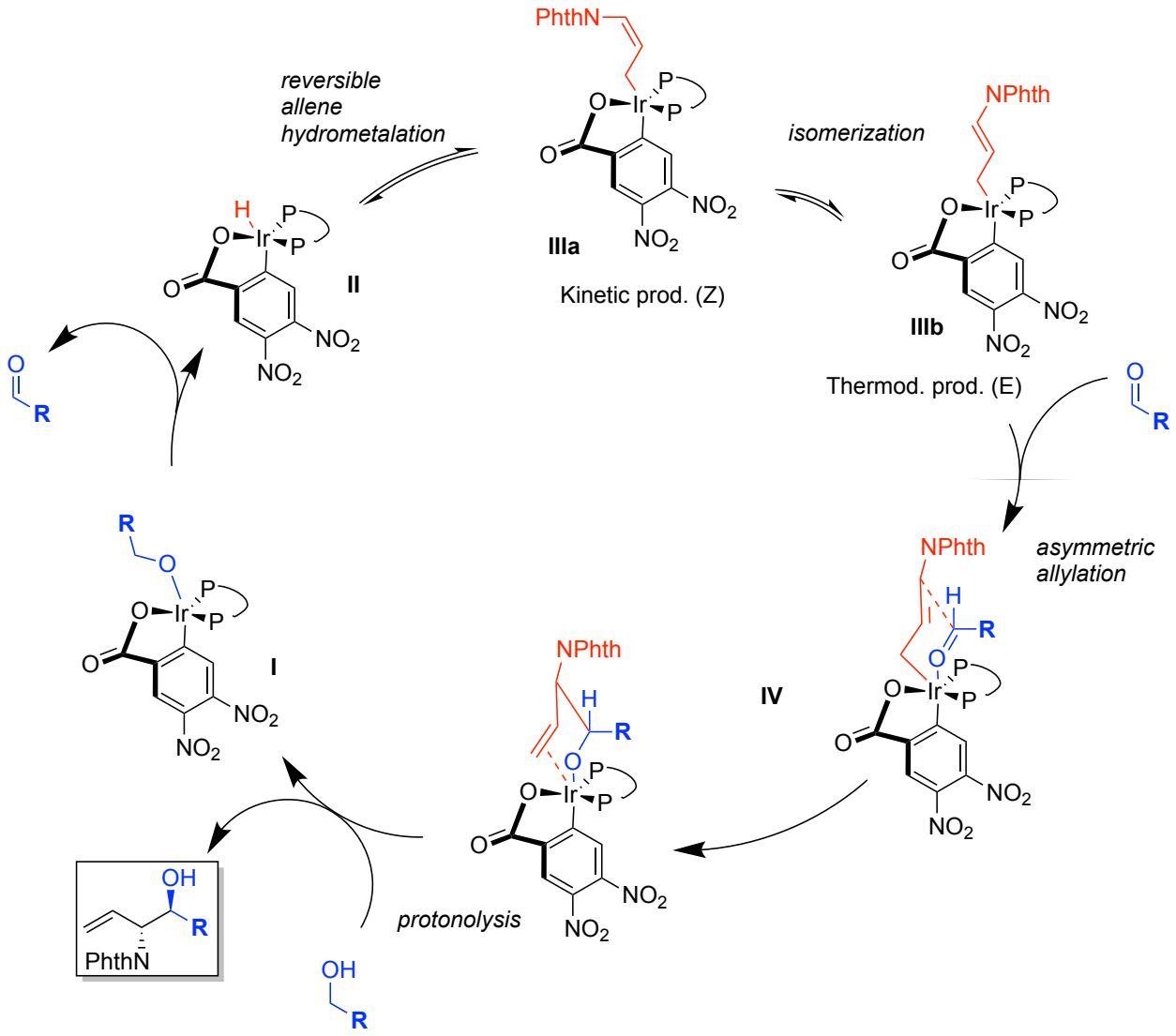


**Scheme 2.3.** Proposed catalytic cycle for Krische allylation based off KIE and DFT calculations.

The potential applicability of this work to generate complex deoxy-amino monosaccharides in a highly diastereoselective fashion was subsequently explored in our lab. In the work discussed in **Section 2.3.3**, we aimed to push the substrate limits of this chemistry by exploring H-transfer on chiral α-amino, β-hydroxy alcohols. Under the right conditions, good yield and high levels of diastereoselectivity were observed, which corroborated with Krische's findings. However, *anti*-diastereoselectivity was not always observed. Additionally, with protected β-hydroxyls (TBS), changing catalyst handedness did *not* show a reversal in alcohol chirality of the product. This led us to believe that there is a ceiling to the level of catalyst control exerted in this reaction and, in some cases, stereoselectivity can be entirely under substrate control. Further mechanistic work must be done to probe this, but it was beyond the scope of this chapter. All in all, delving further into the results described in **Section 2.3.3**. would be an interesting future area of study. Additionally, the Krische allylation is a wonderful tool for the generation of highly diastereoselective 1,2-amino alcohols and has a promising future in the world of carbohydrate chemistry.

## 2.3. Background, Overview, and Total Synthesis of DATDHs

### 2.3.1. Background and Retrosynthetic Analysis

Various methods of synthesis have been reported in the literature for this class of deoxy-amino bacterial sugars. Many of these approaches rely on the stereochemical manipulations of sugar building blocks.[44,47,51,57,93–97] Others start with commercially available amino acids that undergo late-stage cyclization after installation of various chiral centers.[98] While these methods have proven effective, they rely on synthetic routes that

are often limited in scope and/or proceed with low diastereoselectivity in the construction of key intermediates. Herein, we report an efficient, diastereoselective, and versatile protocol for the synthesis of four unique 2,4-diamino-2,4,6-trideoxy sugars. Retrosynthetically, we envisioned that all four 2,4-diamino-2,4,6-trideoxypyranosides **2.20** - **2.23** could arise from threoninols **2.12** – **2.15** via a Krische allylation to set the required stereocenters. In the forward direction, oxidative cleavage of the resulting terminal alkenes followed by anomeric TBS protection would afford the protected deoxy-amino sugars (**Scheme 2.4**).

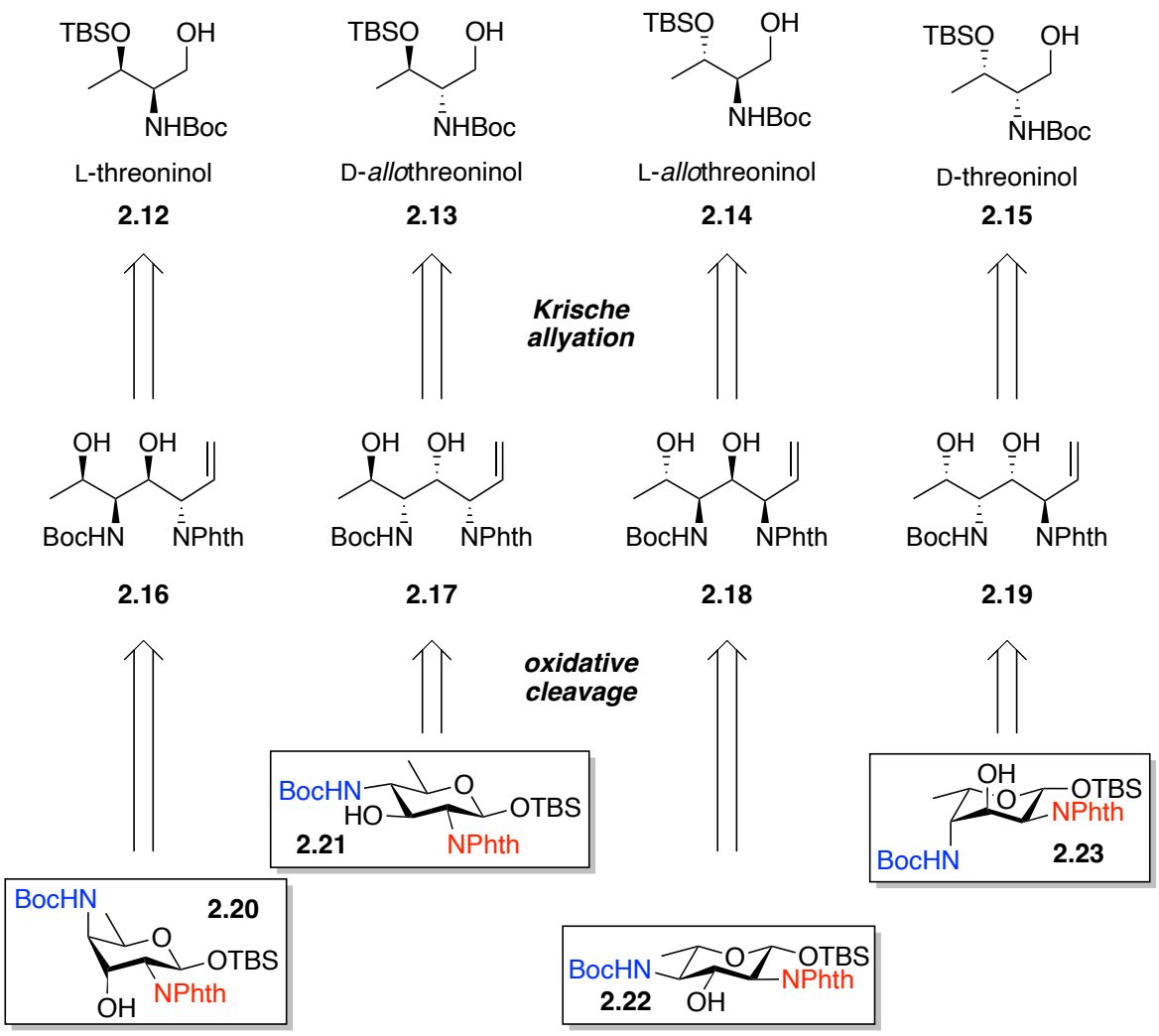


**Scheme 2.4.** Retrosynthetic analysis of deoxy-amino sugar synthesis starting from derivatives of L-threoninol, D-*allo*threoninol, L-*allo*threoninol, and D-threoninol.

## 2.3.2. Threoninol Synthesis

Accessing these deoxy-amino sugars first involved synthesis of the threoninol compounds **2.12 – 2.15** (**Scheme 2.5**). To this end, a commercially available D-threonine **2.24** was first Boc protected at the amine position under standard conditions, giving rise to compound **2.25**. Treating **2.25** with methyl iodide and potassium carbonate ($K_2CO_3$) resulted in the formation of methyl ester **2.26**. This compound was then reduced under

standard conditions with sodium borohydride to yield D-threoninol **2.27** in 80% yield over three steps. It was later found that protecting group adjustments would need to be made to this substrate. See **Section 2.3.5** for further reaction optimizations and protecting group manipulations.

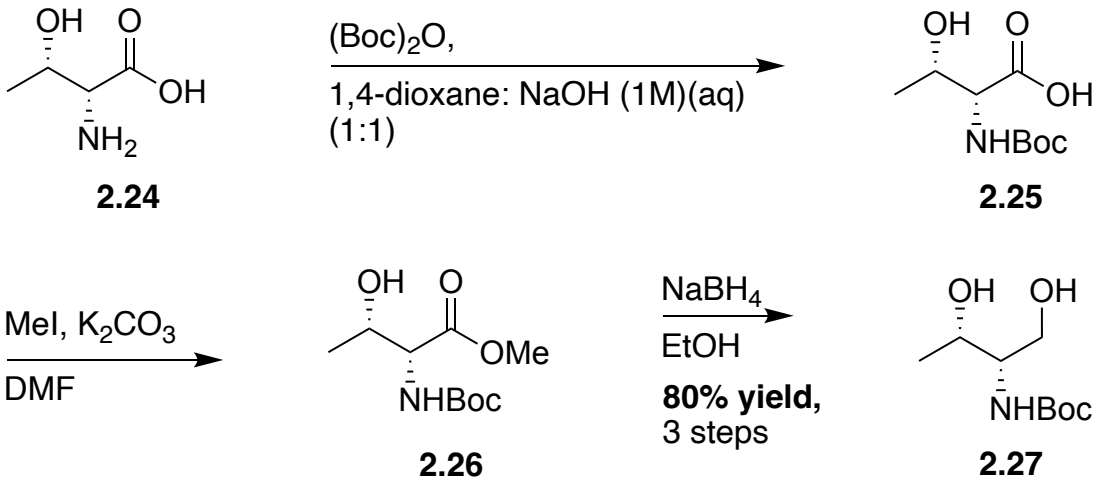


**Scheme 2.5.** Original synthetic pathway toward threoninol compounds for the D-threonine model system.

## 2.3.3. Krische Allylation Optimization and Synthesis

With 1,3-diol **2.27** in hand, we turned our attention to the key allylation reaction (**Table 2.1**). We recognized that optimization of this reaction would be necessary because, to our knowledge, the Krische allylation had never been performed on chiral α-amino, β-hydroxy alcohols (see **Section 2.2.1** for more details).[90] Under the originally reported conditions, only trace amounts of impure allylation product **2.19** were observed (entry 1). Increasing the catalyst loading from 0.05 to 0.1 equivalents led to an increase in conversion (entry 2). The starting material conversion could be further increased by increasing the reaction time (entry 3), with the bulk of starting material consumed within

the first 96 hours. We then further increased the catalyst loading to 0.2 equivalents entry 5) and temperature to 110°C in a sealed tube (entry 7). Pleasingly, these conditions provided the desired allylation product **2.19** as a > 20:1 mixture of diastereomers and showed 58% conversion. Attempts to run the same reaction using the (*S*)-catalyst resulted in lower conversion to product **2.28**, demonstrating a clear case of stereochemical match and mismatch between substrate and catalyst (entries 4 and 6).[80] Additional optimization attempts with alternative chiral catalysts (**Figure 2.2**) failed to provide an improvement (**Table 2.2**). It is unclear whether changes in reaction yield and diastereoselectivity are due to steric or electronic effects of the catalyst used. Alternative solvents also failed to provide any improvement (**Table 2.3**).

**Table 2.1.** Key optimizations of allylation chemistry using D-threoninol as the model substrate.

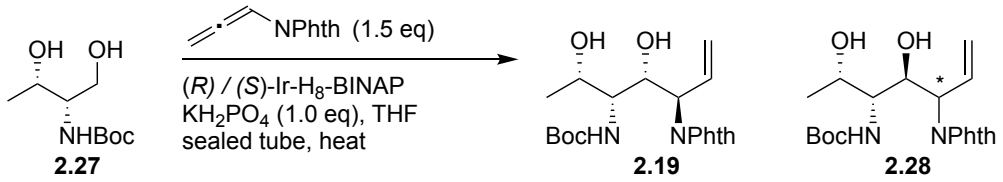


**2.27** **2.19** **2.28**

| Entry | Catalyst Chirality | Catalyst Loading (mol eq.) | Time (days) | Temperature (˚C) | Percent Conversion[a] | Product 2.19:2.28 |
|---|---|---|---|---|---|---|
| 1 | *(R)* | 0.05 | 2 | 100 | trace | 1:0 |
| 2 | *(R)* | 0.1 | 2 | 100 | 27% | 1:0 |
| 3 | *(R)* | 0.1 | 7 | 100 | 41% | 1:0 |
| 4 | *(S)* | 0.1 | 7 | 100 | 27% | 0:1 |
| 5 | *(R)* | 0.2 | 4 | 100 | 51% | 1:0 |
| 6 | *(S)* | 0.2 | 4 | 100 | 37% | 0:1 |
| **7** | ***(R)*** | **0.2** | **4** | **110** | **58%** | 1:0 |

[a] >20:1 diastereomeric ratio

**Table 2.2.** Catalyst screen for allylation optimization.

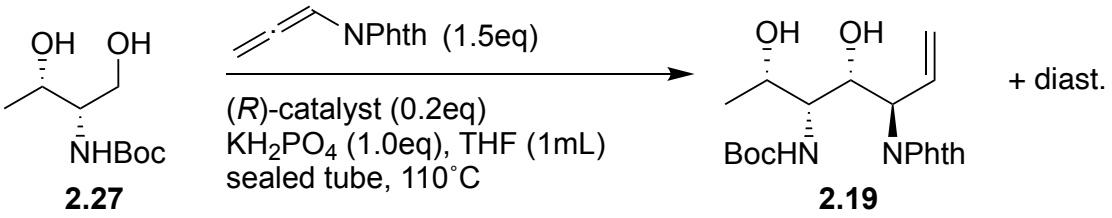


| Entry | Catalyst | Yield | Diastereomeric Ratio (dr) |
|---|---|---|---|
| 22 | (*R*)-Ir-Xyl-GARPHOS | 39% | 1:1 |
| 23 | (*R*)-Ir-Cl-MeO-BIPHEP | 90% | 1:1.3 |
| 24 | (*R*)-Ir-PhanePhos | 0% | N/A |
| **11** | **(*R*)-Ir-$H_8$-BINAP** | **58%** | **>20:1** |

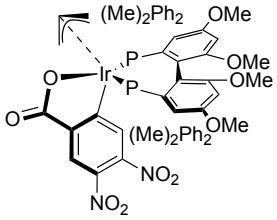


(*R*)-Xyl-GARPHOS

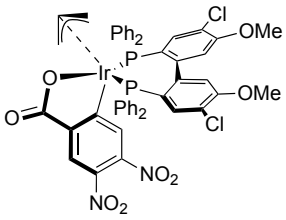


(*R*)-Ir-Cl-MeO-BIPHEP

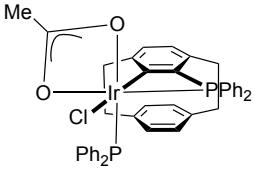


(*R*)-Ir-PhanePhos

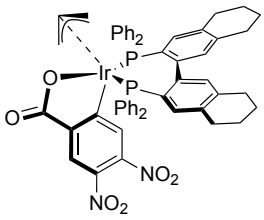


(*R*)-Ir-$H_8$-BINAP

**Figure 2.2.** Catalysts synthesized for catalyst screen in Table 2.2.

**Table 2.3.** Solvent screen for allylation optimization.

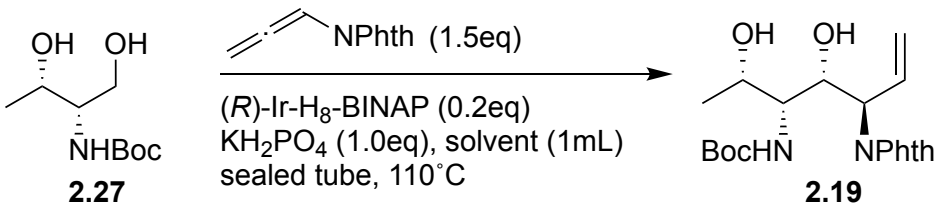


| Entry | Solvent | Yield |
|---|---|---|
| **11** | **THF** | **58%** |
| 14 | toluene | 31% |
| 15 | 1,4-dioxane | 42% |
| 16 | ethyl acetate | 30% |
| 17 | acetone | 56% |
| 18 | N,N-dimethylformamide | 39% |

## 2.3.4. Stereochemical Determinations via Rychnovsky Analysis

To determine stereochemistry of the C-4 hydroxyl on compounds **2.19** and **2.28**, we carried out a Rychnovsky acetonide analysis (**Scheme 2.6**).[99,100] Per this analysis, it is known that an acetonide protected *syn*-1,3-diol will adopt a chair conformation, which is expected to possess acetonide methyl-group $^{13}C$ chemical shifts with a > 9 ppm difference (**Figure 2.3a**). In contrast, the acetonide protected *anti*-1,3-diol will adopt a twist-boat conformation to minimize 1,3-diaxial interactions. This would be identified by diagnostic acetonide methyl-group $^{13}C$ chemical shifts with a < 9 ppm difference, respectively (**Figure 2.3b**). Based off of this analysis, we were able to establish that

compound **2.29** possessed a *syn*-1,3-diol configuration (~19 and 30 ppm $^{13}C$ shifts) while compound **2.30** possessed a *trans*-1,3-diol configuration (~24 and 25 ppm $^{13}C$ shifts).

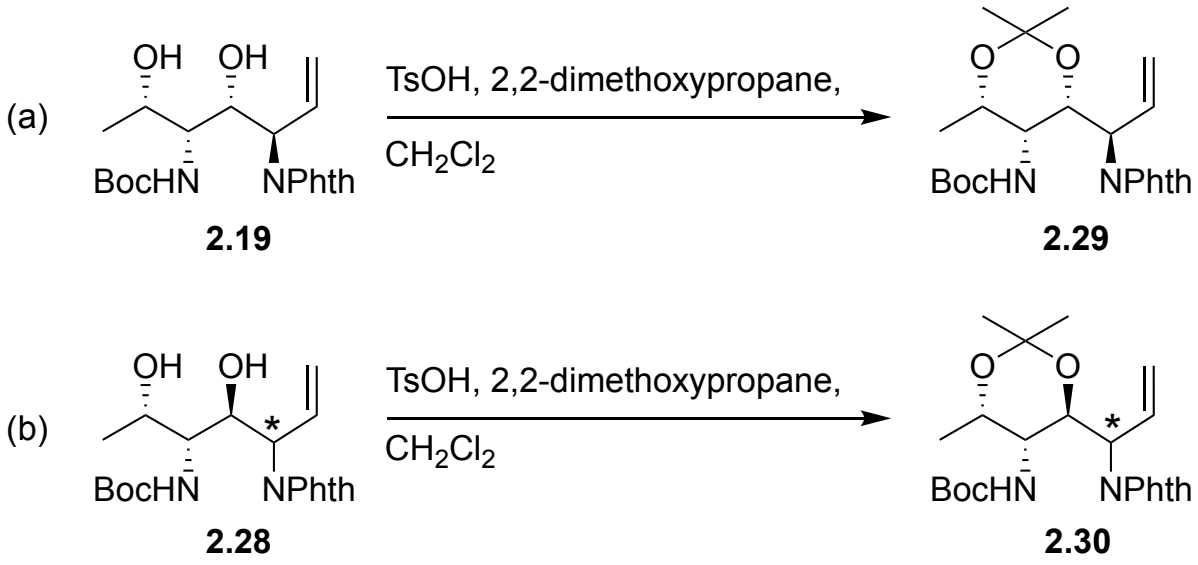


**Scheme 2.6.** Acetonide protection of 1,3-diols for Rychnovsky analysis.

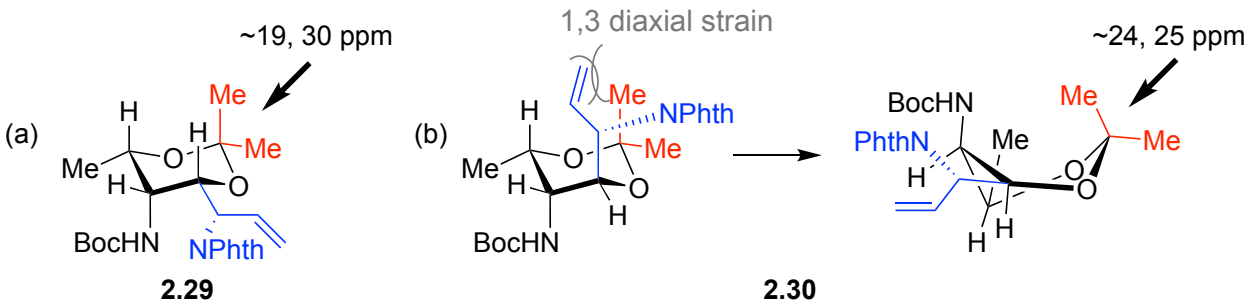


**Figure 2.3.** Stereochemical determination of 1,3-diols using Rychnovsky analysis. (a) The acetonide protected *syn*-1,3-diol with distinct acetonide methyl groups highlighted in red (b) The acetonide protected *anti*-1,3-diol with acetonide methyl groups highlighted in red.

## 2.3.5. Substrate Modifications

It was our initial hope that we could carry the crude allylation product **2.19** on to the subsequent oxidative cleavage. However, all attempts at ozonolysis led to decomposition and trace, impure isolated product. Workups utilizing both $PPh_3$ and $Me_2S$ were attempted and, due to the difficulties removing triphenylphosphine oxide from the product mixture, dimethyl sulfide became the most effective workup reagent. However, and noting the coordinating ability of diols, we reasoned that metal contaminants from the allylation were still causing problems in subsequent steps. To circumvent this, we decided to protect the secondary alcohol prior to allylation. To this end, we examined different silyl protecting groups on the threoninol O3, due to their inability to form a chelate with metal centers. [101,102] We also synthesized an oxazolidine protected threoninol to examine the effect of conformationally constraining substrates on the reaction (**Figure 2.4**).[103]

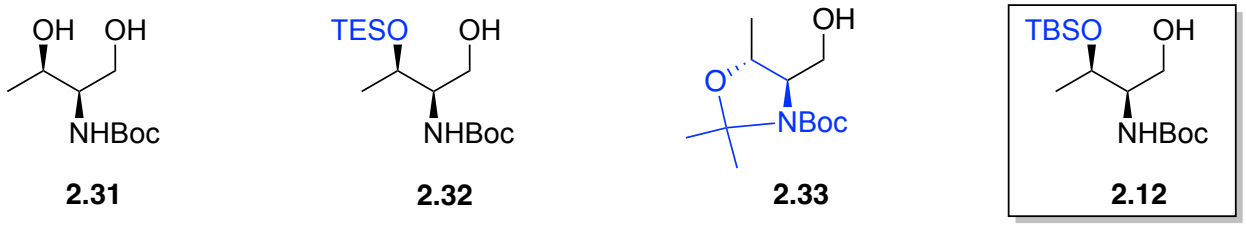


**Figure 2.4.** Starting materials explored for use in the allylation of threoninols to vicinal amino alcohols.

Attempts to synthesis more reactive silyl ethers (TES) were unsuccessful due to the instability of the triethyl silane to regular phase column chromatography. The oxazolidine did not successfully undergo allylation under our optimized conditions, which rendered it unusable. Ultimately, the TBS protected threoninol **2.12** was deemed the optimal substrate, providing the desired allylation product **2.36** in 40% isolated yield as a

20:1 mixture of diastereomers (**Scheme 2.8**). Allylation of TBS protected compound **2.15** was done in the same fashion, generating compound **2.34** in 43% isolated yield as a 20:1 mixture of diastereomers (**Scheme 2.7**). These allylation yields were improved upon after scale-up, which is further elaborated on in Chapter 4 of this thesis (*vide infra*).

Due to the presence of the Boc protecting group on allylation products such as **2.34**, rotamerization in both $^{1}H$ and $^{13}C$ NMR was not surprising and was confirmed using 1-D NOE experimentation according to the procedure of Ley and co-workers.[104] This NMR experimentation is used to show chemical-exchange between rotameric peaks, allowing for rapid distinction of equilibrating small molecules from non-equilibrating diastereomers. This served as a non-destructive, timely way of performing compound characterization and affirming compound purity, while circumventing the need for more complex VT-NMR experimentation or the addition of complexing agents. Broadening of the allylation product **2.34** carbon peaks on $^{13}C$ NMR was also observed, as is expected for carbamate rotamers.[105] The stereochemistry of product **2.34** was confirmed using the Rychnovsky analysis.[99]

### 2.3.6. Oxidative Cleavage and Final Anomeric Protection

Following allylation, attempts to subject **2.34** directly to oxidative cleavage led to complex mixtures resulting from partial loss of the TBS group. To circumvent this, the TBS group was removed prior to ozonolysis. Pleasingly, diol **2.19** then underwent clean oxidative cleavage to afford **2.35a** and **2.35b**, which was directly protected at the anomeric position using TBSCl to generate **2.23** as a single diastereomer (**Scheme 2.7**). Product **2.23** was isolated as a mixture of rotamers at room temperature. [104,105]

Additionally, allylation product **2.19** (**Table 2.1**) and TBS deprotected product **2.19** (**Scheme 2.6**) were found to be the same compound, indicating that the protecting group did not alter the stereochemical outcome of the reaction in this case, but did finally allow for an isolatable product compound.

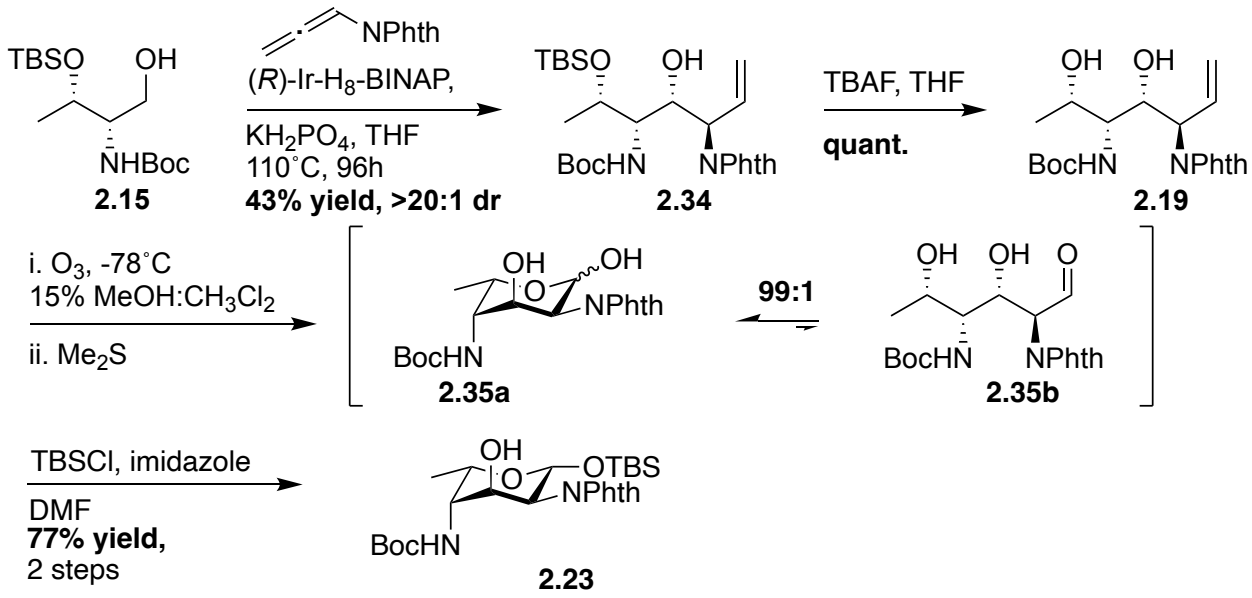


**Scheme 2.7.** Synthesis of protected DATDH from D-threoninol in 43% overall yield, with >20:1 dr.

## 2.3.7. Scope Expansion

Having established a route to **2.23**, we next turned our attention to the construction of other isomers. To this end, the allylation chemistry was applied to threoninols **2.13** and **2.14** under match-pair conditions (**Schemes 2.8 – 2.10**). Yields for each allylation product ranged from 48-56%, with a > 20:1 diastereomeric ratio in each case. Some of these yields were further improved upon scale-up, which is illustrated in Chapter 4 of this thesis (*vide infra*). The presence of rotamers in both $^{1}H$ and $^{13}C$ NMR was observed, in each case.[104,105] This confirmation via NOE experimentation also reaffirmed the purity and

diastereoselectivity of each allylation product. The stereochemical relationship of every 1,3-diol was again confirmed using the Rychnovsky analysis (**Scheme 2.11**). [99] For compounds **2.17** and **2.18**, an alternative acetonide protection procedure[106] was utilized due to a lack in reactivity of the *anti*-1,3-diols under standard conditions.[100] These harsher conditions resulted in loss of the Boc amine protection and led to formation of compounds **2.43** and **2.44**. Luckily, this did not affect the success Rychnovsky analysis, but did require exploration of an additional chromatographic separation strategy for the newly characterized amino compounds.

With clean allylation intermediates **2.36, 2.38,** and **2.40** in hand, facile TBS deprotection under standard conditions yielded the free 1,3-diols **2.16, 2.17,** and **2.18** in quantitative yield. [104,105] Subsequently, ozonolysis was performed on all substrates. Similar to **2.34**, the L-threoninol allylation product **2.36** successfully underwent oxidative cleavage and spontaneous *in situ* cyclization via ozonolysis.[71] Interestingly, the D-*allo* and L-*allo*threoninol allylation products **2.17** and **2.18** underwent decomposition upon exposure to ozone. As an alternative, **2.17** and **2.18** were subject to oxidative cleavage via catalytic $OsO_4$ paired with $NaIO_4$.[107,108]

Subsequently, the hemiacetals of interest (**2.37**, **2.39**, and **2.41**) were TBS protected at the anomeric position to facilitate the stereochemical assignment at the C2 position (**Schemes 2.8 – 2.10**); This could be carried out with the knowledge that TBS protection at the anomeric position strongly favors an equatorial orientation.[109] In all cases, products **2.20**, **2.21**, **2.22**, and **2.23** were obtained exclusively as the β-anomer, as evidenced by J-values > 8.0 Hz at the anomeric position. This analysis also allowed us to establish that the C2 amine substituent was in an equatorial configuration. Notably,

an *anti*-configuration between the C3 and C4 stereocenters was simultaneously established for the D- and L- threoninol products **2.20** and **2.23**, while a *syn*-configuration was established about these positions for the L-*allo* and D-*allo*threoninol products **2.21** and **2.22**. For DATDH **2.21** and **2.22**, high temperature V-T NMR experimentation was conducted due to the presence of rotamers. Overall, this procedure resulted in a highly diastereoselective synthesis of four, protected DATDH products ranging from 22-33% overall yield from their corresponding threoninol starting material. Yields of these total syntheses were further improved upon scale up in Chapter 4 of this thesis (*vide infra*).

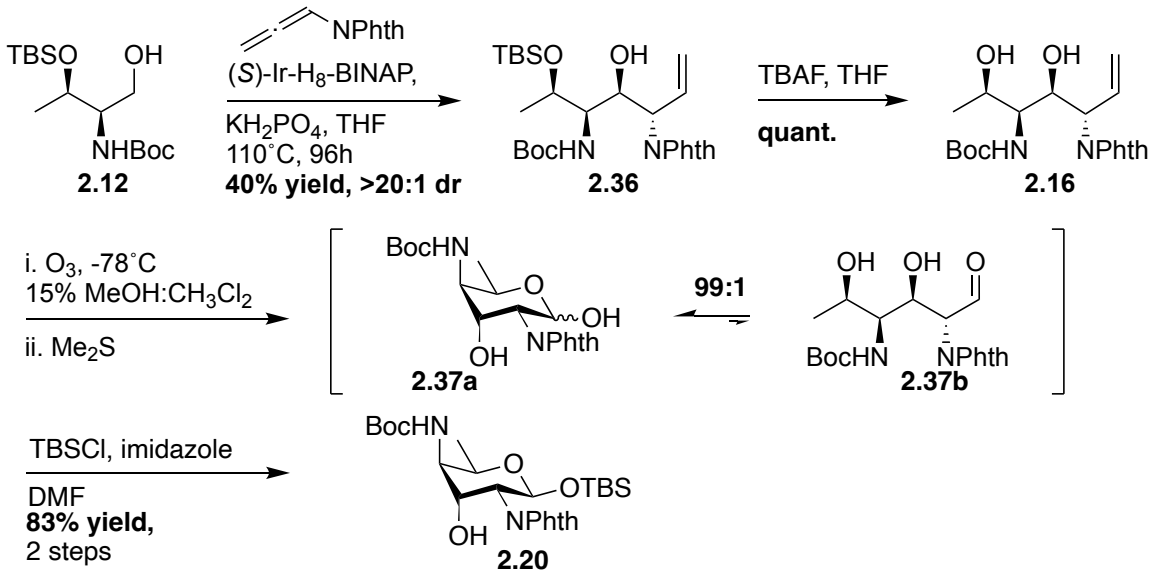


**Scheme 2.8.** Synthesis of protected DATDH from L-threoninol in 33% overall yield, with >20:1 dr.

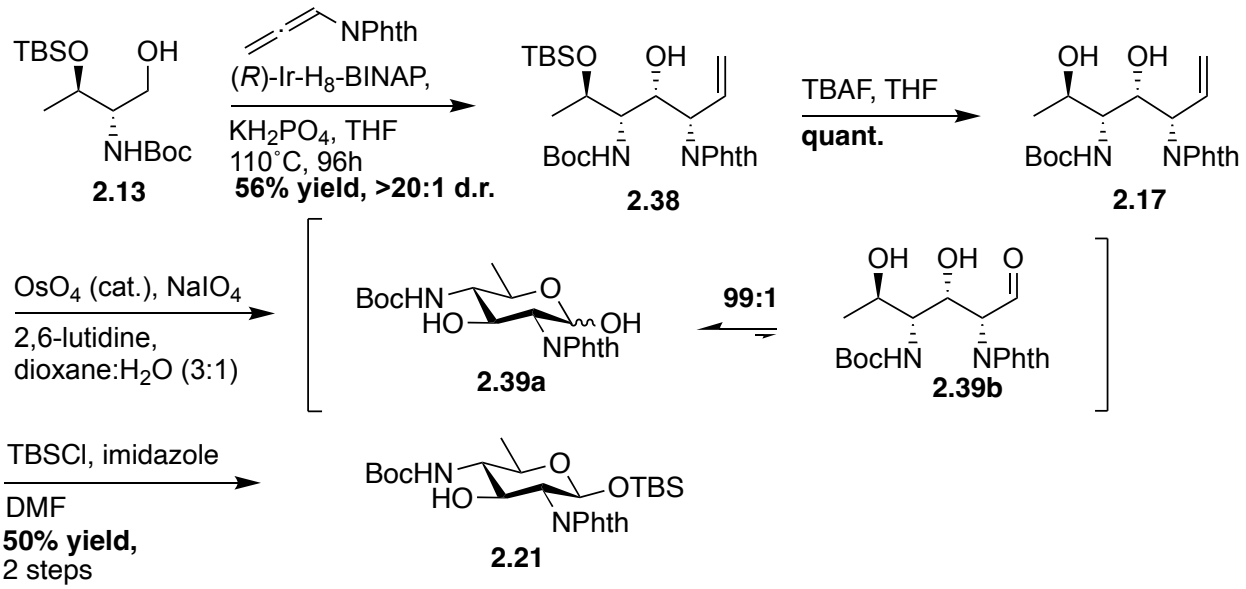


**Scheme 2.9.** Synthesis of protected DATDH from D-*allo*threoninol in 28% overall yield, with >20:1 dr.

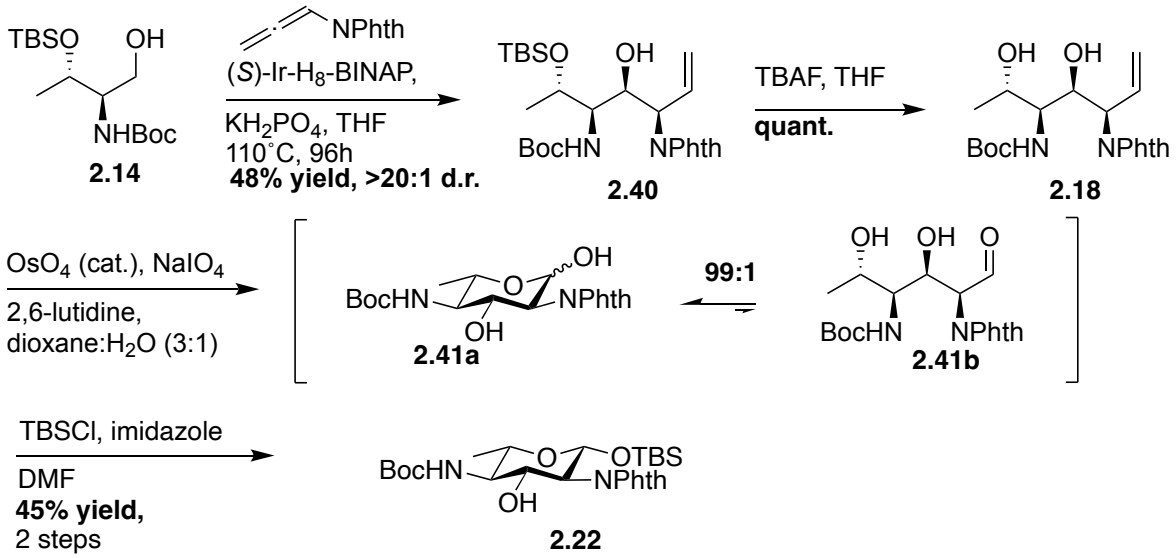


**Scheme 2.10.** Synthesis of protected DATDH from L-*allo*threoninol in 22% overall yield, with >20:1 dr.

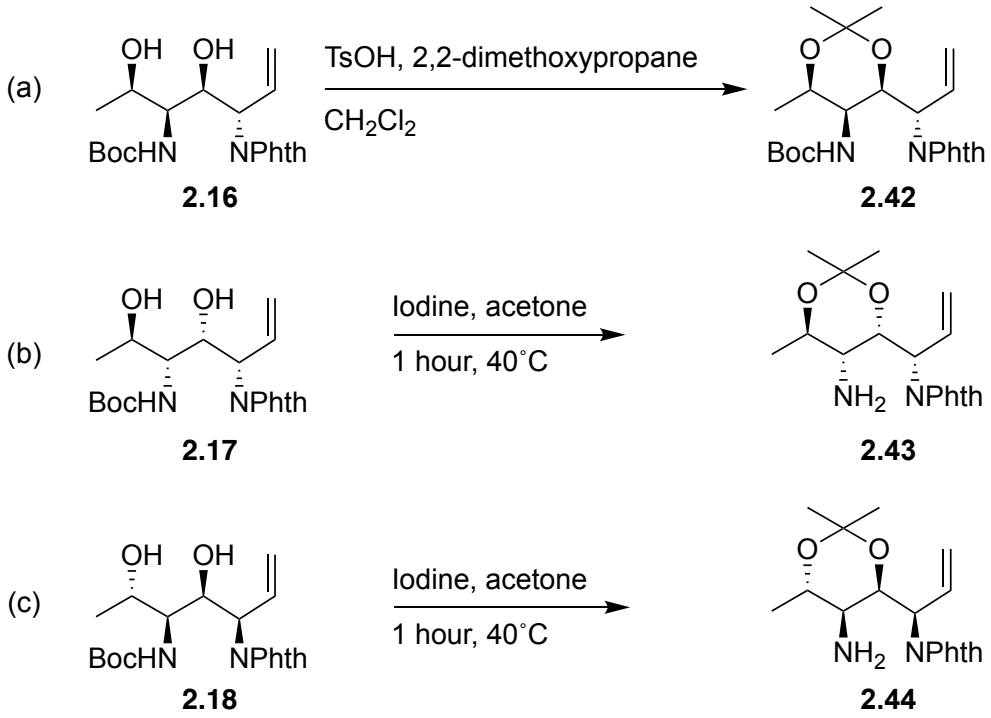


**Scheme 2.11.** Acetonide protection of 1,3-diols for Rychnovsky analysis.

## 2.4. Conclusions

In summary, we developed a highly efficient and versatile route for the synthesis of unusual 2,4-diamino-2,4,6-trideoxyhexoses (DATDH) that is both flexible and highly diastereoselective. This synthetic strategy represents, to the best of our knowledge, the first example which applies Krische allylation chemistry to encumbered $\alpha$-amino alcohols, enabling the establishment of two chiral centers in a single C-C coupling step. The efficiency of this approach permits the construction of DATDHs in seven or fewer steps with good yields, which is a substantial improvement over previous methodology. Moreover, the versatility of this approach enables the generation of two pairs of enantiomers, some of which are not currently accessible from commercial sugars. This flexibility provides access to a range of DATDH derivatives that may have important

biological applications, particularly in the development of carbohydrate-based therapeutics and glycoconjugate vaccines.

## 2.5. Materials and Experimental Methods

### 2.5.1. General Experimental Procedures

Unless otherwise stated, all reactions were carried out under an argon in flame dried reaction vessels. $CH_2Cl_2$, THF, and 1,4-dioxane were rendered anhydrous through a commercial solvent purification system (Inert). All other solvents were dried over activated molecular sieves prior to use. All other chemicals were purchased at the highest possible quality and used as received.

Flash column chromatography was performed on 230−400 mesh silica gel. Analytical and preparative thin layer chromatography was carried out on silica gel 60 F-254 plates. Products were visualized with UV light or by staining with potassium permanganate, 5% aqueous sulfuric acid, ninhydrin, or peroxidase stain, followed by heating.

Resealable pressure tubes (Cat. # 50-974-633) were purchased through Fisher Scientific and oven dried, flame dried in vacuo with septa and needle, and subsequently cooled under a stream of argon prior to use. PTFE pressure tube caps (Cat. # 5846-44) and Chemraz O-rings (Cat. # NC9194340) were purchased through Ace Glass and dried in a desiccator prior to use. Ozone generator (BMT 803N) ozone analyzer (BMT 965ST) were purchased through OSTI. Flow meter to measure gas flow rate for ozonolysis was purchased through Cole-Parmer (Cat. # 32005-04).

## 2.5.2. Spectroscopy, Spectrometry, and Data Collection

NMR spectra were recorded on a Bruker NMR spectrometer at 500 MHz for $^{1}H$ NMR and 125 MHz for $^{13}C$ NMR. Structural assignments were made with additional information from gCOSY and gHSQC experiments. For $CDCl_3$ solvent, chemical shifts are reported in ppm relative to TMS (for $^{1}H$ NMR in $CDCl_3$) or $CDCl_3$ (for $^{13}C$ NMR in $CDCl_3$). For $C_6D_6$ solvent, chemical shifts are reported in ppm relative to $C_6D_6$ (for $^{1}H$ and $^{13}C$ NMR). For $^{1}H$ NMR spectra, data are reported as follows: δ shift, multiplicity (s = singlet, m = multiplet, t = triplet, d = doublet, q = quartet, qd, quartet of doublets, dd = doublet of doublets, ddd = doublet of doublet of doublets), coupling constants are reported in Hz. To prove the existence of rotamers, 1-D NOE experiments were conducted according to procedure reported by Ley, *et al* on a 500 MHz Bruker NMR.[104] Variable temperature (VT) NMR experimentation was carried out on a 500 MHz Varian at Brandeis University. High-resolution mass spectra (HRMS) were obtained on an Agilent 6230 TOF mass spectrometer in the positive ion mode. Optical rotations were measured at 589 nm in a 10 cm cell at 25-23 °C.

## 2.5.3. Experimental Procedures and Spectral Data

***General Procedure A***

To an oven dried and flame dried pressure tube with a magnetic stir bar under argon atmosphere, phthalimido allene (150 mol%), (*S*) / (*R*)-Ir-$H_8$-BINAP (20 mol%), and $KH_2PO_4$ (100 mol%) were added. Threoninol substrate (100 mol%) was weighed out in a vial, dissolved in THF, sonicated (~30 seconds) and added to the mixture. The pressure vessel was flushed with argon and sealed with a PTFE lined cap. The mixture was allowed to stir for 96 hours at 110°C in an oil bath. After 4 days, the mixture was cooled to room temperature, transferred to a round bottom flask, and the solvent removed *in vacuo*. The residual solid was dissolved in a minimal amount of $CH_2Cl_2$ and loaded onto a column to be purified by silica gel chromatography using 20% EtOAc:Hex isocratic to furnish the corresponding product as a clear oil/white solid, which bubbled upon initial exposure to high vacuum.

***General Procedure B***

Allylation product was added to a flame dried flask and dissolved in THF to a concentration of 0.02 M. TBAF (1M in THF) (100 mol%) was added dropwise over the course of 5 minutes to the mixture (reaction turns yellow after addition) and the reaction was allowed to stir at room temperature overnight. The mixture was quenched with sat. $NH_4Cl$ (aq.). The mixture was then diluted with EtOAc and $H_2O$ and the aqueous layer extracted with EtOAc (5x). The pooled organic layers were washed with sat. $NaHCO_3$ (1x), and brine (2x), dried over $Na_2SO_4$, filtered, and concentrated *in vacuo*. The residual oil was purified by silica gel chromatography using 60% EtOAc:Hex to furnish the 1,3-diol compound as a clear oil in quantitative yield.

**Synthesis of (*R*) / (*S*)-Ir-$H_8$-BINAP**

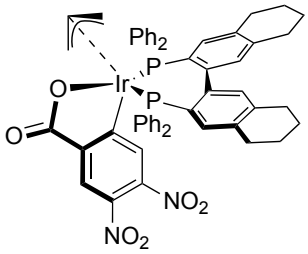


(*R*)-Ir-$H_8$-BINAP

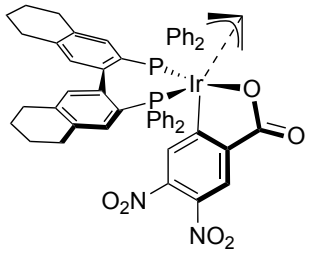


(*S*)-Ir-$H_8$-BINAP

The synthesis of (*R*) / (*S*)-Ir-$H_8$-BINAP was prepared according to literature procedure. Spectroscopic data was in agreement with previously reported data.[90]

**Synthesis of phthalimido allene**

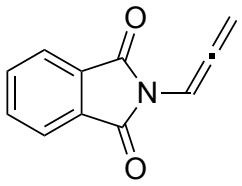

The synthesis of phthalimido allene was prepared according to literature procedure. Spectroscopic data was in agreement with previously reported data.[90]

**Attempted allylation of oxazolidine (2.33)**

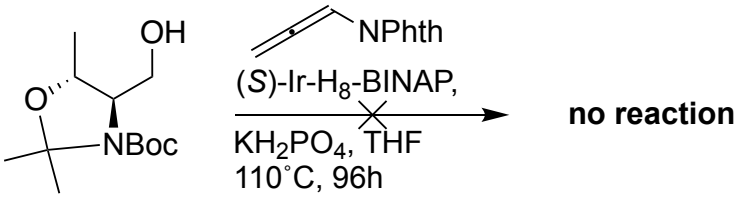


The synthesis of the oxazolidine **2.33** was prepared according to literature procedure. Spectroscopic data was in agreement with previously reported data.[103] The allylation reaction (according to *General Procedure A*) did not proceed.

**Synthesis of 2.15**

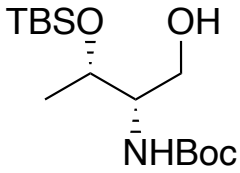


MeOH (16.0 mL) was added to a flame dried flask and cooled to 0°C. $SOCl_2$ (1.22 mL, 0.0168 mol, 100 mol%) was then added dropwise over the course of 5 minutes. The resulting mixture was stirred until the temperature re-cooled to 0°C. D-threonine (2.00 g, 0.0168 mol, 100 mol%) was then added and the reaction was heated to reflux in an oil bath. After 1 hour, the mixture was cooled to room temperature and concentrated *in vacuo*. After evaporation, a mixture of $SOCl_2$ (1.22 mL, 0.0168 mol, 100 mol%) and MeOH (16.0 mL) prepared in the same way as described above was added to the residual yellow oil and the reaction was returned to room temperature. The reaction was then heated to reflux in an oil bath. After 1 hour, the reaction was cooled to room temperature and the solvent removed *in vacuo* to afford D-threonine methyl ester hydrochloride as a yellow oil, which was carried on without further purification.

The crude D-threonine methyl ester hydrochloride mixture was dissolved 1,4-dioxane (8.40 mL) and $H_2O$ (8.40 mL). $(Boc)_2O$ was gently warmed in a water bath slightly above room temperature to be liquified. $NaHCO_3$ (10.4 g, 0.124 mol, 740 mol%) and $(Boc)_2O$ (4.59 mL, 0.0202 mol, 120 mol%) were sequentially added and the mixture was allowed to stir at room temperature for 3 hours. The solution was then partitioned between EtOAc and $H_2O$, and the aqueous layer extracted with EtOAc (3x). The pooled organic layers were washed with 1M HCl(aq.) (1x), sat. $NaHCO_3$(aq.) (1x), and brine (2x), dried over $Na_2SO_4$, filtered, and concentrated *in vacuo* to afford *N*-Boc-D-threonine methyl ester as a colorless oil, which was carried on without further purification.

Substrate was added to a flame dried flask, dissolved in $CH_2Cl_2$ (55 mL), and cooled to 0°C. To this solution, 2,6-lutidine (5.87 mL, 0.0504 mol, 300 mol%) and freshly distilled TBSOTf (4.63 mL, 0.0202 mol, 120 mol%) were added dropwise over the course of 2 minutes. The reaction was allowed to warm to room temperature over 16 hours then was poured into 1M HCl (aq.). The aqueous layer was extracted with $CH_2Cl_2$ (3x), and the pooled organic layers washed with sat. $NaHCO_3$ (aq.) (2x) and brine (1x), dried over $Na_2SO_4$, filtered, and concentrated *in vacuo*. The residual oil was purified by silica gel chromatography using 30% EtOAc:Hex to furnish TBS-protected compound as a colorless oil, which was dried overnight and then carried on to the next step.

Substrate was added to a flame dried flask, dissolved in EtOH (31.0 mL) and cooled to 0°C. $LiBH_4$ (1.02 g, 0.0470 mol, 280 mol%) was added *slowly* and the resulting mixture was removed from the ice bath and gently warmed to room temperature for 1 hour (or until reaction finished vigorous bubbling). Multiple venting needles were placed in septa in anticipation of excess generation of $H_2(g)$. The reaction was then quenched with $H_2O$ and the aqueous layer extracted with EtOAc (3x). The pooled organic layers were dried over $Na_2SO_4$, filtered, and concentrated *in vacuo*. The residual oil was purified by silica gel chromatography using 25% EtOAc:Hex to furnish *N*-Boc-D-threoninol **2.15** as a colorless oil (4.34 g, 0.0136 mol, 81% yield over three steps).

**$^1$H NMR** (500 MHz, $CDCl_3$) δ 4.94 (bd, *J* = 8.6 Hz, 1H), 4.09 (dq, *J* = 6.8, 3.4 Hz, 1H), 3.70 – 3.50 (m, 3H), 2.59 (bs, 1H), 1.46 (s, 9H), 1.18 (d, *J* = 6.3 Hz, 3H), 0.89 (s, 9H), 0.08 (s, 6H)

**$^{13}$C NMR** (126 MHz, $CDCl_3$) δ 156.8, 79.5, 67.3, 63.6, 57.5, 28.4, 25.9, 20.9, 18.0, -4.2, -5.0

HRMS (ESI) *m/z*: $[M + Na]^+$ calcd for $C_{15}H_{33}NO_4Si$+Na: 342.2077; found: 342.2078.

**Synthesis of 2.12**

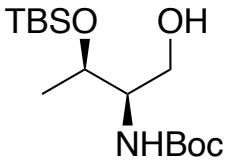


MeOH (16.0 mL) was added to a flame dried flask and cooled to 0°C. $SOCl_2$ (1.22 mL, 0.0168 mol, 100 mol%) was then added dropwise over the course of 5 minutes. The resulting mixture was stirred until the temperature re-cooled to 0°C. L-threonine (2.00 g, 0.0168 mol, 100 mol%) was then added and the reaction was heated to reflux in an oil bath. After 1 hour, the mixture was cooled to room temperature and concentrated *in vacuo*. After evaporation, a mixture of $SOCl_2$ (1.22 mL, 0.0168 mol, 100 mol%) and MeOH (16.0 mL) prepared in the same way described above was added to the residual yellow oil and the reaction returned to room temperature. The reaction was then heated to reflux in an oil bath. After 1 hour, the reaction was cooled to room temperature and the solvent removed *in vacuo* to afford L-threonine methyl ester hydrochloride as a yellow oil, which was carried on without further purification.

The crude L-threonine methyl ester hydrochloride was dissolved 1,4-dioxane (8.40 mL) and $H_2O$ (8.40 mL). $(Boc)_2O$ was gently warmed in a water bath slightly above room temperature to be liquified. $NaHCO_3$ (10.4 g, 0.124 mol, 740 mol%) and $(Boc)_2O$ (4.59 mL, 0.0202 mol, 120 mol%) were sequentially added and the mixture was allowed to stir at room temperature for 3 hours. The solution was then partitioned between EtOAc and $H_2O$, and the aqueous layer extracted with EtOAc (3x). The pooled organic layers were washed with 1M HCl(aq.) (1x), sat. $NaHCO_3$(aq.) (1x), and brine (2x), dried over $Na_2SO_4$, filtered, and concentrated *in vacuo* to afford *N*-Boc-L-threonine methyl ester as a colorless oil, which was carried on without further purification.

Substrate was added to a flame dried flask, dissolved in $CH_2CL_2$ (55 mL), and cooled to 0°C. To this solution, 2,6-lutidine (5.87 mL, 0.0504 mol, 300 mol%) and freshly distilled TBSOTf (4.63 mL, 0.0202 mol, 120 mol%) were added dropwise over the course of 2 minutes. The reaction was allowed to warm to room temperature over 16 hours then was poured into 1M HCl (aq.). The aqueous layer was extracted with $CH_2CL_2$ (3x), and the pooled organic layers washed with sat. $NaHCO_3$ (aq.) (2x) and brine (1x), dried over $Na_2SO_4$, filtered, and concentrated *in vacuo*. The residual oil was purified by silica gel chromatography using 30% EtOAc:Hex to furnish TBS-protected compound as a colorless oil, which was dried overnight and then carried on to the next step.

Substrate was added to a flame dried flask, dissolved in EtOH (31.0 mL), and cooled to 0°C. $LiBH_4$ (1.02 g, 0.0470 mol, 280 mol%) was added *slowly* and the resulting solution was stirred at 0°C for 1 hour (or until reaction finished vigorous bubbling). Multiple venting needles were placed in septa in anticipation of excess generation of $H_2(g)$. The reaction was then quenched with $H_2O$ and the aqueous layer extracted with EtOAc (3x). The pooled organic layers were dried over $Na_2SO_4$, filtered, and concentrated *in vacuo*. The residual oil was purified by silica gel chromatography using 25% EtOAc:Hex to furnish *N*-Boc-L-threoninol **2.12** as a colorless oil (4.13g, 0.0129 mol, 77% yield over three steps).

**$^1$H NMR** (500 MHz, $CDCl_3$) δ 4.93 (bd, *J* = 8.6 Hz, 1H), 4.07 (dq, *J* = 6.5, 3.9 Hz, 1H), 3.69 – 3.50 (m, 3H), 2.49 – 2.40 (bd, 1H), 1.45 (s, 9H), 1.17 (d, *J* = 6.2 Hz, 3H), 0.89 (s, 9H), 0.09 (s, 6H)

**$^{13}$C NMR** (126 MHz, $CDCl_3$) δ 157.0, 79.7, 67.7, 64.2, 57.5, 28.5, 25.9, 21.0, 18.1, -4.1, -4.9

HRMS (ESI) *m/z*: $[M + Na]^+$ calcd for $C_{15}H_{33}NO_4Si$+Na: 342.2077; found: 342.2076

**Synthesis of 2.13**

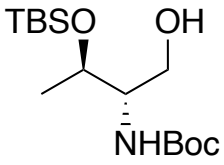


*N*-Boc-D-*allo*threonine (1.84 g, 0.00840 mol, 100 mol%) was added to a flame dried flask and dissolved in DMF (10.0 mL). $K_2CO_3$ (1.74 g, 0.0126 mol, 150 mol%) and MeI (1.57 mL, 0.0252 mol, 300 mol%) were then added to the mixture. The reaction was allowed to stir at room temperature for 4 hours, then the aqueous layer extracted with EtOAc (10x). The pooled organic layers were washed with sat. $NaHCO_3$ (aq) (2x), LiCl (1M) (2x), and bring (2x), dried over $Na_2SO_4$, filtered, and concentrated *in vacuo* to afford the esterified compound as an orange oil, which was carried on without further purification.

The crude ester compound (1.96 g, 0.00840 mol, 100 mol%) was added to a flame dried flask and dissolved in DMF (13.0 mL). Imidazole (1.14 g, 0.0168 mol, 200 mol%) was then added to the mixture, cooled to 0°C, and TBSCl (2.53 g, 0.0168 mol, 200 mol%) added. The reaction was allowed to warm to room temperature over 72 hours, then the aqueous layer extracted with EtOAc (5x). The pooled organic layers were washed with aq. LiCl (1M) (2x) and brine (2x), dried over $Na_2SO_4$, filtered, and concentrated *in vacuo* to afford the TBS-protected compound as a clear-yellow liquid, which was carried on without further purification.

The crude compound was added to a flame dried flask, dissolved in EtOH (8.00 mL), and cooled to 0°C. $NaBH_4$ (1.59 g, 0.0420 mol, 500 mol%) was added to the cooled reaction mixture. The reaction was then warmed in an oil bath to 60°C and allowed to stir for 12 hours, then cooled to 0°C and quenched slowly with sat. $NH_4Cl$ (aq). The aqueous

layer was then extracted with EtOAc (3x) and the pooled organic layers washed with aq. LiCl (1M) (2x) and brine (2x), dried over $Na_2SO_4$, filtered, and concentrated *in vacuo*. The residual oil was purified by silica gel chromatography using 20% EtOAc:Hex to furnish *N*-Boc-D-*allo*threoninol **2.13** as a colorless oil (2.30 g, 0.00720 mol, 86% yield over two steps).

**$^1$H NMR** (500 MHz, $CDCl_3$) δ 5.38 (d, *J* = 5.9 Hz, 1H), 4.21 – 4.15 (m, 1H), 4.13 – 4.07 (m, 1H), 3.64 – 3.57 (m, 1H), 3.39 (dt, *J* = 7.9, 3.8 Hz, 1H), 3.10 (d, *J* = 10.1 Hz, 1H), 1.45 (s, 9H), 1.23 (s, 3H), 0.89 (s, 9H), 0.08 (s, 6H)

**$^{13}$C NMR** (126 MHz, $CDCl_3$) δ 155.9, 79.6, 71.9, 62.1, 55.4, 28.6, 25.9, 20.8, 18.0, -4.6, -5.0

HRMS (ESI) *m/z*: $[M + Na]^+$ calcd for $C_{15}H_{33}NO_4Si$+Na: 342.2077; found: 342.2079

**Synthesis of 2.14**

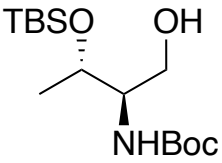


*N*-Boc-L-*allo*threonine (0.460 g, 0.00210 mol, 100 mol%) was added to a flame dried flask and dissolved in DMF (2.50 mL). $K_2CO_3$ (0.435 g, 0.00315 mol, 150 mol%) and MeI (0.392 mL, 0.00630 mol, 300 mol%) were then added to the mixture. The reaction was allowed to stir at room temperature for 4 hours, then the aqueous layer extracted with EtOAc (10x). The pooled organic layers were washed with sat. $NaHCO_3$ (aq) (2x), LiCl (1M) (2x), and bring (2x), dried over $Na_2SO_4$, filtered, and concentrated *in vacuo* to afford the esterified compound as an orange oil, which was carried on without further purification.

The crude ester compound (0.490 g, 0.00210 mol, 100 mol%) was added to a flame dried flask and dissolved in DMF (4.00 mL). Imidazole (0.286 g, 0.00420 mol, 200 mol%) was then added to the mixture, cooled to 0°C, and TBSCl (0.633 g, 0.00420 mol, 200 mol%) added. The reaction was allowed to warm to room temperature over 72 hours, then the aqueous layer extracted with EtOAc (5x). The pooled organic layers were washed with aq. LiCl (1M) (2x), and brine (2x), dried over $Na_2SO_4$, filtered, and concentrated *in vacuo* to afford the TBS-protected compound as a clear-yellow liquid, which was carried on without further purification.

The crude compound was added to a flame dried flask, dissolved in EtOH (2.00 mL), and cooled to 0°C. $NaBH_4$ (0.397 g, 0.0105 mol, 500 mol%) was added to the cooled mixture. The reaction was then warmed in an oil bath to 60°C and the reaction was allowed to stir for 12 hours, then cooled to 0°C and quenched slowly with sat. $NH_4Cl$ (aq).

The aqueous layer was extracted with EtOAc (3x) and the pooled organic layers washed with aq. LiCl (1M) (2x) and brine (2x), dried over $Na_2SO_4$, filtered, and concentrated *in vacuo*. The residual oil was purified by silica gel chromatography using 20% EtOAc:Hex to furnish *N*-Boc-L-*allo*threoninol **2.14** as a colorless oil (0.536 g, 0.00168 mol, 80% yield over two steps).

**$^1$H NMR** (500 MHz, $CDCl_3$) δ 5.38 (d, *J* = 8.2 Hz, 1H), 4.22 – 4.16 (m, 1H), 4.14 – 4.08 (m, 1H), 3.61 (td, *J* = 10.8, 3.4 Hz, 1H), 3.42 – 3.37 (m, 1H), 3.09 (d, *J* = 10.0 Hz, 1H), 1.45 (s, 9H), 1.24 (d, *J* = 6.5 Hz, 3H), 0.89 (s, 9H), 0.09 (s, 6H)

**$^{13}$C NMR** (126 MHz, $CDCl_3$) δ 155.9, 79.6, 71.9, 62.1, 55.4, 28.6, 25.9, 20.8, 18.0, -4.6, -5.0

HRMS (ESI) *m/z*: $[M + Na]^+$ calcd for $C_{15}H_{33}NO_4Si$+Na: 342.2077; found: 342.2079

**Synthesis of 2.27**

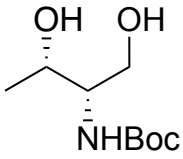


D-threonine (1.00 g, 0.00840 mol, 100 mol%) was added to a flame dried flask and dissolved in aq. NaOH (1M) (10.0 mL). $(Boc)_2O$ (2.31 mL, 0.0101 mol, 120 mol%) was gently warmed in a water bath to a liquid, added to a separate flame dried flask, dissolved in 1,4-dioxane (10.0 mL), and cooled to 0°C. The solution was transferred to the substrate/NaOH (1M) solution, allowed to stir at room temperature for 24 hours, then cooled to 0°C and quenched with aq. $KHSO_4$ (1M). The aqueous layer was extracted with EtOAc (6x), dried over $Na_2SO_4$, filtered, concentrated *in vacuo*, dried through azeotropic distillation with toluene (3x), and concentrated again *in vacuo* to afford Boc-protected product as a clear oil, which was carried on without further purification.

The crude compound (1.84 g, 0.00840 mol, 100 mol%) was added to a flame dried flask, suspended in DMF (18.0 mL), $K_2CO_3$ (1.74 g, 0.0126 mol, 150 mol%) and MeI (1.57 mL, 0.0252 mol, 300 mol%) added, and the reaction was allowed to stir at room temperature for 1 hour. The aqueous layer was then extracted with EtOAc (10x) and the pooled organic layers washed with sat. $NaHCO_3$ (aq.) (3x), aq. LiCl (1M) (2x) and brine (2x), dried over $Na_2SO_4$, filtered, and concentrated *in vacuo* to afford ester compound as a clear-yellow oil, which was carried on without further purification.

The crude compound (1.96 g, 0.00840 mol, 100 mol%) was added to a flame dried flask, dissolved in EtOH (14.3 mL), and cooled to 0°C. $NaBH_4$ (0.636 g, 0.0168 mol, 200 mol%) was added to the cooled mixture, allowed to stir for 1 hour, then allowed to warm to room temperature for 2 hours. The reaction was then cooled down to 0°C, quenched

*slowly* with sat. $NH_4Cl$ (aq). and the aqueous layer extracted with EtOAc (5x). The pooled organic layers were washed with aq. LiCl (1M) (2x) and brine (2x), dried over $Na_2SO_4$, filtered, and concentrated *in vacuo.* The residual oil was purified by silica gel chromatography using 90% EtOAc:Hex to furnish compound **2.27** as a white amorphous solid (1.38 g, 0.00672 mol, 80% yield over three steps).

**$^1$H NMR** (500 MHz, $CDCl_3$) δ 5.27 (d, *J* = 8.7 Hz, 1H), 4.14 (d, *J* = 6.9 Hz, 1H), 3.81 (s, 2H), 3.52 (s, 1H), 2.85 (s, 2H), 1.46 (s, 9H), 1.22 (d, *J* = 6.4 Hz, 3H)

**$^{13}$C NMR** (126 MHz, $CDCl_3$) δ 156.8, 79.9, 69.2, 65.3, 55.8, 28.5, 20.6

HRMS (ESI) *m/z*: $[M + Na]^+$ calcd for $C_9H_{19}NO_4$+Na: 228.1212; found: 228.1213

**Synthesis of 2.19 / 2.28**

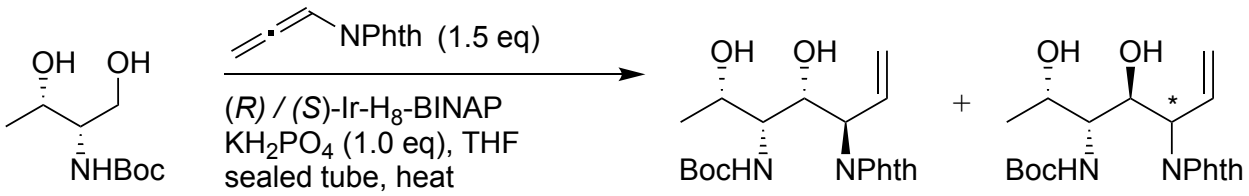


Allylation product **2.19 / 2.28** were prepared according to *General Procedure A*: Starting material **2.27** (41.0 mg, 0.200 mmol, 100 mol%), phthalimido allene (55.0 mg, 0.300 mmol, 150 mol%), chiral Ir-$H_8$-BINAP (42.8 mg, 0.0400 mmol, 20 mol%), $KH_2PO_4$ (27.2 mg, 0.200 mmol, 100 mol%) and dissolved in THF (1.0 mL). Allylation product **2.19** (0.0453 g, 0.116 mmol, 58% yield) **/ 2.28** (0.0289 g, 0.0740 mmol, 37% yield) was afforded as a brown solid after silica gel chromatography using 40% EtOAc:Tol.[1] The resulting crude product was carried on directly to acetonide protection to establish the stereochemical relationship of the 1,3 diols. (See **S2.21 / S2.22**).

[1] Yield based on percent conversion

**Synthesis of 2.34**

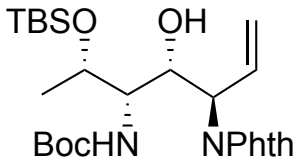


According to *General Procedure A*, allylation product **2.34** was prepared from compound **2.15** (150. mg, 0.469 mmol, 100 mol%), phthalimido allene (129. mg, 0.704 mmol, 150 mol%), (*R*)-Ir-$H_8$-BINAP (101. mg, 0.0938 mmol, 20 mol%), $KH_2PO_4$ (65.2 mg, 0.469 mmol, 100 mol%) and dissolved in THF (2.30 mL). Allylation product **2.34** was afforded as a clear-white amorphous solid (0.101 g, 0.200 mmol, 43% yield, >20:1 diastereomeric ratio), which was present as a mixture of rotamers in the $^1$H and $^{13}$C NMR spectrum.

**$^1$H NMR** (500 MHz, $CDCl_3$) δ 7.80 (dd, *J* = 5.5, 3.1 Hz, 2H), 7.69 (dd, *J* = 5.5, 3.0 Hz, 2H), 6.25 (ddd, *J* = 16.5, 10.4, 5.9 Hz, 1H), 5.29 – 5.23 (m, 2H), 5.10 (d, *J* = 10.2 Hz, 1H), 4.77 – 4.66 (m, 2H), 4.19 – 4.12 (m, 1H), 3.43 (dd, *J* = 10.5, 4.0 Hz, 1H), 1.43 (s, 9H), 1.12 (d, *J* = 6.3 Hz, 3H), 0.89 (s, 9H), 0.13 (s, 3H), 0.10 (s, 3H)

**$^{13}$C NMR** (126 MHz, $CDCl_3$) δ 168.0, 156.2, 134.1, 133.4, 132.2, 123.4, 118.7, 79.6, 72.9, 72.5, 55.3, 54.6, 28.5, 26.0, 20.7, -3.7, -4.6

HRMS (ESI) *m/z*: $[M + Na]^+$ calcd for $C_{26}H_{40}N_2O_6Si$+Na: 527.2549; found: 527.2580

$[\alpha]^{23}_D$: +23.3 ($CH_2Cl_2$, c = .0107 g/mL)

**Synthesis of 2.36**

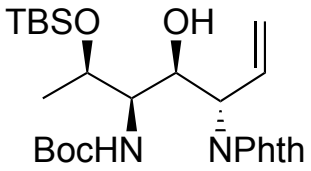


According to *General Procedure A*, allylation product **2.36** was prepared from compound **2.12** (150. mg, 0.469 mmol, 100 mol%), phthalimido allene (129. mg, 0.704 mmol, 150 mol%), (*S*)-Ir-$H_8$-BINAP (101. mg, 0.0938 mmol, 20 mol%), $KH_2PO_4$ (65.2 mg, 0.469 mmol, 100 mol%) and dissolved in THF (2.30 mL). Allylation product **2.36** was afforded as a clear-white amorphous solid (0.095 g, 0.188 mmol, 40% yield, >20:1 diastereomeric ratio), which was present as a mixture of rotamers in the $^1$H and $^{13}$C NMR spectrum.

**$^1$H NMR** (500 MHz, $CDCl_3$) δ 7.80 (dd, *J* = 5.4, 3.0 Hz, 2H), 7.70 (dd, *J* = 5.5, 3.0 Hz, 2H), 6.25 (ddd, *J* = 16.6, 10.3, 6.0 Hz, 1H), 5.29 – 5.23 (m, 2H), 5.10 (d, *J* = 10.0 Hz, 1H), 4.76 – 4.70 (m, 2H), 4.18 – 4.13 (m, 1H), 3.43 (dd, *J* = 10.5, 4.1 Hz, 1H), 1.43 (s, 9H), 1.12 (d, *J* = 6.1 Hz, 3H), 0.89 (s, 9H), 0.13 (s, 3H), 0.10 (s, 3H)

**$^{13}$C NMR** (126 MHz, $CDCl_3$) δ 168.0, 156.2, 134.1, 133.4, 132.2, 123.5, 118.7, 79.6, 72.9, 72.5, 55.3, 54.5, 28.5, 26.0, 20.7, -3.7, -4.6

HRMS (ESI) *m/z*: $[M + Na]^+$ calcd for $C_{26}H_{40}N_2O_6Si$+Na: 527.2549; found: 527.2560

$[\alpha]^{23}_D$: -20.7 ($CH_2Cl_2$, c =.0104 g/mL)

**Synthesis of 2.38**

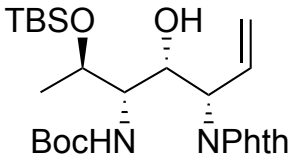


According to *General Procedure A*, allylation product **2.38** was prepared from compound **2.13** (150. mg, 0.469 mmol, 100 mol%), phthalimido allene (129. mg, 0.704 mmol, 150 mol%), (*R*)-Ir-$H_8$-BINAP (101. mg, 0.0938 mmol, 20 mol%), $KH_2PO_4$ (65.2 mg, 0.469 mmol, 100 mol%) and dissolved in THF (2.30 mL). Allylation product **2.38** was afforded as a clear-white amorphous solid (0.133 g, 0.263 mmol, 56% yield, >20:1 diastereomeric ratio), which was present as a mixture of rotamers in the $^1H$ and $^{13}C$ NMR spectrum.

**$^1H$ NMR** (500 MHz, $CDCl_3$) δ 7.78 (dd, *J* = 5.5, 3.0 Hz, 2H), 7.69 (dd, *J* = 5.5, 3.1 Hz, 2H), 6.26 (ddd, *J* = 17.3, 10.2, 7.3 Hz, 1H), 5.32 – 5.24 (m, 3H), 5.04 (d, *J* = 9.5 Hz, 1H), 4.76 – 4.71 (m, 1H), 4.05 (qd, *J* = 6.6, 2.9 Hz, 1H), 3.30 (dd, *J* = 9.6, 1.7 Hz, 1H), 1.40 (s, 9H), 1.24 (d, *J* = 6.4 Hz, 3H), 0.88 (s, 9H), 0.07 (s, 3H), 0.07 (s, 3H)

**$^{13}C$ NMR** (126 MHz, $CDCl_3$) δ 167.8, 155.3, 134.1, 133.5, 132.1, 123.4, 118.9, 79.6, 73.0, 68.8, 54.8, 53.4, 28.5, 25.9, 20.6, -4.6, -5.1

HRMS (ESI) *m/z*: $[M + Na]^+$ calcd for $C_{26}H_{40}N_2O_6Si$+Na: 527.2549; found: 527.2551

$[\alpha]^{23}_D$: +6.9 ($CH_2Cl_2$, c = .0105 g/mL)

**Synthesis of 2.40**

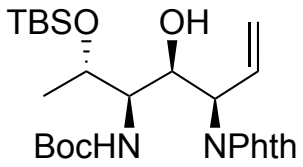


According to *General Procedure A*, allylation product **2.40** was prepared from compound **2.14** (150. mg, 0.469 mmol, 100 mol%), phthalimido allene (129. mg, 0.704 mmol, 150 mol%), (*S*)-Ir-$H_8$-BINAP (101. mg, 0.0938 mmol, 20 mol%), $KH_2PO_4$ (65.2 mg, 0.469 mmol, 100 mol%) and dissolved in THF (2.30 mL). Allylation product **2.40** was afforded as a clear-white amorphous solid (0.113 g, 0.223 mmol, 48% yield, >20:1 diastereomeric ratio), which was present as a mixture of rotamers in the $^1$H and $^{13}$C NMR spectrum.

**$^1$H NMR** (500 MHz, $CDCl_3$) δ 7.79 (dd, *J* = 5.5, 3.1 Hz, 2H), 7.70 (dd, *J* = 5.5, 3.0 Hz, 2H), 6.28 (ddd, *J* = 17.3, 10.3, 7.3 Hz, 1H), 5.33 – 5.26 (m, 3H), 5.05 (d, *J* = 9.5 Hz, 1H), 4.78 – 4.72 (m, 1H), 4.07 (qd, *J* = 6.5, 2.9 Hz, 1H), 3.32 (dd, *J* = 9.3, 1.4 Hz, 1H), 1.41 (s, 9H), 1.25 (d, *J* = 6.4 Hz, 3H), 0.90 (s, 9H), 0.08 (s, 3H), 0.07 (s, 3H)

**$^{13}$C NMR** (126 MHz, $CDCl_3$) δ 167.8, 155.3, 134.0, 133.5, 132.1, 123.4, 118.8, 79.5, 72.9, 68.8, 54.8, 53.4, 28.4, 25.9, 20.6, -4.7, -5.1

HRMS (ESI) *m/z*: $[M + Na]^+$ calcd for $C_{26}H_{40}N_2O_6Si$+Na: 527.2549; found: 527.2556

$[\alpha]^{23}_D$: -1.0 ($CH_2Cl_2$, c = .0107g/mL)

**Synthesis of 2.19**

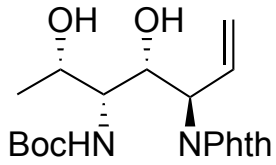


According to *General Procedure B*, the 1,3-diol compound **2.19** was prepared from compound **2.34** (75.4 mg, 0.149 mmol, 100 mol%), TBAF (1M in THF) (0.149 mL, 0.149 mmol, 100 mol%), and THF (10.0 mL). Product **2.34** was afforded as a white amorphous solid (58.0 mg, 0.149 mmol), in quantitative yield, which was present as a mixture of rotamers in the $^{1}H$ and $^{13}C$ NMR spectrum.

**$^{1}$H NMR** (500 MHz, $CDCl_3$) δ 7.80 (dd, *J* = 5.5, 3.1 Hz, 2H), 7.71 (dd, *J* = 5.5, 3.1 Hz, 2H), 6.21 (ddd, *J* = 17.5, 10.2, 7.6 Hz, 1H), 5.38 – 5.29 (m, 2H), 5.24 (d, *J* = 10.2 Hz, 1H), 4.80 – 4.68 (m, 2H), 4.15 – 4.09 (m, 1H), 3.55 (d, *J* = 10.2 Hz, 1H), 1.41 (s, 9H), 1.10 (d, *J* = 6.3 Hz, 3H)

**$^{13}$C NMR** (126 MHz, $CDCl_3$) δ 168.1, 156.5, 134.2, 132.6, 132.1, 123.5, 120.3, 79.7, 74.3, 71.2, 55.9, 53.7, 28.4, 20.1

HRMS (ESI) *m/z*: $[M + Na]^+$ calcd for $C_{20}H_{26}N_2O_6$+Na: 413.1684; found: 413.1686

$[\alpha]^{23}_D$: +26.9 ($CH_2Cl_2$, c = .0104 g/mL)

**Synthesis of 2.16**

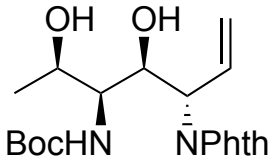


According to *General Procedure B*, the 1,3-diol compound **2.16** was prepared from compound **2.36** (50.0 mg, 0.099 mmol, 100 mol%), TBAF (1M in THF) (0.099 mL, 0.099 mmol, 100 mol%), and THF (6.70 mL). Product **2.16** was afforded as a white amorphous solid (38.7 mg, 0.099 mmol) in quantitative yield which was present as a mixture of rotamers in the $^{1}H$ and $^{13}C$ NMR spectrum.

**$^{1}H$ NMR** (500 MHz, $C_6D_6$) δ 7.52 (dd, *J* = 5.5, 3.0 Hz, 2H), 6.94 (dd, *J* = 5.4, 3.0 Hz, 2H), 6.31 (ddd, *J* = 17.3, 10.3, 7.1 Hz, 1H), 5.45 (d, *J* = 10.2 Hz, 1H), 5.22 (d, *J* = 17.2 Hz, 1H), 5.08 (d, *J* = 10.3 Hz, 1H), 5.05 – 5.00 (m, 1H), 4.83 (d, *J* = 8.8 Hz, 1H), 3.94 – 3.89 (m, 1H), 3.74 (d, *J* = 10.2 Hz, 1H), 1.46 (s, 9H), 1.04 (d, *J* = 6.3 Hz, 3H)

**$^{13}C$ NMR** (126 MHz, $CDCl_3$) δ 168.1, 156.7, 133.7, 133.6, 132.6, 123.2, 118.8, 79.3, 74.3, 71.3, 56.0, 54.1, 28.5, 20.3

HRMS (ESI) *m/z*: $[M + Na]^+$ calcd for $C_{20}H_{26}N_2O_6$+Na: 413.1684; found: 413.1701

$[\alpha]^{23}_D$: -30.4 ($CH_2Cl_2$, c =.01305g/mL)

**Synthesis of 2.17**

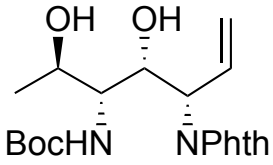


According to *General Procedure B*, the 1,3-diol compound **2.17** was prepared from compound **2.38** (26.6 mg, 0.053 mmol, 100 mol%), TBAF (1M in THF) (0.053 mL, 0.053 mmol, 100 mol%), and THF (3.50 mL). Product **2.17** was afforded as a white amorphous solid in quantitative yield which was present as a mixture of rotamers in the $^{1}H$ and $^{13}C$ NMR spectrum.

**$^{1}$H NMR** (500 MHz, $CDCl_3$) δ 7.81 (dd, *J* = 5.5, 3.1 Hz, 2H), 7.71 (dd, *J* = 5.5, 3.1 Hz, 2H), 6.24 (ddd, *J* = 17.5, 10.2, 7.6 Hz, 1H), 5.35 – 5.28 (m, 3H), 4.93 (d, *J* = 6.7 Hz, 1H), 4.78 – 4.74 (m, 1H), 3.93 – 3.88 (m, 1H), 3.49 – 3.45 (m, 1H), 1.41 (s, 9H), 1.26 (d, *J* = 6.6 Hz, 3H)

**$^{13}$C NMR** (126 MHz, $CDCl_3$) δ 168.0, 155.8, 134.2, 132.8, 132.1, 123.5, 120.0, 79.8, 70.8, 69.4, 55.8, 54.6, 28.5, 20.6

HRMS (ESI) *m/z*: $[M + Na]^+$ calcd for $C_{20}H_{26}N_2O_6$+Na: 413.1684; found: 413.1696

$[\alpha]^{23}_D$: +17.4 ($CH_2Cl_2$, c = .0142 g/mL)

**Synthesis of 2.18**

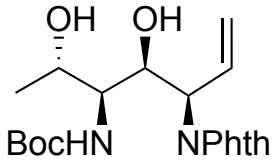


According to *General Procedure B*, the 1,3-diol compound **2.18** was prepared from compound **2.40** (50.0 mg, 0.099 mmol, 100 mol%), TBAF (1M in THF) (0.099 mL, 0.099 mmol, 100 mol%), and THF (7.1 mL). Product **2.18** was afforded as a white amorphous solid (40.2 mg, 0.103 mmol) in quantitative yield, which was present as a mixture of rotamers in the $^{1}H$ and $^{13}C$ NMR spectrum.

**$^{1}H$ NMR** (500 MHz, $CDCl_3$) δ 7.81 (dd, *J* = 5.5, 3.0 Hz, 2H), 7.71 (dd, *J* = 5.5, 3.1 Hz, 2H), 6.24 (ddd, *J* = 17.6, 10.2, 7.7 Hz, 1H), 5.36 – 5.28 (m, 3H), 4.92 (dd, *J* = 8.2, 1.8 Hz, 1H), 4.78 – 4.74 (m, 1H), 3.94 – 3.88 (m, 1H), 3.49 – 3.45 (m, 1H), 1.41 (s, 9H), 1.27 (d, *J* = 6.5 Hz, 3H)

**$^{13}C$ NMR** (126 MHz, $CDCl_3$) δ 168.0, 155.8, 134.2, 132.9, 132.1, 123.5, 119.7, 79.8, 70.6, 69.3, 55.6, 54.7, 28.5, 20.6

HRMS (ESI) *m/z*: $[M + Na]^+$ calcd for $C_{20}H_{26}N_2O_6$+Na: 413.1684; found: 413.1695

$[\alpha]^{23}_D$: -19.1 ($CH_2Cl_2$, c = 0.01315 g/mL)

**Synthesis of 2.23**

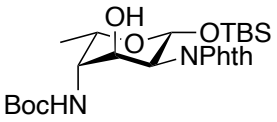


Compound **2.19** (28.7 mg, 0.0735 mmol, 100 mol%) was added to a flame dried, 3-neck round bottom secured with glass fittings, dissolved in a mixture of $CH_2Cl_2$ (2.50 mL) and MeOH (0.250 mL), and cooled to -78°C. The mixture was purged with argon, followed by $O_2$ (*g*). Ozone (via ozone generator) was bubbled through the solution for ~10 minutes, until the solution turned dark purple. [$O_2/O_3$ flow controlled by flow meter]. Excess $O_3$ was blown off by $O_2$ until solution lost all purple color (~1min) and the system was then purged with argon.

*N.B. Excess $O_3$(g) was quenched immediately via bubbling through two 10% aq. KI solutions following exposure to the reaction flask. The first KI solution turned orange, while the second remained clear, indicating that all $O_3$ was successfully destroyed.* (See photo below for setup details).

$Me_2S$ (0.100 mL, 1.36 mmol, 2000% mol) was added to the cooled mixture and the reaction was allowed to stir at room temperature for 12 hours. The solution was tested via peroxidase stain/peroxidase test strips for complete consumption of hazardous intermediates, concentrated *in vacuo*, diluted with a minimal amount of $CH_2Cl_2$, and purified via preparatory thin layer chromatography (1000 μm, 60:39:1 EtOAc:Hex:$Et_3N$). The products (both **2.35a** and **2.35b**) were recombined to furnish intermediate **2.35** as a white solid, which was immediately carried on to the next step without further purification. All equipment used to handle $Me_2S$ was handled in the fume hood and subsequently washed with bleach, acetone, and disposed of using secondary waste containment.

Intermediate **2.35** was added to a flame dried flask, dissolved in $CH_2Cl_2$ (1 mL), and cooled to 0°C. Imidazole (25.0 mg, 0.0735 mmol, 500 mol%) and TBSCl (55.5 mg, 0.368 mmol, 500 mol%) were added and the reaction was allowed to warm to room temperature for 12 hours. The aqueous layer was extracted with EtOAc (3x), and the pooled organic layers washed with sat. $NaHCO_3$ (1x) (aq.), brine (1x), dried over $Na_2SO_4$, filtered, and concentrated *in vacuo*. The resulting solution was diluted with a minimal amount of $CH_2Cl_2$, and purified via preparatory thin layer chromatography (1000 μm, 40% EtOAc:Hex to furnish compound **2.23** as a clear-white film (0.0287 g, 0.0566 mmol, 77% yield over 2 steps).

**$^1$H NMR** (500 MHz, $C_6D_6$) δ 7.38 (dd, *J* = 5.4, 3.1 Hz, 2H), 6.84 (dd, *J* = 5.5, 3.0 Hz, 2H), 5.93 (d, *J* = 8.5 Hz, 1H), 5.00 (d, *J* = 9.0 Hz, 1H), 4.75 (s, 1H), 4.62 (dd, *J* = 8.6, 2.4 Hz, 1H), 4.50 – 4.46 (m, 2H), 4.12 – 4.07 (m, 1H), 1.40 (s, 9H), 1.03 (d, *J* = 6.5 Hz, 3H), 0.72 (s, 9H), 0.12 (s, 3H), -0.04 (s, 3H)

**$^{13}$C NMR** (126 MHz, $C_6D_6$) δ 155.9, 134.0, 132.1, 123.4, 91.9, 79.4, 72.3, 68.6, 56.8, 55.6, 28.4, 25.6, 16.5, -3.9, -5.4

HRMS (ESI) *m/z*: $[M + Na]^+$ calcd for $C_{25}H_{38}N_2O_7Si$+Na: 529.2341; found: 529.2345

$[\alpha]^{23}_D$: +6.4 ($CH_2Cl_2$, c = 0.0132 g/mL)

## Ozonolysis General Setup

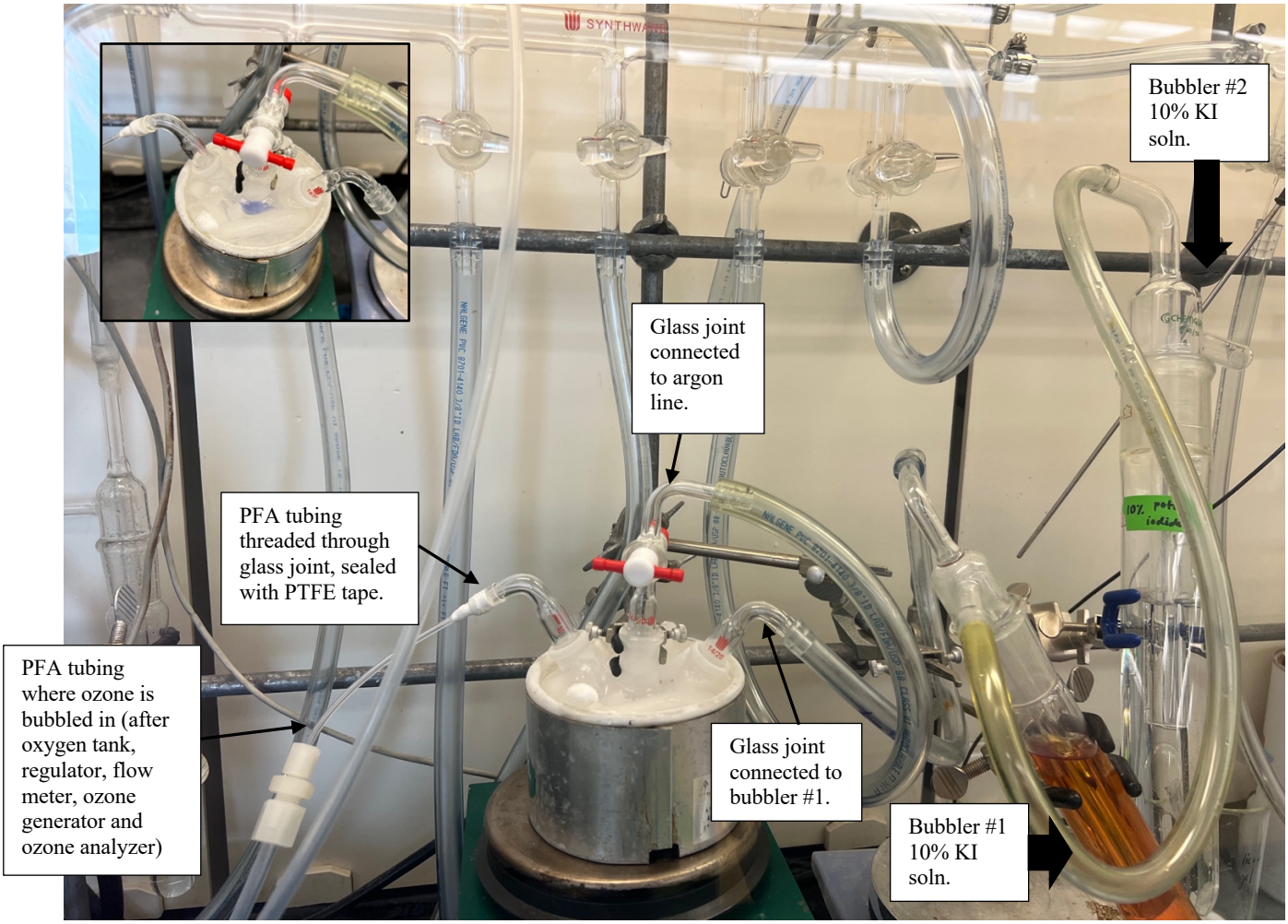

**Synthesis of 2.20**

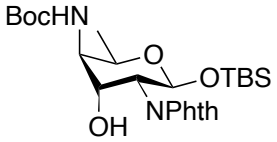


Compound **2.16** (21.1 mg, 0.540 mmol, 100 mol%) was added to a flame dried, 3-neck round bottom secured with glass fittings, dissolved in a mixture of $CH_2Cl_2$ (2.50 mL) and MeOH (0.250 mL), and cooled to -78°C. The reaction was purged with argon, followed by $O_2$ (*g*). Ozone (via ozone generator) was bubbled through the solution for ~10 minutes, until the solution turned purple. [$O_2/O_3$ flow was controlled by flow meter.] Excess $O_3$ was blown off by $O_2$ until solution lost all purple color (~1min) and the system then purged with argon.

*N.B. Excess $O_3$ was quenched immediately via bubbling through two 10% aq. KI solutions following exposure to the reaction flask. The first KI solution turned orange, while the second remained clear, indicating that all $O_3$ was successfully destroyed.* (See photo above for setup details)

$Me_2S$ (0.100 mL, 1.36 mol, 2000 mol%) was added to the cooled mixture and was allowed to stir at room temperature for 12 hours. The reaction was tested via peroxidase stain for complete consumption of hazardous intermediates, concentrated *in vacuo*, and purified via preparatory thin layer chromatography (1000 μm, 60:39:1 EtOAc:Hex:$Et_3N$). The products (both **2.37a** and **2.37b**) were recombined to furnish intermediate **2.37** as a white solid, which was immediately carried on to the next step without further purification. All equipment used to handle $Me_2S$ was handled in the fume hood and subsequently washed with bleach, acetone, and disposed of using secondary waste containment.

Intermediate **2.37** was added to a flame dried flask, dissolved in $CH_2CL_2$ (1.00 mL), and cooled to 0°C. Imidazole (18.3 mg, 0.269 mmol, 500 mol%) and TBSCl (40.5 mg, 0.269 mmol, 500 mol%) were added and the reaction was allowed to warm to room temperature for 12 hours. The aqueous layer was extracted with EtOAc (3x) and the pooled organic layers washed with sat. $NaHCO_3$ (1x) (aq.), brine (1x), dried over $Na_2SO_4$, filtered, and concentrated *in vacuo*. The resulting solution was diluted with a minimal amount of $CH_2Cl_2$ and purified via preparatory thin layer chromatography (1000 μm, 40% EtOAc:Hex to furnish compound **2.20** as a clear-white film (0.0227 g, 0.0448 mmol, 83% yield over two steps).

**$^1$H NMR** (500 MHz, $C_6D_6$) δ 7.37 (dd, *J* = 5.4, 3.1 Hz, 2H), 6.83 (dd, *J* = 5.5, 3.0 Hz, 2H), 5.90 (d, *J* = 8.5 Hz, 1H), 5.00 (d, *J* = 9.1 Hz, 1H), 4.63 (dd, *J* = 8.6, 2.5 Hz, 1H), 4.49 – 4.44 (m, 2H), 4.14 – 4.07 (m, 1H), 1.41 (s, 9H), 1.03 (d, *J* = 6.5 Hz, 3H), 0.72 (s, 9H), 0.12 (s, 3H), -0.05 (s, 3H)

**$^{13}$C NMR** (126 MHz, $C_6D_6$) δ 155.9, 134.0, 132.1, 123.4, 91.9, 79.3, 72.3, 68.6, 56.8, 55.5, 28.4, 25.6, 16.5, -3.9, -5.5

HRMS (ESI) *m/z*: $[M + Na]^+$ calcd for $C_{25}H_{38}N_2O_7Si$+Na: 529.2341; found: 529.2354

$[\alpha]^{23}_D$: -4.8 ($CH_2Cl_2$, c = 0.0144g/mL)

**Synthesis of 2.21**

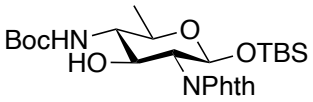


Compound **2.17** (49.8 mg, 0.128 mmol, 100 mol%) was added to a flame dried flask and dissolved in a mixture of 1,4-dioxane: $H_2O$ (3:1) (1.30 mL). 2,6-lutidine (0.030 mL 0.256 mmol, 200 mol%), $OsO_4$ (0.700 mg, 0.003 mmol, 2 mol%), and $NaIO_4$ (110. mg, 0.512 mmol, 400 mol%) were added and the reaction was allowed to stir at room temperature for 16 hours. The mixture was partitioned between $CH_2Cl_2$ and $H_2O$, the aqueous layer extracted with $CH_2Cl_2$ (3x) and the pooled organic layers washed with brine (2x), dried over $Na_2SO_4$, filtered, and concentrated *in vacuo.* The resulting solution was diluted with a minimal amount of $CH_2Cl_2$ and purified via preparatory thin layer chromatography (1000 μM, 70:30:1 EtOAc:Hex:$Et_3N$) and the products (both **2.39a** and **2.39b**) recombined to furnish intermediate **2.39**, which was immediately carried on to the next step without further purification.

*N.B. Osmium tetraoxide is a hazardous chemical compound. Extreme caution should be taken when handling and the appropriate SDS referred to. All equipment which encountered osmium was quenched in a fume hood with corn oil and disposed of in secondary containment.*

Intermediate **2.39** was added to a flame dried flask, dissolved in DMF (3.00 mL), and cooled to 0°C. Imidazole (43.6 mg, 0.640 mmol, 500 mol%) and TBSCl (96.5 mg, 0.640 mmol, 500 mol%) were added and the reaction was allowed to warm to room temperature for 12 hours. The aqueous layer was extracted with EtOAc (3x), and the pooled organic layers washed with sat. $NaHCO_3$ (aq.) (1x), brine (1x), dried over $Na_2SO_4$, filtered, and concentrated *in vacuo*. The resulting solution was diluted with a minimal

amount of $CH_2Cl_2$ and purified via preparatory thin layer chromatography (1000 μm, 40% EtOAc:Hex) to furnish compound **2.21** as a clear-white film (32.4 mg, 0.0639 mmol, 50% yield over 2 steps).

**$^1$H NMR** (400 MHz, $CDCl_3$) δ 7.83 (dd, *J* = 5.5, 3.1 Hz, 2H), 7.70 (dd, *J* = 5.5, 3.1 Hz, 2H), 5.36 (d, *J* = 7.8 Hz, 1H), 4.38 (s, 1H), 4.31 – 4.24 (m, 1H), 4.10 (dd, *J* = 10.7, 8.0 Hz, 1H), 3.57 – 3.49 (m, 1H), 3.45 – 3.36 (m, 1H), 1.44 (s, 9H), 1.34 (d, *J* = 6.1 Hz, 3H), 0.70 (s, 9H), 0.05 (s, 3H), -0.06 (s, 3H)

**$^{13}$C NMR** (126 MHz, $CDCl_3$) δ 134.2, 132.0, 123.4, 93.2, 71.3, 60.1, 29.9, 28.4, 25.5, 18.3, 17.8, -4.1, -5.3

HRMS (ESI) *m/z*: $[M + Na]^+$ calcd for $C_{25}H_{38}N_2O_7Si$+Na: 529.2341; found: 529.2352/506.5304

$[\alpha]^{23}_D$: +0.35 ($CH_2Cl_2$, c = 0.0171 g/mL)

**Synthesis of 2.22**

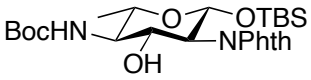


Compound **2.18** (26.3 mg, 0.0674 mmol, 100 mol%) was added to a flame dired flask and dissolved in a mixture of 1,4-dioxane: $H_2O$ (3:1) (0.700 mL). 2,6-lutidine (0.0200 mL 0.135 mmol, 200 mol%), $OsO_4$ (0.300 mg, 0.00135 mmol, 2 mol%) and $NaIO_4$ (57.7 mg, 0.270 mmol, 400 mol%) were added and the reaction was allowed to stir at room temperature for 16 hours. The mixture was partitioned between $CH_2Cl_2$ and $H_2O$, the aqueous layer extracted with $CH_2Cl_2$ (3x) and the pooled organic layers washed with brine (2x), dried over $Na_2SO_4$, filtered, and concentrated *in vacuo.* The resulting solution was purified via preparatory thin layer chromatography (1000 μM, 70:30:1 EtOAc:Hex:$Et_3N$) and the products (both **2.41a** and **2.41b**) recombined to furnish intermediate **2.41**, which was immediately carried on to the next step without further purification.

*N.B. Osmium tetraoxide is a hazardous chemical compound. Extreme caution should be taken when handling and the appropriate SDS referred to. All equipment which encountered osmium was quenched in a fume hood with corn oil and disposed of in secondary containment.*

Intermediate **2.41** was added to a flame dried flask, dissolved in DMF (1.60 mL), and cooled to 0°C. Imidazole (22.9 mg, 0.337 mmol, 500 mol%) and TBSCl (50.8 mg, 0.337 mmol, 500 mol%) were added and the reaction was allowed to warm to room temperature for 12 hours. The aqueous layer was extracted with EtOAc (3x), and the pooled organic layers washed with sat. $NaHCO_3$ (aq.) (1x), brine (1x), dried over $Na_2SO_4$, filtered, and concentrated *in vacuo*. The resulting solution was diluted with a minimal amount of $CH_2Cl_2$ and purified via preparatory thin layer chromatography (1000 μm, 40%

EtOAc:Hex) to furnish compound **2.22** as a clear-white film (15.4 mg, 0.0304 mmol, 44% yield over 2 steps).

**$^{1}$H NMR** (400 MHz, $CDCl_3$) δ 7.83 (dd, *J* = 5.7, 2.8 Hz, 2H), 7.70 (dd, *J* = 6.1, 2.4 Hz, 2H), 5.36 (d, *J* = 8.0 Hz, 1H), 4.39 (s, 1H), 4.32 – 4.24 (m, 1H), 4.10 (dd, *J* = 10.6, 8.1 Hz, 1H), 3.58 – 3.49 (m, 1H), 3.45 – 3.36 (m, 1H), 1.45 (s, 9H), 1.34 (d, *J* = 6.1 Hz, 3H), 0.70 (s, 9H), 0.05 (s, 3H), -0.06 (s, 3H)

**$^{13}$C NMR** (126 MHz, $CDCl_3$) δ 134.2, 132.0, 123.4, 93.2, 71.3, 60.1, 29.9, 28.4, 25.5, 18.3, 17.8, -4.1, -5.3

HRMS (ESI) *m/z*: $[M + Na]^+$ calcd for $C_{25}H_{38}N_2O_7Si$+Na: 529.2341; found: 529.2347/506.5303

$[\alpha]^{23}_D$: - 0.096 ($CH_2Cl_2$, c = 0.0125 g/mL)

**Synthesis of 2.29**

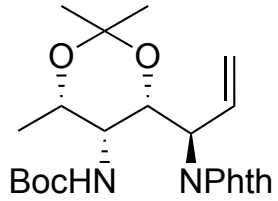


Compound **2.19** (100.0 mg, 0.256 mmol, 100 mol%) was added to a flame dried flask, dissolved in $CH_2Cl_2$ (10 mL), and cooled to 0°C. TsOH (4.40 mg, 0.0256 mmol, 10 mol%) and 2,2-dimethoxypropane (.0380 mL, 0.307 mmol, 120 mol%) were added and the reaction was allowed to warm to room temperature for 12 hours. Afterwards, the reaction was concentrated *in vacuo,* diluted with minimal $CH_2Cl_2$, and purified via preparatory thin layer chromatography (500μM, 40% EtOAc:Hex) to furnish compound **2.29** as a clear-white film (59.7 mg, 54% yield).

**$^1$H NMR** (500 MHz, $CDCl_3$) δ 7.78 (dd, *J* = 5.4, 3.1 Hz, 2H), 7.69 (dd, *J* = 5.5, 3.1 Hz, 2H), 6.13 – 6.05 (m, 1H), 5.21 – 5.14 (m, 2H), 5.04 (d, *J* = 10.6 Hz, 1H), 4.79 (m, 2H), 4.10 – 4.05 (m, 1H), 3.35 (d, *J* = 10.6 Hz, 1H), 1.51 (s, 3H), 1.43 (s, 3H), 1.36 (s, 9H), 1.26 (d, *J* = 2.3 Hz, 3H), 1.03 (d, *J* = 6.1 Hz, 3H)

**$^{13}$C NMR** (126 MHz, $CDCl_3$) δ 155.9, 133.8, 133.1, 123.2, 117.4, 99.8, 79.4, 71.6, 68.0, 52.7, 47.8, 29.8, 29.7, 28.2, 19.4, 17.1

HRMS (ESI) *m/z*: $[M + Na]^+$ calcd for $C_{23}H_{30}N_2O_6$+Na: 453.2002; found: 453.2012

$[\alpha]^{23}_D$: +18.2 ($CH_2Cl_2$, c = 0.0072 g/mL)

**Synthesis of 2.30**

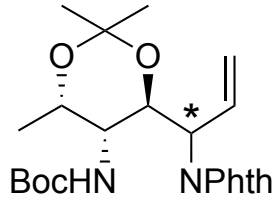


Compound **2.28** (29.0 mg, .0743 mmol, 100 mol%) was added to a flame dried flask, dissolved in $CH_2Cl_2$ (2.9 mL), and cooled to 0°C. TsOH (1.28 mg, .00743 mmol, 10 mol%) and 2,2-dimethoxypropane ( 0.0110 mL, 0.0891 mmol, 120 mol%) were added and the reaction was allowed to warm to room temperature for 12 hours. Afterwards, the reaction was concentrated *in vacuo,* diluted with minimal $CH_2Cl_2$, and purified via preparatory thin layer chromatography (500μM, 40% EtOAc:Hex) to furnish compound **2.30** as a clear-white film (18.0 mg, 0.0418 mmol, 56% yield).

**$^1$H NMR** (500 MHz, $CDCl_3$) δ 7.82 (dd, *J* = 5.5, 3.0 Hz, 2H), 7.67 (dd, *J* = 5.4, 3.0 Hz, 2H), 6.28 – 6.20 (m, 1H), 5.26 – 5.23 (m, 1H), 5.23 – 5.21 (m, 1H), 4.92 – 4.88 (m, 1H), 4.61 (d, *J* = 10.7 Hz, 1H), 4.13 – 4.07 (m, 2H), 3.72 – 3.66 (m, 1H), 1.38 (s, 3H), 1.36 (s, 3H), 1.00 (d, 3H), 0.97 (s, 9H)

**$^{13}$C NMR** (126 MHz, $CDCl_3$) δ 168.3, 133.9, 133.4, 132.3, 123.4, 118.9, 101.4, 79.1, 71.5, 66.1, 55.6, 54.8, 29.9, 27.9, 25.1, 23.8

HRMS (ESI) *m/z*: $[M + Na]^+$ calcd for $C_{23}H_{30}N_2O_6$+Na: 453.2002; found: 453.2003

$[\alpha]^{23}_D$: - 2.3 ($CH_2Cl_2$, c= 0.009 g/mL)

**Synthesis of 2.42**

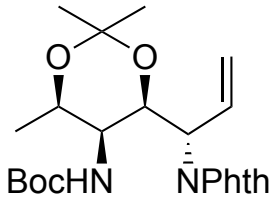


Compound **2.16** (20.0 mg, 0.0512 mmol, 100 mol%) was added to a flame dried flask, dissolved in $CH_2Cl_2$ (2 mL), and cooled to 0°C. TsOH (0.880 mg, 0.00512 mmol, 10 mol%) and 2,2-dimethoxypropane (.00750 mL, 0.0615 mmol, 120 mol%) were added and the reaction was allowed to warm to room temperature for 12 hours. Afterwards, the reaction was concentrated *in vacuo,* diluted with minimal $CH_2Cl_2$, and purified via preparatory thin layer chromatography (500μM, 40% EtOAc:Hex) to furnish compound **2.42** as a clear-white film (15.65 mg, 0.0364 mmol, 71% yield).

**$^1$H NMR** (500 MHz, $CDCl_3$) δ 7.78 (dd, *J* = 5.4, 3.1 Hz, 2H), 7.69 (dd, *J* = 5.4, 3.1 Hz, 2H), 6.09 (m, 1H), 5.20 – 5.13 (m, 2H), 5.04 (d, *J* = 10.6 Hz, 1H), 4.79 (m, 2H), 4.07 (m, 1H), 3.35 (d, *J* = 10.6 Hz, 1H), 1.51 (s, 3H), 1.43 (s, 3H), 1.36 (s, 9H), 1.03 (d, *J* = 6.2 Hz, 3H)

**$^{13}$C NMR** (126 MHz, $CDCl_3$) δ 156.0, 134.0, 133.2, 123.3, 117.6, 99.9, 79.5, 71.8, 68.2, 52.9, 48.0, 30.0, 29.9, 28.4, 19.6, 17.2

HRMS (ESI) *m/z*: $[M + Na]^+$ calcd for $C_{23}H_{30}N_2O_6$+Na: 453.2002; found: 453.2004

$[\alpha]^{23}_D$: -29.4 ($CH_2Cl_2$, c = 0.0051 g/mL)

**Synthesis of 2.43**

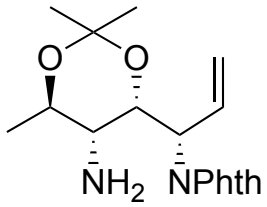


Compound **2.17** (10.0 mg, 0.0256 mmol, 100 mol%) was added to a flame dried flask and dissolved in acetone (1 mL). Iodine (1.96 mg, 0.00768 mmol, 30 mol%) was added, allowed to stir in an oil bath at 40°C for 1 hour, and quenched with a 10% solution of $Na_2S_2O_3$ (aq.) until the solution turned from brown to clear. The aqueous layer was extracted with EtOAc (3x) and the pooled organic layers washed with $H_2O$ (2x), brine (1x), dried over $Na_2SO_4$, filtered, concentrated *in vacuo,* and purified via preparatory thin layer chromatography (500 μM, 40% EtOAc:Hex) to furnish compound **2.43** as a clear-white film (5.07 mg, 0.0153 mmol, 62% yield).

**$^1$H NMR** (500 MHz, $CDCl_3$) δ 7.90 (dd, *J* = 25.6, 7.3 Hz, 2H), 7.65 (m, 2H), 5.83 (m, 1H), 5.23 (dd, *J* = 10.5, 1.6 Hz, 1H), 5.03 (dd, *J* = 17.1, 1.7 Hz, 1H), 4.83 (m, 1H), 4.12 (m, 1H), 3.81 (m, 1H), 3.53 (m, 1H), 1.53 (d, *J* = 6.4 Hz, 3H), 1.41 (s, 3H), 1.29 (s, 3H)

**$^{13}$C NMR** (126 MHz, $CDCl_3$) δ 132.7, 131.9, 123.4, 121.8, 117.6, 71.2, 63.8, 60.7, 52.7, 32.1, 29.9, 25.6, 23.8, 20.4

HRMS (ESI) *m/z*: $[M - H_2O]^+$ calcd for $C_{18}H_{23}N_2O_4$: 313.1552; found: 313.1547

$[\alpha]^{23}_D$: -0.26 $CH_2Cl_2$, c = 0.0116 g/mL)

**Synthesis of 2.44**

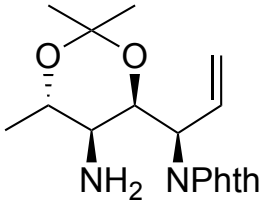


Compound **2.18** (20.0 mg, 0.0512 mmol, 100 mol%) was added to a flame dried flask and dissolved in acetone (2 mL). Iodine (3.90 mg, 0.0154 mmol, 30 mol%) was added, allowed to stir in an oil bath at 40°C for 1 hour, and quenched with a 10% solution of $Na_2S_2O_3$ (aq) until the solution turned from brown to clear. The aqueous layer was extracted with EtOAc (3x) and the pooled organic layers washed with $H_2O$ (2x), brine (1x), dried over $Na_2SO_4$, filtered, concentrated *in vacuo,* and purified via preparatory thin layer chromatography (500 μM, 40% EtOAc:Hex) to furnish compound **2.44** as a clear-white film (11.7 mg, 0.0354 mmol, 69% yield).

**$^1$H NMR** (500 MHz, $CDCl_3$) δ 7.94 – 7.85 (m, 2H), 7.65 (m, 2H), 5.83 (ddd, *J* = 17.1, 10.4, 5.1 Hz, 1H), 5.23 (dd, *J* = 10.4, 1.6 Hz, 1H), 5.03 (dd, *J* = 17.1, 1.8 Hz, 1H), 4.84 – 4.81 (m, 1H), 4.12 (dd, *J* = 3.8, 1.9 Hz, 1H), 3.83 – 3.77 (m, 1H), 3.54 (dd, *J* = 6.9, 3.9 Hz, 1H), 1.53 (d, *J* = 6.3 Hz, 3H), 1.41 (s, 3H), 1.29 (s, 3H)

**$^{13}$C NMR** (126 MHz, $CDCl_3$) δ 133.1, 132.7, 131.9, 123.4, 121.8, 117.5, 101.4, 71.2, 63.8, 60.7, 52.7, 29.9, 25.6, 23.8, 20.4

HRMS (ESI) *m/z*: $[M - H_2O]^+$ calcd for $C_{18}H_{23}N_2O_4$: 313.1552; found: 313.1547

$[\alpha]^{23}_{D}$: +0.62 ($CH_2Cl_2$, c = 0.0081 g/mL)

## 2.6. References


(1) De Oliveira, D. M. P.; Forde, B. M.; Kidd, T. J.; Harris, P. N. A.; Schembri, M. A.; Beatson, S. A.; Paterson, D. L.; Walker, M. J. Antimicrobial Resistance in ESKAPE Pathogens. *Clin. Microbiol. Rev.* **2020**, *33* (3).

(2) Lewis, A. L.; Szymanski, C. M.; Schnaar R.L.; et al. Bacterial and Viral Infections. In *Essentials of Glycobiology [Internet]*; Varki, A., Cummings, R. D., Esko, J. D., et al., Eds.; Cold Spring Harbor (NY): Cold Spring Harbor Laboratory Press, 2022.

(3) Kay, E.; Lesk, V. I.; Tamaddoni-Nezhad, A.; Hitchen, P. G.; Dell, A.; Sternberg, M. J.; Muggleton, S.; Wren, B. W. Systems Analysis of Bacterial Glycomes. *Biochem. Soc. Trans.* **2010**, *38* (5), 1290–1293.

(4) Morrison, M. J.; Imperiali, B. The Renaissance of Bacillosamine and Its Derivatives: Pathway Characterization and Implications in Pathogenicity. *Biochemistry* **2014**, *53* (4), 624–638.

(5) Nishat, S.; Andreana, P. Entirely Carbohydrate-Based Vaccines: An Emerging Field for Specific and Selective Immune Responses. *Vaccines (Basel)* **2016**, *4* (2), 19.

(6) Astronomo, R. D.; Burton, D. R. Carbohydrate Vaccines: Developing Sweet Solutions to Sticky Situations? *Nat. Rev. Drug Discov.* **2010**, *9* (4), 308–324.

(7) Micoli, F.; Del Bino, L.; Alfini, R.; Carboni, F.; Romano, M. R.; Adamo, R. Glycoconjugate Vaccines: Current Approaches towards Faster Vaccine Design. *Expert Rev. Vaccines* **2019**, *18* (9), 881–895.

(8) Clark, E. L.; Emmadi, M.; Krupp, K. L.; Podilapu, A. R.; Helble, J. D.; Kulkarni, S. S.; Dube, D. H. Development of Rare Bacterial Monosaccharide Analogs for Metabolic Glycan Labeling in Pathogenic Bacteria. *ACS Chem. Biol.* **2016**, *11* (12), 3365–3373.

(9) Young, N. M.; Brisson, J.-R.; Kelly, J.; Watson, D. C.; Tessier, L.; Lanthier, P. H.; Jarrell, H. C.; Cadotte, N.; St. Michael, F.; Aberg, E.; Szymanski, C. M. Structure of the N-Linked Glycan Present on Multiple Glycoproteins in the Gram-Negative Bacterium, Campylobacter Jejuni. *J. Biol. Chem.* **2002**, *277* (45), 42530–42539.

(10) Emmadi, M.; Kulkarni, S. S. Synthesis of Orthogonally Protected Bacterial, Rare-Sugar and D-Glycosamine Building Blocks. *Nat. Protoc.* **2013**, *8* (10), 1870–1889.

(11) Stimson, E.; Virji, M.; Makepeace, K.; Dell, A.; Morris, H. R.; Payne, G.; Saunders, J. R.; Jennings, M. P.; Barker, S.; Panico, M.; Blench, I.; Moxon, E. R. Meningococcal Pilin: A Glycoprotein Substituted with Digalactosyl 2,4-Diacetamido-2,4,6-Trideoxyhexose. *Mol. Microbiol.* **1995**, *17* (6), 1201–1214.

(12) Ovchinnikova, O. G.; Kocharova, N. A.; Bialczak-Kokot, M.; Shashkov, A. S.; Rozalski, A.; Knirel, Y. A. Structure of the O-Polysaccharide of Providencia Alcalifaciens O22 Containing D-Glyceramide 2-Phosphate. *Eur. J. Org. Chem.* **2012**, *2012* (18), 3500–3506.

(13) Spielmann, K.; Xiang, M.; Schwartz, L. A.; Krische, M. J. Direct Conversion of Primary Alcohols to 1,2-Amino Alcohols: Enantioselective Iridium-Catalyzed Carbonyl Reductive Coupling of Phthalimido-Allene via Hydrogen Auto-Transfer. *J. Am. Chem. Soc.* **2019**, *141* (36), 14136–14141.

(14) Doerksen, R. S.; Meyer, C. C.; Krische, M. J. Feedstock Reagents in Metal-Catalyzed Carbonyl Reductive Coupling: Minimizing Preactivation for Efficiency in Target-Oriented Synthesis. *Angew. Chem. Int. Ed.* **2019**, *58* (40), 14055–14064.

(15) Shezaf, J. Z.; Santana, C. G.; Ortiz, E.; Meyer, C. C.; Liu, P.; Sakata, K.; Huang, K.-W.; Krische, M. J. Leveraging the Stereochemical Complexity of Octahedral Diastereomeric-at-Metal Catalysts to Unlock Regio-, Diastereo-, and Enantioselectivity in Alcohol-Mediated C–C Couplings via Hydrogen Transfer. *J. Am. Chem. Soc.* **2024**, *146* (12), 7905–7914.

(16) Flack, E. K. P.; Chidwick, H. S.; Guchhait, G.; Keenan, T.; Budhadev, D.; Huang, K.; Both, P.; Mas Pons, J.; Ledru, H.; Rui, S.; Stafford, G. P.; Shaw, J. G.; Galan, M. C.; Flitsch, S.; Thomas, G. H.; Fascione, M. A. Biocatalytic Transfer of Pseudaminic Acid (Pse5Ac7Ac) Using Promiscuous Sialyltransferases in a Chemoenzymatic Approach to Pse5Ac7Ac-Containing Glycosides. *ACS Catal.* **2020**, *10* (17), 9986–9993.

(17) Dhara, D.; Bouchet, M.; Mulard, L. A. Scalable Synthesis of Versatile Rare Deoxyamino Sugar Building Blocks from D-Glucosamine. *J. Org. Chem.* **2023**, *88* (11), 6645–6663.

(18) Amin, M. N.; Ishiwata, A.; Ito, Y. Synthesis of Asparagine-Linked Bacillosamine. *Carbohydr. Res.* **2006**, *341* (11), 1922–1929.

(19) Amin, M. N.; Ishiwata, A.; Ito, Y. Synthesis of N-Linked Glycan Derived from Gram-Negative Bacterium, Campylobacter Jejuni. *Tetrahedron* **2007**, *63* (34), 8181–8198.

(20) Emmadi, M.; Kulkarni, S. S. Orthogonally Protected D-Galactosamine Thioglycoside Building Blocks via Highly Regioselective, Double Serial and Double Parallel Inversions of β-d-Thiomannoside. *Org. Biomol. Chem.* **2013**, *11* (29), 4825.

(21) Eradi, P.; Ghosh, S.; Andreana, P. R. Total Synthesis of Zwitterionic Tetrasaccharide Repeating Unit from *Bacteroides Fragilis* ATCC 25285/NCTC 9343 Capsular Polysaccharide PS A1 with Alternating Charges on Adjacent Monosaccharides. *Org. Lett.* **2018**, *20* (15), 4526–4530.

(22) Emmadi, M.; Kulkarni, S. S. Total Synthesis of the Bacillosamine Containing α-L-Serine Linked Trisaccharide of Neisseria Meningitidis. *Carbohydr. Res.* **2014**, *399*, 57–63.

(23) Ghosh, B.; Bhattacharjee, N.; Podilapu, A. R.; Puri, K.; Kulkarni, S. S. Total Synthesis of the Repeating Units of *O*-Specific Polysaccharide of *Pseudomonas Chlororaphis* Subsp. *Aureofaciens* UCM B-306 via One-Pot Glycosylation. *Org. Lett.* **2022**, *24* (20), 3696–3701.

(24) Pragani, R.; Stallforth, P.; Seeberger, P. H. De Novo Synthesis of a 2-Acetamido-4-Amino-2,4,6-Trideoxy-D-Galactose (AAT) Building Block for the Preparation of a *Bacteroides Fragilis* A1 Polysaccharide Fragment. *Org. Lett.* **2010**, *12* (7), 1624–1627.

(25) Masamune, S.; Choy, W.; Petersen, J. S.; Sita, L. R. Double Asymmetric Synthesis and a New Strategy for Stereochemical Control in Organic Synthesis. *Angew. Chem., Int. Ed. Engl.* **1985**, *24* (1), 1–30.

(26) Rychnovsky, S. D.; Rogers, B.; Yang, G. Analysis of Two Carbon-13 NMR Correlations for Determining the Stereochemistry of 1,3-Diol Acetonides. *J. Org. Chem.* **1993**, *58* (13), 3511–3515.

(27) Gelas, J.; Horton, D. Kinetic Acetonation of D-Mannose: Preparation of 4,6-Mono- and 2,3:4,6-Di-O-Isopropylidene-D-Mannopyranose. *Carbohydr. Res.* **1978**, *67* (2), 371–387.

(28) Overman, L. E.; McCready, R. J. Highly Stereocontrolled Reduction of A′-Alkoxyenones to Give Either the Threo or Eryhtro Allylic 1,2-Diol. Assignment of the Threo Configuration to the C-15, C-16 Diol of Pumiliotoxin B.1. *Tetrahedron Lett.* **1982**, *23* (23), 2355–2358.

(29) Evans, D. A.; Allison, B. D.; Yang, M. G.; Masse, C. E. The Exceptional Chelating Ability of Dimethylaluminum Chloride and Methylaluminum Dichloride. The Merged Stereochemical Impact of α- and β-Stereocenters in Chelate-Controlled Carbonyl Addition Reactions with Enolsilane and Hydride Nucleophiles. *J. Am. Chem. Soc.* **2001**, *123* (44), 10840–10852.

(30) Dondoni, A.; Marra, A.; Massi, A. Design and Use of an Oxazolidine Silyl Enol Ether as a New Homoalanine Carbanion Equivalent for the Synthesis of Carbon-Linked Isosteres of *O*-Glycosyl Serine and *N*-Glycosyl Asparagine. *J. Org. Chem.* **1999**, *64* (3), 933–944.

(31) Hu, D. X.; Grice, P.; Ley, S. V. Rotamers or Diastereomers? An Overlooked NMR Solution. *J. Org. Chem.* **2012**, *77* (11), 5198–5202.

(32) Deetz, M. J.; Jonas, M.; Malerich, J. P.; Smith, B. D. Conformational Switches: Controlling the Carbamate C-N Rotamer Equilibrium. *Supramol. Chem.* **2002**, *14* (6), 487–489.

(33) Kartha, K. P. R. Iodine, a Novel Catalyst in Carbohydrate Reactions I. O-Isopropylidination of Carbohydrates. *Tetrahedron Lett.* **1986**, *27* (29), 3415–3416.

(34) Liu, H.; Zhang, Y.; Wei, R.; Andolina, G.; Li, X. Total Synthesis of *Pseudomonas Aeruginosa* 1244 Pilin Glycan via *de Novo* Synthesis of Pseudaminic Acid. *J. Am. Chem. Soc.* **2017**, *139* (38), 13420–13428.

(35) Yu, W.; Mei, Y.; Kang, Y.; Hua, Z.; Jin, Z. Improved Procedure for the Oxidative Cleavage of Olefins by OsO4 −NaIO4. *Org. Lett.* **2004**, *6* (19), 3217–3219.

(36) Pappo, R.; Allen, Jr. , D.; Lemieux, R.; Johnson, W. Osmium Tetroxide-Catalyzed Periodate Oxidation of Olefinic Bonds. *J. Org. Chem.* **1956**, *21* (4), 478–479.

(37) Soliman, S. E.; Bennett, C. S. Reagent-Controlled Synthesis of the Branched Trisaccharide Fragment of the Antibiotic Saccharomicin B. *Org. Lett.* **2018**, *20* (11), 3413–3417.

# Chapter 3: The Derivatization and Characterization of 2,4,6-Trideoxy-2-Amino-4-Acetamidohexoses and 2,4,6-Trideoxy-2,4-Diacetamidohexoses for Enzymatic Testing and Biologic Studies

## 3.1. Introduction

Due to the presence of rare, prokaryote-specific sugars on the *O*-Antigen of Gram-negative pathogens, there is an interest in exploring how they interact with and affect cells.[1,6,11–13,110] It has been suggested that these sugars protect bacteria from cell death,[1,9,10] but it is generally unclear how 6-deoxy sugars specifically play a role in this phenomenon.[7,11] To better understand this, among other functions, testing that explores what biologic pathways some 6-deoxy-containing bacterial glycans undergo has been pursued.[111] However, the biosynthesis of DATDH containing bacterial glycans, specifically, has not yet been explored. This is mainly attributed to the lack of access scientists have to DATDH-containing moieties. To circumvent this issue, we first developed an efficient synthesis of two enantiomeric pairs of DATDHs (see Chapter 2). Subsequently, we developed various protecting group modifications to the originally synthesized DATDHs (**Figure 3.1**). By providing DATDHs in their deprotected and/or acetylated form, we open the door to possible enzymatic transformations that would allow us to better study the role(s) these compounds play in nature. Furthermore, a better understanding of the biosynthesis of complex bacterial glycans may allow for the potential development of novel strategies to combat bacterial infection.[6]

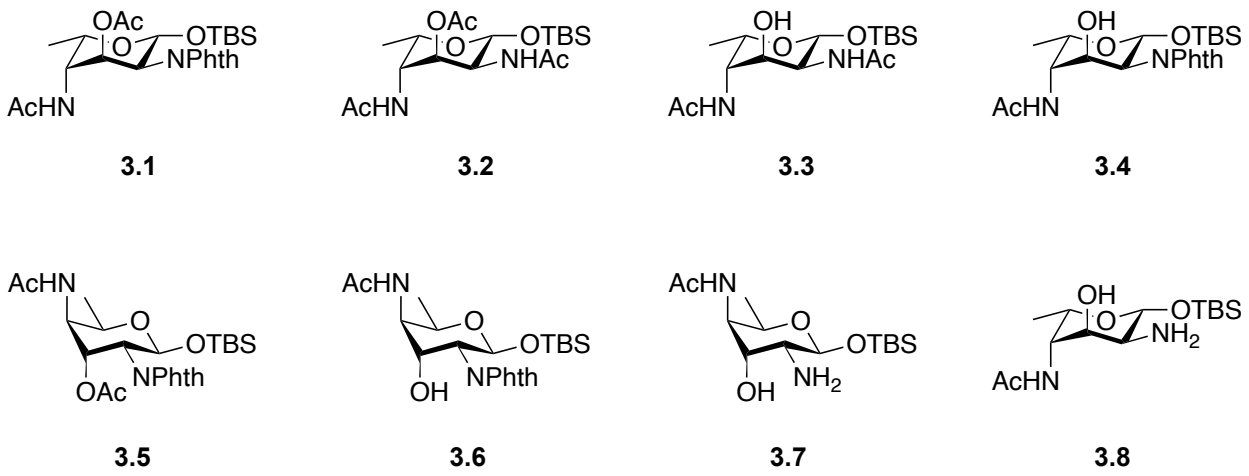


**Figure 3.1.** Deoxy-amino sugars synthesized for enzymatic testing and biologic studies.

In addition to sugar derivatization for biological testing, it was hypothesized that deprotected 6-carbon DATDHs could be chemoenzymatically elongated to 9-carbon nonulosonic acids (NulOs) when exposed to the appropriate aldolase enzyme (**Scheme 3.1**).[112,113] In collaboration with the Pohl lab at Indiana University, various aldolase enzymes were expressed, with the intent of testing them on 2,4-diacetamido-derived hexoses to determine whether the enzyme's promiscuity would be sufficient to facilitate the elongation process. Successful enzymatic transformation through this method would provide a more accessible and efficient route to nonulosonic acids than was previously thought possible. Additionally, the ability to generate nonulosonic acids through this strategy could have significant implications for understanding their role in bacterial pathogenicity and fitness.[43] Chapter 1 includes additional details on previous syntheses of NulOs and potential therapeutic applications (*vide supra*).

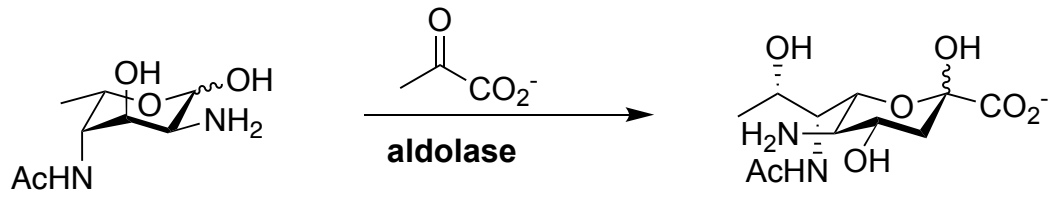


**3.9** **3.10**

**Scheme 3.1.** Proposed chemoenzymatic route to 8epiLeg via chemoenzymatic elongation with an aldolase enzyme.

## 3.1.1. Enzymatic Transformations of 6-Deoxy Sugars

After the synthesis of DATDH **3.18**, a series of deprotections were developed toward generation of derivatized compound **3.23** (see **Section 3.2.3**). This involved the synthetic installation of an acetamide at C4, a free amino substituent at C2, and the removal of a silyl group at C1. The resulting deoxy-amino sugar could then be primed for further enzymatic modification.[114] To this end, and through a collaborative effort, the deprotected sugar would be exposed to sugar-1-kinase or related phosphorylating enzyme to install a phosphate group at C1, generating a sugar-1-phosphate intermediate.[115–117] Once formed, the sugar-1-phosphate would be transformed into nucleoside diphosphate sugar (NDP-sugar) using a sugar-1-phosphate nucleotidyltransferase enzyme.[118,119] This transformation is an essential step in the activation of the sugar for downstream biosynthetic processes.[119] Whether the NDP-2,4-diamino-2,4,6-trideoxy sugar can be successfully synthesized using the techniques described by Lupoli and co-workers is yet to be discovered. In previously reported methodology, the enzymatic synthesis of activated 6-deoxy sugars was performed on simpler, commercially available substrates.[6]

If successfully made, the NDP-6-deoxy sugars, could then undergo various biosynthetic pathways, which may be studied to explore their biological functions and

roles in pathogen-host interactions. By investigating these biosynthetic routes, we may then gain deeper insight into the metabolic processes that control the production of key sugar-based molecules involved in bacterial virulence. These studies have the potential to reveal new targets for therapeutic intervention and improve our understanding of the complex roles theses sugars plan in microbial pathogenesis (*vide supra*).

## 3.2. Synthetic Manipulations Toward Deprotected DATDHs

### 3.2.1. Scale-up of D-threonine Derived DATDH Synthesis

To provide "enzyme ready" sugars for further biologic studies, scale-up and improved overall yield to the synthesis of compound **3.18**, first discussed in Chapter 2, was imperative (**Scheme 3.2**). It was discovered that gram-scale synthesis of the D-threonine allylation could successfully be performed, with the only real hindrance to further scaleup being the amount of iridium-$H_8$-BINAP on hand. On gram scale, up to 53% isolated yield of the desired allylation product **3.15** was observed. Following generation of this alkene intermediate, ozonolysis followed by TBS protection of the anomeric position resulted in generation of compound **3.18** in 98% yield over two steps, as compared to the 77% two-step yield previously reported.[120] Further details regarding synthesis of compounds **3.12** though **3.16** are detailed in Chapter 2 of this thesis (*vide supra*). *In sum*, scale-up led to an improvement of 33% overall yield to 52% overall yield for this synthetic pathway, starting from D-threoninol.

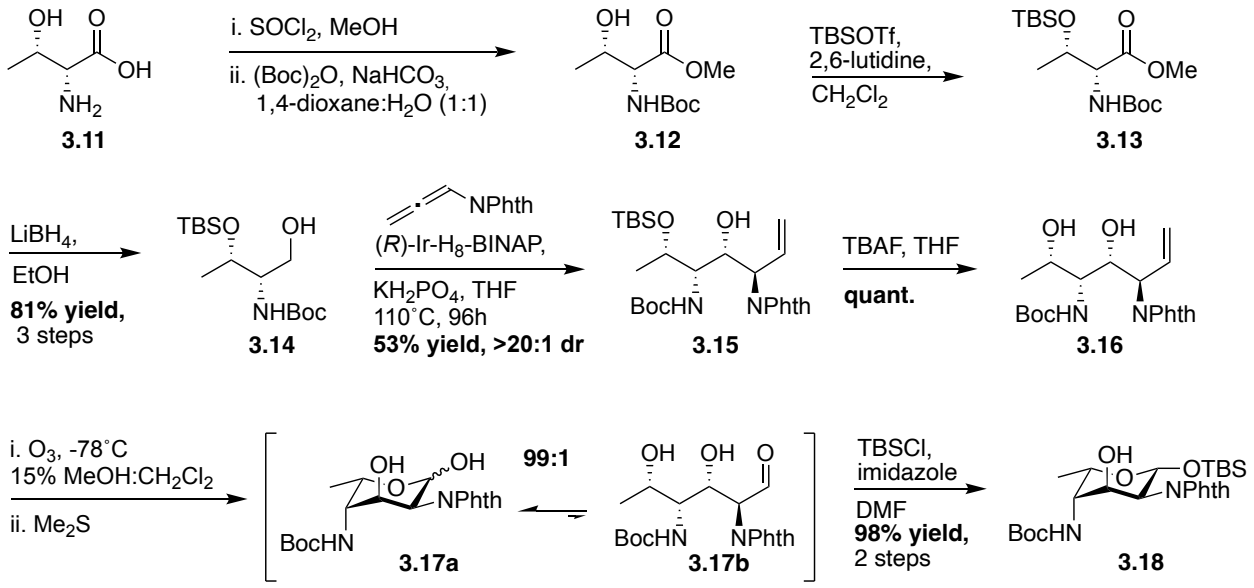


**Scheme 3.2.** Scaled up d*e novo* synthesis of derivatized DATDHs from threonine starting material, using D-threonine as the model substrate.

## 3.2.2. Exploration of Conditions for Boc and Phthalimide Removal

Following generation of compound **3.18**, protecting group manipulations were explored to synthesize various acetamido and free amine derivatives of the DATDH, to use as both probes for studying their biosynthesis and precursors for enzymatic elongation. Both phthalimide removal and Boc removal of compound **3.18** were first explored. Phthalimide removal was attempted under standard conditions with sodium borohydride[121] followed by acetylation.[121] No product was observed in this instance, and decomposition of the starting material was additionally seen (**Scheme 3.3**). Conversely, Boc removal under standard TFA conditions [121] followed by acetylation of compound **3.18** delightfully provided the diacetylated product **3.19** in quantitative yield (**Scheme 3.4**).

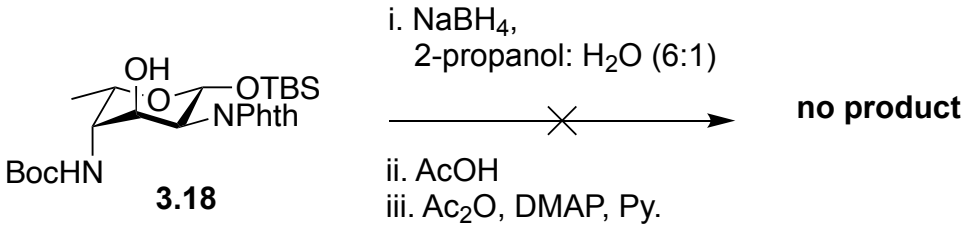


**Scheme 3.3.** Attempted phthalimide removal of DATDH.

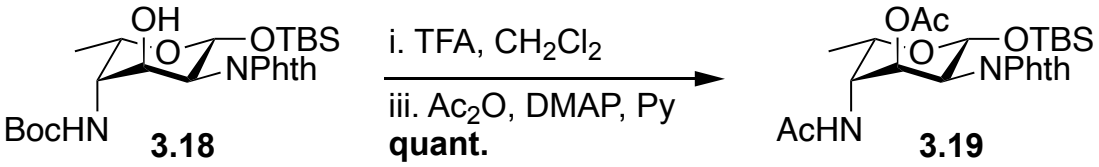


**Scheme 3.4.** Boc removal of DATDH under standard TFA conditions.

After Boc removal of **3.18**, various conditions for phthalimide removal of newly synthesized compound **3.19** were explored (**Table 3.1**). Under standard conditions utilizing sodium borohydride, trace amounts of product **3.20** were observed.[121] Utilizing an alternative procedure with ethylene diamine, there was no conversion to the desired compound.[121] However, utilization of hydrazine monohydrate followed by acetylation resulted in a 91% isolated yield of compound **3.20** and full consumption of starting material.[121] Content with these results, deacetylation of the C3 hydroxyl was next explored. It was observed that Zemplen deacetylation utilizing catalytic amounts of sodium methoxide in methanol resulted in the desired diacetamide, compound **3.21**.[121] **Scheme 3.5** depicts the pathway from protected DATDH **3.18** to derivatized 2,4-diacetamide, hexose **3.21**. The temporary anomeric protecting group was left on for stability purposes and is thought to be easily removed with TBAF once ready for further enzymatic testing.[120,121]

**Table 3.1.** Conditions screened for phthalimide removal of DATDH.

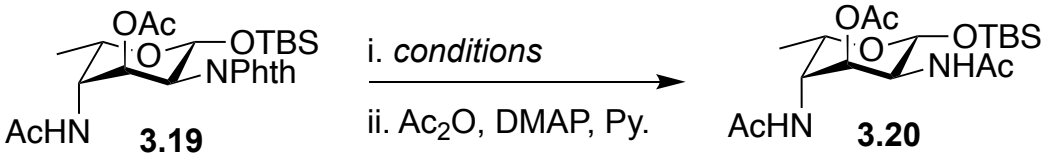


| Entry | Reaction Conditions | Percent Yield |
|---|---|---|
| 1 | $NaBH_4$, 2-propanol: $H_2O$ (6:1) | trace |
| 2 | ethylene diamine, EtOH | 0 |
| **3** | **$H_2NNH_2 \cdot H_2O$, EtOH** | **91** |

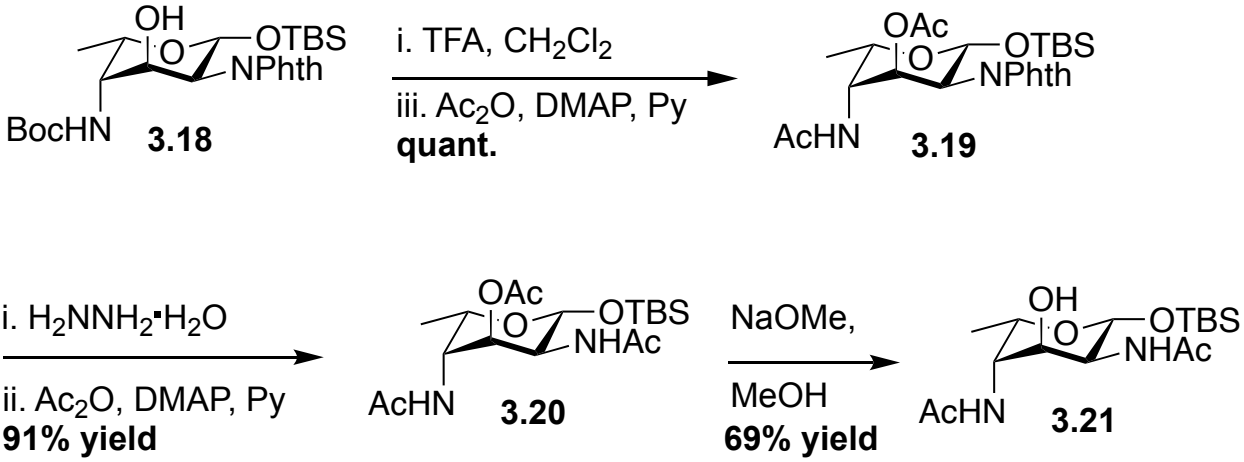


**Scheme 3.5.** Optimized pathway from protected DATDH to 2,4-diacetamido-2,4,6-trideoxyhexose.

## 3.2.3. Expansion of Derivatization to C2 Free Amines

In addition to the -2,4-diacetamido-2,4,6-trideoxyhexose **3.21**, a C2 free amino derivative of **3.18** was also desired for subsequent enzymatic testing. Due to the strategic differentiation in protection at the C2 and C4 position of DATDH **3.18**, this was possible after optimization of reaction conditions. To this end, the conditions for a one-pot Boc

removal and acetylation were revisited. It was found that careful addition of 1.0 equivalent of acetic anhydride (as opposed to 10.0 molar eq., excess) could generate high amounts of C4 acetamide while retaining a free hydroxyl at C3, which can be attributed to nitrogen's higher nucleophilicity when compared to the competing C3 nucleophile. Overall, this resulted in a 40% isolated yield of compound **3.22**. The temporary anomeric protecting group was left on for stability purposes and is thought to be easily removed with TBAF once ready for further enzymatic testing.[120,121]

Following generation of the C4 acetamide, phthalimide removal utilizing hydrazine monohydrate was performed. Under standard conditions, only trace amounts of compound **3.23** were observed. Generation of white precipitate (the phthalhydrazide byproduct) is expected when the reaction proceeds successfully, which was not visualized. As a result, excess amounts of hydrazine were additionally added to the reaction. Upon addition, the reaction was observed via TLC to go to completion and significant amounts of precipitate were visually observed. After purification, an isolated 80% yield of the desired 2-amino-4-acetamido compound **3.23** was obtained. **Scheme 3.6** represents the optimized pathway from compound **3.18** to the desired 2-amino-4-diacetamide, hexose **3.23**. Again, the temporary anomeric protecting group was left on for stability purposes and is thought to be easily removed with TBAF once ready for further enzymatic testing. Due to the previous variability in success of phthalimide removal under standard conditions, all subsequent reactions were performed in an excess of hydrazine monohydrate and run until precipitate generation was visually observed.

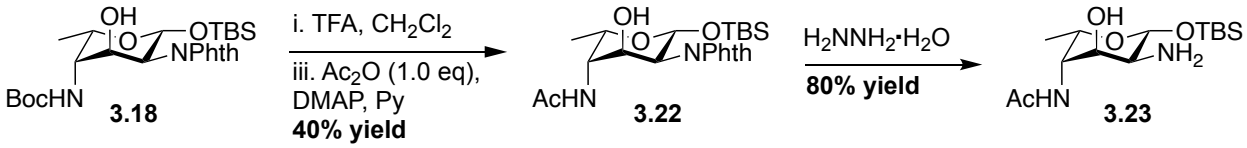


**Scheme 3.6.** Optimized pathway from D-threonine derived DATDH to the 2-amino-4-acetamido-2,4,6-trideoxyhexose.

## 3.2.4. Scope Expansion

After an establishing a route to D-threonine derivatized compounds **3.21** and **3.23**, scope expansion was performed to access other isomeric 2-amino-4-acetamido-2,4,6-trideoxyhexoses. Regarding the L-threonine derived compound **3.24**, a one-pot, two step Boc removal and acetylation to generate sugar **3.25** was performed in 42% yield in the same manner as was done for generation of compound **3.21**. A one-pot, two step phthalimide removal and acetylation of **3.25** followed, which successfully generated the desired compound **3.26** in 20% yield (**Scheme 3.7**). Though yields could be improved for this pathway through additional optimization and more careful handling of material, it was more imperative that biological studies go underway in a timely manner. As a result, this route was not further optimized.

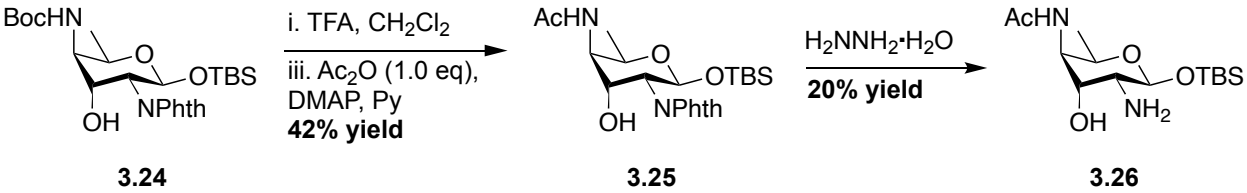


**Scheme 3.7.** Route from L-threonine derived DATDH toward the 2-amino-4-acetamido-2,4,6-trideoxyhexose.

Additional work on the D-*allo* and L-*allo*threonine derived sugars, to access their 2-amino-4-acetamido-2,4,6-trideoxyhexose derivatives, was done. Along the way, improved yield of the allylation chemistry from L-*allo*threoninol can be noted. A 70% isolated yield of the allylation product **2.40** was reported, which is compared to the previously reported 48% yield in Chapter 2 (*vide supra*). While scale up of the L-*allo* and D-*allo* derived allylations and subsequent TBS removal to access compound **2.18** and **2.17** was straightforward, oxidative cleavage of these species was not. Various attempts at isolation of the oxidatively cleaved products **2.41** and **2.39** was attempted with no success. All starting material was consumed, but product could not be collected in any attempts. Decomposition in high amounts can be reported. Due to these difficulties, as well as the inherent safety concerns that come with working with $OsO_4$, this pathway was temporarily tabled. Alternative oxidative conditions for scale-up of this pathway should be pursued in the future, to avoid inherent scalability and safety issues. However, this fell beyond the scope of work deemed necessary for this project, as it stands.

## 3.3. Conclusions

Conclusively, seven routes to newly derivatized deoxy-amino compounds were developed and characterized. These compounds are now ready for various methods of enzymatic testing and/or for the potential of further chemical transformations. It is envisioned that access to these kinds of deoxy-amino compounds will shed light on their mechanisms of action in biologic systems and could be further utilized for the development of novel therapeutics. Additionally, small modifications to these sugars at the anomeric position could allow for glycosylation ready donors, opening the door for even more complex oligosaccharide syntheses.

## 3.4. Materials and Experimental Methods

### 3.4.1. General Experimental Procedures

Unless otherwise stated, all reactions were carried out under an argon in flame dried reaction vessels. $CH_2Cl_2$, THF, and 1,4-dioxane were rendered anhydrous through a commercial solvent purification system (Inert). All other solvents were dried over activated molecular sieves prior to use. All other chemicals were purchased at the highest possible quality and used as received.

Flash column chromatography was performed on 230−400 mesh silica gel. Analytical and preparative thin layer chromatography was carried out on silica gel 60 F-254 plates. Products were visualized with UV light or by staining with potassium permanganate, 5% aqueous sulfuric acid, or ninhydrin followed by heating.

### 3.4.2. Spectroscopy, Spectrometry, and Data Collection

NMR spectra were recorded on a Bruker NMR spectrometer at 500 MHz for $^{1}H$ NMR and 125 MHz for $^{13}C$ NMR. Structural assignments were made with additional information from gCOSY and gHSQC experiments. For $CDCl_3$ solvent, chemical shifts are reported in ppm relative to TMS (for $^{1}H$ NMR in $CDCl_3$) or $CDCl_3$ (for $^{13}C$ NMR in $CDCl_3$). For $C_6D_6$ solvent, chemical shifts are reported in ppm relative to $C_6D_6$ (for $^{1}H$ and $^{13}C$ NMR). For $^{1}H$ NMR spectra, data are reported as follows: δ shift, multiplicity (s = singlet, m = multiplet, t = triplet, d = doublet, q = quartet, qd, quartet of doublets, dd = doublet of doublets, ddd = doublet of doublet of doublets), coupling constants are reported in Hz. To prove the existence of rotamers, 1-D NOE experiments were conducted according to procedure reported by Ley, et al on a 500 MHz Bruker NMR.[104] High-resolution mass spectra (HRMS) were obtained on an Agilent 6230 TOF mass spectrometer in the positive ion mode. Optical rotations were measured at 589 nm in a 10 cm cell at 23 °C.

## 3.4.3. Experimental Procedures and Spectral Data

**Synthesis of 3.19**

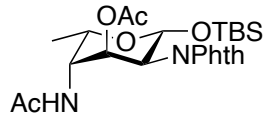


Compound **3.18** (20.0 mg, 0.0395 mmol, 100 mol%) was added to a flame dried flask and dissolved in in $CH_2Cl_2$ (0.40 mL). TFA (0.07 mL, .0998 mmol, 250 mol%) was added dropwise and the reaction allowed to run at room temperature for 1 hour, in which time the reaction mixture was observed to turn pink in color. The resulting mixture was then concentrated *in vacuo*. Ten minutes after drying, the resulting solid was dissolved in pyridine (2 mL). DMAP (5 mol%) and acetic anhydride (2 mL) were added, and the reaction was allowed to run at room temperature for 12 hours, then concentrated *in vacuo* to remove excess pyridine. The mixture was partitioned between EtOAc and $H_2O$ and the organic layer washed with an aqueous $Cu(II)SO_4$ x $5H_2O$ solution (1x), $H_2O$ (3x), brine (1x), dried over $Na_2SO_4$, filtered, and concentrated *in vacuo*. The resulting solution was diluted with minimal $CH_2Cl_2$, and purified via preparatory plate chromatography (50% EtOAc:Hex) to furnish compound **3.19** as a clear-white film (20.1 mg, 0.0410 mmol, quant. yield).

**$^1$H NMR** (500 MHz, $CDCl_3$) δ 7.86 – 7.74 (m, 2H), 7.73 – 7.68 (m, 2H), 6.09 (d, *J* = 9.1 Hz, 1H), 5.99 (d, *J* = 8.4 Hz, 1H), 5.30 – 5.25 (m, 1H), 4.35 (qd, *J* = 6.5, 1.9 Hz, 1H), 4.22 (dd, *J* = 8.5, 2.9 Hz, 1H), 4.09 – 4.04 (m, 1H), 2.14 (s, 3H), 2.03 (s, 3H), 1.23 (d, *J* = 6.6 Hz, 3H), 0.70 (s, 9H), 0.11 (s, 3H), 0.04 (s, 3H).

**$^{13}$C NMR** (126 MHz, $CDCl_3$) δ 170.2, 170.1, 168.3, 134.3, 132.0, 131.5, 123.6, 123.1, 92.0, 71.4, 69.0, 84.5, 51.7, 25.5, 23.4, 21.0, 16.7, -3.9, -5.5.

HRMS (ESI) *m/z*: $[M + Na]^+$ calcd for $C_{24}H_{34}N_2O_7Si$+Na: 513.2032; found: 513.2033

$[\alpha]^{23}_D$: +12.5 ($CH_2Cl_2$, c = 0.01153 g/mL)

**Synthesis of 3.22**

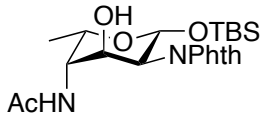


Compound **3.18** (371.8 mg, 0.734 mmol, 100 mol%) was added to a flame dried flask and dissolved in in $CH_2Cl_2$ (7.5 mL). TFA (0.56 mL, 7.34 mmol, 1000 mol%) was added dropwise and the reaction allowed to run at room temperature for 2 hours, in which time the reaction mixture was observed to turn red in color. The resulting mixture was then concentrated *in vacuo*. Ten minutes after drying, the resulting solid was dissolved in pyridine (10.9 mL). DMAP (4.12 mg, 0.03367 mmol, 5 mol%) and acetic anhydride (0.14 mL, 1.47 mmol, 200 mol%) were added, and the reaction was allowed to run at room temperature for 12 hours, then concentrated *in vacuo* to remove excess pyridine. The mixture was partitioned between EtOAc and $H_2O$ and the organic layer washed with an aqueous $Cu(II)SO_4$ x $5H_2O$ solution (1x), $H_2O$ (3x), brine (1x), dried over $Na_2SO_4$, filtered, and concentrated *in vacuo*. The resulting solution was diluted with minimal $CH_2Cl_2$, and purified via column chromatography (60-80% EtOAc:Hex) to furnish a mixture of desired compound **3.22** as a white solid (131.6 mg, 0.294 mmol, 40% yield). Peracetylated compound **3.19** was also generated, which was to be expected.

**$^1$H NMR** (500 MHz, $CDCl_3$) δ 7.87 (dd, *J* = 5.4, 3.0 Hz, 2H), 7.76 (dd, *J* = 5.5, 3.0 Hz, 2H), 6.04 (d, *J* = 8.9 Hz, 1H), 5.71 (d, *J* = 8.5 Hz, 1H), 4.83 (d, *J* = 1.9 Hz, 1H), 4.51 (qd, *J* = 6.5, 1.8 Hz, 1H), 4.22 (dd, *J* = 8.6, 2.5 Hz, 1H), 4.17 – 4.12 (m, 1H), 4.08 – 4.04 (m, 1H), 2.07 (s, 3H), 1.21 (d, *J* = 6.6 Hz, 3H), 0.65 (s, 9H), 0.05 (s, 3H), -0.06 (s, 3H).

**$^{13}$C NMR** (126 MHz, $CDCl_3$) δ 170.39, 134.59, 131.63, 123.67, 91.48, 71.44, 68.01, 56.25, 53.85, 25.39, 23.45, 17.56, 16.68, -4.01, -5.61.

HRMS (ESI) *m/z*: $[M + Na]^+$ calcd for $C_{22}H_{32}N_2O_6Si$+Na: 471.1928; found: 471.1931

$[\alpha]^{24}_D$: +24.2 ($CH_2Cl_2$, c = 0.009912 g/mL)

**Synthesis of 3.20**

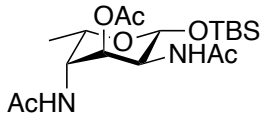


Compound **3.19** (100.0 mg, 0.204 mmol, 100 mol%) was added to a flame dried flask and dissolved in EtOH (8.0 mL). Hydrazine monohydrate (0.013 mL, 0.265 mmol, 130 mol%) was added dropwise and the reaction was allowed to reflux for 12 hours. Upon completion of the reaction, a white solid is observed at the bottom of the reaction flask. (If this byproduct is not observed, an additional 130 mol% of hydrazine is additionally added and the reaction is allowed to continue refluxing until ppt. formation is visibly observed.) Upon completion, the solid byproduct was filtered, and the mother liquor was concentrated *in vacuo*. Two hours after drying, the resulting solid was dissolved in pyridine (1 mL). DMAP (1.14 mg, .0102 mmol, 5 mol%) and acetic anhydride (1 mL) were added, and the reaction was allowed to run at room temperature for 12 hours, then concentrated *in vacuo* to remove excess pyridine. The mixture was partitioned between EtOAc and $H_2O$ and the organic layer washed with an aqueous $Cu(II)SO_4x5H_2O$ solution (1x), $H_2O$ (3x), brine (1x), dried over $Na_2SO_4$, filtered, and concentrated *in vacuo*. The resulting solution was diluted with minimal $CH_2Cl_2$, and purified via preparatory thin layer chromatography (1000μM, 60% EtOAc:Hex) to furnish compound **3.20** as a clear-white film (74.7 mg, 0.186 mmol, 91% yield).

**$^1$H NMR** (500 MHz, $CDCl_3$) δ 5.89 (d, *J* = 9.5 Hz, 1H), 5.34 (d, *J* = 9.4 Hz, 1H), 5.09 – 5.06 (m, 1H), 4.74 (d, *J* = 8.2 Hz, 1H), 4.18 – 4.11 (m, 2H), 4.04 – 4.00 (m, 1H), 2.16 (s,

3H), 2.07 (s, 3H), 1.97 (s, 3H), 1.15 (d, *J* = 6.5 Hz, 3H), 0.89 (s, 9H), 0.12 (s, 3H), 0.11 (s, 3H).

**$^{13}$C NMR** (126 MHz, $CDCl_3$) δ 170.02, 169.57, 95.56, 72.44, 68.67, 50.30, 50.10, 25.69, 23.58, 23.45, 21.23, 18.03, 16.64, -3.73, -5.29.

HRMS (ESI) *m/z*: $[M + Na]^+$ calcd for $C_{18}H_{34}N_2O_6Si$+Na: 425.2084; found: 425.2082

$[\alpha]^{23}_D$: +1.96 ($CH_2Cl_2$, c = 0.0143 g/mL)

**Synthesis of 3.21**

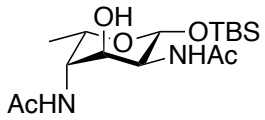


Compound **3.20** (15.8 mg, 0.0392 mmol, 100 mol%) was added to a flame dried flask and dissolved in MeOH (2.0 mL). NaOMe (0.42 mg, 0.0078 mmol, 20 mol%) was added and the reaction was allowed to stir and room temperature for 12 hours. Upon completion, the reaction mixture was concentrated *in vacuo*. The resulting solution was diluted with minimal $CH_2Cl_2$ and purified via preparatory thin layer chromatography (500μM, 5% MeOH: $CH_2Cl_2$) to furnish compound **3.21** as a clear-white film (9.8 mg, 0.0272 mmol, 69% yield).

**$^1$H NMR** (400 MHz, $CDCl_3$) δ 6.00 (d, *J* = 8.8 Hz, 1H), 5.90 (d, *J* = 9.2 Hz, 1H), 4.82 (d, *J* = 8.3 Hz, 1H), 4.29 – 4.23 (m, 1H), 4.03 – 3.98 (m, 1H), 3.98 – 3.92 (m, 2H), 3.38 (s, 1H), 2.06 (s, 3H), 2.03 (s, 3H), 1.19 (d, *J* = 6.6 Hz, 3H), 0.92 (s, 10H), 0.14 (s, 3H), 0.12 (s, 3H).

**$^{13}$C NMR** (101 MHz, $CDCl_3$) δ 171.85, 166.07, 95.28, 77.36, 70.43, 67.28, 56.14, 53.78, 51.59, 29.85, 25.70, 23.77, 23.49, 16.73, -5.36.

HRMS (ESI) *m/z*: $[M + Na]^+$ calcd for $C_{16}H_{32}N_2O_5Si$+Na: 383.1978; found: 383.1977

$[\alpha]^{24}_D$: +2.80 ($CH_2Cl_2$, c = 0.0075 g/mL)

**Synthesis of 3.23**

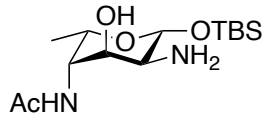


Compound **3.22** (79.3 mg, 0.162 mmol, 100 mol%) was added to a flame dried flask and dissolved in EtOH (6.35 mL). Hydrazine monohydrate (0.013 mL, 0.259 mmol, 160 mol%) was added dropwise and the reaction was allowed to reflux for 12 hours. Upon completion of the reaction, a white solid is observed at the bottom of the reaction flask. (If this byproduct is not observed, an additional 130 mol% of hydrazine is additionally added and the reaction is allowed to continue refluxing until ppt. formation is visibly observed.) Upon completion, the solid byproduct was filtered, and the mother liquor was concentrated *in vacuo*. The resulting solution was diluted with minimal $CH_2Cl_2$ and purified via preparatory thin layer chromatography (1000μM, 20% MeOH: $CH_2Cl_2$,1% $Et_3N$) to furnish compound **3.23** as a clear-white film (41.3 mg, 0.106 mmol, 80% yield).

**$^1$H NMR** (500 MHz, $CDCl_3$) δ 5.92 (d, *J* = 8.7 Hz, 1H), 4.68 (d, *J* = 8.0 Hz, 1H), 4.20 (qd, *J* = 6.6, 1.6 Hz, 1H), 3.98 – 3.93 (m, 2H), 3.49 (s, 1H), 2.77 (s, 1H), 2.64 – 2.61 (m, 1H), 2.02 (s, 3H), 1.16 (d, *J* = 6.5 Hz, 3H), 0.93 (s, 9H), 0.14 (s, 3H), 0.14 (s, 3H).

**$^{13}$C NMR** (126 MHz, $CDCl_3$) δ 170.60, 97.83, 70.08, 68.04, 54.07, 53.85, 45.62, 26.18, 23.67, 18.50, 16.98, -3.62, -4.78.

HRMS (ESI) *m/z*: $[M + Na]^+$ calcd for $C_{14}H_{30}N_2O_4Si$+Na: 341.1873; found: 341.1884; 319.2039

$[\alpha]^{24}_{D}$: +13.5($CH_2Cl_2$, c = 0.011 g/mL)

**Synthesis of 3.25**

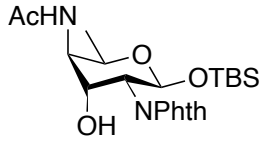


Compound **3.24** (146.0 mg, 0.288 mmol, 100 mol%) was added to a flame dried flask and dissolved in in $CH_2Cl_2$ (2.9 mL). TFA (0.22 mL, 2.88 mmol, 1000 mol%) was added dropwise and the reaction allowed to run at room temperature for 1 hour, in which time the reaction mixture was observed to turn dark pink in color. The resulting mixture was then concentrated *in vacuo*. Five minutes after drying, the resulting solid was dissolved in pyridine (4.27 mL). DMAP (1.62 mg, 0.0144 mmol, 5 mol%) and acetic anhydride (0.027 mL, 0.288 mmol, 100 mol%) were added, and the reaction was allowed to run at room temperature for 12 hours, then concentrated *in vacuo* to remove excess pyridine. The mixture was partitioned between EtOAc and $H_2O$ and the organic layer washed with an aqueous $Cu(II)SO_4 \times 5H_2O$ solution (1x), $H_2O$ (2x), brine (1x), dried over $Na_2SO_4$, filtered, and concentrated *in vacuo*. The resulting solution was diluted with minimal $CH_2Cl_2$, and purified via preparatory plate chromatography (1000μM, 70% EtOAc:Hex) to furnish a mixture of desired compound **3.25** as a white amorphous solid (54.8 mg, 0.122 mmol, 42% yield). Peracetylated compound was also generated in appreciable amounts, which was to be expected.

**$^1$H NMR** (500 MHz, $CDCl_3$) δ 7.87 (dd, *J* = 5.5, 3.1 Hz, 2H), 7.76 (dd, *J* = 5.5, 3.0 Hz, 2H), 6.01 (d, *J* = 8.9 Hz, 1H), 5.69 (d, *J* = 8.5 Hz, 1H), 4.80 (d, *J* = 1.8 Hz, 1H), 4.51 (qd, *J* = 6.4, 1.7 Hz, 1H), 4.24 – 4.21 (m, 1H), 4.17 – 4.14 (m, 1H), 4.08 – 4.05 (m, 1H), 1.21 (d, *J* = 6.4 Hz, 3H), 0.65 (s, 9H), 0.05 (s, 3H), -0.06 (s, 3H).

**$^{13}$C NMR** (126 MHz, $CDCl_3$) δ 170.37, 134.62, 131.63, 123.70, 91.48, 71.48, 68.02, 56.25, 53.85, 25.39, 23.47, 17.57, 16.68, -4.00, -5.60.

HRMS (ESI) *m/z*: $[M + Na]^+$ calcd for $C_{22}H_{32}N_2O_6Si$+Na: 471.1928; found: 471.1929

$[\alpha]^{24}_D$: -21.9 ($CH_2Cl_2$, c = 0.011 g/mL)

## 3.5. References


(1) Schmidt, M. A.; Riley, L. W.; Benz, I. Sweet New World: Glycoproteins in Bacterial Pathogens. *Trends Microbiol.* **2003**, *11* (12), 554–561.

(2) Morrison, M. J.; Imperiali, B. The Renaissance of Bacillosamine and Its Derivatives: Pathway Characterization and Implications in Pathogenicity. *Biochemistry* **2014**, *53* (4), 624–638.

(3) Upreti, R. K.; Kumar, M.; Shankar, V. Bacterial Glycoproteins: Functions, Biosynthesis and Applications. *Proteomics* **2003**, *3* (4), 363–379.

(4) Harnagel, A. P.; Sheshova, M.; Zheng, M.; Zheng, M.; Skorupinska-Tudek, K.; Swiezewska, E.; Lupoli, T. J. Preference of Bacterial Rhamnosyltransferases for 6-Deoxysugars Reveals a Strategy To Deplete O-Antigens. *J. Am. Chem. Soc.* **2023**, *145* (29), 15639–15646.

(5) Varki, A. ; S. R. L. ; S. R. Sialic Acids and Other Nonulosonic Acids. In *Essentials of Glycobiology*; Cold Spring Harbor Laboratory Press, 2017.

(6) Varki, A.; Cummings, R.; Esko, J.; Freeze, H.; Hart, G.; Marth, J. *Essentials of Glycobiology*; Varki, A., Ed.; Cold Spring Harbor Laboratory Press: Cold Spring Harbor, New York, 1999.

(7) Van Deun, K.; Pasmans, F.; Ducatelle, R.; Flahou, B.; Vissenberg, K.; Martel, A.; Van den Broeck, W.; Van Immerseel, F.; Haesebrouck, F. Colonization Strategy of Campylobacter Jejuni Results in Persistent Infection of the Chicken Gut. *Vet. Microbiol.* **2008**, *130* (3–4), 285–297.

(8) Nothaft, H.; Szymanski, C. M. Bacterial Protein N-Glycosylation: New Perspectives and Applications. *J. Biol. Chem.* **2013**, *288* (10), 6912–6920.

(9) Liu, B.; Furevi, A.; Perepelov, A. V; Guo, X.; Cao, H.; Wang, Q.; Reeves, P. R.; Knirel, Y. A.; Wang, L.; Widmalm, G. Structure and Genetics of *Escherichia Coli* O Antigens. *FEMS Microbiol. Rev.* **2020**, *44* (6), 655–683.

(10) Maki, M. Biosynthesis of 6-Deoxyhexose Glycans in Bacteria. *Glycobiology* **2003**, *14* (3), 1R – 15.

(11) Li, W.; McArthur, J. B.; Chen, X. Strategies for Chemoenzymatic Synthesis of Carbohydrates. *Carbohydr. Res.* **2019**, *472*, 86–97.

(12) Gijsen, H. J. M.; Qiao, L.; Fitz, W.; Wong, C.-H. Recent Advances in the Chemoenzymatic Synthesis of Carbohydrates and Carbohydrate Mimetics. *Chem. Rev.* **1996**, *96* (1), 443–474.

(13) Schauer, R.; Corfield, A. P. Isolation and Purification of Sialic Acids; 1982; pp 51–57.

(14) White-Phillip, J.; Thibodeaux, C. J.; Liu, H. Enzymatic Synthesis of TDP-Deoxysugars; 2009; pp 521–544.

(15) Kay, H. D.; Robison, R. The Role of Phosphates in Carbohydrate Metabolism. *Biochem. J.* **1924**, *18* (5), 1139–1151.

(16) Liu, Y.; Nishimoto, M.; Kitaoka, M. Facile Enzymatic Synthesis of Sugar 1-Phosphates as Substrates for Phosphorylases Using Anomeric Kinases. *Carbohydr. Res.* **2015**, *401*, 1–4.

(17) Naught, L. E.; Tipton, P. A. Formation and Reorientation of Glucose 1,6-Bisphosphate in the PMM/PGM Reaction: Transient-State Kinetic Studies. *Biochemistry* **2005**, *44* (18), 6831–6836.

(18) Zheng, M.; Zheng, M.; Lupoli, T. J. Expanding the Substrate Scope of a Bacterial Nucleotidyltransferase via Allosteric Mutations. *ACS Infect. Dis.* **2022**, *8* (10), 2035–2044.

(19) Ahmadipour, S.; Beswick, L.; Miller, G. J. Recent Advances in the Enzymatic Synthesis of Sugar-Nucleotides Using Nucleotidylyltransferases and Glycosyltransferases. *Carbohydr. Res.* **2018**, *469*, 38–47.

(20) Vasquez, O.; Alibrandi, A.; Bennett, C. S. De Novo Synthetic Approach to 2,4-Diamino-2,4,6-Trideoxyhexoses (DATDH): Bacterial and Rare Deoxy-Amino Sugars. *Org. Lett.* **2023**, *25* (43), 7873–7877.

(21) Greene, T. W.; Wuts, P. G. M. *Protective Groups in Organic Synthesis*, 3rd ed.; John Wiley & Sons, Inc.: New York, 1999.

(22) Hu, D. X.; Grice, P.; Ley, S. V. Rotamers or Diastereomers? An Overlooked NMR Solution. *J. Org. Chem.* **2012**, *77* (11), 5198–5202.

# Chapter 4: Toward the Synthesis of 8-*epi*-Legionaminic Acid (8epiLeg)

## 4.1 Introduction

### 4.1.1. Overview and Retrosynthetic Analysis

As was discussed in Chapter 1 (*vide supra*), nonulosonic acids (NulOs) play a significant role in bacterial pathogenicity and fitness. However, their structural complexity (resulting difficult chemical synthesis) as well as their inability to be isolated from their native CPS/LPS, prevents access to significant amounts of these sugars to be studied and, consequently, better understood. Previous syntheses of these compounds have been performed either semi-synthetically or synthetically, but with varying levels of diastereoselectivity and low overall yield (see **Section 1.2**). Herein, we propose and attempt various *de novo* synthetic approaches toward 8-*epi*-legionaminic acid (8epiLeg) that could result in a higher yielding, more efficient, and more diastereoselective route toward this NulO than was previously available.

Retrosynthetically, we envision 8epiLeg arising via a late stage 6-member ring cyclization from long-chain intermediate **4.2**. Intermediate **4.2** is to be generated via a diastereoselective C4 hydroxyl insertion using conditions and starting material **4.3**. Compound **4.3** will arise from a Krische allylation of D-threoninol **4.4**. **Scheme 4.1** depicts the retrosynthetic analysis of 8epiLeg from threoninol **4.4**. In the forward direction, from compound **4.3** to compound **4.2**, various sets of conditions are explored. **Sections 4.2.1 – 4.2.3** describes three different hypothesized routes toward the generation of 8epiLeg from allylation intermediate **4.3**, each of which are met with varying levels of success thus far.

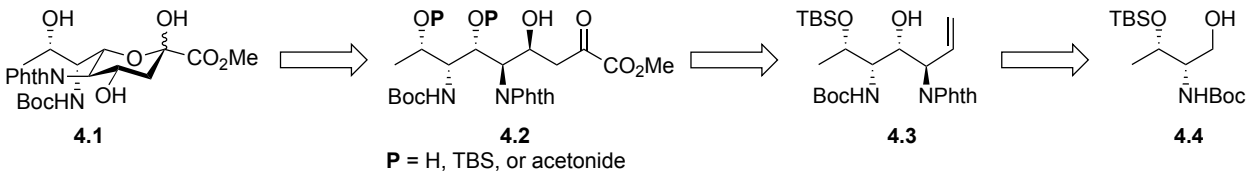


**Scheme 4.1.** Retrosynthetic analysis of 8-*epi*-Legionaminic acid from protected D-threoninol starting material.

## 4.2 Chemical Elongation Strategies Toward 8-epi-Leg

### 4.2.1. Olefin Cross Metathesis Strategy

Originally, it was envisioned that an olefin cross metathesis of allylation product **4.3** with a 4- or 5-carbon enone facilitated by the Grubbs II ruthenium catalyst could give rise to a cross-coupling product **4.5** in a key C-C bond forming step (**Scheme 4.2**).[122] In the forward direction, a substrate controlled, NHC-catalyzed, stereoselective conjugate addition utilizing an NHC-ligand (**Figure 4.1**) could generate the C4 stereocenter needed to complete the synthesis of a 9-carbon 8epiLeg derivative **4.6**.[123–127] With TBS protection at the C8 position, differentiation between both secondary hydroxyls is given, which would allow for selectivity between C8 and C4, should that be desired. For the purposes of this work, however, the alcohol protection is proposed to be removed to generate the deprotected sugar target **4.7**. Additional differentiation between amino sites arises via a Boc and phthalimide protection at C7 and C5, which could subsequently be removed under the right deprotection conditions, if desired. **Scheme 4.2** demonstrates the theorized pathway toward 8epiLeg. **Figure 4.1** depicts the potential catalyst candidates, boron source, and NHC-ligand for the proposed route.

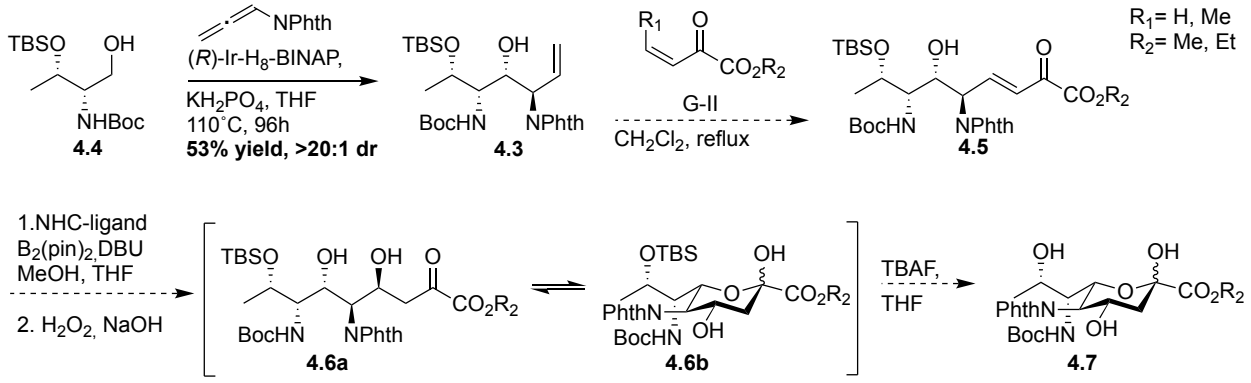


**Scheme 4.2.** Proposed synthetic route to 8epiLeg using an olefin cross metathesis strategy followed by stereoselective conjugate addition.

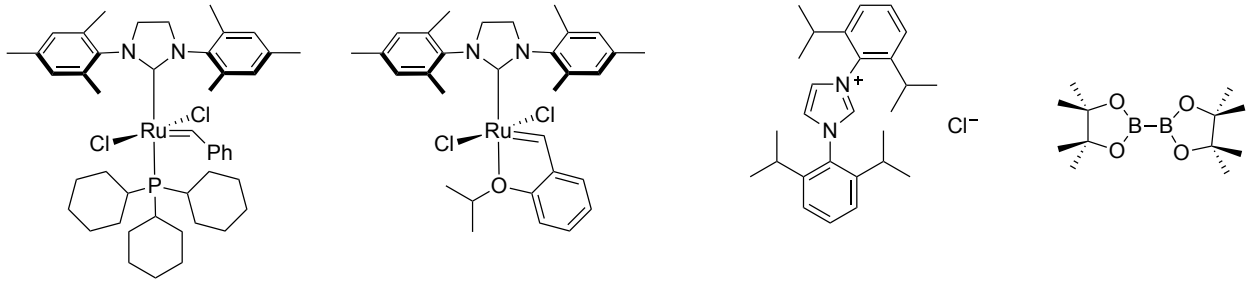


**Figure 4.1.** Chemical structure of catalysts and additives in the proposed synthesis of 8epiLeg using olefin cross metathesis followed by stereoselective conjugate addition.

To screen Grubbs cross-metathesis conditions, 4- and 5-carbon enones were first generated as cross coupling partners. As a prerequisite for olefin cross metathesis, enones of a certain Grubbs "type" had to be selected.[122] Which enones were chosen was based on their predicted reactivity with olefin cross-coupling partner **4.3** under Grubbs II catalyst, cross metathesis conditions, and their inability to quickly homodimerize.[122] Additional factors, such as high volatility of these low molecular weight enones, had to also be considered. To this end, a variety of conditions were explored and optimized to successfully synthesis two desired enone cross-coupling partners.

Toward desired enone **4.9**, *cis*-propenyl magnesium bromide was first synthesized, and its molarity subsequently determined.[128] To generate the *cis*-propenyl magnesium bromide, a reaction between *cis*-1-bromopropene, magnesium turnings, and iodine was performed under varying solvent concentrations (**Table 4.1**). [128] Due to concerns pertaining the generated exotherm of the Grignard reaction (loss in THF due to aggressive boiling), reaction concentration was incrementally increased until a 0.69 M concentration in THF was obtained, and the product concentration determined to be sufficient for the following reaction. Upon completion of each reaction, a titration with iodine was performed to determine molarity of the Grignard reagent (see **Section 4.4.3** for experimental details).

**Table 4.1**. Generation of desired Grignard reagent from *cis*-propenyl bromide.

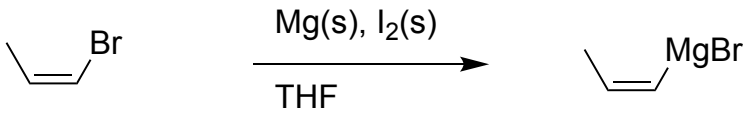


| Entry | Reaction Conc (M) | % yield | Prod. Conc in THF (M) |
|---|---|---|---|
| 1 | 0.5 | assumed quant. | — |
| 2 | 0.5 | 42 | 0.21 |
| 3 | 0.5 | 34 | 0.17 |
| 4 | 1.0 | 39 | 0.39 |
| **5** | **2.0** | **34** | **0.69** |

Immediately following generation of the Grignard reagent, a Grignard reaction utilizing the *cis*-propenyl magnesium bromide and commercially available diethyl oxalate **4.8** was performed. This generated the desired enone compound **4.9**. Various sets of conditions were explored toward synthesis of this compound (**Table 4.2**).[129,130] Molarity of the Grignard, solvent choice, reaction temperature, and reaction time were all optimized. Additionally, development of a gas chromatography (GC) method was required to monitor product formation, since the product was too unstable and volatile for formation monitoring via thin-layer chromatography (TLC). Entry 4 of **Table 4.2** shows the optimized conditions,[129] which resulted in a 30% product yield (mixture of (*E)* / (*Z*) isomers) and, additionally, a small amount of overreacted starting material byproduct. Due to the nature of the next reaction, it was not imperative that this be purified further before moving on to olefin cross metathesis. In addition to the generation of enone **4.9**, enone **4.11** was also synthesized. Starting with methyl vinyl glycolate (MVG) **4.10**, an oxidation utilizing Dess-Martin periodinane generated the desired methyl 2-oxobut-3-enoate **4.11**.[131] As a result of product volatility, compound **4.11** was obtained as a solution in dichloromethane.

**Table 4.2.** Optimization of conditions for the generation of enone **4.9**.

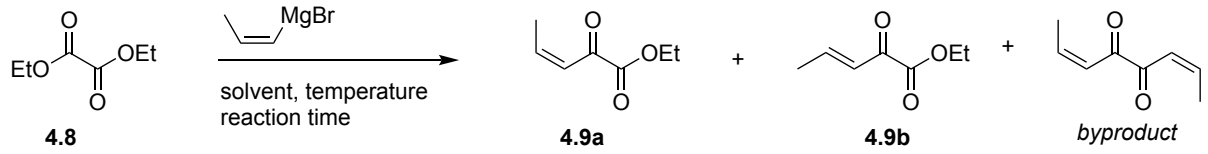


| Entry | Grignard mol. eq. | Grignard Molarity | Solvent | Reaction Temperature (˚C) | Reaction Time | % Yield | Notes |
|---|---|---|---|---|---|---|---|
| 1 | 1.4 | 0.21M | THF | -78 | 7hrs | 0 | S.M. recovered |
| 2 | 1.4 | 0.17M | THF | 0 to r.t. | 12 hrs | 0 | no distillation prod. |
| 3 | 1.2 | 0.39M | THF | -78 to -60 | 4 hrs | 0 | no product |
| **4** | **1.2** | **0.69M** | **THF: Ether (1:1)** | **-80 to -60** | **3 hrs** | **30** | *E/Z* prod. mixture & over-reacted byproduct |

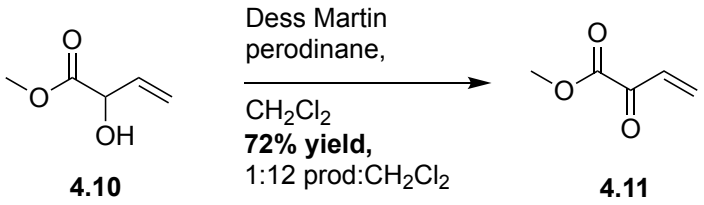


**4.10** **4.11**

**Scheme 4.3.** Synthesis of methyl 2-oxobut-3-enoate.

The resulting enones were then tested for viability as coupling partners for olefin cross metathesis with substrate **4.3**. Variables for optimization included reaction time, Lewis acid additive, solvent, and bath temperature, in attempts to push the reaction forward (**Table 4.3**). Because previous reports suggested allylamines could be challenging cross-coupling partners in OCM, the use of chlorodicyclohexylborane was deemed necessary to attempt improved substrate reactivity.[122,132,133] It was observed, however, that compound **4.3** acted as a "spectator," even with additional Lewis acid additive. This raised concerns over the C4 hydroxyl potentially causing deactivation of the ruthenium catalyst, the enones not being a reactive enough coupling partner, or the allylamine species not being a reactive enough species in general for this kind of olefin cross-metathesis.[122]

**Table 4.3.** Optimization of olefin cross metathesis.

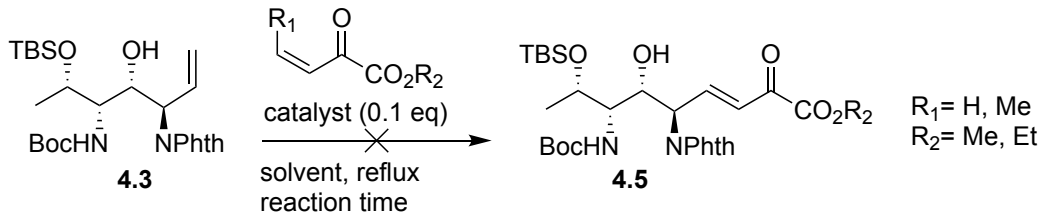


| Entry | $R_1$ | $R_2$ | Catalyst | Solvent | Reaction Temperature (˚C) | Reaction Time (h) | 10% L.A.? | % Yield* |
|---|---|---|---|---|---|---|---|---|
| 1 | Me | Et | G-II | $CH_2Cl_2$ | 40 | 24 | none | 0 |
| 2 | Me | Et | G-II | $CH_2Cl_2$ | 40 | 48 | $Cy_2BCl$ | 0 |
| 3 | Me | Et | M720 | toluene | 80 | 72 | $Cy_2BCl$ | 0 |
| 4 | H | Me | G-II | $CH_2Cl_2$ | 40 | 24 | none | 0 |
| 5 | H | Me | G-II | $CH_2Cl_2$ | 40 | 72 | $Cy_2BCl$ | 0 |

* No reaction. Starting material (**4.3**) recollected in all cases.

To disprove some of these theories, additional optimization under altered conditions was performed (**Table 4.4**). First, acetonide protected species **4.12** was generated from **4.14** (procedural details in Chapter 2, *vide supra*). Compound **4.12** was used to disprove substrate deactivation of the catalyst via the C4 hydroxyl. Additionally, allyl alcohol, a “type I” olefin known to be extremely reactive in OCM was utilized as a cross coupling partner.[122] With and without the addition of a titanium (IV) isopropoxide (TTIP) co-catalyst,[132,134,135] compound **4.12** remained a spectator in the reaction. As a result, and even with a variety of altered variables, it was concluded that the lack of reactivity of compound **4.3** / **4.12** was the problem with this chemistry.

**Table 4.4.** Additional optimizations to attempt chemical elongation via OCM.

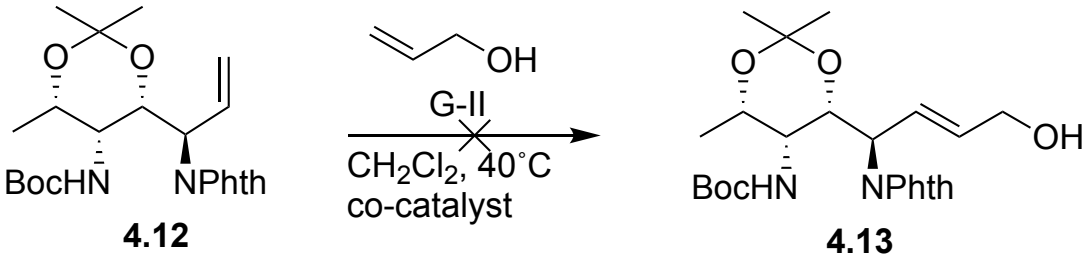


**4.12** **4.13**

| Entry | co-catalyst | % Yield* |
|---|---|---|
| 1 | N/A | 0 |
| 2 | TTIP | 0 |

* No reaction. Starting material (**4.12**) recollected in all cases.

The low reactivity of **4.3** / **4.12** in OCM is attributed to the electron withdrawing nature of the phthalimido amine, which removes electron density from the alkene moiety. The same difficulties have been faced for Boc protected secondary amines during olefin cross metathesis. Additionally, protecting group removal was not a modification that could be made to overcome the electron withdrawing effect of amino-protecting groups and increase substrate reactivity. This is because free amines have been reported to deactivate Grubbs catalysts.[136] Alternative amine protecting groups could, however, provide a more reactive alternative. As a result, these were to be explored. Unfortunately, phthalimide removal of the allylation product **4.12** was relatively unsuccessful (**Table 4.6** *vide infra*) because of its existing terminal alkene substituent. As a result, alternative strategies were pursued toward synthesis of the target 8epiLeg compound.

## 4.2.2. Mukaiyama Aldol Strategy

Given the lability of substrate **4.3** in olefin cross metathesis, a stereoselective Mukaiyama aldol reaction was proposed as an alternative. Hypothetically, this reaction would allow for a stereoselective aldol addition to generate desired 8epiLeg **4.1** from substrate **4.15**. **Scheme 4.4** depicts the proposed route. In the forward direction, an acetonide protection of allylation product **4.14** generates the isopropylidene **4.12**. Following this, oxidative cleavage via ozonolysis generates compound **4.15**. After generation of aldehyde **4.15**, a Mukaiyama aldol reaction with a silyl enol ether and lewis acid is theorized to generate compound **4.2** with high levels of stereocontrol. Standard acetonide removal would then generate the target compound **4.1** in its protected form.

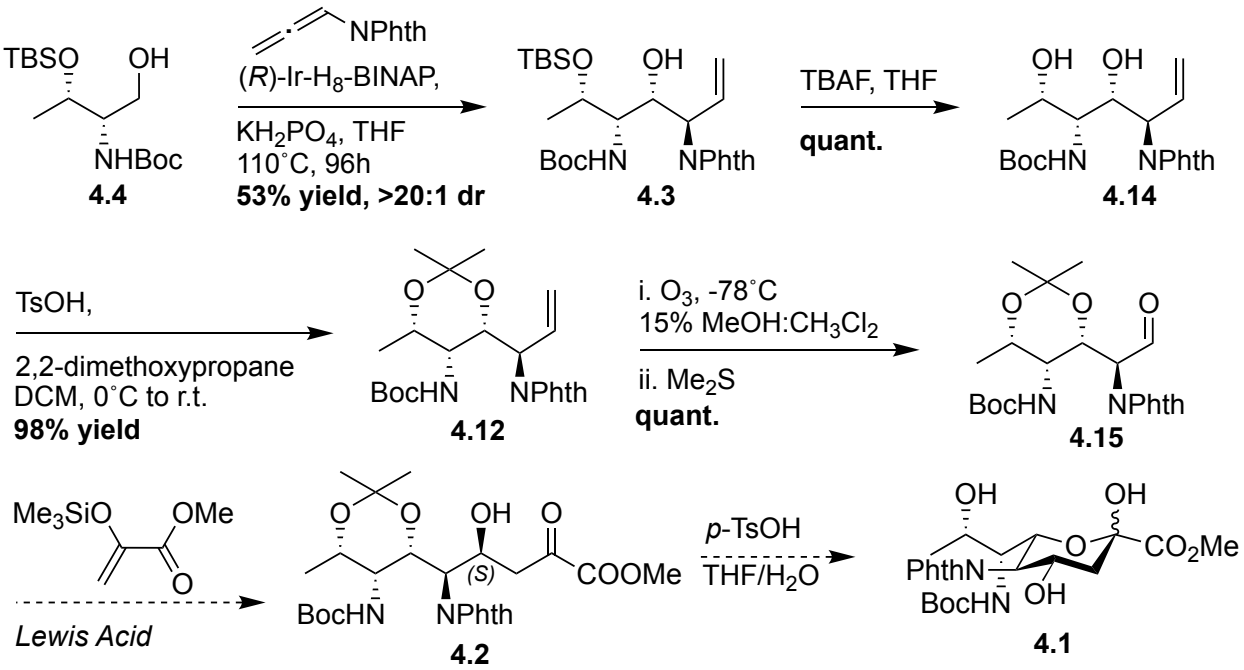


**Scheme 4.4.** Proposed forward synthesis of 8epiLeg from D-threoninol utilizing a stereoselective Mukaiyama aldol reaction.

To predict and tune stereochemical control over the aldol reaction, a Felkin or chelate control model was implemented to theorize over steric preferences during nucleophilic addition to the carbonyl. Under β-chelate control, it is hypothesized that orientation of the carbonyl would favor the desired product. Through Felkin control, it is theorized that sterics would allow preferential nucleophilic attack to generate the undesired product stereochemistry. However, and due to the complexity of the aldehyde **4.15**, it was possible that secondary steric interactions and/or, in the presence of chelation agents, secondary chelation effects could interfere with the proposed model for stereocontrol. As a result, we turned to experimental data to attempt to elucidate stereoselectivity outcome.

First, a Mukaiyama aldol reaction with free 1,3-diol **4.16**, silyl enol ether, and $BF_3$ etherate was carried out (**Scheme 4.5**). Under these conditions, no product formation was observed. It was reasoned that free alcohols could interfere with the reactivity, so further reactions were carried out with an isopropylidene-protected 1,3-diol substrate **4.15**.

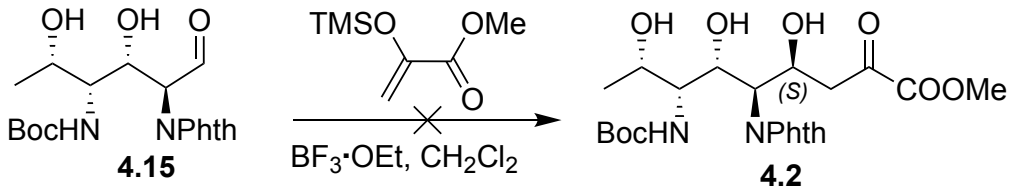


**Scheme 4.5.** Attempted Mukaiyama aldol reaction on 1,3-diol substrate.

To generate the acetonide protected aldehyde **4.15**, standard 1,3-diol isopropylidene protection of substrate **4.14** was first carried out utilizing TsOH and 2,2-

dimethoxypropane, synthesizing compound **4.12** in excellent yield. Following this, ozonolysis of the protected diol **4.12** was successfully performed, resulting in generation of compound **4.15** in quantitative yield. Formation of both acetonide protected compounds **4.12** and **4.15** resulted in observable rotamers on $^{1}H$ and $^{13}C$ NMR. As a result, standard NOE experimentation utilizing the Ley procedure was carried out as proof of rotamerization and as additional support of compound purity after chromatographic purification.[104] Following the generation of compound **4.15**, multiple aldol reactions with additives of varying levels of Lewis acidity and chelation potential were performed (see **Table 4.5**).[137,138] In all cases, no product was formed. In the case of entries 1 and 2, starting material **4.15** was fully recovered. In the case of entry 3, it was theorized that the high levels of acidity caused starting material **4.15** decomposition as well as a lack of product formation.

Regarding future directions, a broader scope of Lewis acids and solvent conditions should be explored to draw definitive conclusions about substrate reactivity. However, and in the interest of exploring an exciting new strategy, we turned our attention temporarily away from the Mukaiyama aldol route.

**Table 4.5.** Attempted optimization of Mukaiyama aldol chemistry on acetonide, exploring different Lewis acid additives.

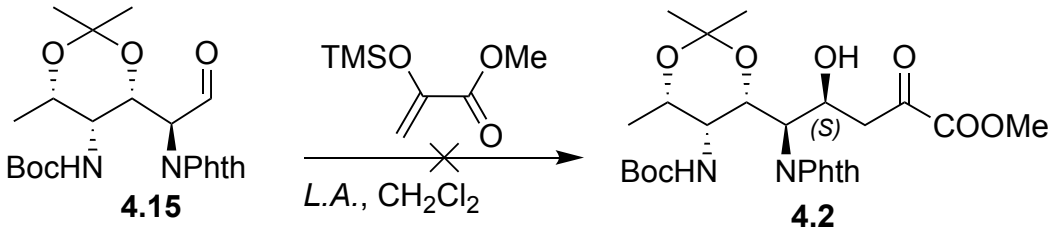


| Entry | Lewis Acid | Percent Yield |
|---|---|---|
| 1 | $MgBr_2$ | 0* |
| 2 | TTIP | 0* |
| 3 | $SnCl_4$ | 0 |

* No reaction. Starting material (**4.15**) recollected.

## 4.2.3. Diborylation Strategy

A third route toward 8epiLeg was proposed because of the lack in substrate reactivity for both the Mukaiyama aldol chemistry and olefin cross metathesis. **Scheme 4.6** illustrates this route in the forward direction from D-threoninol. Again, adapted Krische allylation chemistry allows for generation of a diastereoselective late-stage intermediate **4.3**.[90] After removal of the TBS group, acetonide protection of compound **4.14** is performed to generate isopropylidene **4.12**.[121] Afterward, it is hypothesized that a stereoselective diborylation of alkene **4.12** will generate dipinacol boron species **4.16.**[139–142] Subsequently, a Suzuki-Miyaura coupling of the generated organoborane species with methyl oxalyl chloride followed by oxidation would result in late stage intermediate **4.2**.[139] Upon removal of the acetonide protection under standard conditions, target 8epiLeg **4.1**

would be synthesized in a highly stereoselective fashion. **Figure 4.2** displays the chemical structures of the commercially available ligand, boron species, and electrophile required to execute this chemistry.

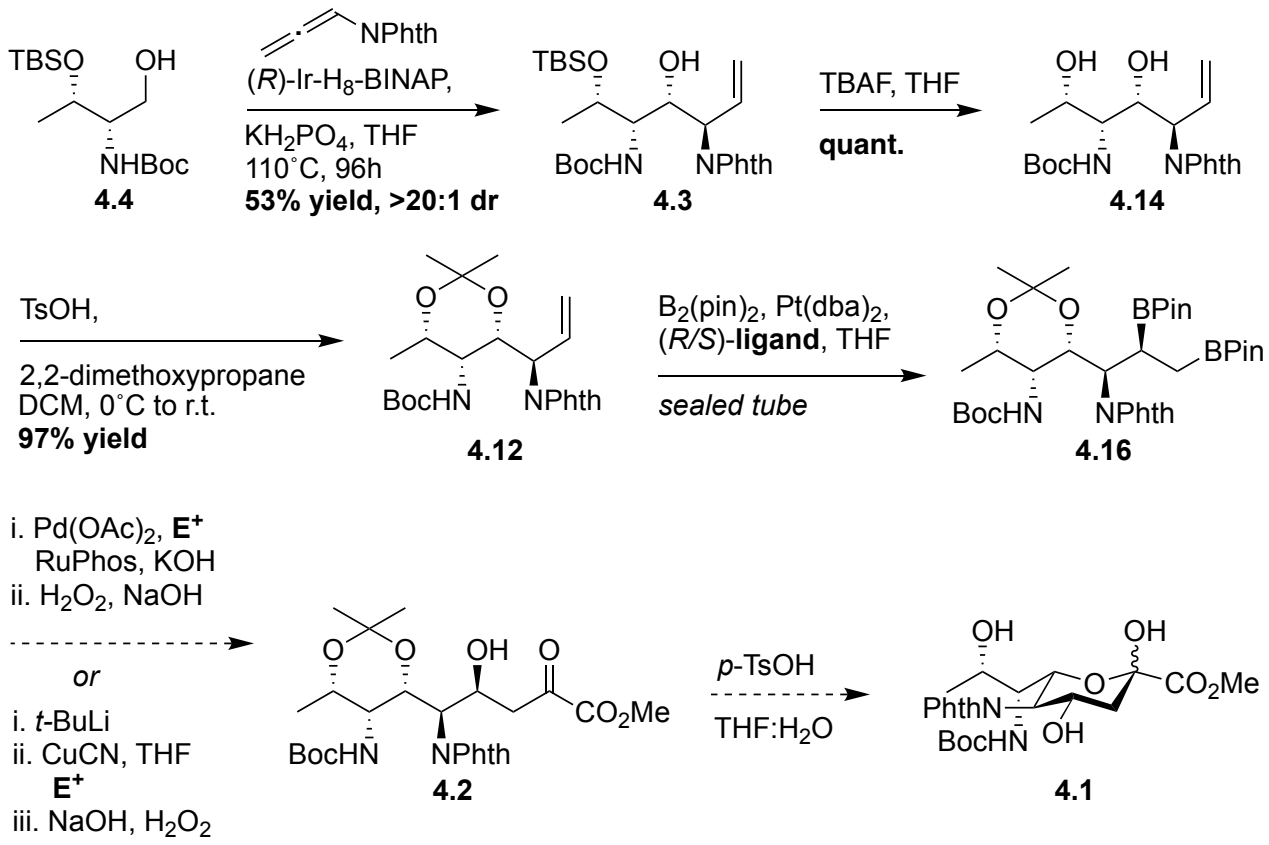


**Scheme 4.6.** Proposed forward synthesis of 8epiLeg from D-threoninol utilizing a diborylation, Suzuki-Miyaura coupling, oxidation strategy.

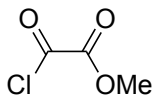


**$E^+$**

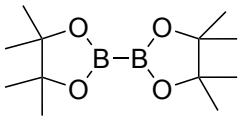


**$B_2(Pin)_2$**

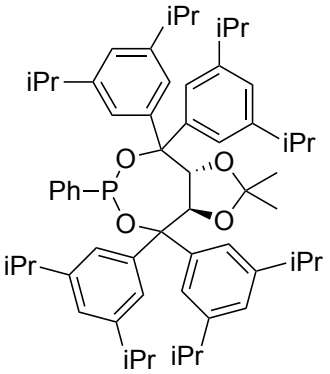


**Ligand**: (3aR,8aR)-(-)-4,4,8,8-Tetrakis(3,5-di-i-propylphenyl) tetrahydro-2,2-dimethyl-6-phenyl-1,3-dioxolo[4,5-e]dioxaphosphepin

**Figure 4.2.** Chemical structure of catalysts and additives proposed for the forward synthesis of 8epiLeg using a diborylation followed by Suzuki-Miyaura coupling and oxidation.

From the OCM route (*vide supra*), synthesis and characterization of compound **4.12** was already established. Toward generation of the diboron species from **4.12**, we were inspired by Morken and co-workers, who developed a stereoselective diborylation of terminal alkenes utilizing $Pt(dba)_3$, $B_2(pin)_2$, and a chiral dioxaphosphepin ligand (**Figure 4.2**).[139,142] To establish that a diastereoselective diborylation of substrate **4.12** using the Morken chemistry was feasible, a diborylation-oxidation procedure (also by Morken and co-workers) was first attempted.[140,141] Should this have worked on our substrate, a subsequent diborylation followed immediately by cross-coupling would have taken place.

Under the proposed conditions for diborylation-oxidation, no product was observed, though there was full consumption of starting material **4.12** (**Scheme 4.7**). Instead of the desired dihydroxylation product, a partially opened phthalimide byproduct **4.17** was isolated as the main species (confirmed via NMR and ESI) in the final reaction mixture. This indicated that reactivity of the phthalimide moiety with sodium hydroxide

was the only reaction that proceeded. Because neither diborylation nor dihydroxylation product was observed, we reasoned that steric and/or electron withdrawing effects of the phthalimide led to a lack in alkene **4.12** reactivity. This was supported after a model reaction with 1-hexene showed quantitative yield of the dihydroxylation product under Morken's proposed conditions, proving the viability of the chemistry in our hands with an adequate substrate.

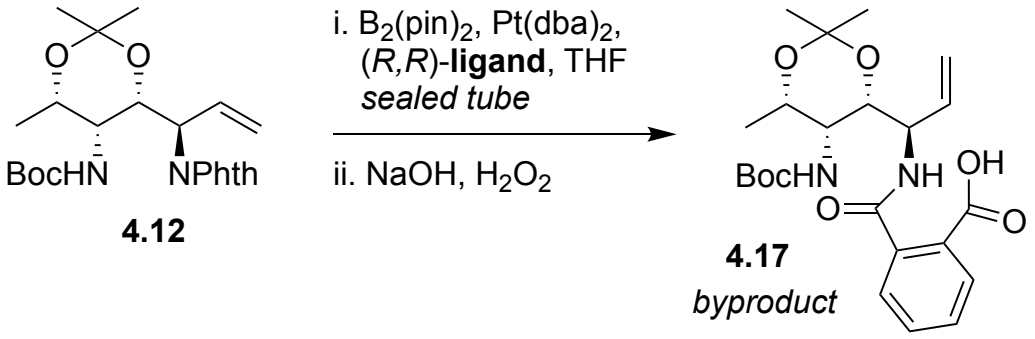


**Scheme 4.7.** One-pot, two step diborylation-oxidation inspired by work from Morken and co-workers, which did not yield the desired dihydroxylation product. See Figure 4.2 for structure of chiral ligand.

To combat substrate reactivity issues, we subsequently attempted C3 phthalimide removal, followed by acetylation. To this end, only trace amounts of the desired substrate **4.18** was synthesized after various optimization attempts (**Table 4.6**). As a first pass, a one-pot two-step phthalimide removal/acetylation with hydrazine monohydrate (1.6 eq) followed by standard acetylation conditions were employed.[121] While the C3 acetamide was successfully formed under these conditions, a loss of alkene functionality was also observed due to an undesirable diimide reduction reaction (**Table 4.6**, entry 1). As a result, alternative conditions were employed that utilized a sacrificial alkene, 4-penten-1-ol or *E/Z* crotyl alcohol, to scavenge for any diimide formed from hydrazine oxidation.[143–145] As a first attempt, a one pot, two-step phthalimide removal, acetylation with 4-pentanol

scavenger resulted in 15% yield of the desired acetamide **4.18** (entry 2). However, this required various preparatory plate purifications due to the complex mixtures formed throughout the reaction. To try and circumvent purification challenges in the next attempt, a crude preparatory plate purification after phthalimide removal was performed. It was our hope that by removing excess pentanol and hydrazine byproducts from the reaction mixture, it would make the acetylation product easier to abstract. When carrying the isolated free amine intermediate on to the acetamide protection, however, significant amounts of diimide reduction product were still observed (entries 3 and 4). We attributed this to small amounts of diimide being carried through after the crude purification (observed via NMR), which proceeded to react with the desired free amine and/or acetamide **4.18** once the scavenger was removed from the reaction. Since phthalimide removal proved to be significantly more challenging than was expected, we suggest further route development in the area of the Krische allylation with an alternative allene pronucleophile. This would circumvent the need for tedious phthalimide protecting group removal strategies in later reactions and may reduce step count of the overall synthetic route. Additionally, access to a compound like **4.18** could be the key to successful long chain elongation to 8epiLeg, since preliminary evidence points to a lack in protected allylamine reactivity being the main issue for route development.

**Table 4.6.** One-pot, two-step acetamide formation optimizations, attempting to avoid undesired diimide reduction byproduct.

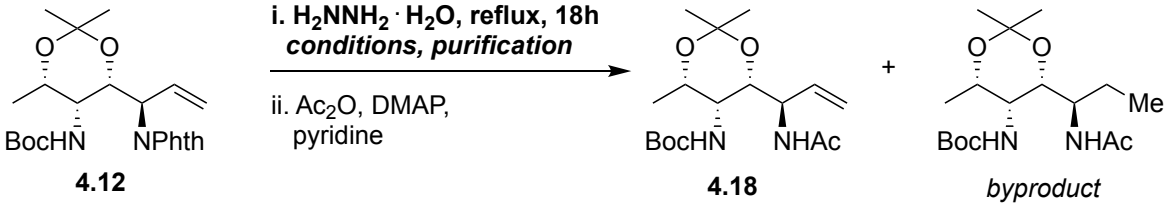


**4.12** **4.18** *byproduct*

| Entry | Solvent | Reaction Conc. (M) | Scavenger | Purification of amine? | % Yield | Notes |
|---|---|---|---|---|---|---|
| 1 | EtOH | .025 | none | none | trace | mostly byprod. |
| **2** | **EtOH** | **.025** | **4-penten-1-ol** | **none** | **15** | **3 prep plates to isolate** |
| 3 | MeOH | .003 | 4-penten-1-ol | yes | 0 | reaction did not proceed after 24 hrs. Additional hydrazine added and byprod observed. |
| 4 | MeOH | .058 | *E/Z* crotyl alcohol | yes | trace | mix of byprod/prod. |

## 4.3. Conclusions

In this chapter, we explored and evaluated several synthetic strategies toward the efficient and diastereoselective synthesis of 8-epi-legionaminic acid (8epiLeg), a compound of significant interest in bacterial pathogenicity and fitness. Despite the inherent challenges posed by the structural complexity of nonulosonic acids (NulOs), we proposed and investigated multiple synthetic routes that could potentially overcome these obstacles. The retrosynthetic analysis of 8epiLeg led to the identification of three distinct synthetic approaches: the olefin cross-metathesis strategy, the Mukaiyama aldol strategy, and the diborylation strategy. Each route was preliminarily optimized and tested; however, we encountered significant difficulties in all three approaches. The olefin cross metathesis strategy suffered from low reactivity of the allylamine intermediate, while the Mukaiyama

aldol approach was hindered by poor reactivity of the aldehyde substrate with the silyl enol ether of interest. The diborylation strategy, despite initial promise, was limited by issues related to the phthalimide protecting group and the low reactivity of key intermediates.

Although these strategies did not lead to the successful synthesis of 8epiLeg under the conditions explored, the challenges faced in each approach have provided valuable insights into the limitations and potential pitfalls of working with NulO-based compounds. These setbacks have highlighted the need for further method development of reactive intermediates and/or alternative protection-deprotection strategies, particularly concerning the phthalimide group. As such, the failure of these synthetic routes does not mark the end of this endeavor, but rather lays the groundwork for future efforts in overcoming these barriers. Moving forward, exploring alternative reaction conditions, different protecting group strategies, and more reactive intermediates may be essential in achieving a successful and scalable synthesis of 8epiLeg through one of our proposed approaches.

## 4.4. Materials and Experimental Methods

### 4.4.1. General Experimental Procedures

Unless otherwise stated, all reactions were carried out under an argon in flame dried reaction vessels. $CH_2Cl_2$, THF, and 1,4-dioxane were rendered anhydrous through a commercial solvent purification system (Inert). All other solvents were dried over activated molecular sieves prior to use. All other chemicals were purchased at the highest possible quality and used as received.

Flash column chromatography was performed on 230−400 mesh silica gel. Analytical and preparative thin layer chromatography was carried out on silica gel 60 F-254 plates. Products were visualized with UV light or by staining with potassium permanganate, 5% aqueous sulfuric acid, or ninhydrin followed by heating.

### 4.4.2. Spectroscopy, Spectrometry, and Data Collection

NMR spectra were recorded on a Bruker NMR spectrometer at 500 MHz for $^{1}H$ NMR and 125 MHz for $^{13}C$ NMR. Structural assignments were made with additional information from gCOSY and gHSQC experiments. For $CDCl_3$ solvent, chemical shifts are reported in ppm relative to TMS (for $^{1}H$ NMR in $CDCl_3$) or $CDCl_3$ (for $^{13}C$ NMR in $CDCl_3$). For $C_6D_6$ solvent, chemical shifts are reported in ppm relative to $C_6D_6$ (for $^{1}H$ and $^{13}C$ NMR). For $^{1}H$ NMR spectra, data are reported as follows: δ shift, multiplicity (s = singlet, m = multiplet, t = triplet, d = doublet, q = quartet, qd, quartet of doublets, dd = doublet of doublets, ddd = doublet of doublet of doublets), coupling constants are reported in Hz. To prove the existence of rotamers, 1-D NOE experiments were conducted according to procedure reported by Ley, et al on a 500 MHz Bruker NMR.[104] High-resolution mass spectra (HRMS) were obtained on an Agilent 6230 TOF mass spectrometer in the positive ion mode. Optical rotations were measured at 589 nm in a 10 cm cell at 23 °C.

## 4.4.3. Experimental Procedures and Spectral Data

**Synthesis of *cis*-propenyl magnesium bromide**

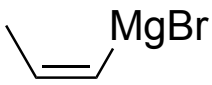


Magnesium turnings (1.81 g, 0.0744 mol, 150 mol%) were activated with a mortar and pestle and added to a flame dried 2-neck flask set up with a reflux condenser. Iodine (125.4 mg, 0.496 mmol, 10 mol%) was then added and the mixture stirred vigorously for ten minutes. *Cis*-1-bromo-propene (4.26 mL, .0496 mol, 100 mol%) was added to a separate flame dried flask and dissolved in THF (25 mL). 2 mL of the propene/THF mixture was added dropwise to the $Mg/I_2$ which, upon addition, began bubbling/heating and a color change from brown to grey was observed. (Depending on reaction concentration, this color change may need to be facilitated by gentle heating with a heat gun. Under these conditions, it was not deemed necessary.). The remainder of the propene/THF mixture was added *slowly* via canula and the reaction stirred at room temperature for three hours. The dark brown reaction mixture was then titrated to determine Molar concentration of the generated Grignard reagent.

Titration: Iodine (0.0140 g) was dissolved in THF (0.5 mL) to generate a 0.110 M solution. Grignard reagent was added dropwise to the $I_2$ solution until a color change from brown to clear was visibly observed. 0.08 mL of Grignard was required to titrate the solution, meaning a 0.69 M concentration of Grignard reagent ($M_1V_1=M_2V_2$) was generated in this instance.

**Synthesis of 4.9 a/b**

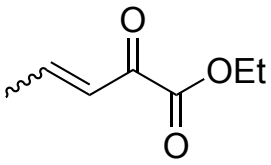


The synthesis of (*E*)/(*Z*) enone **4.9** was prepared according to literature procedure. Spectroscopic data was in agreement with previously reported data. [129]

**Synthesis of 4.11**

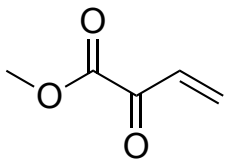


The synthesis of enone **4.11** was prepared according to literature procedure. Spectroscopic data was in agreement with previously reported data. [131]

GC Method: Compound **14.11** (20 μL) was dissolved in LCMS grade hexanes (1.5 mL). An Agilent GC method was run, 60°C isocratic for 5 minutes, then incrementally increasing at a gradient of 10°C/minute until reaching 200°C. Starting material diethyl oxalate was observed to elute at the 4–5-minute mark, which was confirmed by utilizing an external standard for comparison. Once the reaction was complete, no starting material was observed at this time stamp.

**Synthesis of 4.12**

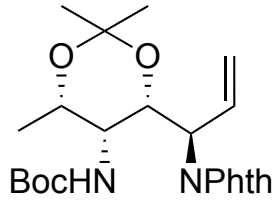


Compound **4.14** (100.0 mg, 0.256 mmol, 100 mol%) was added to a flame dried flask, dissolved in $CH_2Cl_2$ (10 mL), and cooled to 0°C. TsOH (4.40 mg, 0.0256 mmol, 10 mol%) and 2,2-dimethoxypropane (.0380 mL, 0.307 mmol, 120 mol%) were added and the reaction was allowed to warm to room temperature for 12 hours. Afterwards, the reaction was concentrated *in vacuo,* diluted with minimal $CH_2Cl_2$, and purified via preparatory thin layer chromatography (500μM, 40% EtOAc:Hex) to furnish compound **4.12** as a clear-white film (59.7 mg, 54% yield).

**$^1$H NMR** (500 MHz, $CDCl_3$) δ 7.78 (dd, *J* = 5.4, 3.1 Hz, 2H), 7.69 (dd, *J* = 5.5, 3.1 Hz, 2H), 6.13 – 6.05 (m, 1H), 5.21 – 5.14 (m, 2H), 5.04 (d, *J* = 10.6 Hz, 1H), 4.79 (m, 2H), 4.10 – 4.05 (m, 1H), 3.35 (d, *J* = 10.6 Hz, 1H), 1.51 (s, 3H), 1.43 (s, 3H), 1.36 (s, 9H), 1.26 (d, *J* = 2.3 Hz, 3H), 1.03 (d, *J* = 6.1 Hz, 3H)

**$^{13}$C NMR** (126 MHz, $CDCl_3$) δ 155.9, 133.8, 133.1, 123.2, 117.4, 99.8, 79.4, 71.6, 68.0, 52.7, 47.8, 29.8, 29.7, 28.2, 19.4, 17.1

HRMS (ESI) *m/z*: $[M + Na]^+$ calcd for $C_{23}H_{30}N_2O_6$+Na: 453.2002; found: 453.2012

$[\alpha]^{23}_D$: +18.2 ($CH_2Cl_2$, c = 0.0072 g/mL)

**Synthesis of 4.15**

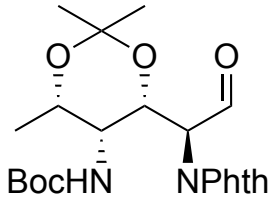


Compound **4.12** (7.4 mg, 0.0172 mmol, 100 mol%) was added to a flame dried, 3-neck round bottom secured with glass fittings, dissolved in a mixture of $CH_2Cl_2$ and MeOH and cooled to -78°C. The reaction was purged with argon, followed by $O_2$ (g). Ozone (via ozone generator) was bubbled through the solution for ~10 minutes, until the solution turned purple. [$O_2$/$O_3$ flow was controlled by flow meter.] Excess $O_3$ was blown off by $O_2$ until solution lost all purple color (~1min) and the system then purged with argon.

*N.B. Excess $O_3$ was quenched immediately via bubbling through two 10% aq. KI solutions following exposure to the reaction flask. The first KI solution turned orange, while the second remained clear, indicating that all $O_3$ was successfully destructed.* (See photo in Section 2.5.3 for further experimental detail).

$Me_2S$ (0.100 mL, excess) was added to the cooled mixture and was allowed to stir at room temperature for 12 hours. The reaction was tested via peroxidase stain for complete consumption of hazardous intermediates, concentrated *in vacuo*, and purified via preparatory thin layer chromatography (500 μm, 40:59:1 EtOAc:Hex:$Et_3N$) to furnish compound **4.15** as a clear-white film (7.4 mg, quant. yield). All equipment used to handle $Me_2S$ was handled in the fume hood and subsequently washed with bleach, acetone, and disposed of using secondary waste containment.

**$^{1}$H NMR** (500 MHz, $CDCl_3$) δ 9.77 (s, 1H), 7.80 (dd, *J* = 8.1, 3.9 Hz, 2H), 7.71 (dd, *J* = 5.7, 3.0 Hz, 2H), 5.12 – 5.07 (m, 2H), 4.86 (d, *J* = 10.2 Hz, 1H), 4.15 (q, *J* = 6.4 Hz, 1H), 3.36 (d, *J* = 10.9 Hz, 1H), 1.58 (s, 3H), 1.49 (s, 3H), 1.37 (s, 10H), 1.06 (d, *J* = 6.2 Hz, 3H).

**$^{13}$C NMR** (126 MHz, $CDCl_3$) δ 195.69, 167.67, 155.95, 134.22, 132.06, 123.63, 100.36, 79.93, 69.19, 68.14, 58.51, 47.96, 29.87, 28.31, 19.74, 17.25.

HRMS (ESI) *m/z*: $[M + Na]^+$ calcd for $C_{22}H_{28}N_2O_7$+Na: 455.1795; found: 455.1992

$[\alpha]^{23}_D$: + 9.9 ($CH_2Cl_2$, c = 0.0106 g/mL)

**Synthesis of 4.17**

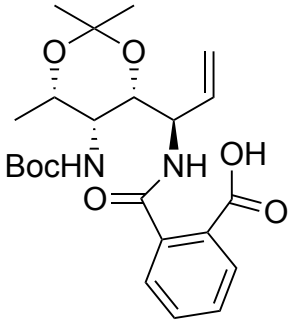


Pt $(dba)_3$ (0.723 mg, 0.0008 mmol, 10 mol%), (R,R)-**ligand** (0.862 mg, 0.0095 mmol, 12 mol%), and $B_2(pin)_2$ (21.06 mg, 0.0820 mmol, 105 mol%) were added to a flame dried pressure vessel dissolved in THF (0.079 mL). The reaction was heated to 80°C for 30 minutes, then cooled to room temperature. Compound **4.12** (34.00 mg, 0.0790 mmol, 100 mol%) was added to the reaction mixture, flushed with argon, and allowed to stir at 60°C for 3 hours. Then the reaction was cooled to 0°C and 3M NaOH (0.21 mL) and 30% $H_2O_2$ (0.103 mL) were added dropwise. The reaction was allowed to warm to room temperature overnight, then cooled to 0°C and sodium thiosulfate (1 mL) was added dropwise. The aqueous layer was extracted with EtOAc (3x), dried over $Na_2SO_4$, filtered, and concentrated *in vacuo.* The resulting mixture was diluted with a minimal amount of $CH_2Cl_2$ and purified via preparatory thin layer chromatography (1000μM, 15% MeOH:$CH_2Cl_2$) to furnish byproduct **4.17** as an off-white film.

**$^1$H NMR** (500 MHz, MeOD) δ 7.67 (dd, *J* = 33.4, 7.2 Hz, 2H), 7.41 – 7.34 (m, 3H), 6.04 – 5.97 (m, 1H), 5.45 (d, *J* = 17.4 Hz, 1H), 5.10 (d, *J* = 10.6 Hz, 1H), 4.58 (t, *J* = 6.8 Hz, 1H), 4.13 – 4.05 (m, 1H), 4.01 (d, *J* = 9.6 Hz, 1H), 3.67 (s, 1H), 3.32 (d, *J* = 2.3 Hz, 2H), 1.42

(s, 4H), 1.40 (d, *J* = 2.3 Hz, 9H), 1.38 (s, 5H), 1.24 (s, 2H), 1.18 (d, *J* = 2.4 Hz, 1H), 1.06 (dd, *J* = 6.4, 2.4 Hz, 3H).

**$^{13}$C NMR** (126 MHz, MeOD) δ 156.65, 135.01, 134.88, 130.14, 129.17, 128.27, 128.23, 128.08, 127.71, 115.06, 99.45, 78.99, 73.60, 68.55, 68.43, 51.58, 48.36, 46.09, 28.57, 27.50, 27.47, 27.17, 23.67, 18.21, 16.84, 16.47, 8.41.

LRMS (ESI) *m/z*: $[M + Na]^+$ calcd for $C_{23}H_{32}N_2O_7$+Na: 471.22; found: 472.02

## 4.5. References


(1) Chatterjee, A. K.; Choi, T.-L.; Sanders, D. P.; Grubbs, R. H. A General Model for Selectivity in Olefin Cross Metathesis. *J. Am. Chem. Soc.* **2003**, *125* (37), 11360–11370.

(2) Radomkit, S.; Hoveyda, A. H. Enantioselective Synthesis of Boron-Substituted Quaternary Carbon Stereogenic Centers through NHC-Catalyzed Conjugate Additions of (Pinacolato)Boron Units to Enones. *Angew. Chem. Int. Ed.* **2014**, *53* (13), 3387–3391.

(3) Tsutsumi, R.; Taguchi, R.; Yamanaka, M. Chiral Bipyridine Ligand with Flexible Molecular Recognition Site: Development and Application to Copper-Catalyzed Asymmetric Borylation of α,B-Unsaturated Ketones. *ChemCatChem* **2022**, *14* (2).

(4) Lee, K.; Hoveyda, A. H. Monodentate Non-$C_2$-Symmetric Chiral *N*-Heterocyclic Carbene Complexes for Enantioselective Synthesis. Cu-Catalyzed Conjugate Additions of Aryl- and Alkenylsilylfluorides to Cyclic Enones. *J. Org. Chem.* **2009**, *74* (12), 4455–4462.

(5) Radomkit, S.; Hoveyda, A. H. Enantioselective Synthesis of Boron-Substituted Quaternary Carbon Stereogenic Centers through NHC-Catalyzed Conjugate Additions of (Pinacolato)Boron Units to Enones. *Angew. Chem. Int. Ed.* **2014**, *53* (13), 3387–3391.

(6) Nyalata, S.; Raghavan, S. Convergent Stereoselective Synthesis of the C16–C37 Subunit of Sorangicin A. *Org. Lett.* **2019**, *21* (19), 7778–7781.

(7) Paul, D.; Mague, J. T.; Sathyamoorthi, S. Sulfamate-Tethered *Aza* -Wacker Cyclization Strategy for the Syntheses of 2-Amino-2-Deoxyhexoses: Preparation of Orthogonally Protected D -Galactosamines. *J. Org. Chem.* **2023**, *88* (3), 1445–1456.

(8) Rambaud, M.; Bakasse, M.; Duguay, G.; Villieras, J. A One-Step Synthesis of Alkyl 2-Oxo-3-Alkenoates from Alkenyl Grignard Reagents and Dialkyl Oxalates. *Synthesis (Stuttg)* **1988**, *1988* (07), 564–566.

(9) Evans, D. A.; Beiger, J. J.; Burch, J. D.; Fuller, P. H.; Glorius, F.; Kattnig, E.; Thaisrivongs, D. A.; Trenkle, W. C.; Young, J. M.; Zhang, J. Total Synthesis of Aflastatin A. *J. Am. Chem. Soc.* **2022**, *144* (43), 19953–19972.

(10) Jessen, B. M.; Taarning, E.; Madsen, R. Synthesis, Stability, and Diels-Alder Reactions of Methyl 2-Oxobut-3-enoate. *Eur. J. Org. Chem.* **2021**, *2021* (29), 4049–4053.

(11) Vedrenne, E.; Dupont, H.; Oualef, S.; Elkaïm, L.; Grimaud, L. Dramatic Effect of Boron-Based Lewis Acids in Cross-Metathesis Reactions. *Synlett.* **2005**, No. 4, 670–672.

(12) Shafi, S.; Kędziorek, M.; Grela, K. Cross Metathesis of N-Allylamines and α,β-Unsaturated Carbonyl Compounds: A One-Pot Synthesis of Substituted Pyrroles. *Synlett.* **2011**, *2011* (01), 124–128.

(13) Fujioka, K.; Yokoe, H.; Yoshida, M.; Shishido, K. Total Synthesis of Penostatin B. *Org. Lett.* **2012**, *14* (1), 244–247.

(14) Huo, H.-H.; Zhang, H.-K.; Xia, X.-E.; Huang, P.-Q. A Formal Enantioselective Total Synthesis of FR901483. *Org. Lett.* **2012**, *14* (18), 4834–4837.

(15) Lummiss, J. A. M.; Ireland, B. J.; Sommers, J. M.; Fogg, D. E. Amine-Mediated Degradation in Olefin Metathesis Reactions That Employ the Second-Generation Grubbs Catalyst. *ChemCatChem* **2014**, *6* (2), 459–463.

(16) Hu, D. X.; Grice, P.; Ley, S. V. Rotamers or Diastereomers? An Overlooked NMR Solution. *J. Org. Chem.* **2012**, *77* (11), 5198–5202.

(17) Delas, C.; Blacque, O.; Moïse, C. Use of Chiral Enolsilanes and Chiral Aldehydes in a Mukaiyama-Type Aldol Reaction Promoted by Titanium(IV)Isopropoxide. *Tetrahedron Lett.* **2000**, *41* (43), 8269–8272.

(18) Corey, E. J.; Li, W.; Reichard, G. A. A New Magnesium-Catalyzed Doubly Diastereoselective *Anti*-Aldol Reaction Leads to a Highly Efficient Process for the Total Synthesis of Lactacystin in Quantity. *J. Am. Chem. Soc.* **1998**, *120* (10), 2330–2336.

(19) Spielmann, K.; Xiang, M.; Schwartz, L. A.; Krische, M. J. Direct Conversion of Primary Alcohols to 1,2-Amino Alcohols: Enantioselective Iridium-Catalyzed Carbonyl Reductive Coupling of Phthalimido-Allene via Hydrogen Auto-Transfer. *J. Am. Chem. Soc.* **2019**, *141* (36), 14136–14141.

(20) Greene, T. W.; Wuts, P. G. M. *Protective Groups in Organic Synthesis*, 3rd ed.; John Wiley & Sons, Inc.: New York, 1999.

(21) Xu, N.; Holmgren, J. L.; Morken, J. P. Site-Selective Activation and Stereospecific Functionalization of Bis(Boronic Esters) Derived from 2-Alkenes: Construction of Propionates and Other 1,2-Difunctional Motifs. *Angew. Chem. Int. Ed.* **2024**.

(22) Mlynarski, S. N.; Schuster, C. H.; Morken, J. P. Asymmetric Synthesis from Terminal Alkenes by Cascades of Diboration and Cross-Coupling. *Nature* **2014**, *505* (7483), 386–390.

(23) Coombs, J. R.; Haeffner, F.; Kliman, L. T.; Morken, J. P. Scope and Mechanism of the Pt-Catalyzed Enantioselective Diboration of Monosubstituted Alkenes. *J. Am. Chem. Soc.* **2013**, *135* (30), 11222–11231.

(24) Yan, L.; Meng, Y.; Haeffner, F.; Leon, R. M.; Crockett, M. P.; Morken, J. P. Carbohydrate/DBU Cocatalyzed Alkene Diboration: Mechanistic Insight Provides Enhanced Catalytic Efficiency and Substrate Scope. *J. Am. Chem. Soc.* **2018**, *140* (10), 3663–3673.

(25) Maryanoff, B. E.; Greco, M. N.; Zhang, H.-C.; Andrade-Gordon, P.; Kauffman, J. A.; Nicolaou, K. C.; Liu, A.; Brungs, P. H. Macrocyclic Peptide Inhibitors of Serine Proteases. Convergent Total Synthesis of Cyclotheonamides A and B via a Late-Stage Primary Amine Intermediate. Study of Thrombin Inhibition under Diverse Conditions. *J. Am. Chem. Soc.* **1995**, *117* (4), 1225–1239.

(26) Maryanoff, B. E.; Zhang, H.-C.; Greco, M. N.; Glover, K. A.; Kauffman, J. A.; Andrade-Gordon, P. Cyclotheonamide Derivatives: Synthesis and Thrombin Inhibition. Exploration of Specific Structure-Function Issues. *Bioorg. Med. Chem.* **1995**, *3* (8), 1025–1038.

(27) Barsu, C.; Cheaib, R.; Chambert, S.; Queneau, Y.; Maury, O.; Cottet, D.; Wege, H.; Douady, J.; Bretonnière, Y.; Andraud, C. Neutral Push-Pull Chromophores for Nonlinear Optical Imaging of Cell Membranes. *Org. Biomol. Chem.* **2010**, *8* (1), 142–150.

# Appendix A: NMR Spectra of Novel Compounds

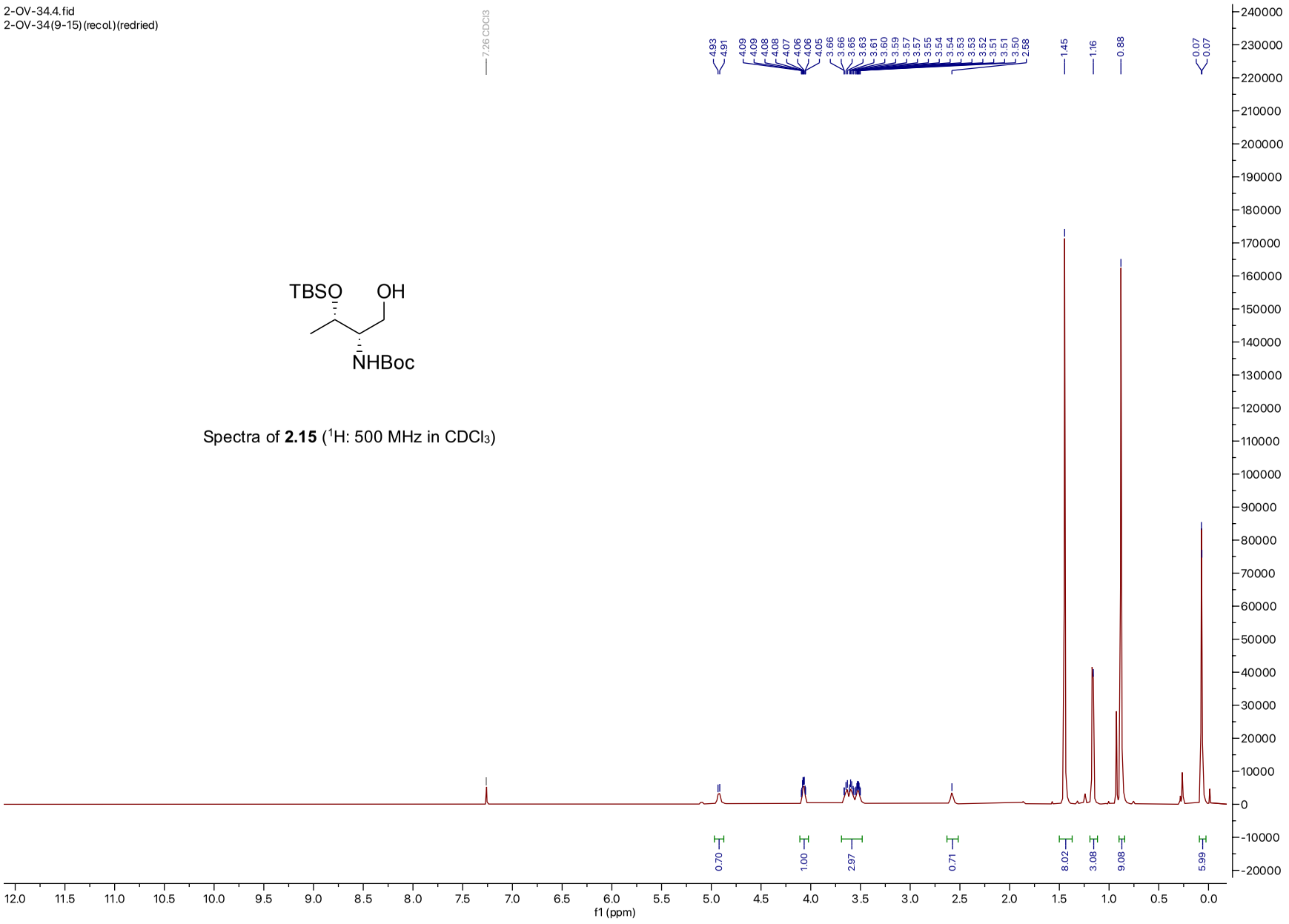


Spectra of **2.15** ($^1$H: 500 MHz in $CDCl_3$)

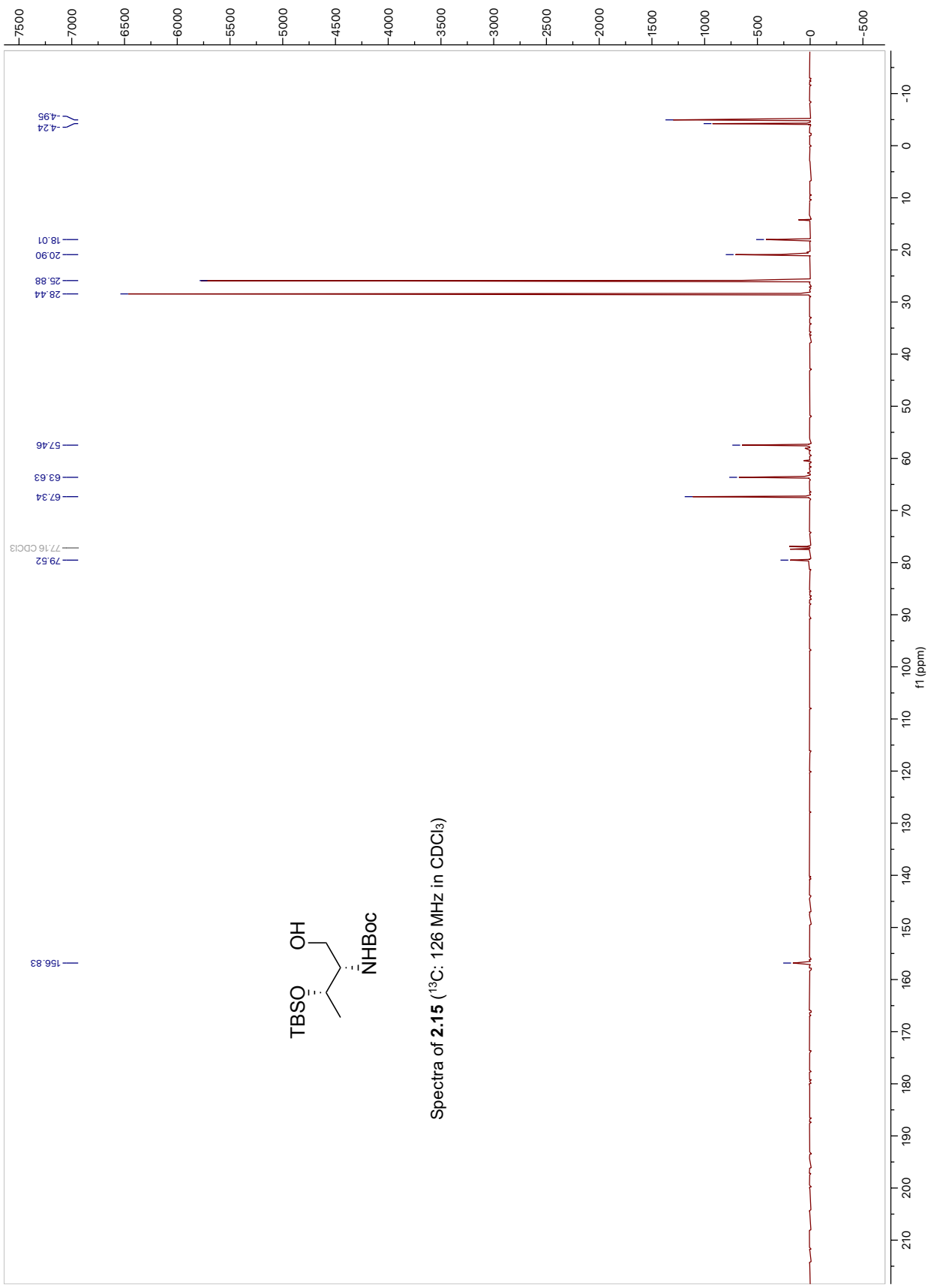
-4.95
-4.24
18.01
20.90
25.88
28.44
57.46
63.63
67.34
77.16 CDCl3
79.52
156.83
TBSO
OH
NHBoc
Spectra of 2.15 (13C: 126 MHz in CDCl3)
f1 (ppm)

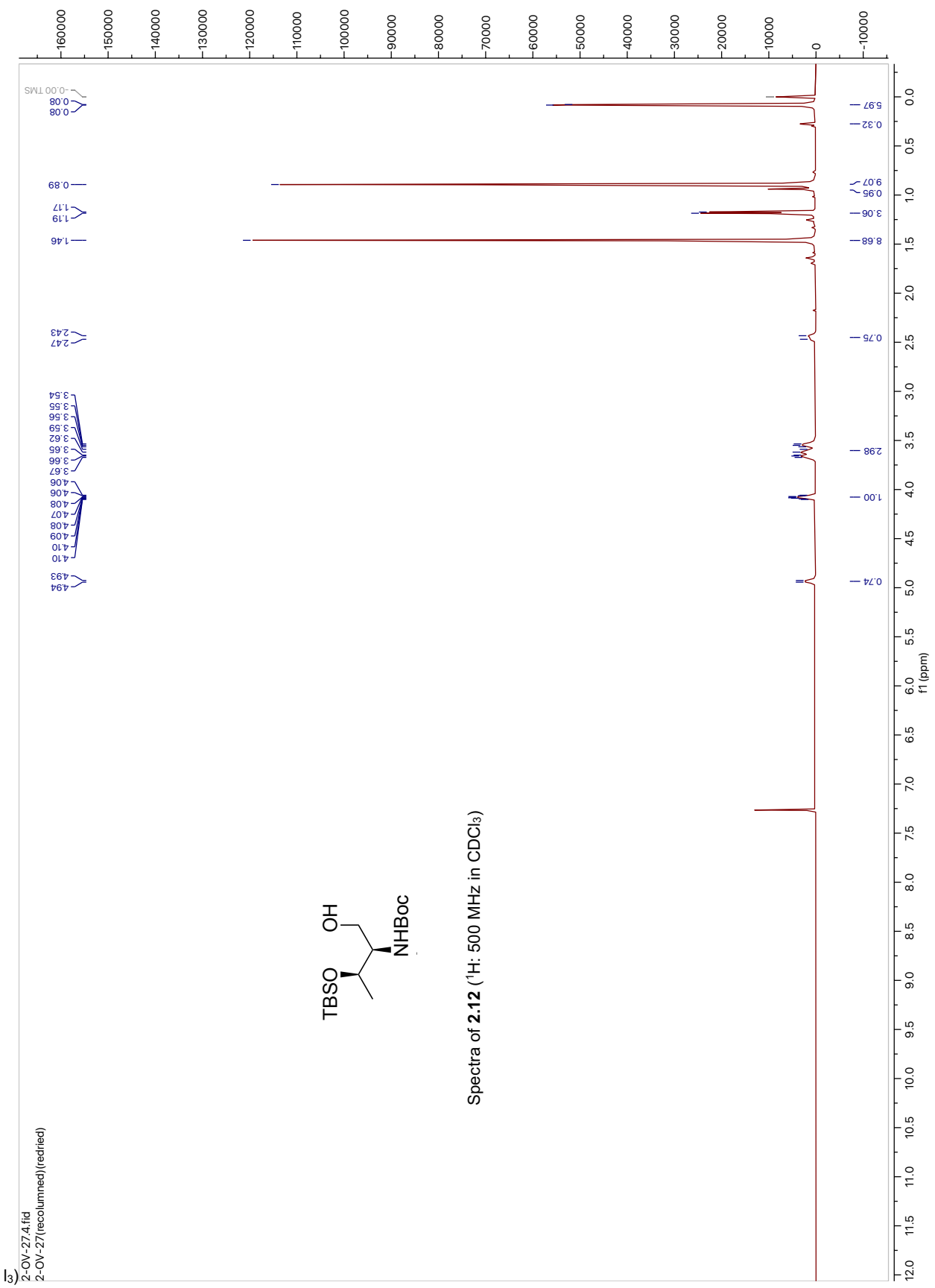
I3)
2-OV-27.4.fid
2-OV-27(recolumned)(redried)
TBSO
OH
NHBoc
Spectra of 2.12 (1H: 500 MHz in CDCl3)
f1 (ppm)

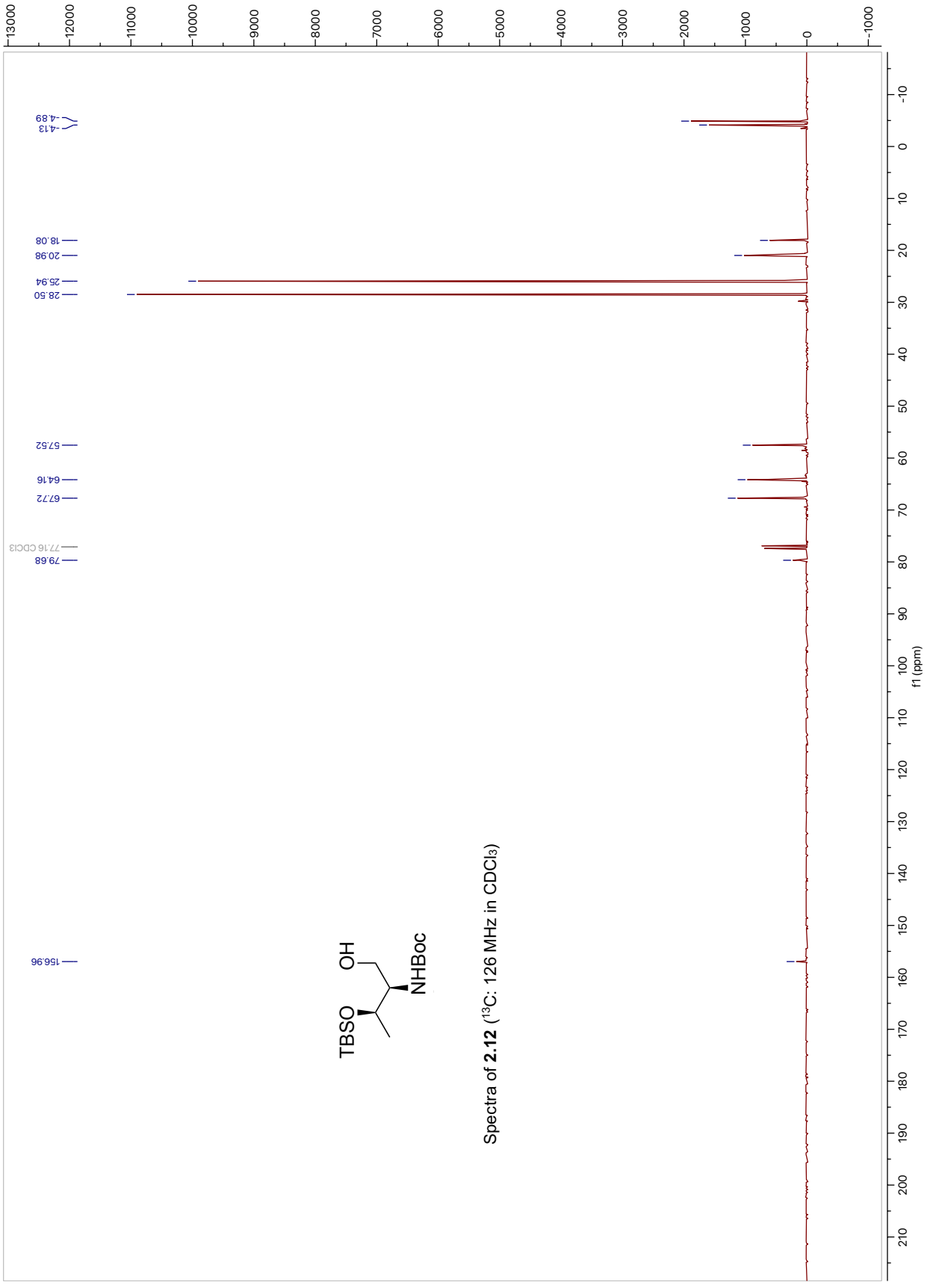


Spectra of **2.12** ($^{13}$C: 126 MHz in $CDCl_3$)

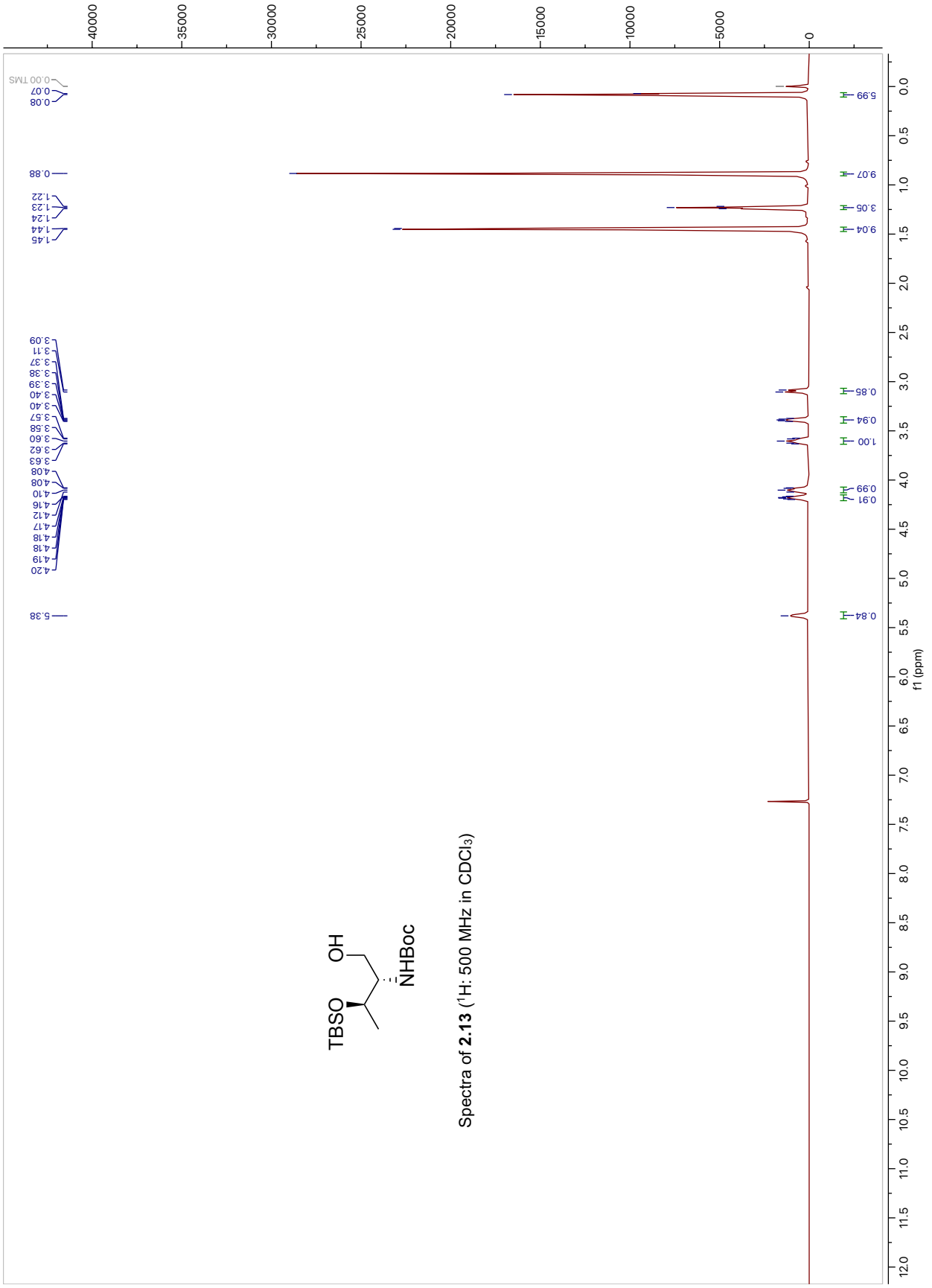


Spectra of **2.13** ($^1$H: 500 MHz in $CDCl_3$)

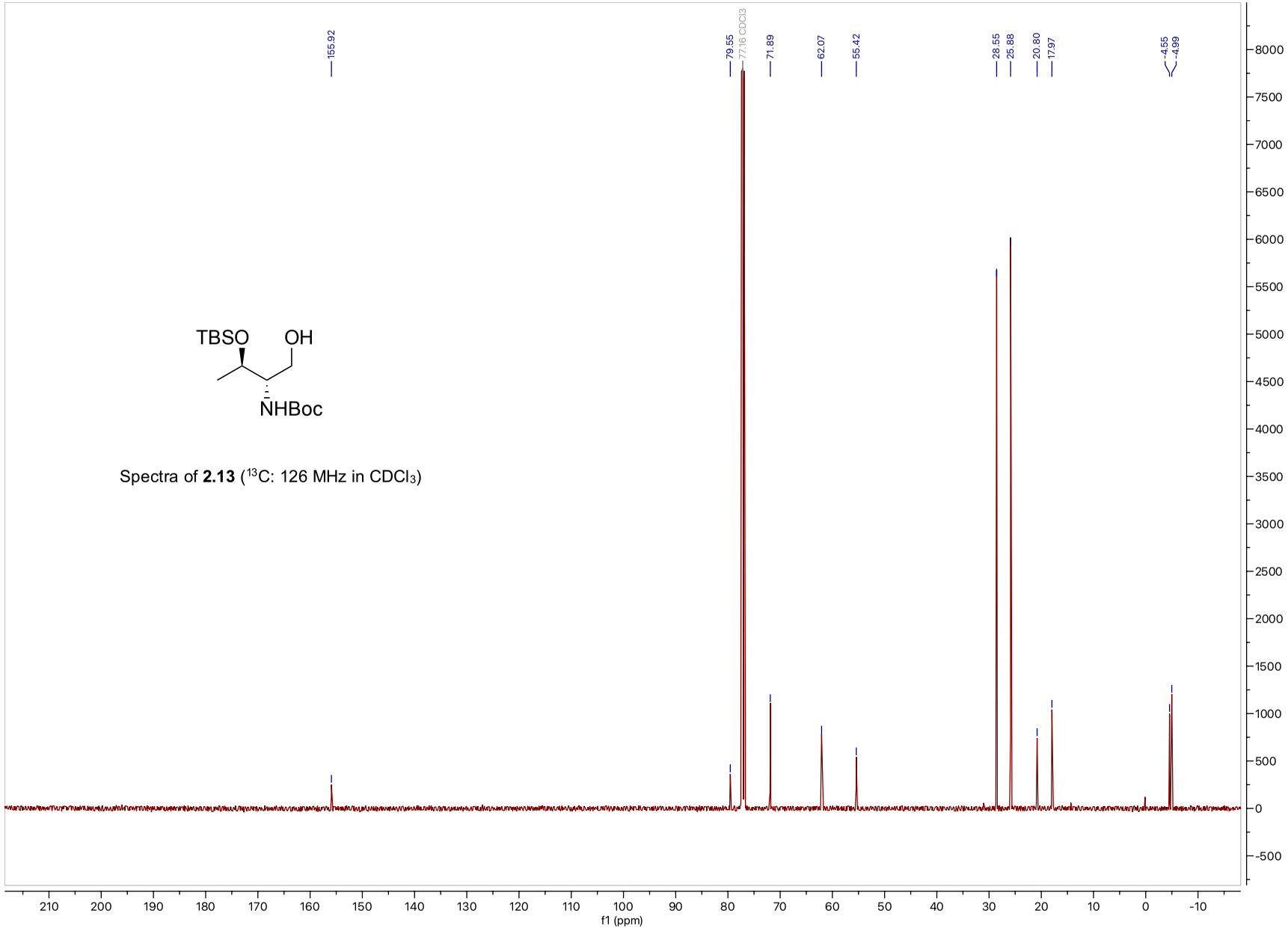


Spectra of **2.13** ($^{13}C$: 126 MHz in $CDCl_3$)

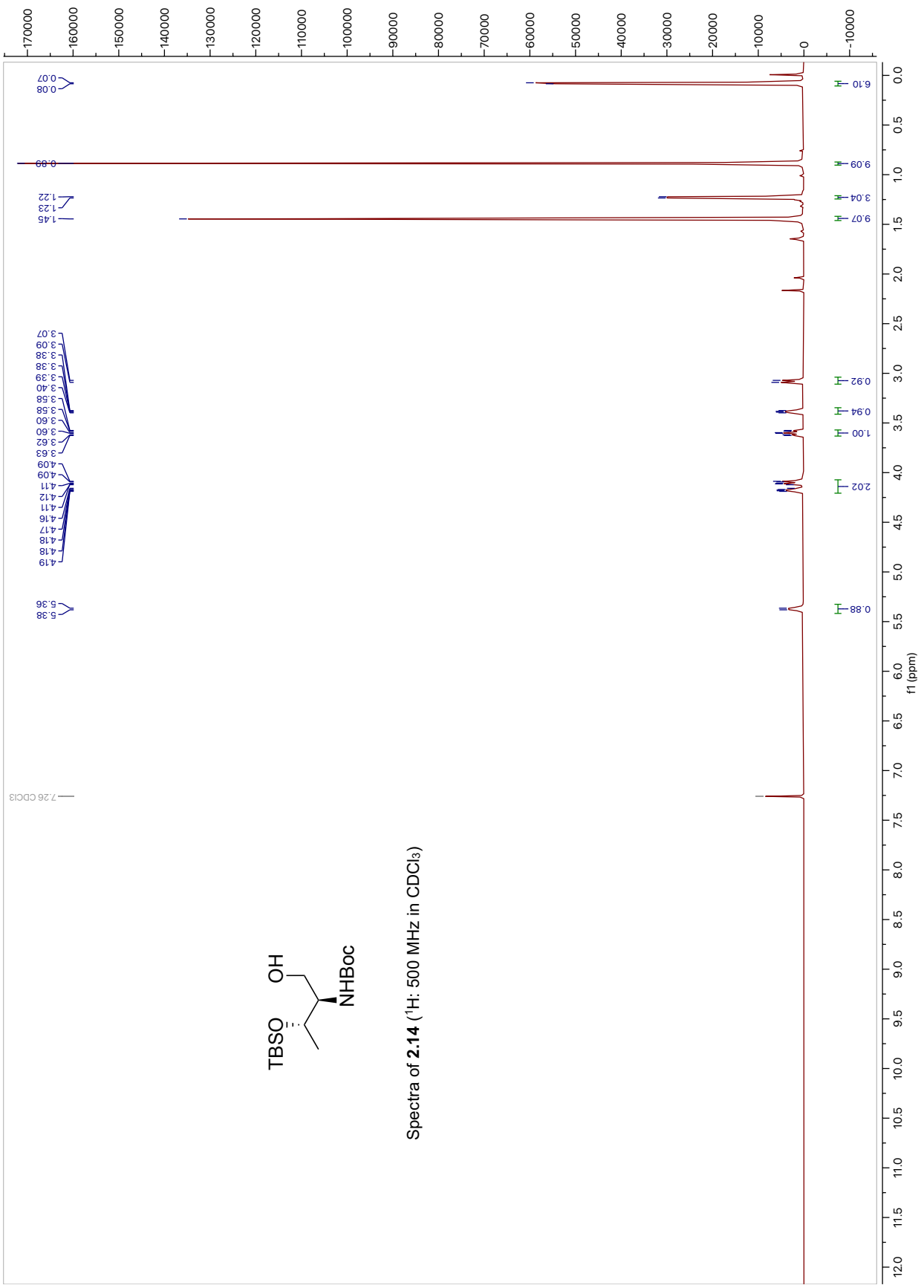


Spectra of **2.14** ($^1$H: 500 MHz in $CDCl_3$)

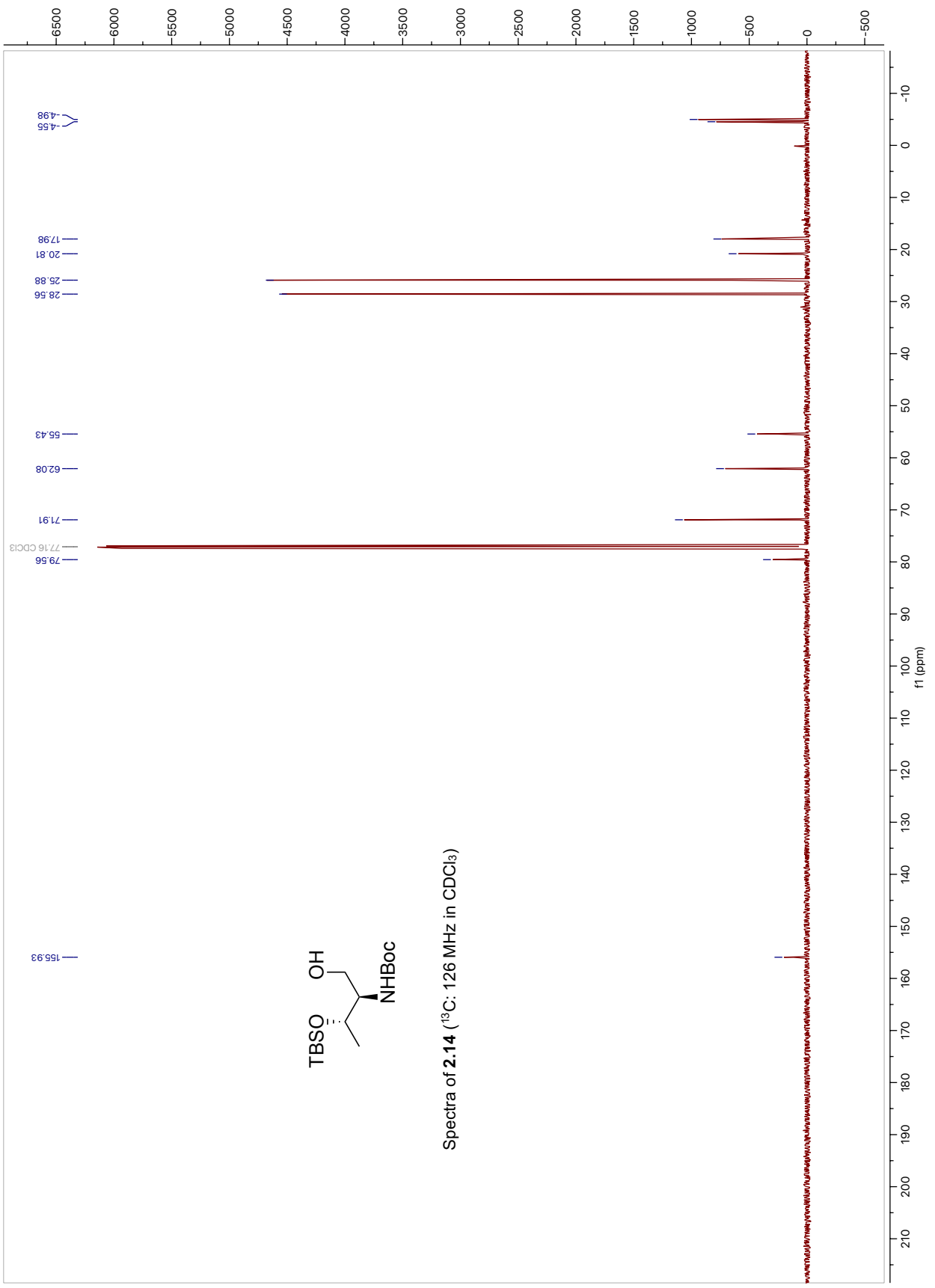


Spectra of **2.14** ($^{13}$C: 126 MHz in $CDCl_3$)

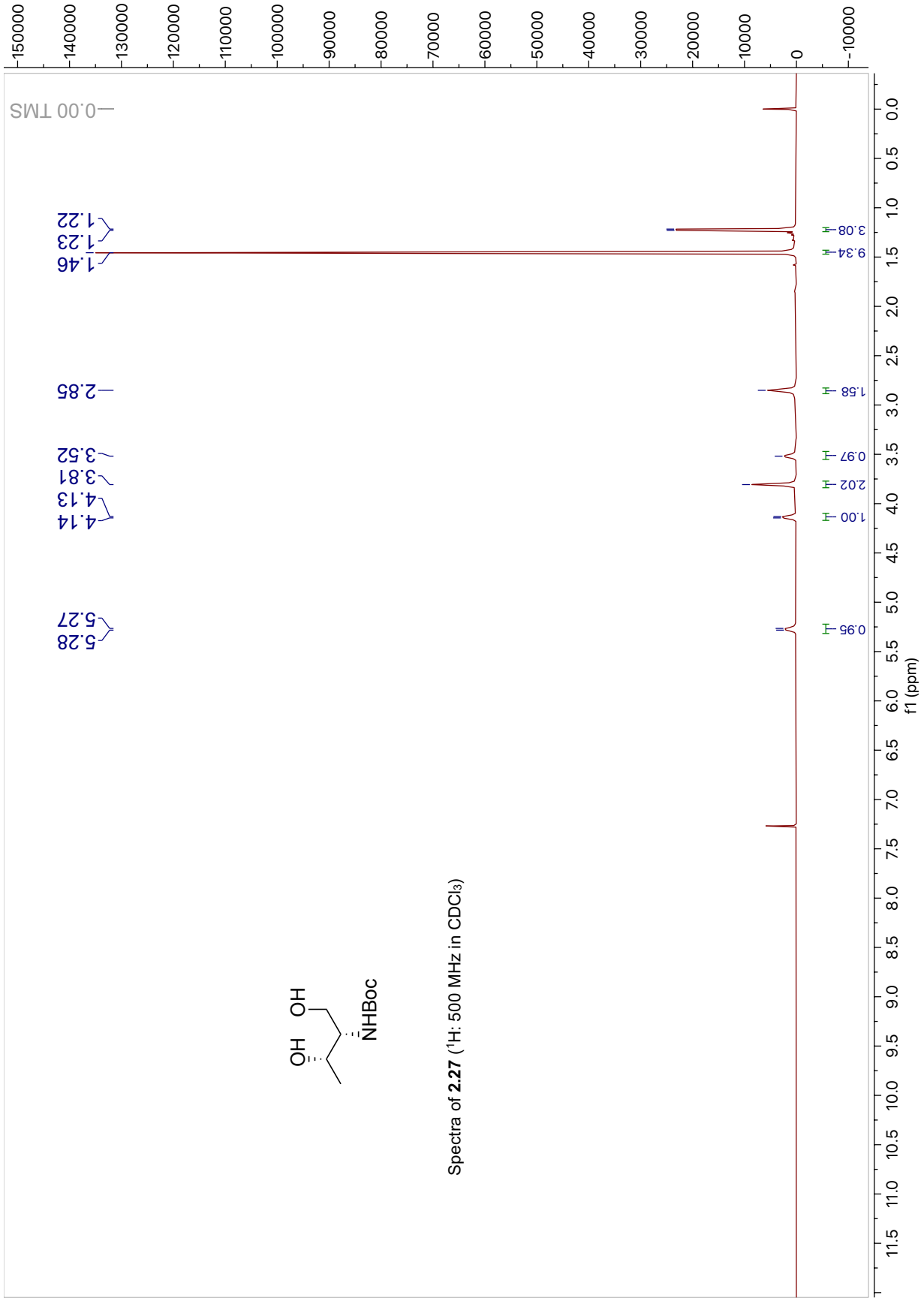
Spectra of 2.27 (1H: 500 MHz in CDCl3)
OH
OH
NHBoc
TMS 0.00
1.46
1.23
1.22
2.85
3.52
3.81
4.13
4.14
5.28
5.27
3.08
9.34
1.58
0.97
2.02
1.00
0.95
f1 (ppm)

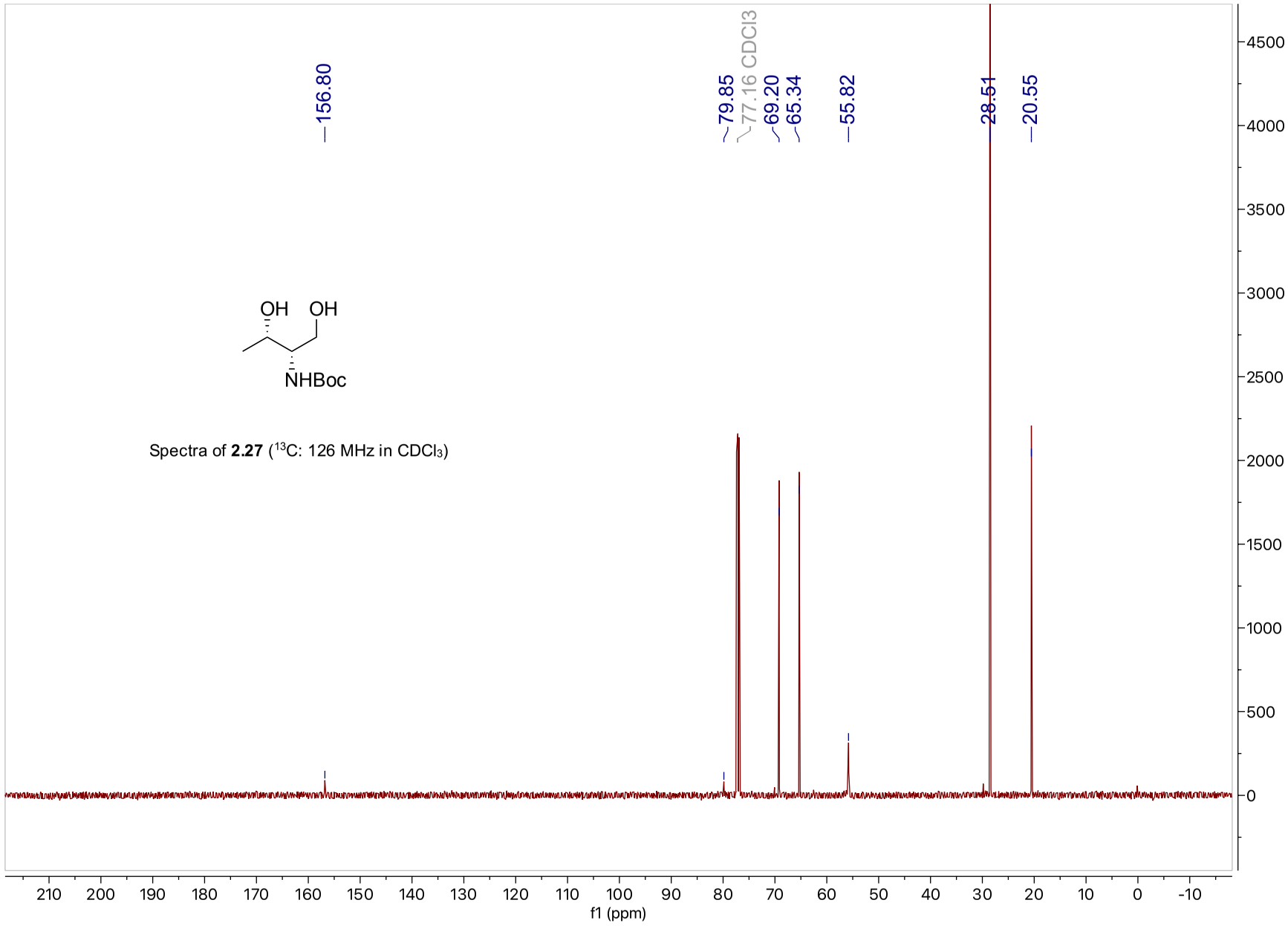
156.80
79.85
77.16 CDCl3
69.20
65.34
55.82
28.51
20.55
OH
OH
NHBoc
Spectra of 2.27 (13C: 126 MHz in CDCl3)
4500
4000
3500
3000
2500
2000
1500
1000
500
0
210
200
190
180
170
160
150
140
130
120
110
100
90
80
70
60
50
40
30
20
10
0
-10
f1 (ppm)

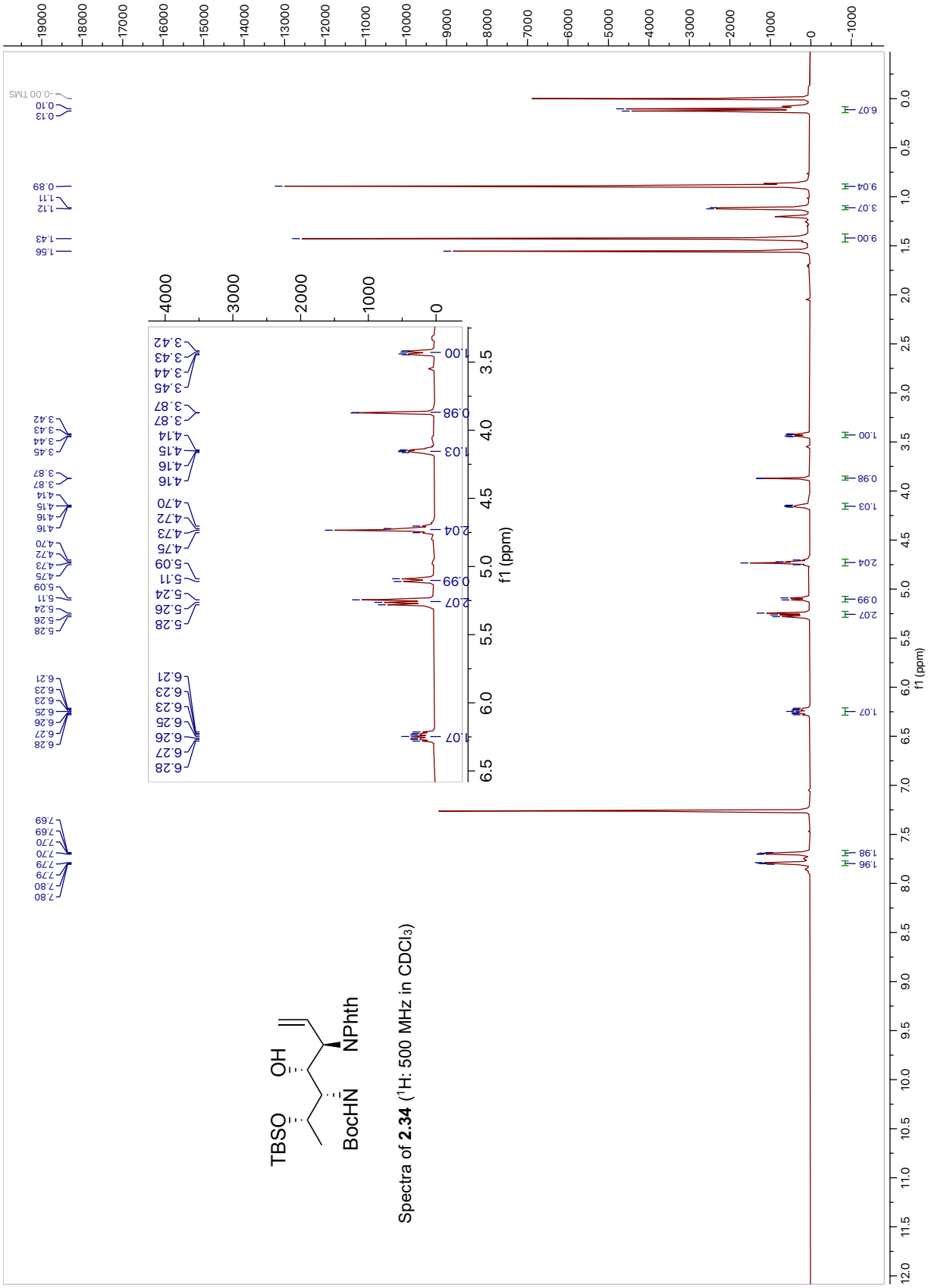
TBSO
OH
BocHN
NPhth
Spectra of 2.34 (1H: 500 MHz in CDCl3)
f1 (ppm)

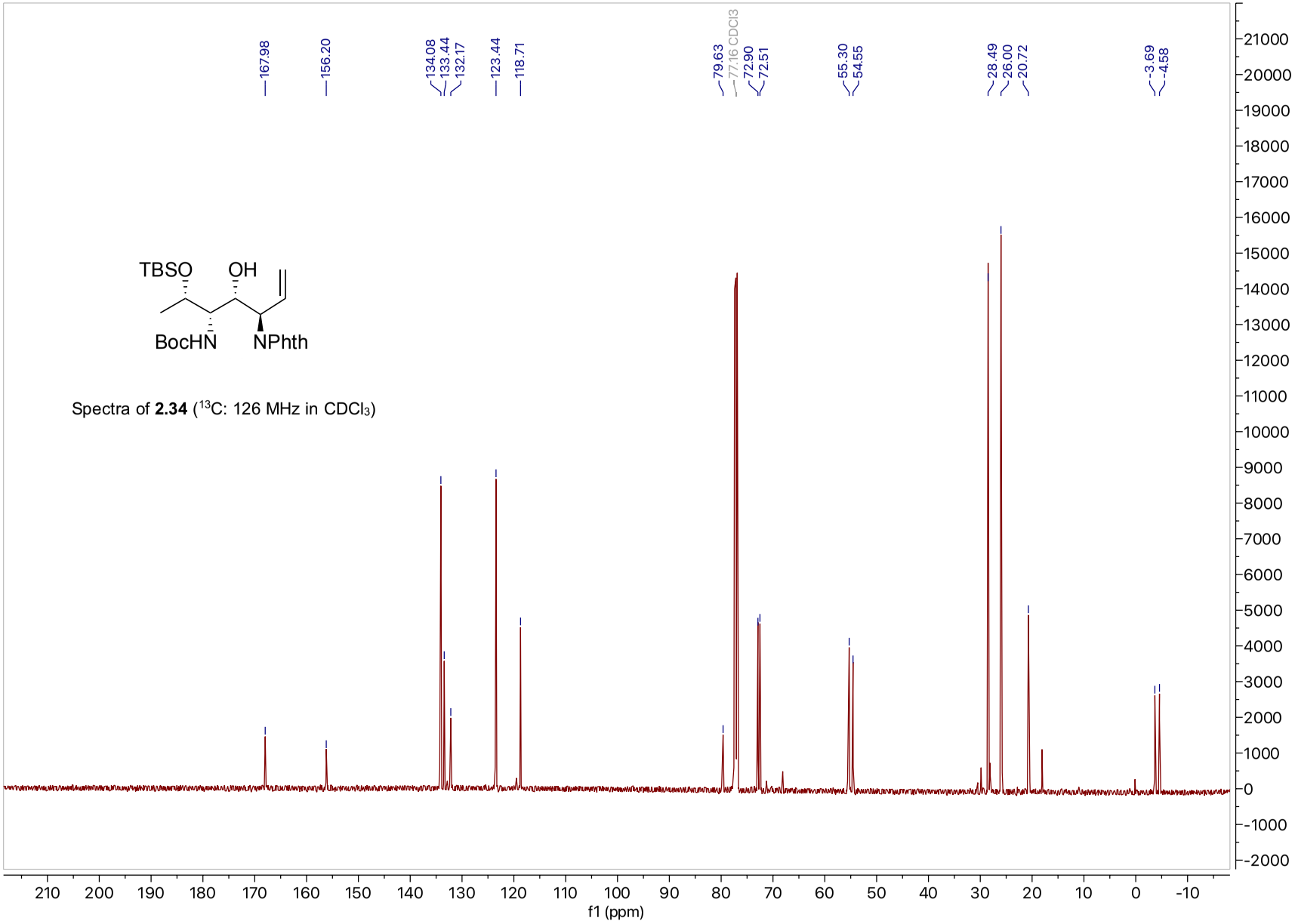
167.98
156.20
134.08
133.44
132.17
123.44
118.71
79.63
77.16 CDCl3
72.90
72.51
55.30
54.55
28.49
26.00
20.72
-3.69
-4.58
TBSO
OH
BocHN
NPhth
Spectra of 2.34 (13C: 126 MHz in CDCl3)
f1 (ppm)

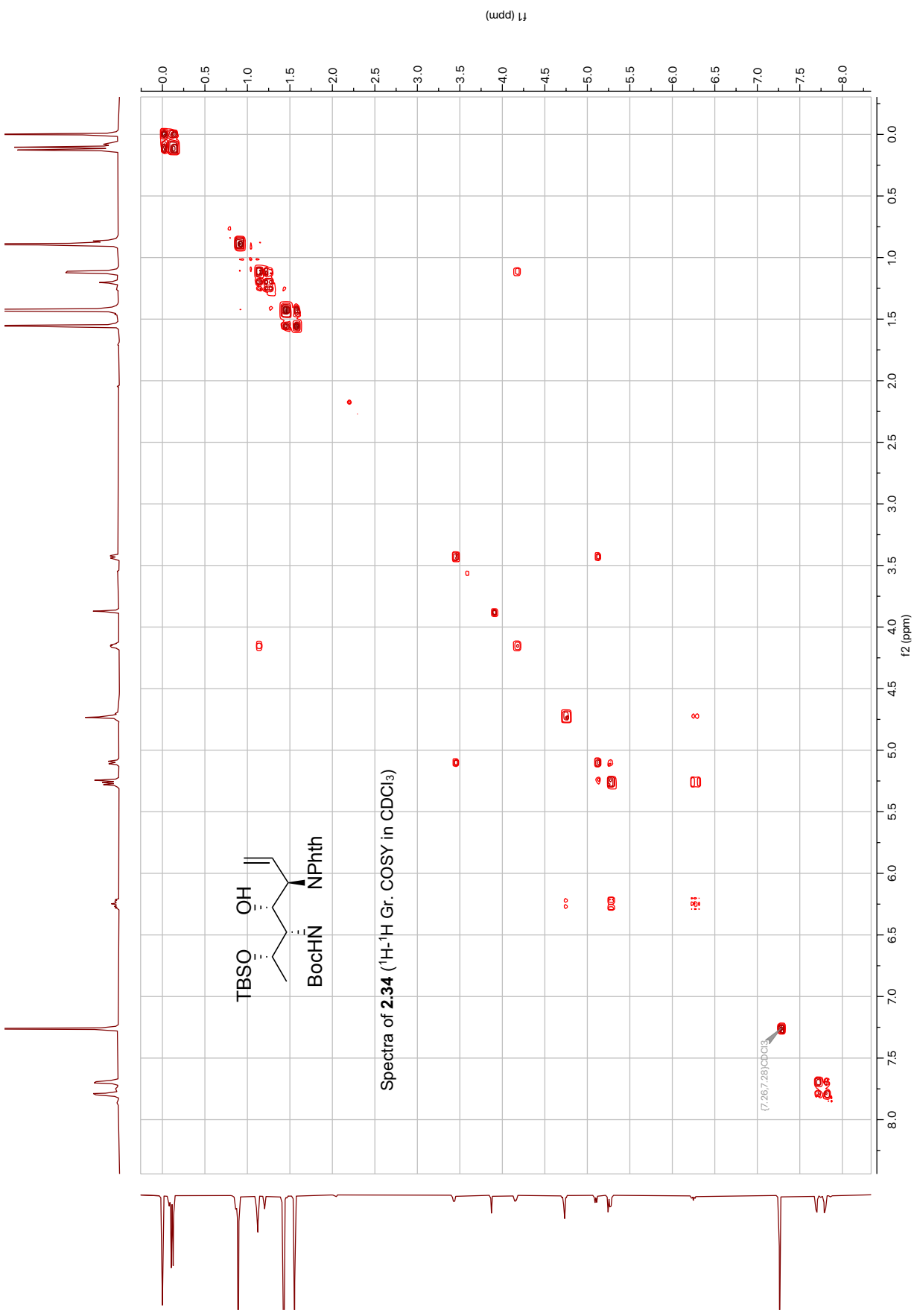
f1 (ppm)
f2 (ppm)
Spectra of 2.34 (1H-1H Gr. COSY in CDCl3)
TBSO
OH
BocHN
NPhth
{7.26,7.28}CDCl3

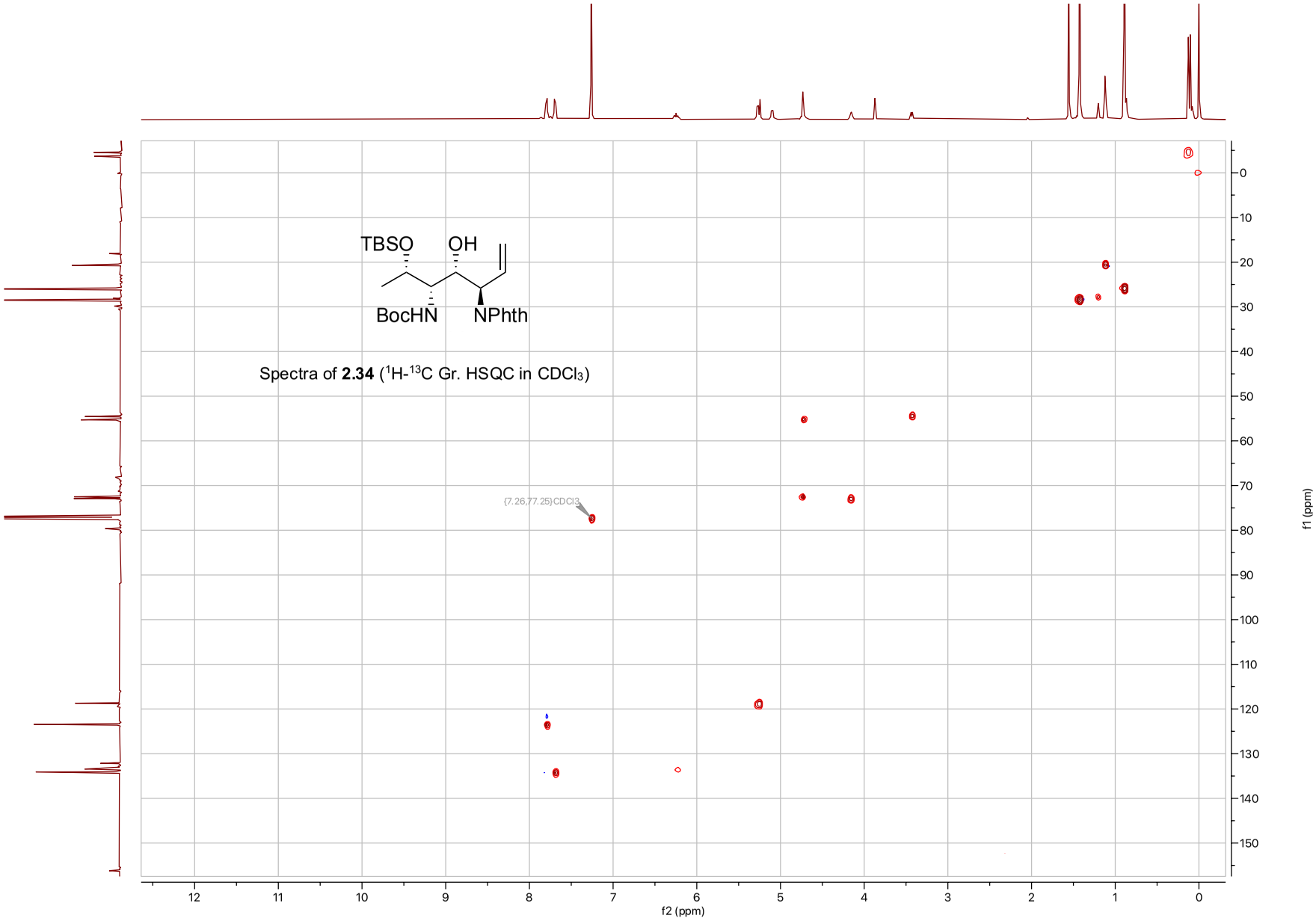
TBSO
OH
BocHN
NPhth
Spectra of **2.34** ($^{1}$H-$^{13}$C Gr. HSQC in $CDCl_3$)
{7.26,77.25}CDCl3
f2 (ppm)
f1 (ppm)

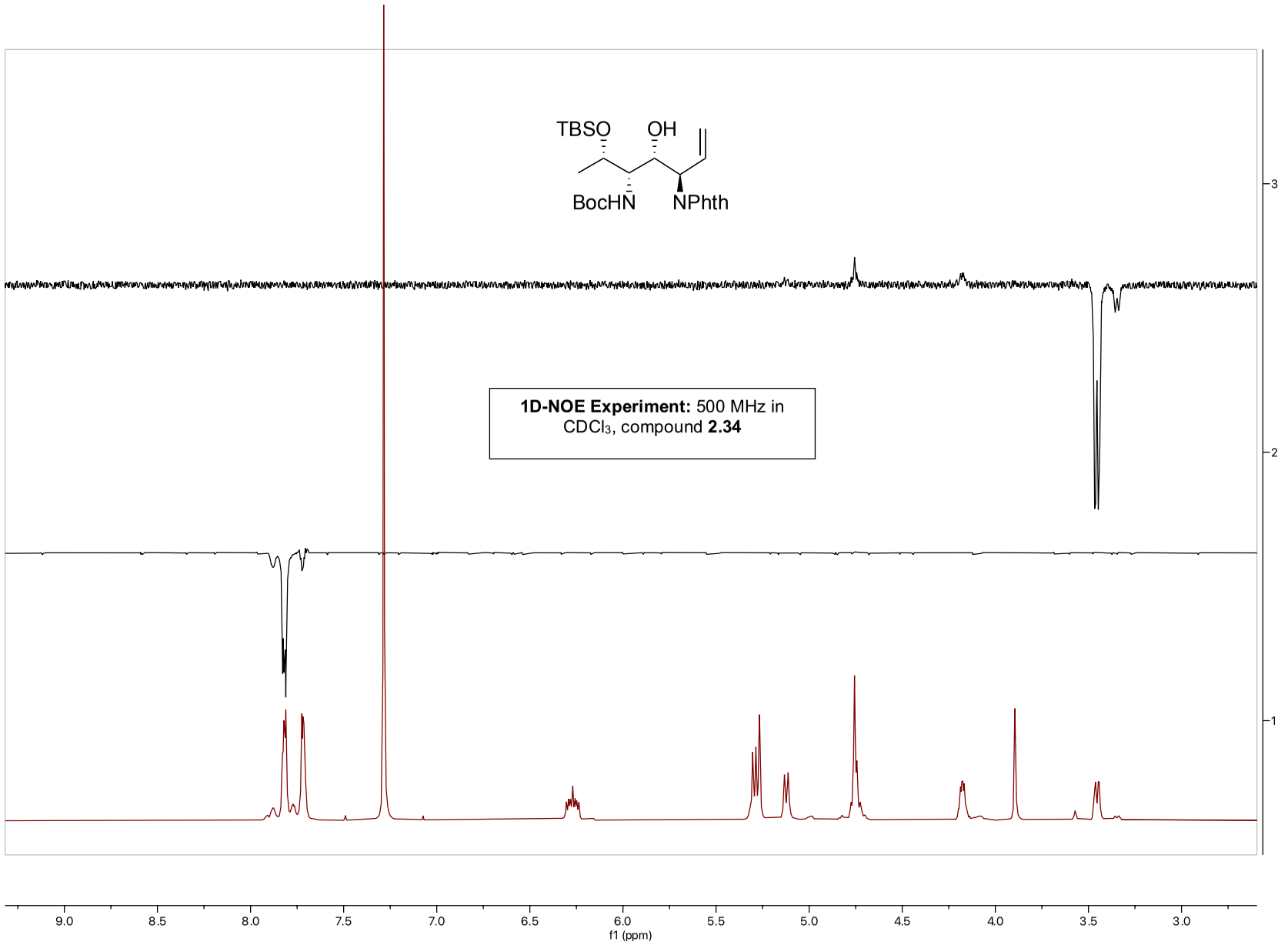
TBSO
OH
BocHN
NPhth
1D-NOE Experiment: 500 MHz in CDCl3, compound 2.34
3
2
1
9.0
8.5
8.0
7.5
7.0
6.5
6.0
5.5
5.0
4.5
4.0
3.5
3.0
f1 (ppm)

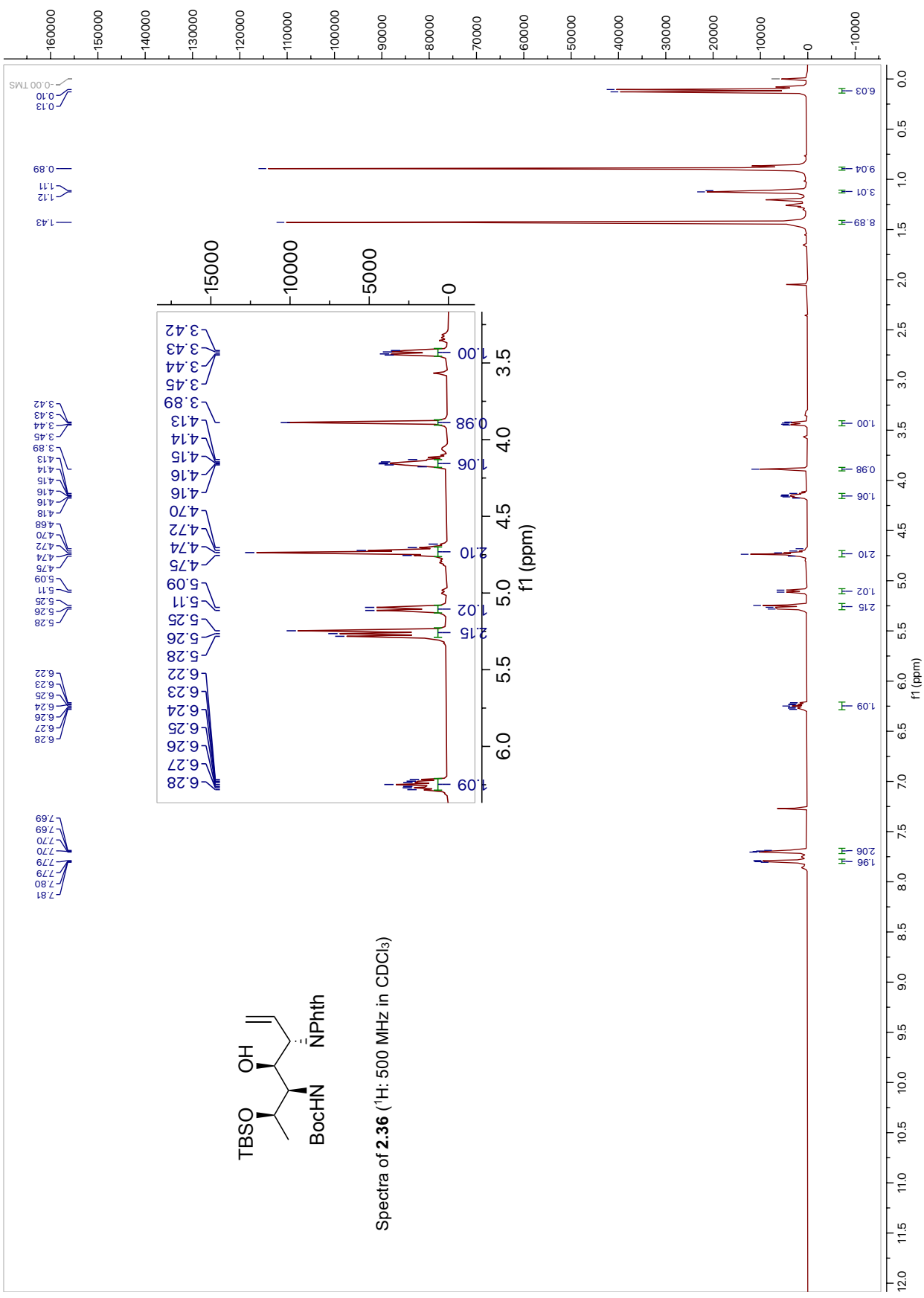


Spectra of **2.36** ($^1$H: 500 MHz in $CDCl_3$)

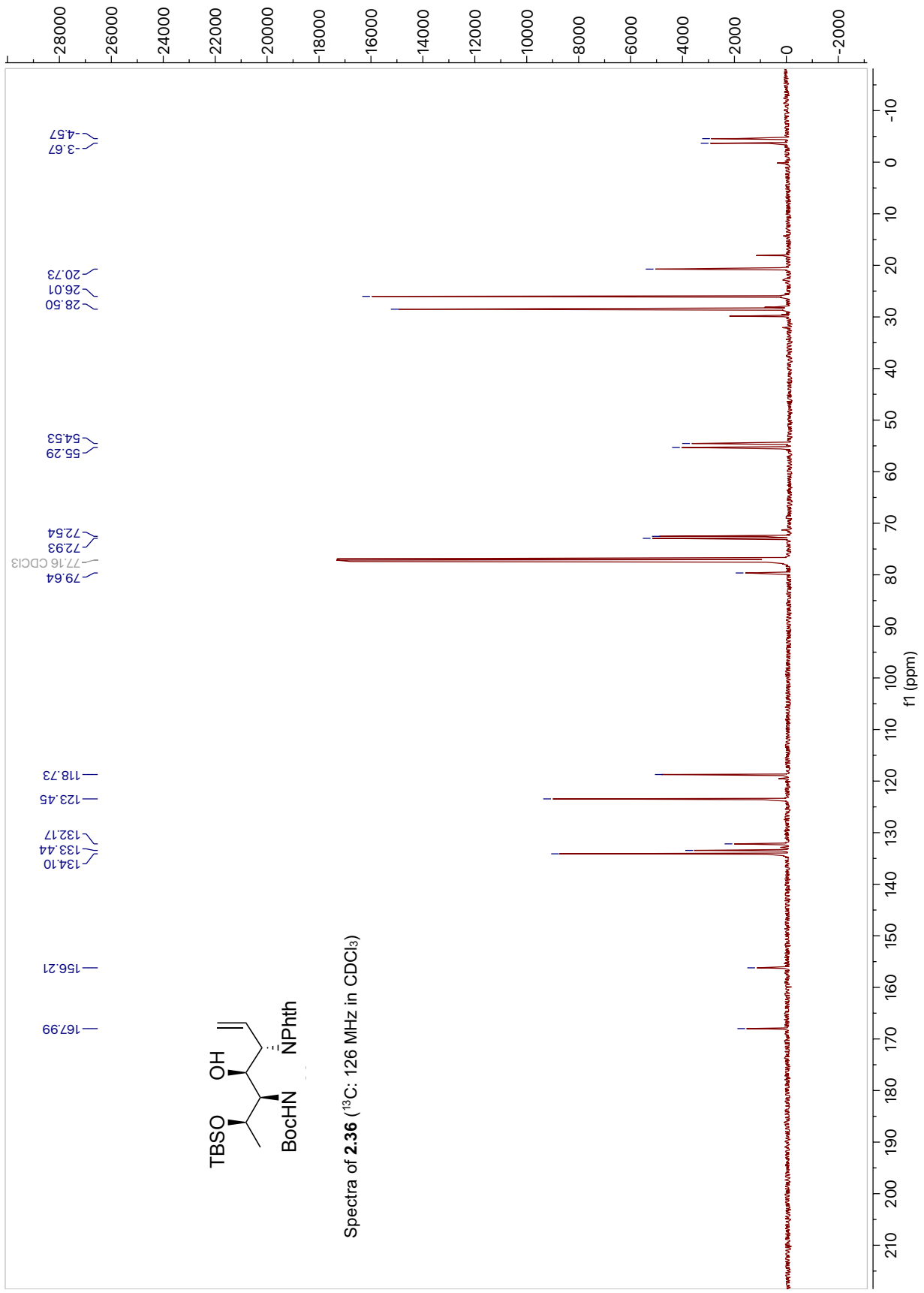
TBSO
OH
BocHN
NPhth
Spectra of 2.36 (13C: 126 MHz in CDCl3)
167.99
156.21
134.10
133.44
132.17
123.45
118.73
79.64
77.16 CDCl3
72.93
72.54
55.29
54.53
28.50
26.01
20.73
-3.67
-4.57
f1 (ppm)

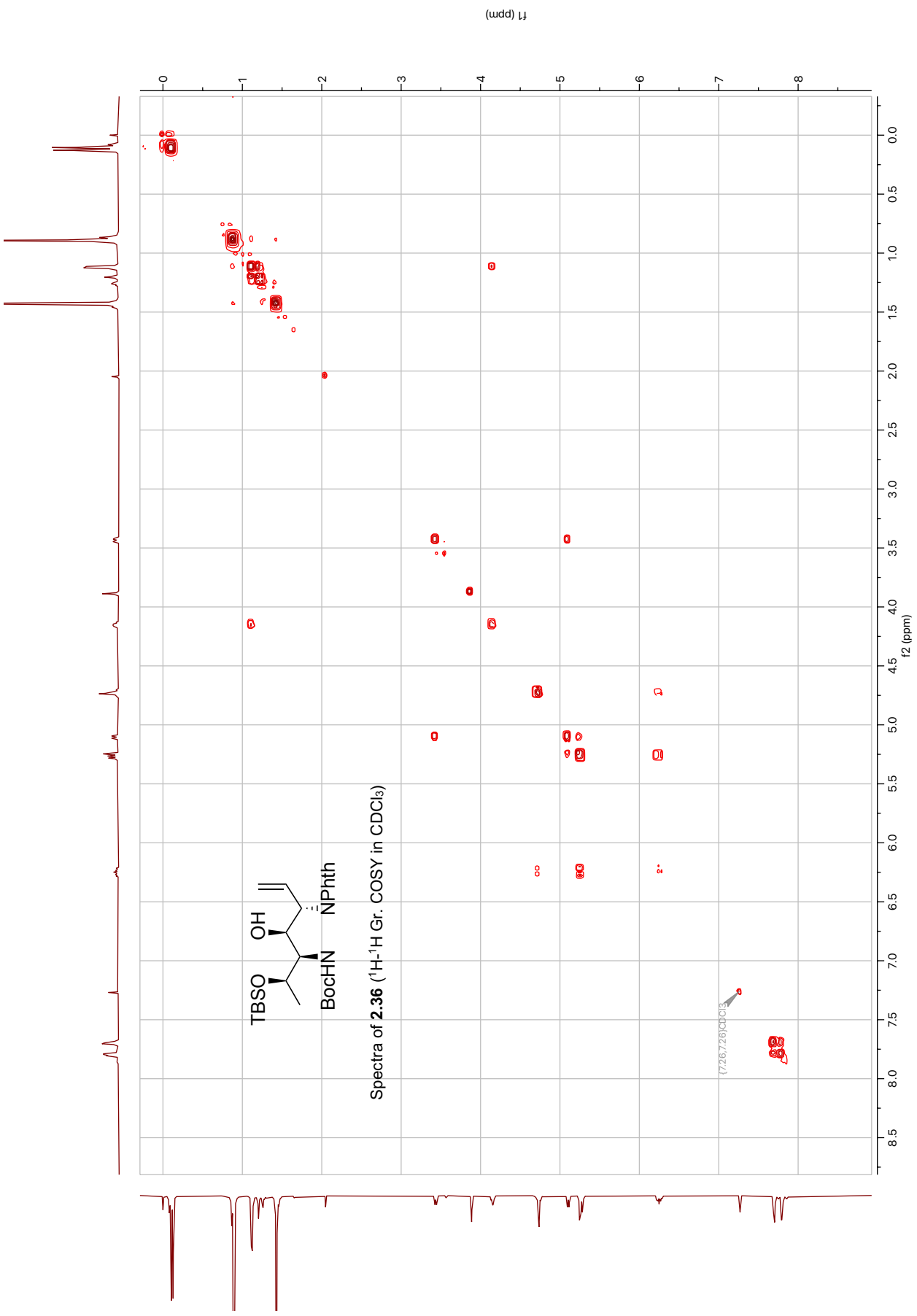
f1 (ppm)
f2 (ppm)
TBSO
OH
BocHN
NPhth
Spectra of 2.36 (1H-1H Gr. COSY in CDCl3)
{7.26,7.26}CDCl3

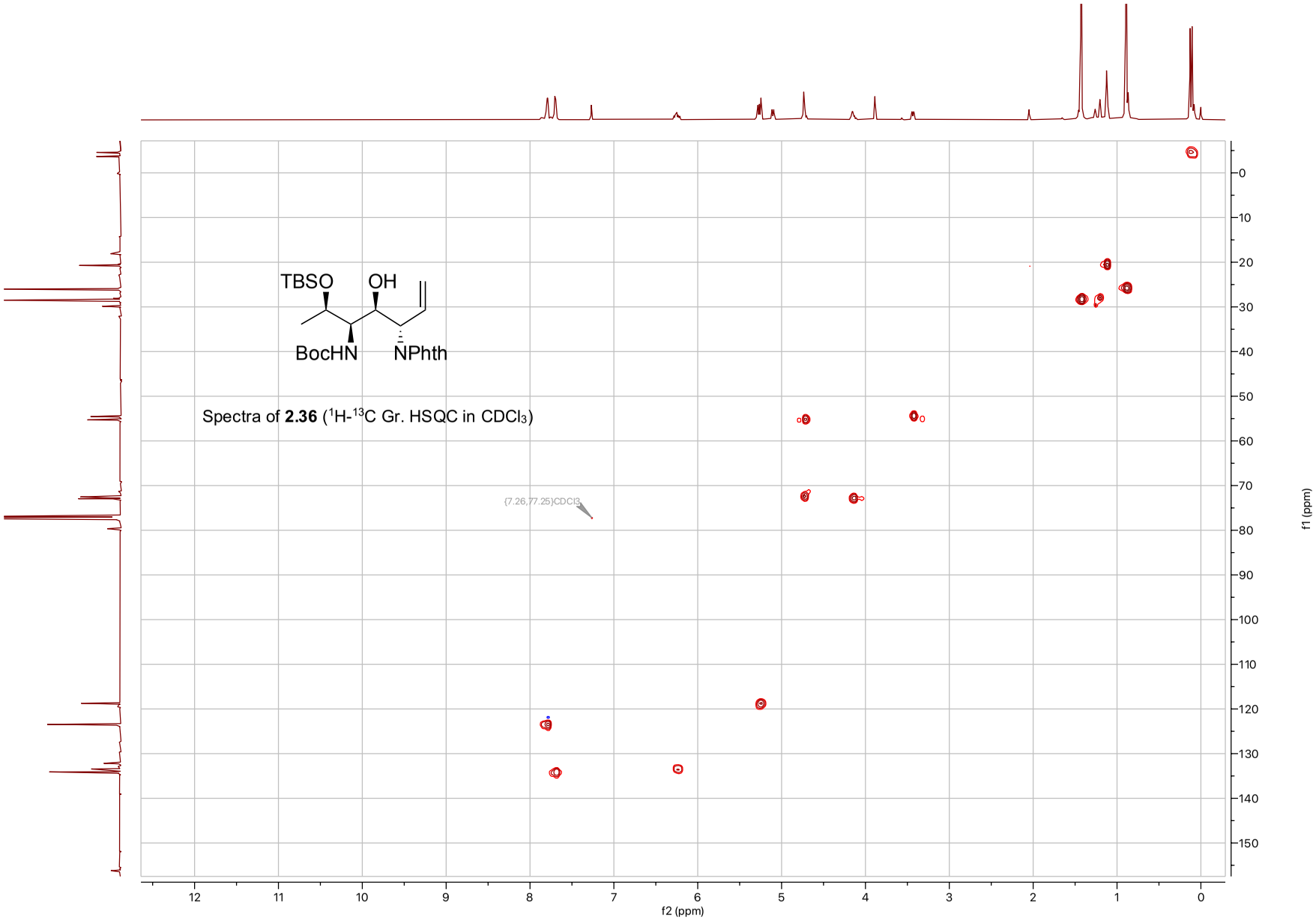
TBSO
OH
BocHN
NPhth
Spectra of **2.36** ($^{1}$H-$^{13}$C Gr. HSQC in $CDCl_3$)
{7.26,77.25}CDCl3
f2 (ppm)
f1 (ppm)

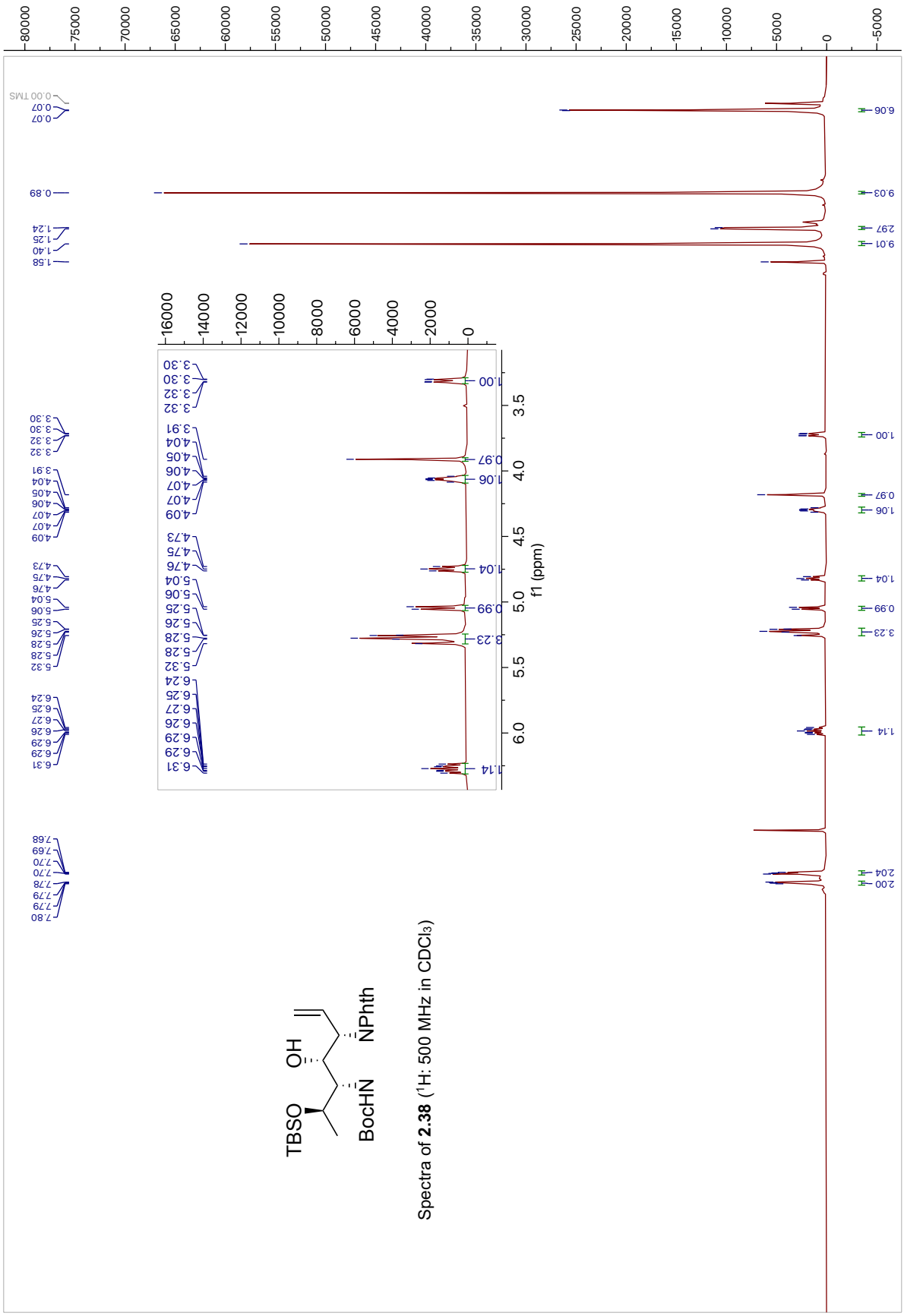
TBSO
OH
BocHN
NPhth
Spectra of 2.38 (1H: 500 MHz in CDCl3)
f1 (ppm)

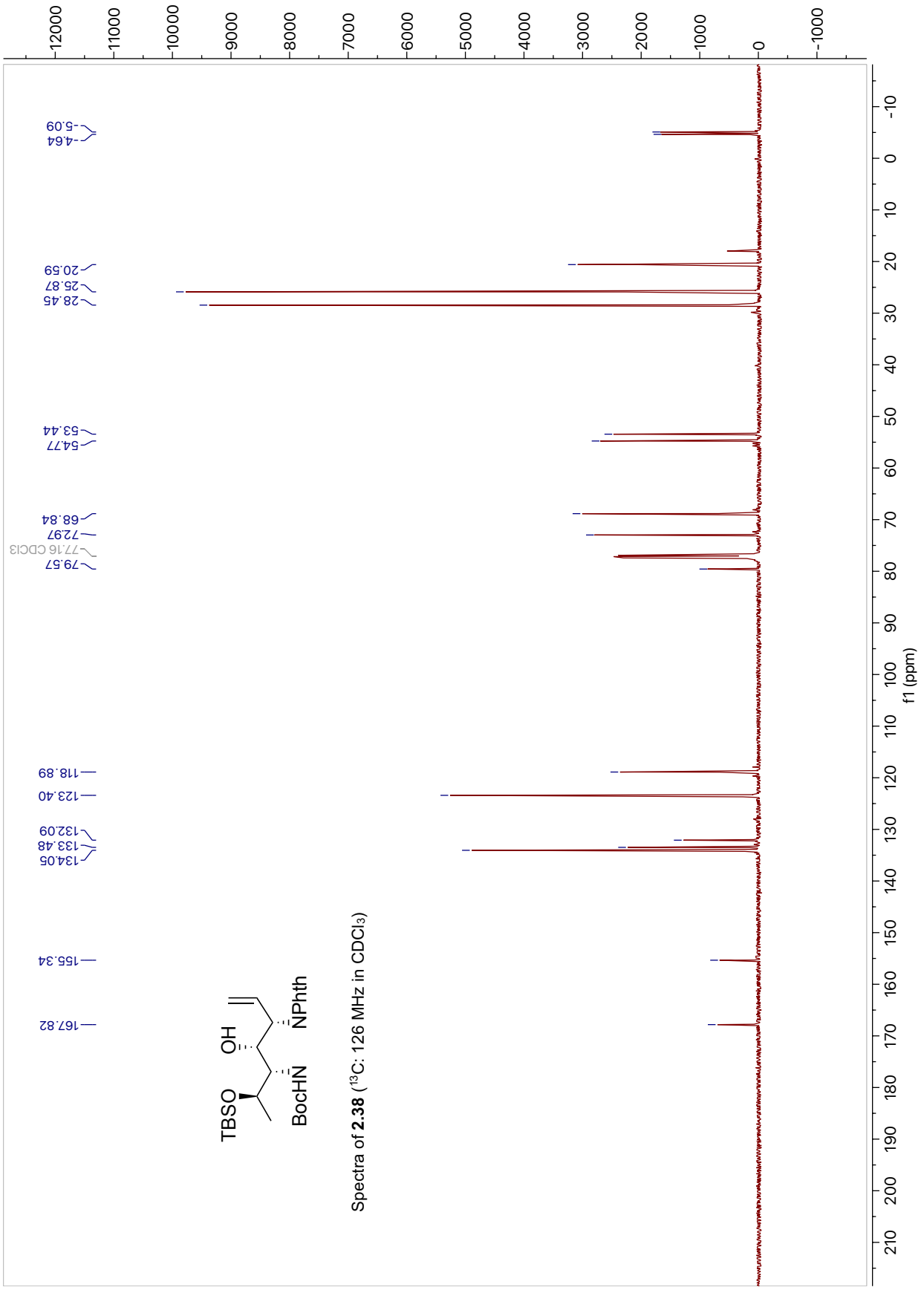
Spectra of 2.38 ($^{13}$C: 126 MHz in $CDCl_3$)
TBSO
OH
BocHN
NPhth
167.82
155.34
134.05
133.48
132.09
123.40
118.89
79.57
77.16 CDCl3
72.97
68.84
54.77
53.44
28.45
25.87
20.59
-4.64
-5.09
f1 (ppm)

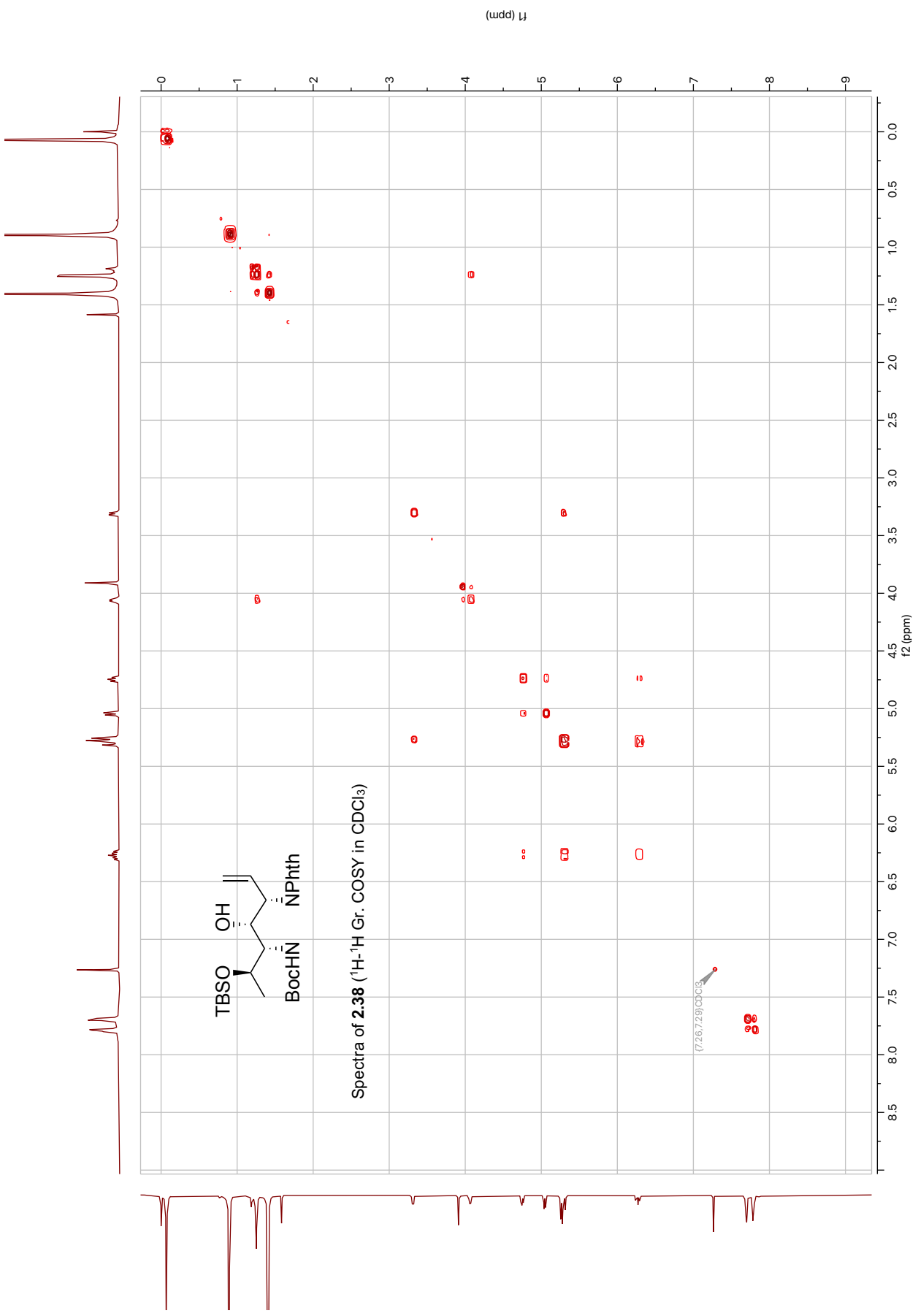
f1 (ppm)
f2 (ppm)
Spectra of 2.38 (1H-1H Gr. COSY in CDCl3)
TBSO
OH
BocHN
NPhth
{7.26,7.29}CDCl3

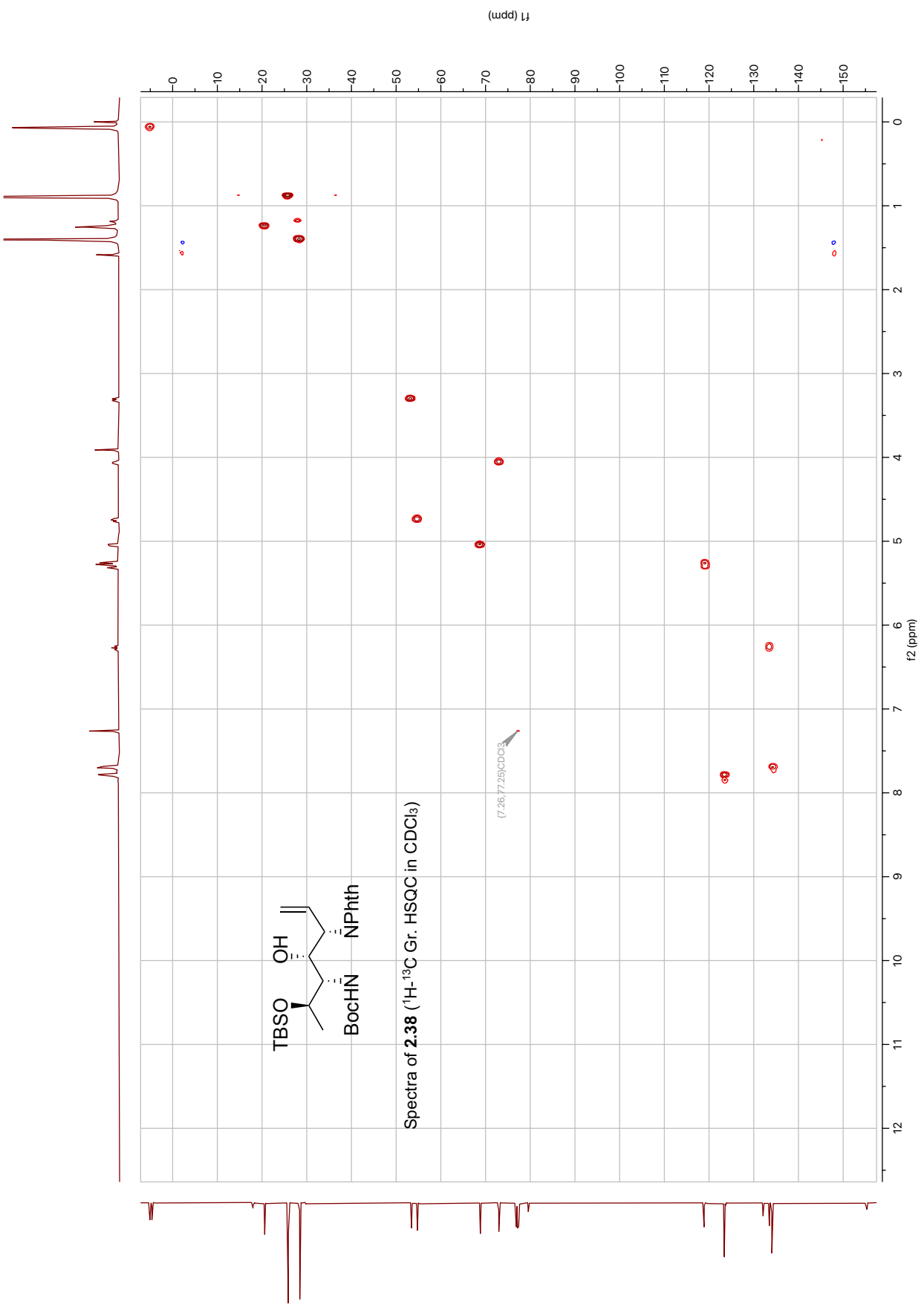
Spectra of 2.38 (1H-13C Gr. HSQC in CDCl3)
TBSO
OH
BocHN
NPhth
(7.26,77.25)CDCl3
f2 (ppm)
f1 (ppm)

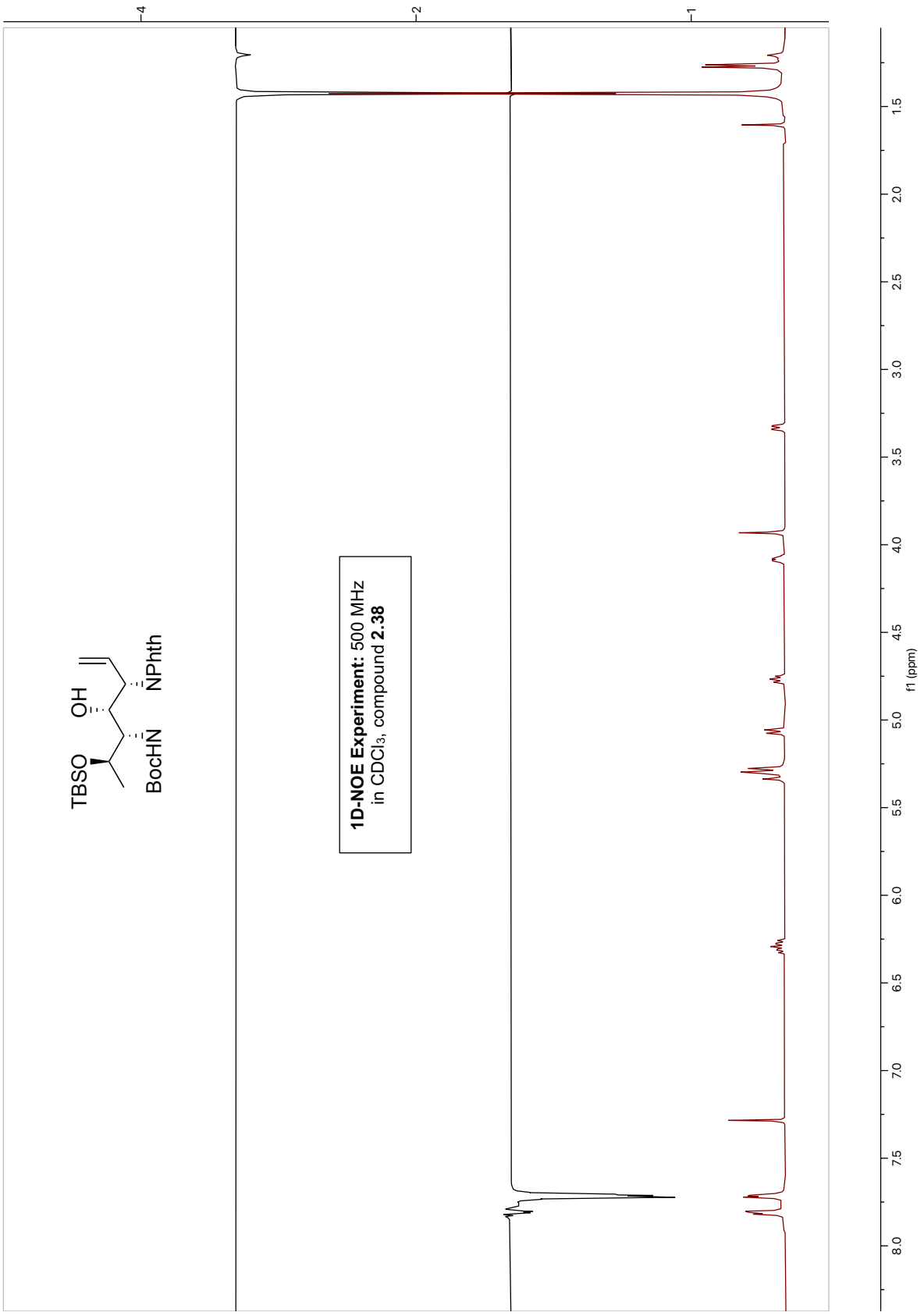
TBSO
OH
BocHN
NPhth
**1D-NOE Experiment:** 500 MHz
in $CDCl_3$, compound **2.38**
4
2
1
8.0
7.5
7.0
6.5
6.0
5.5
5.0
4.5
4.0
3.5
3.0
2.5
2.0
1.5
f1 (ppm)

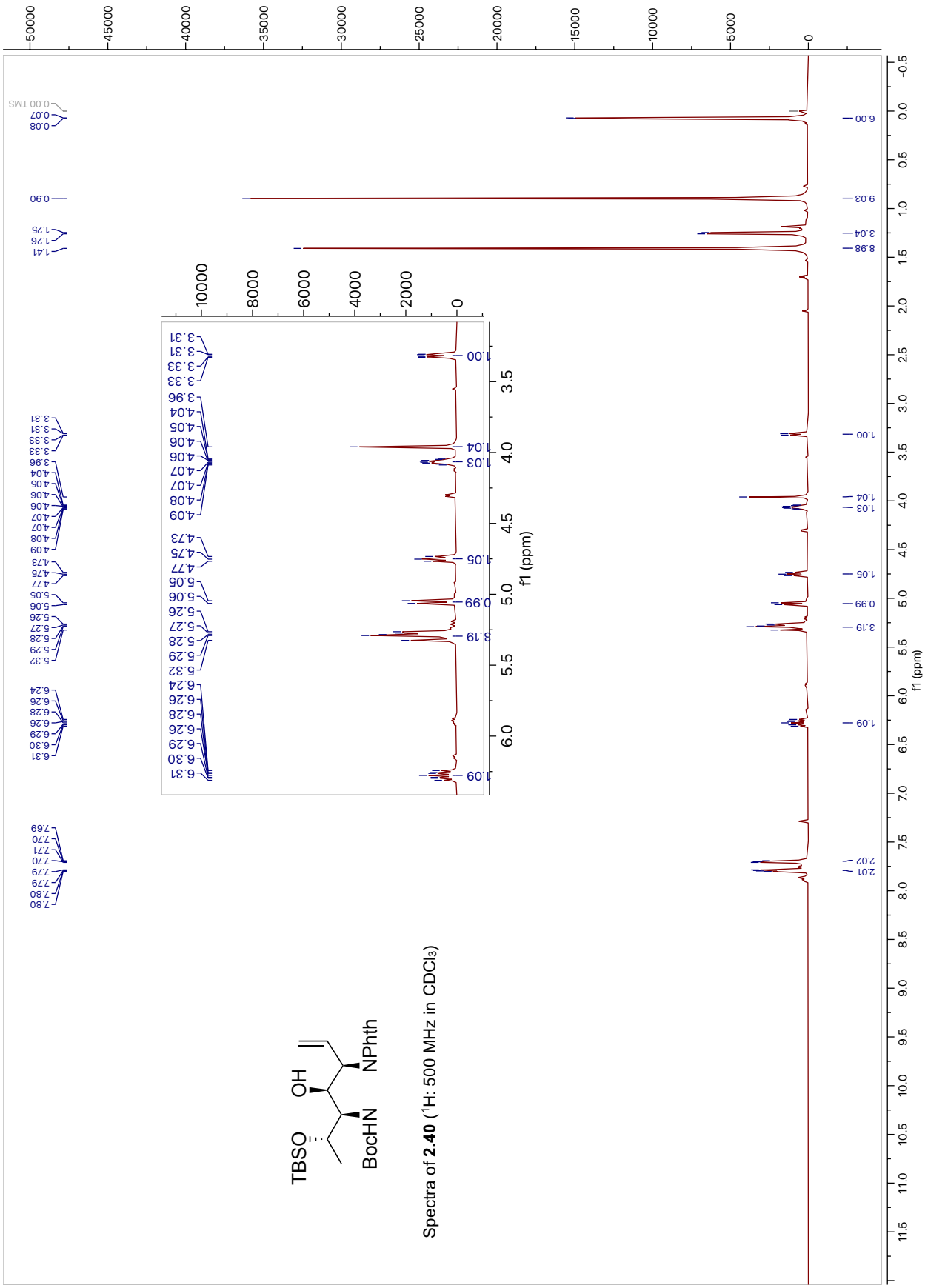


Spectra of **2.40** ($^1$H: 500 MHz in $CDCl_3$)

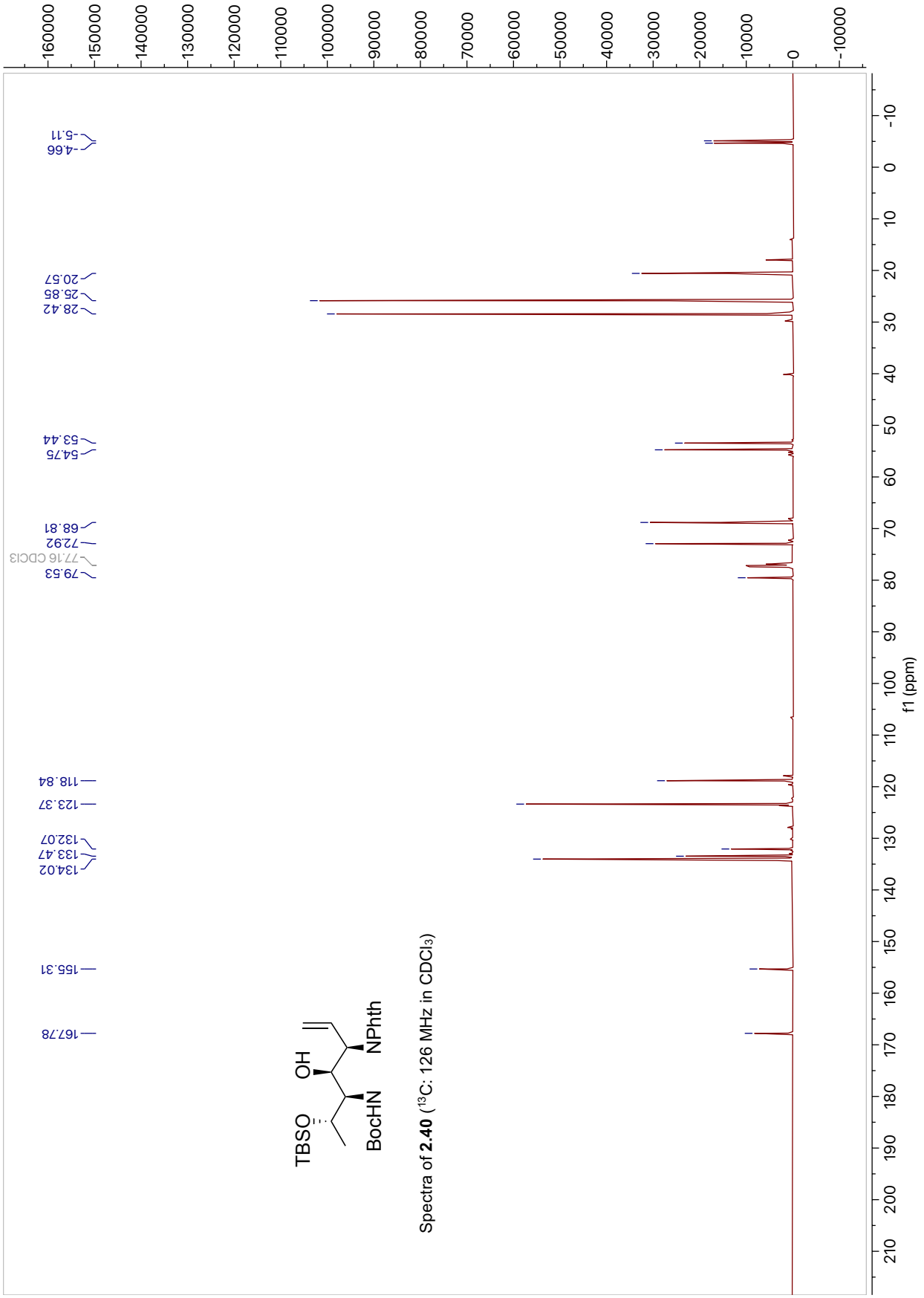
TBSO
OH
BocHN
NPhth
Spectra of 2.40 (13C: 126 MHz in CDCl3)
167.78
155.31
134.02
133.47
132.07
123.37
118.84
79.53
77.16 CDCl3
72.92
68.81
54.75
53.44
28.42
25.85
20.57
-4.66
-5.11
f1 (ppm)

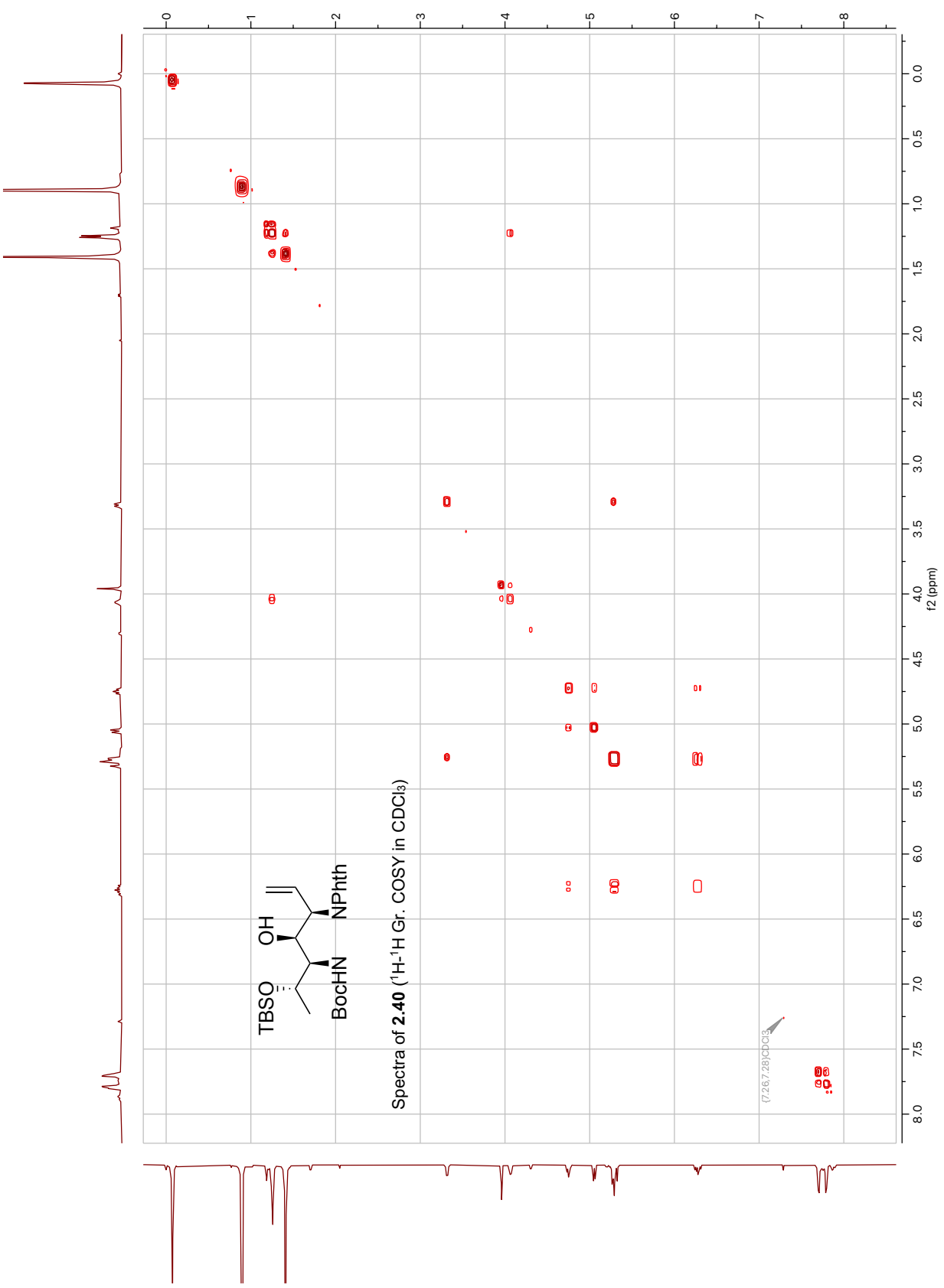
f1 (ppm)
f2 (ppm)
Spectra of 2.40 (1H-1H Gr. COSY in CDCl3)
TBSO
OH
BocHN
NPhth
{7.26,7.28}CDCl3

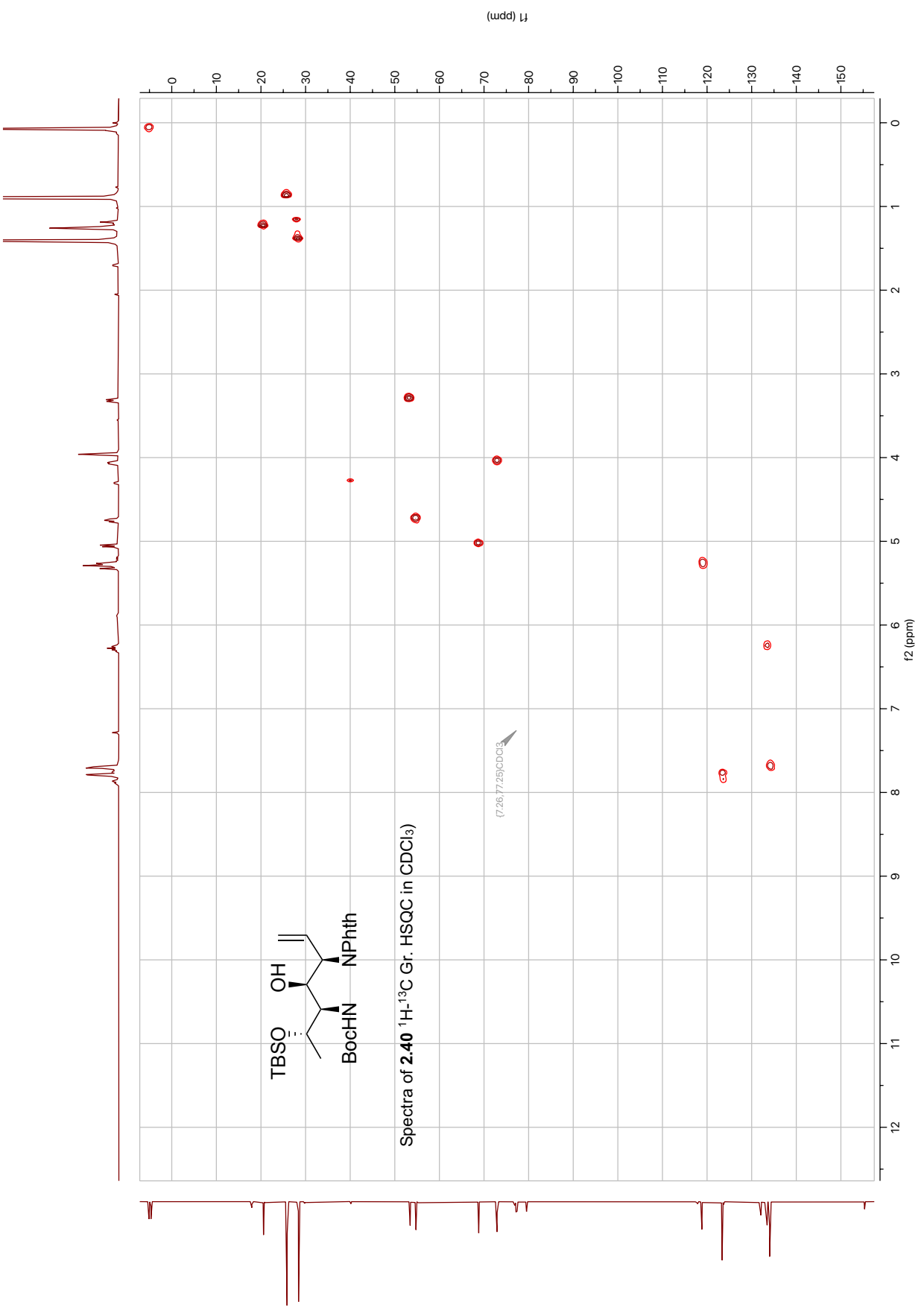
Spectra of **2.40** $^{1}H$-$^{13}C$ Gr. HSQC in $CDCl_3$)
TBSO
OH
BocHN
NPhth
{7.26,77.25}CDCl3
f2 (ppm)
f1 (ppm)

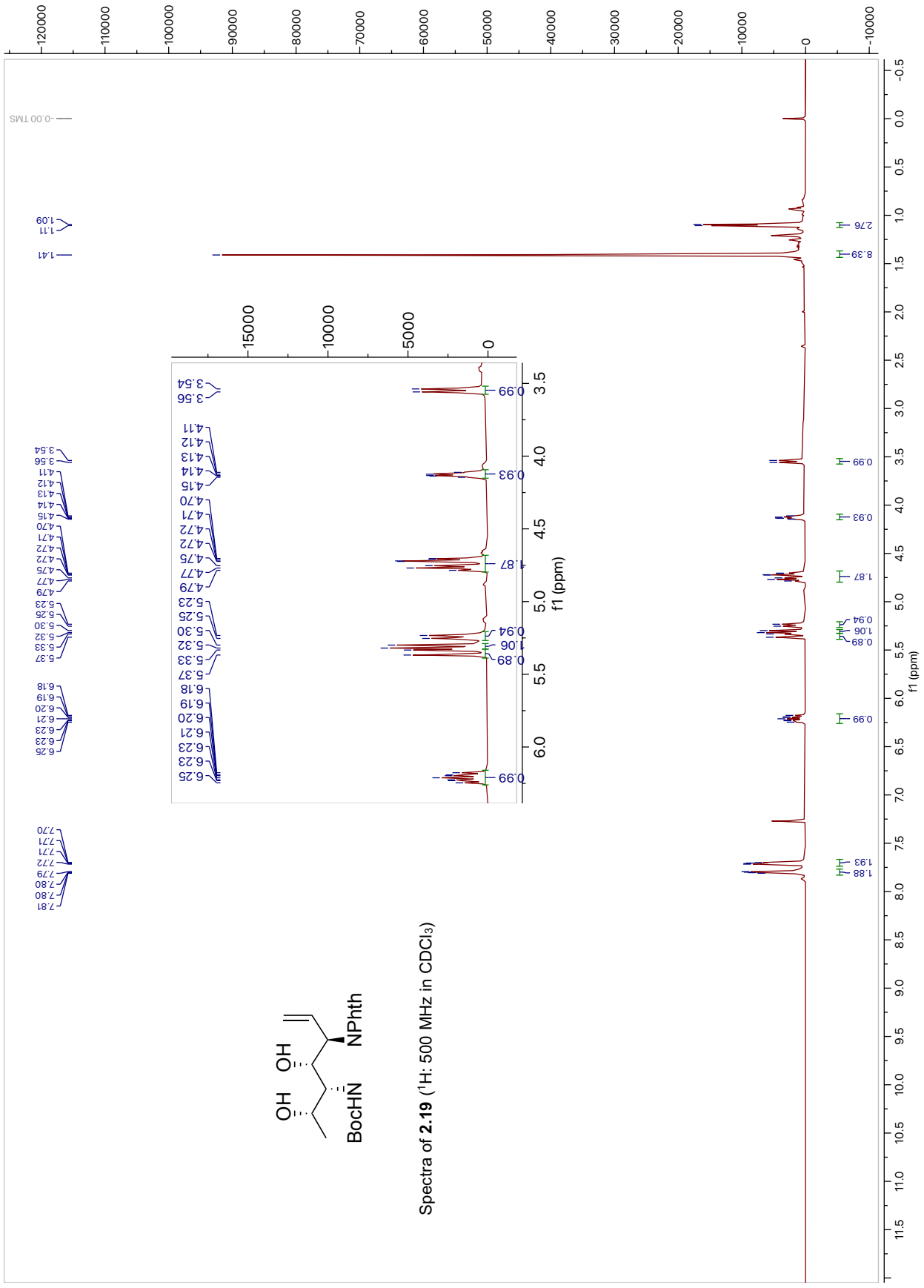


Spectra of **2.19** ($^1$H: 500 MHz in $CDCl_3$)

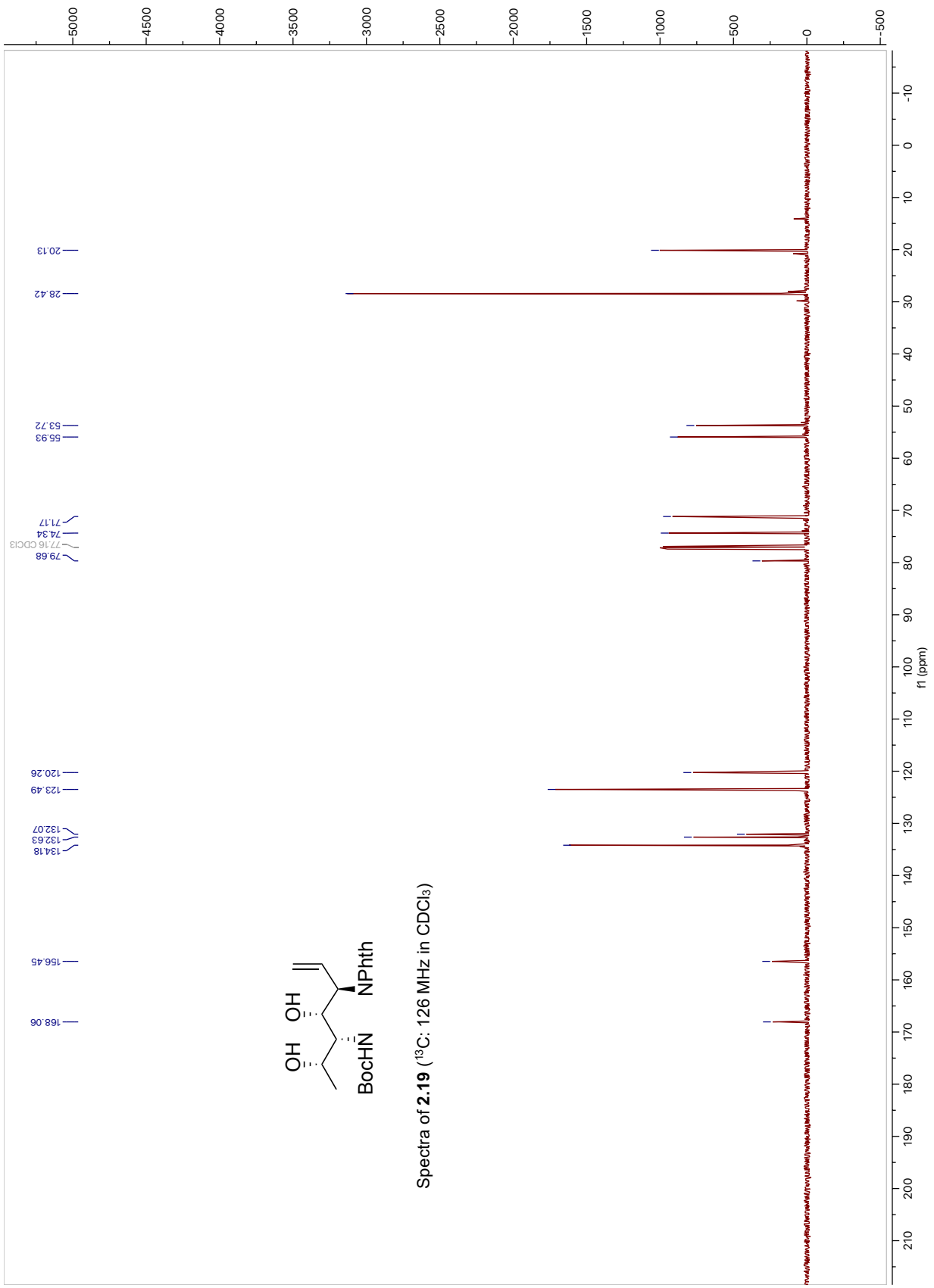
OH
OH
BocHN
NPhth
Spectra of 2.19 (13C: 126 MHz in CDCl3)
168.06
156.45
134.18
132.63
132.07
123.49
120.26
79.68
77.16 CDCl3
74.34
71.17
55.93
53.72
28.42
20.13
f1 (ppm)

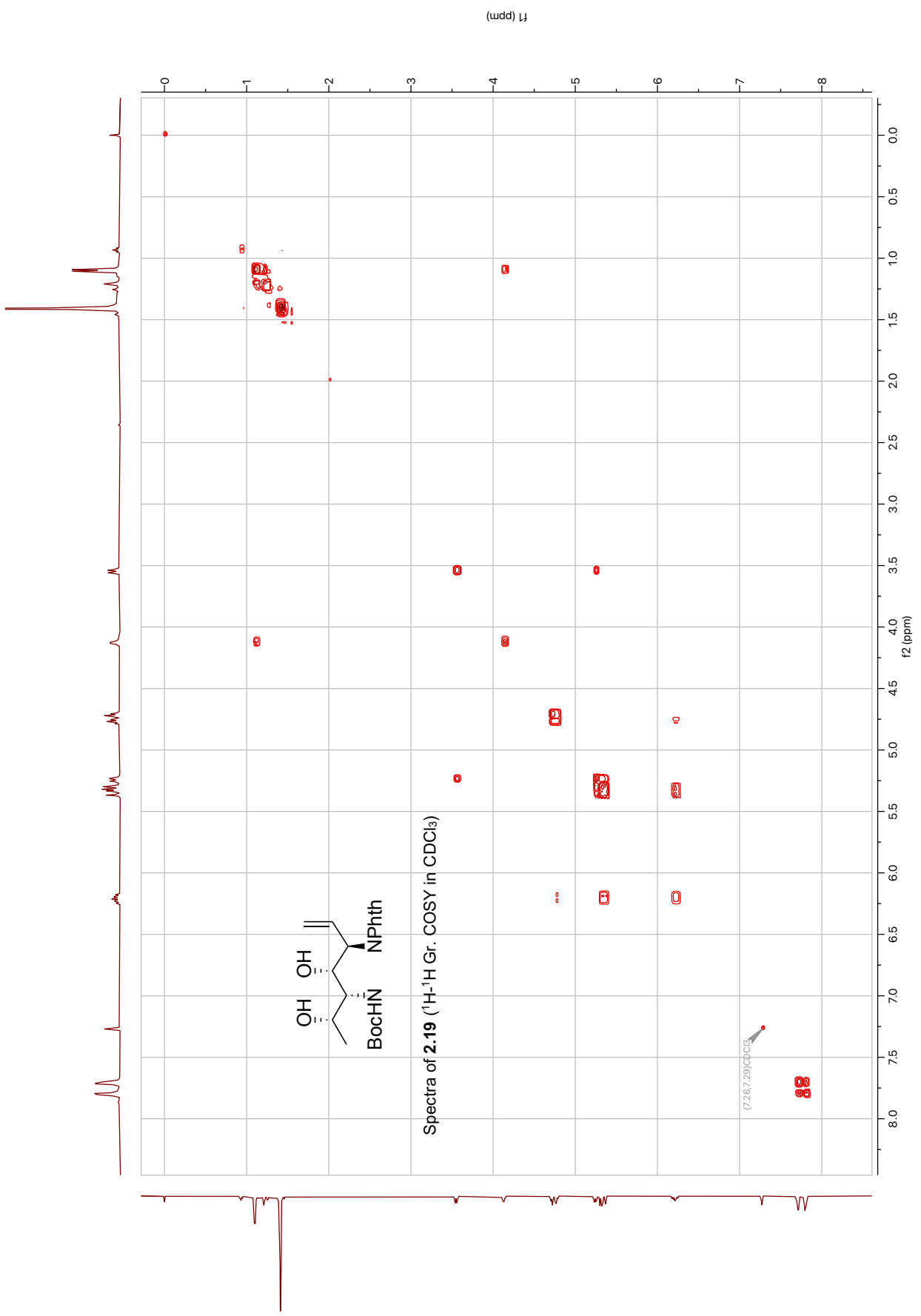
f1 (ppm)
f2 (ppm)
Spectra of 2.19 (1H-1H Gr. COSY in CDCl3)
OH
OH
BocHN
NPhth
(7.26,7.29)CDCl3

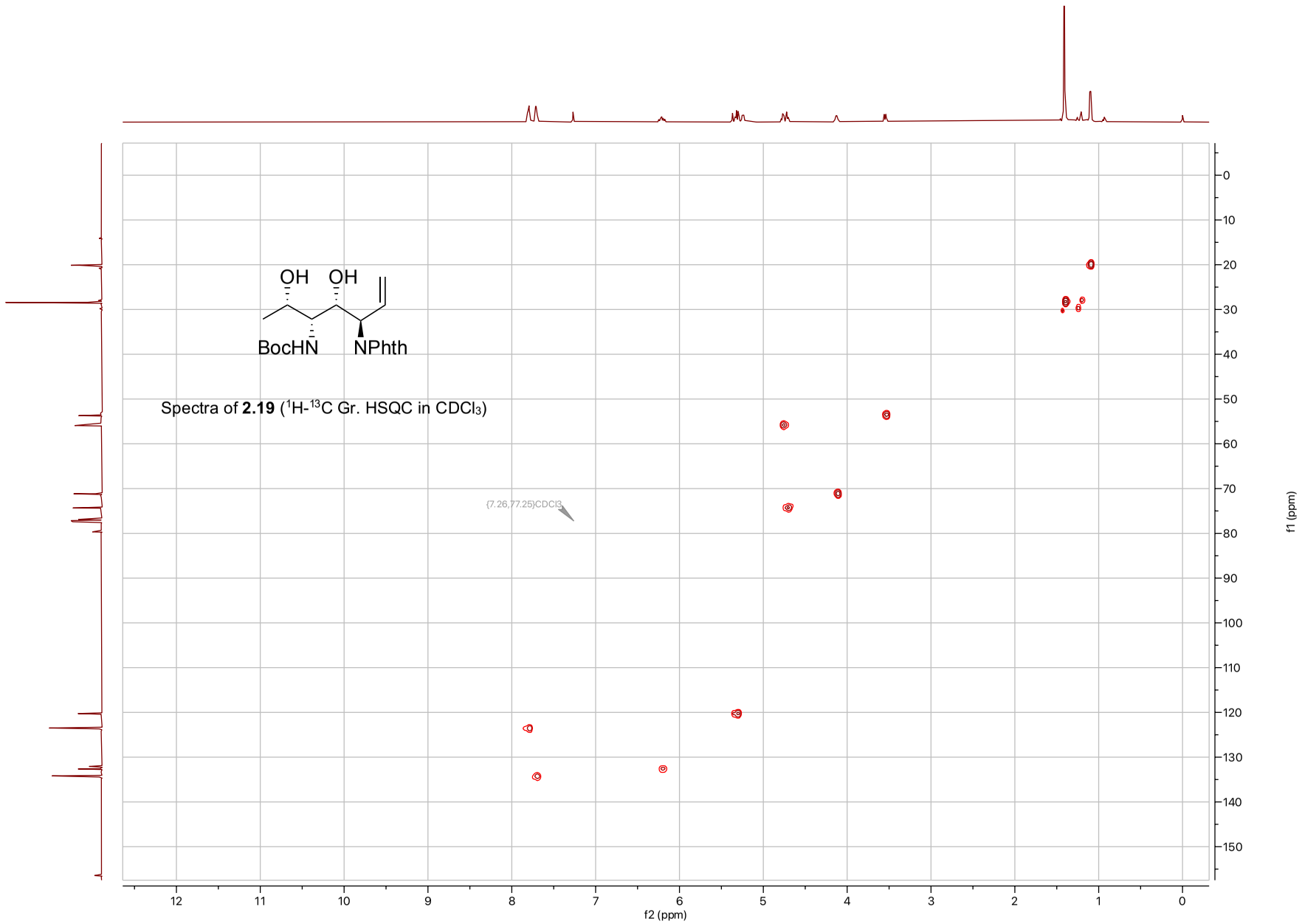
OH
OH
BocHN
NPhth
Spectra of **2.19** ($^{1}$H-$^{13}$C Gr. HSQC in $CDCl_3$)
{7.26,77.25}CDCl3
f2 (ppm)
f1 (ppm)

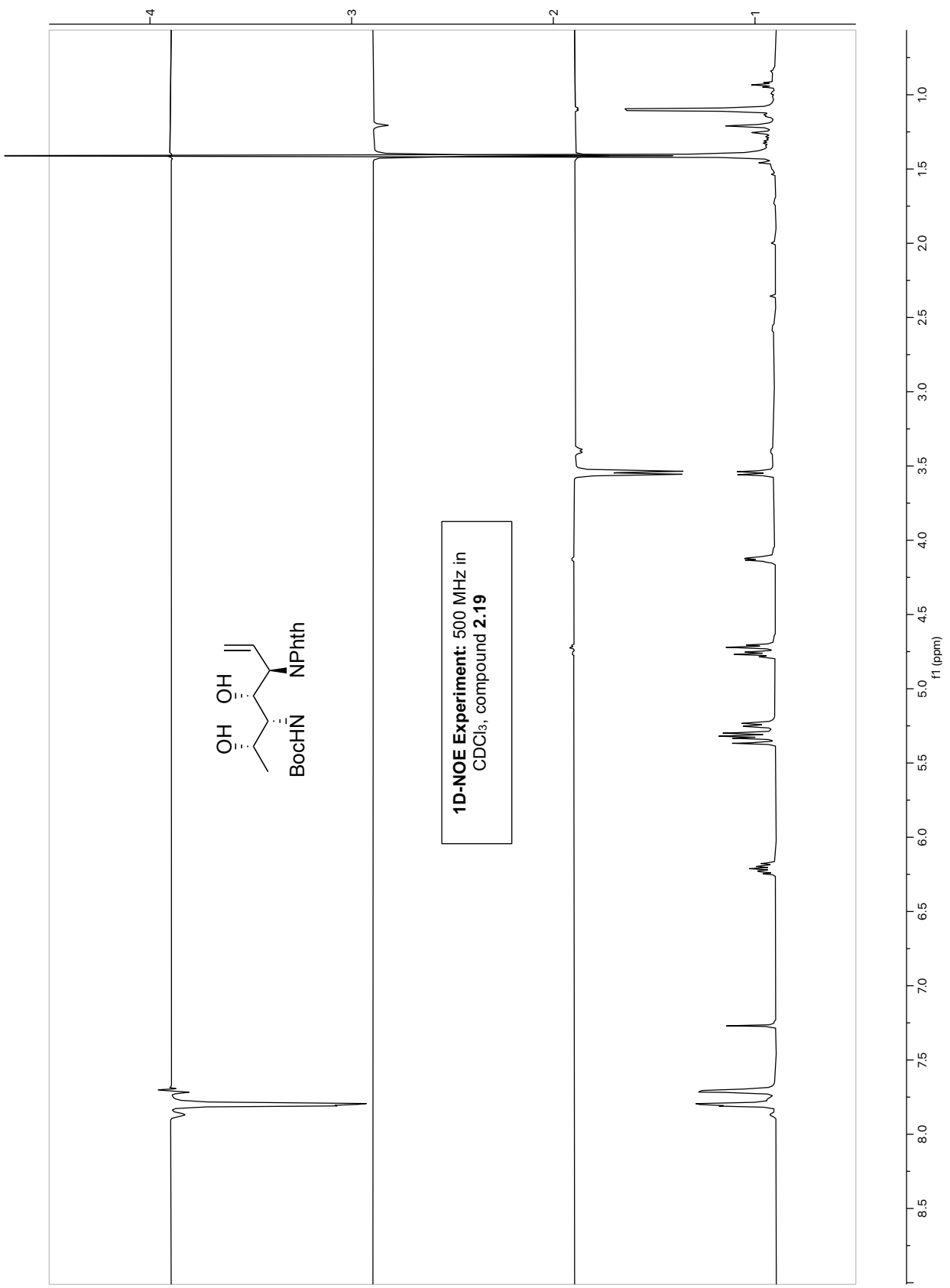
OH
OH
BocHN
NPhth
1D-NOE Experiment: 500 MHz in CDCl3, compound 2.19
f1 (ppm)

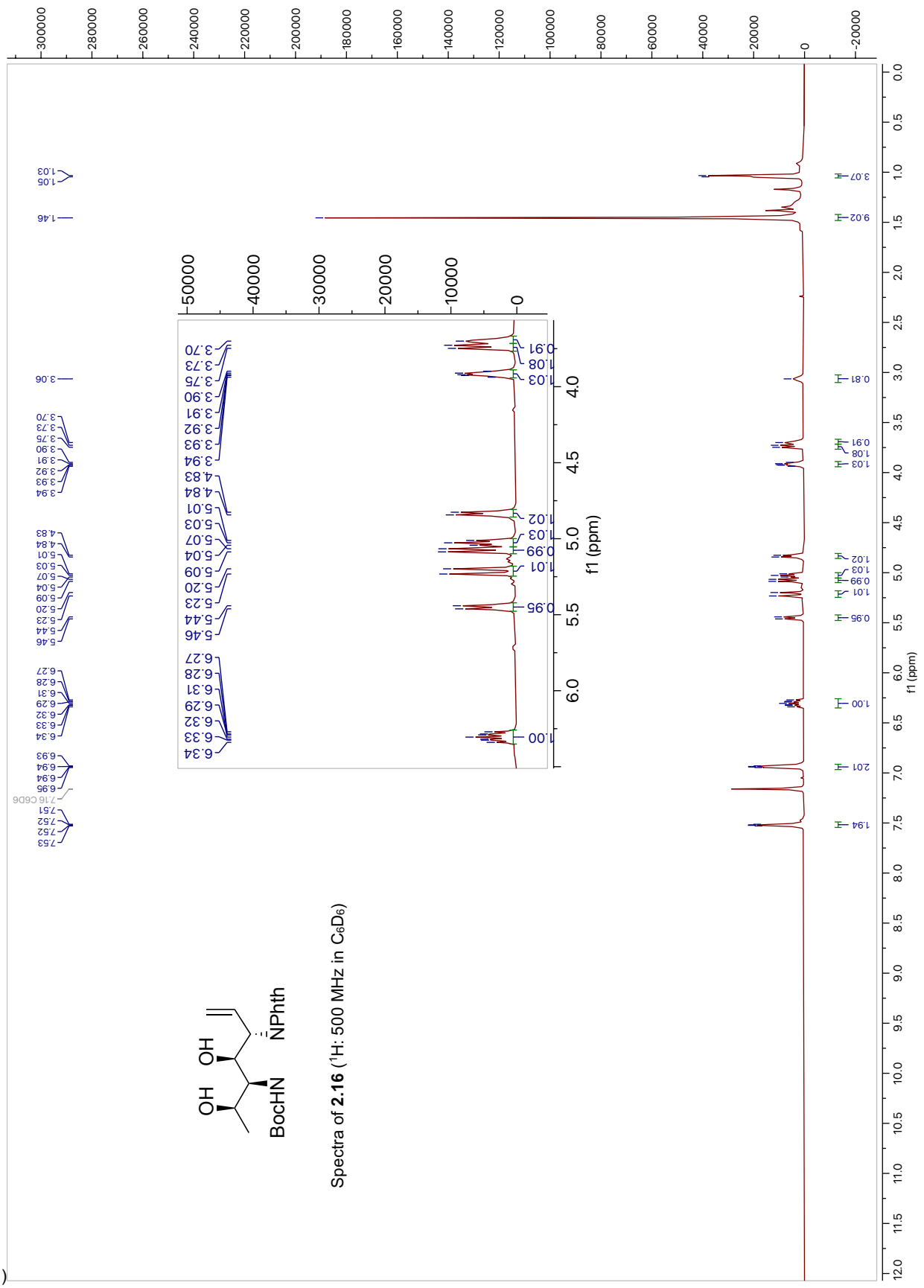


Spectra of **2.16** ($^1$H: 500 MHz in $C_6D_6$)

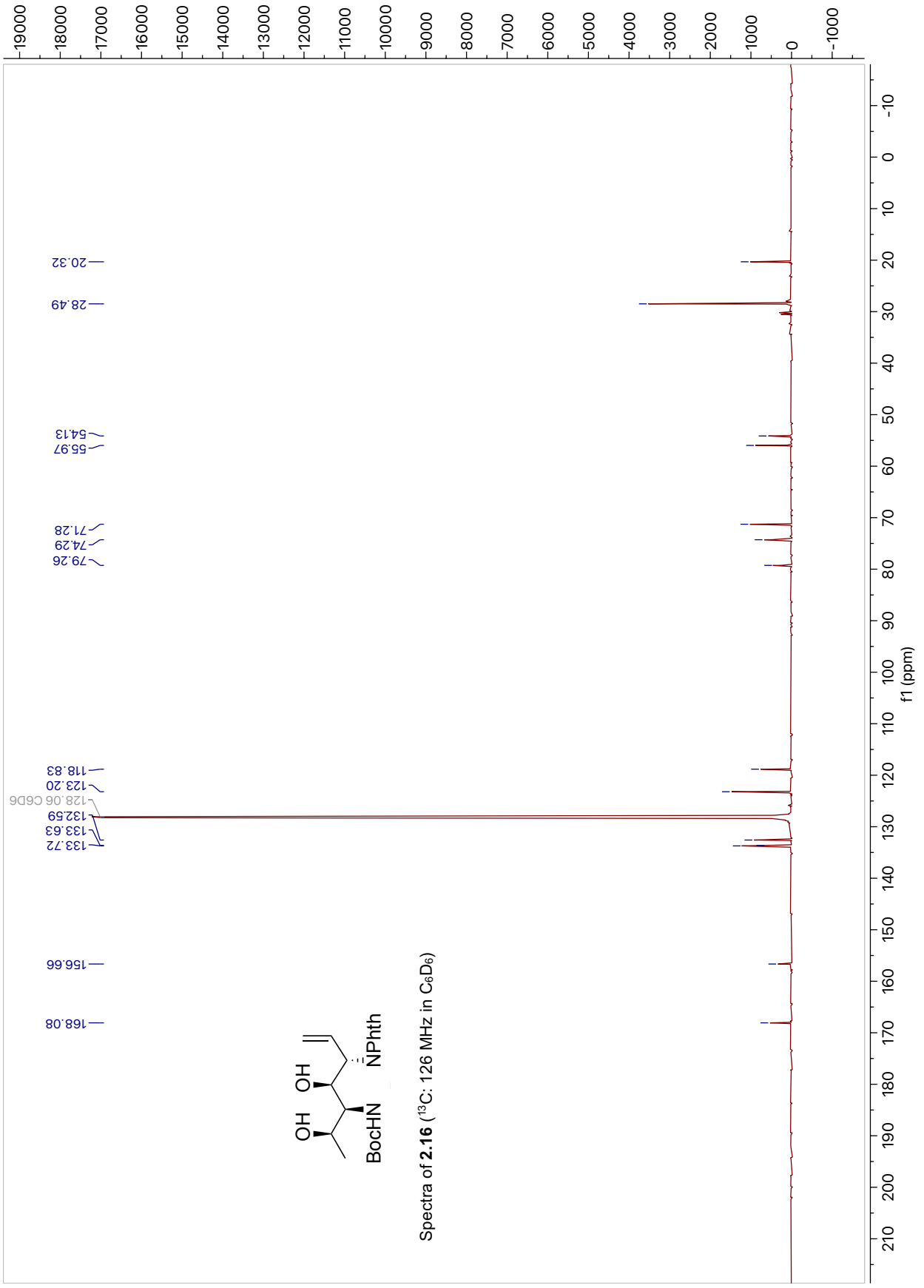
19000
18000
17000
16000
15000
14000
13000
12000
11000
10000
9000
8000
7000
6000
5000
4000
3000
2000
1000
0
-1000
168.08
156.66
133.72
133.63
132.59
128.06 C6D6
123.20
118.83
79.26
74.29
71.28
55.97
54.13
28.49
20.32
OH
OH
BocHN
NPhth
Spectra of 2.16 (13C: 126 MHz in C6D6)
f1 (ppm)
-10
0
10
20
30
40
50
60
70
80
90
100
110
120
130
140
150
160
170
180
190
200
210

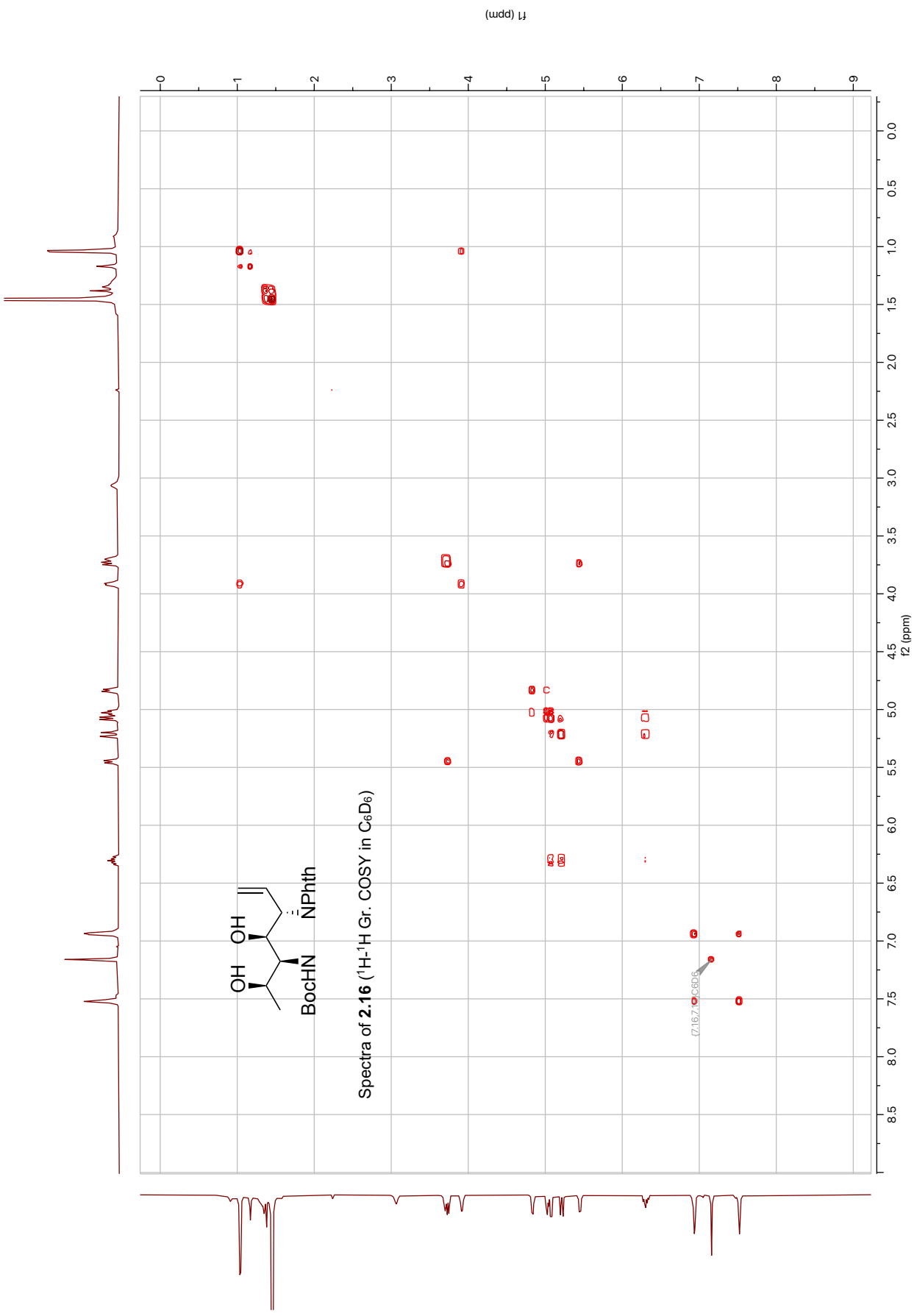
f1 (ppm)
f2 (ppm)
Spectra of 2.16 (1H-1H Gr. COSY in C6D6)
OH
OH
BocHN
NPhth

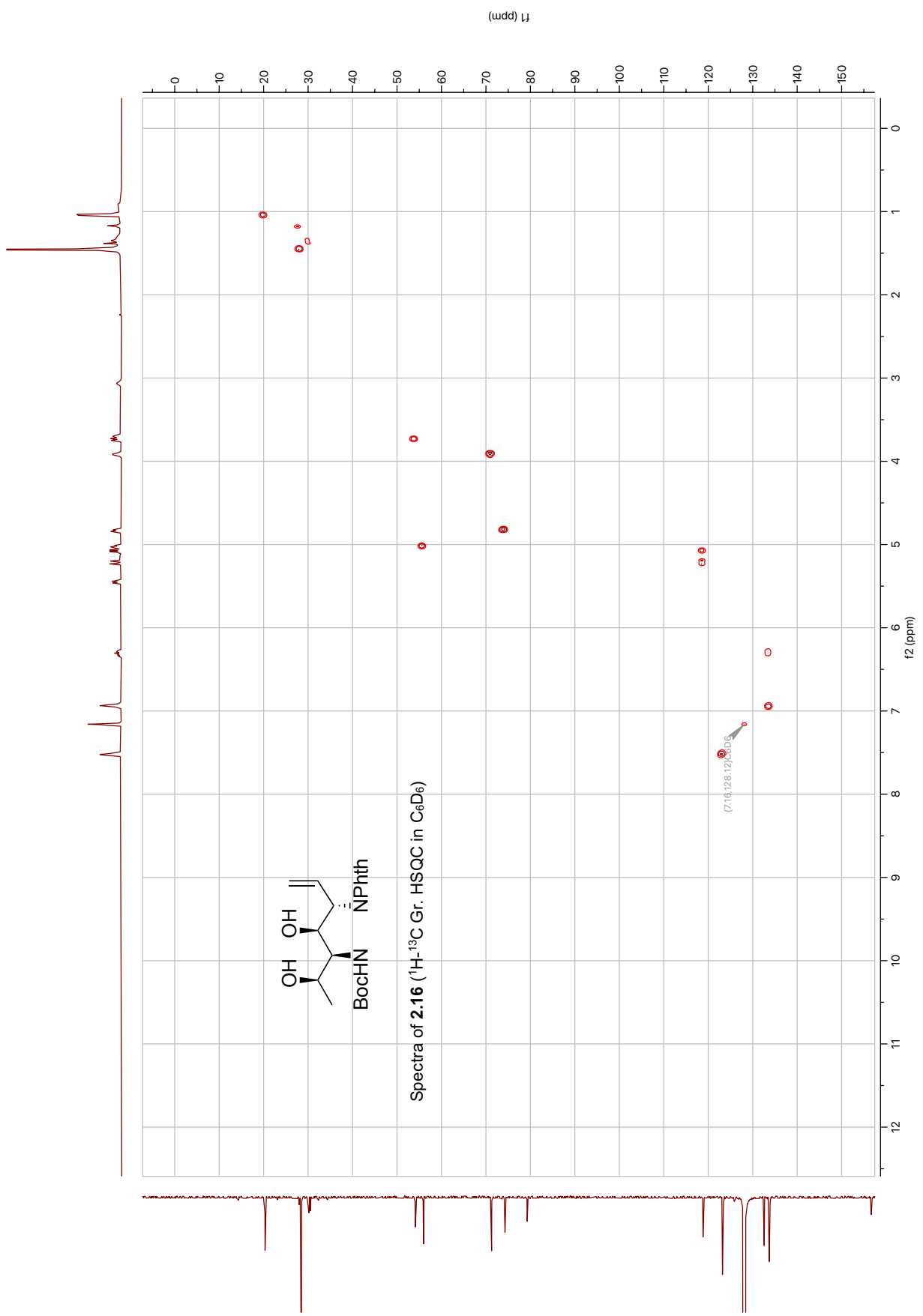
Spectra of 2.16 (1H-13C Gr. HSQC in C6D6)
OH
OH
BocHN
NPhth
f2 (ppm)
f1 (ppm)

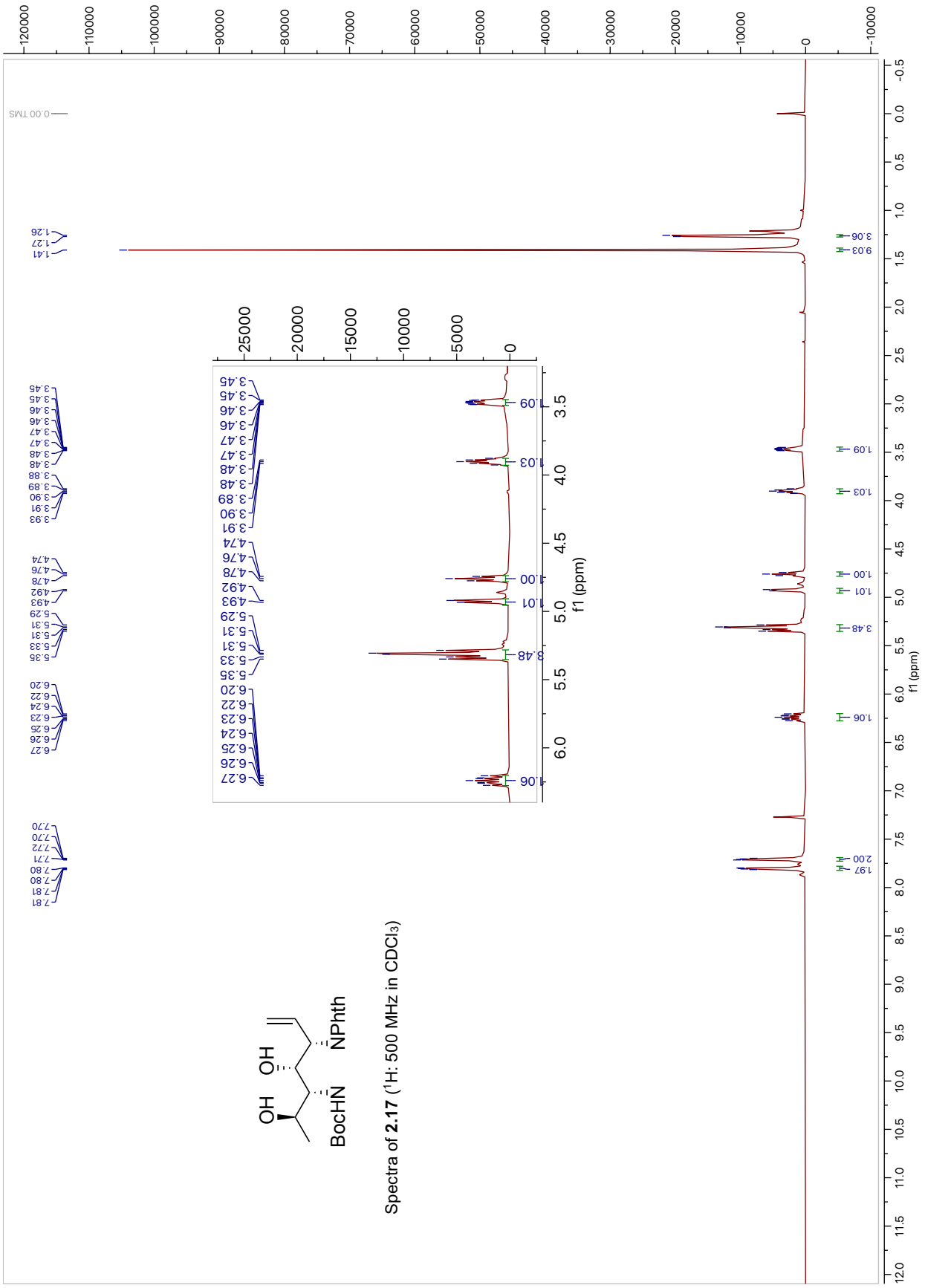


Spectra of **2.17** ($^1$H: 500 MHz in $CDCl_3$)

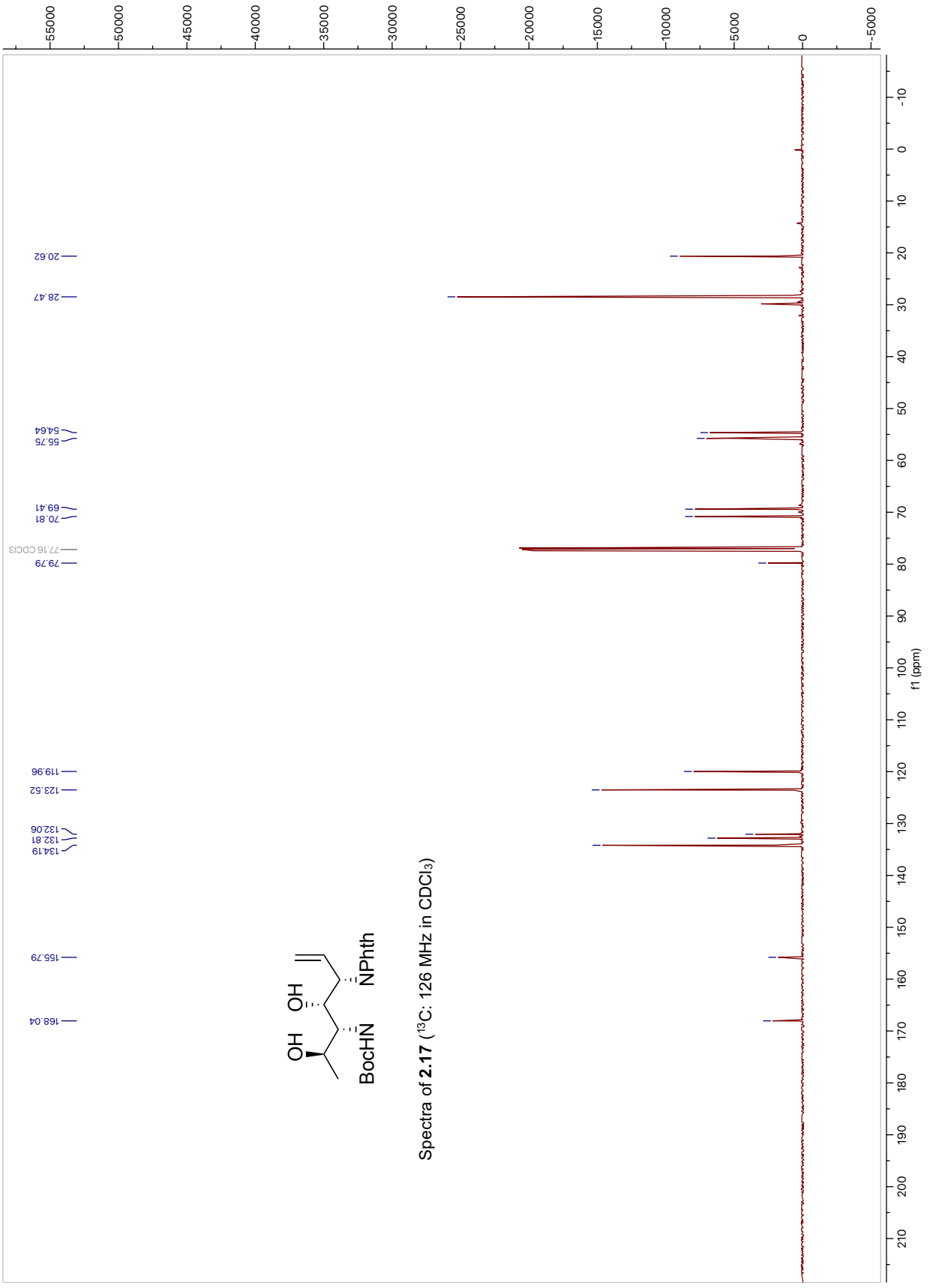


Spectra of **2.17** ($^{13}C$: 126 MHz in $CDCl_3$)

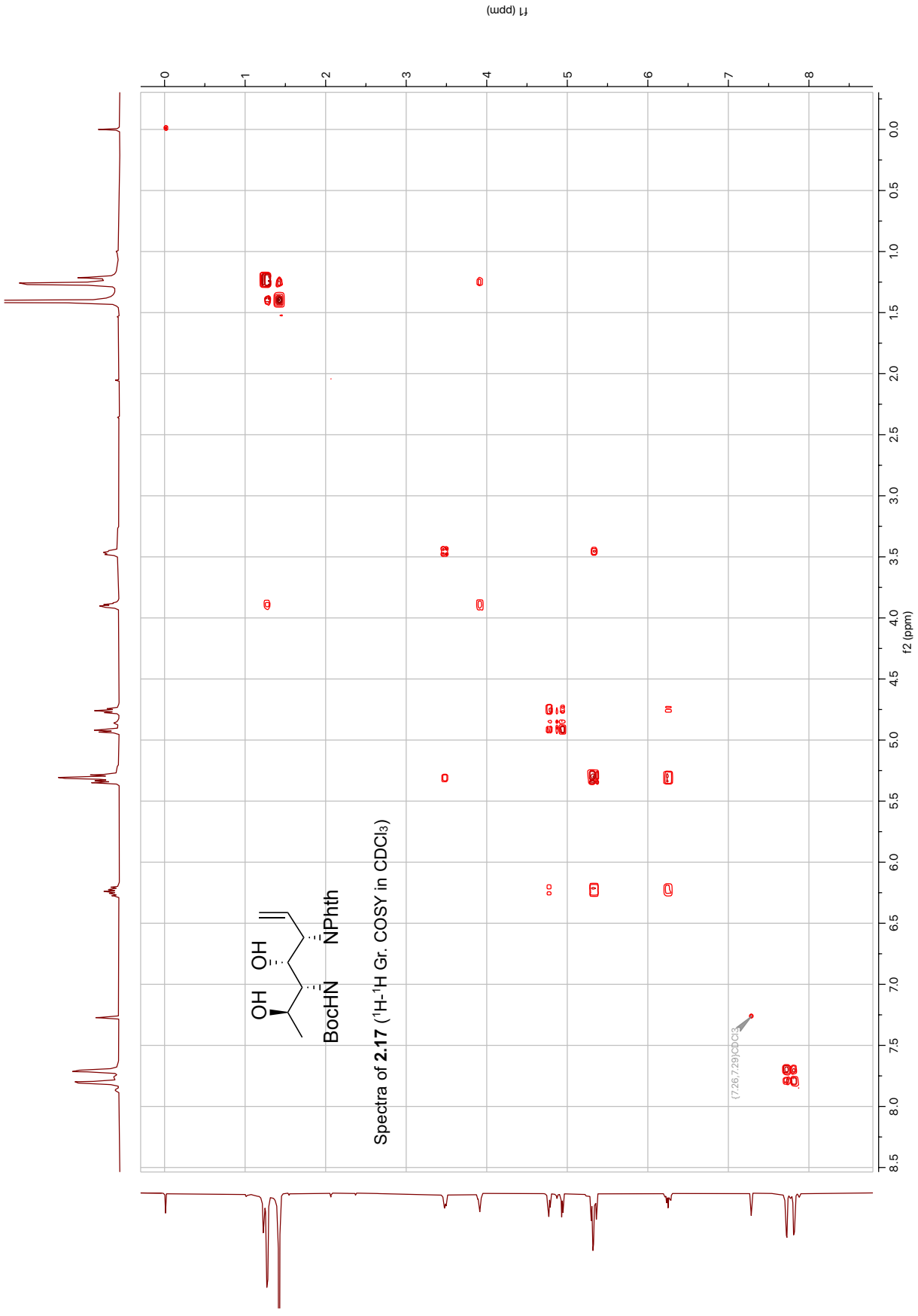
Spectra of 2.17 (1H-1H Gr. COSY in CDCl3)
OH
OH
BocHN
NPhth
f1 (ppm)
f2 (ppm)
{7.26,7.29}CDCl3

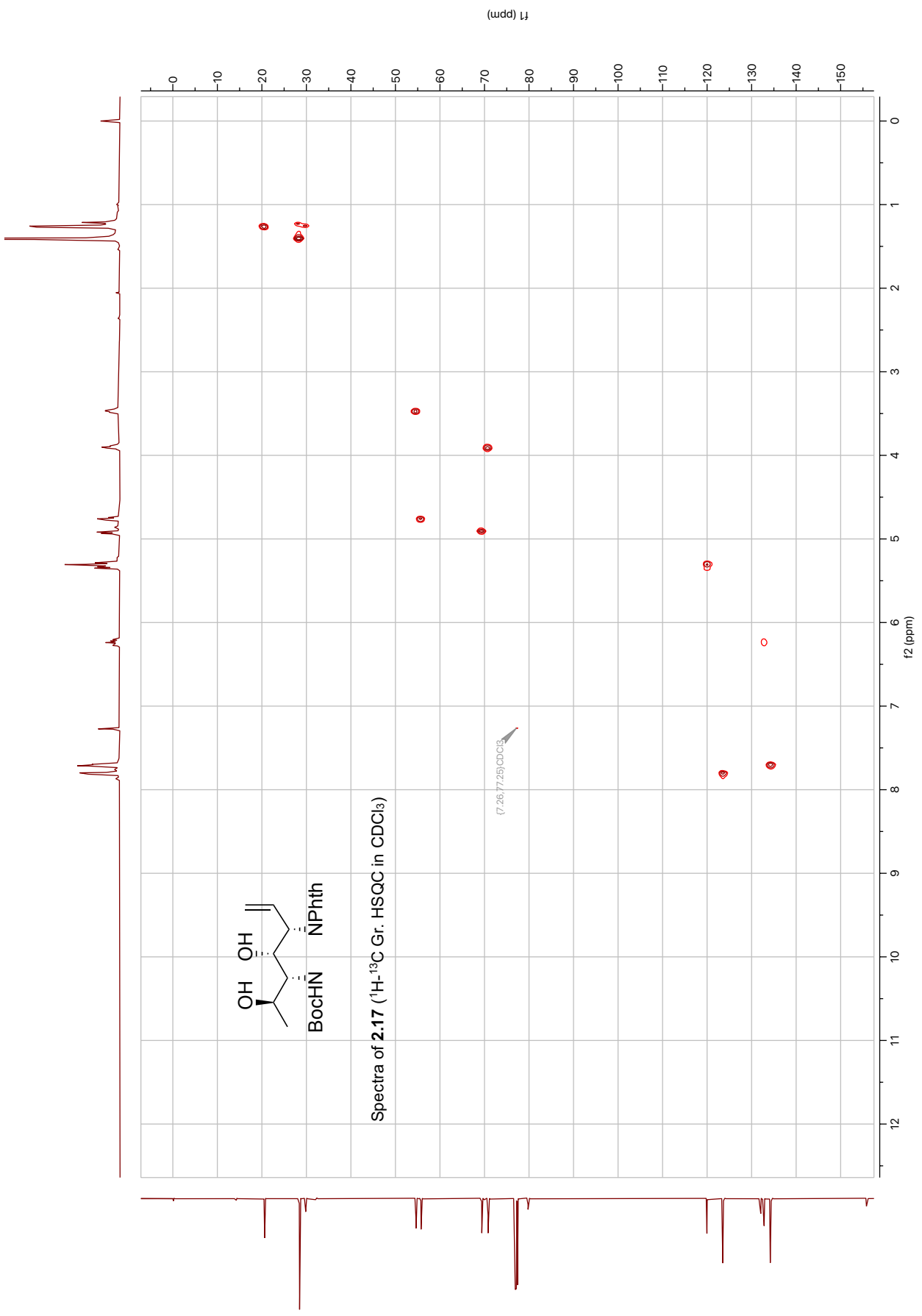
Spectra of 2.17 (1H-13C Gr. HSQC in CDCl3)
OH OH
BocHN NPhth
{7.26;77.25}CDCl3
f2 (ppm)
f1 (ppm)

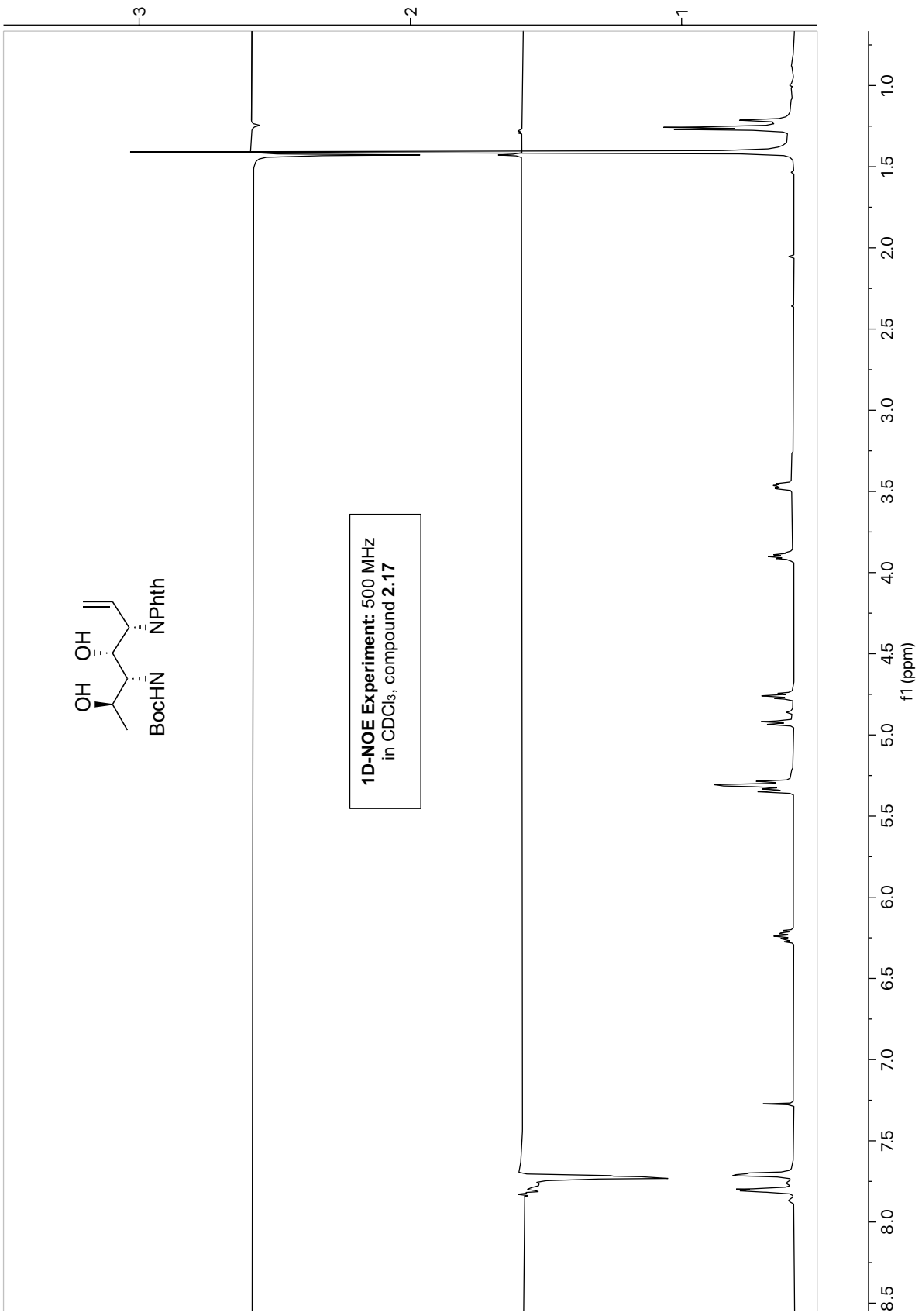
OH
OH
BocHN
NPhth
1D-NOE Experiment: 500 MHz
in CDCl3, compound 2.17
f1 (ppm)

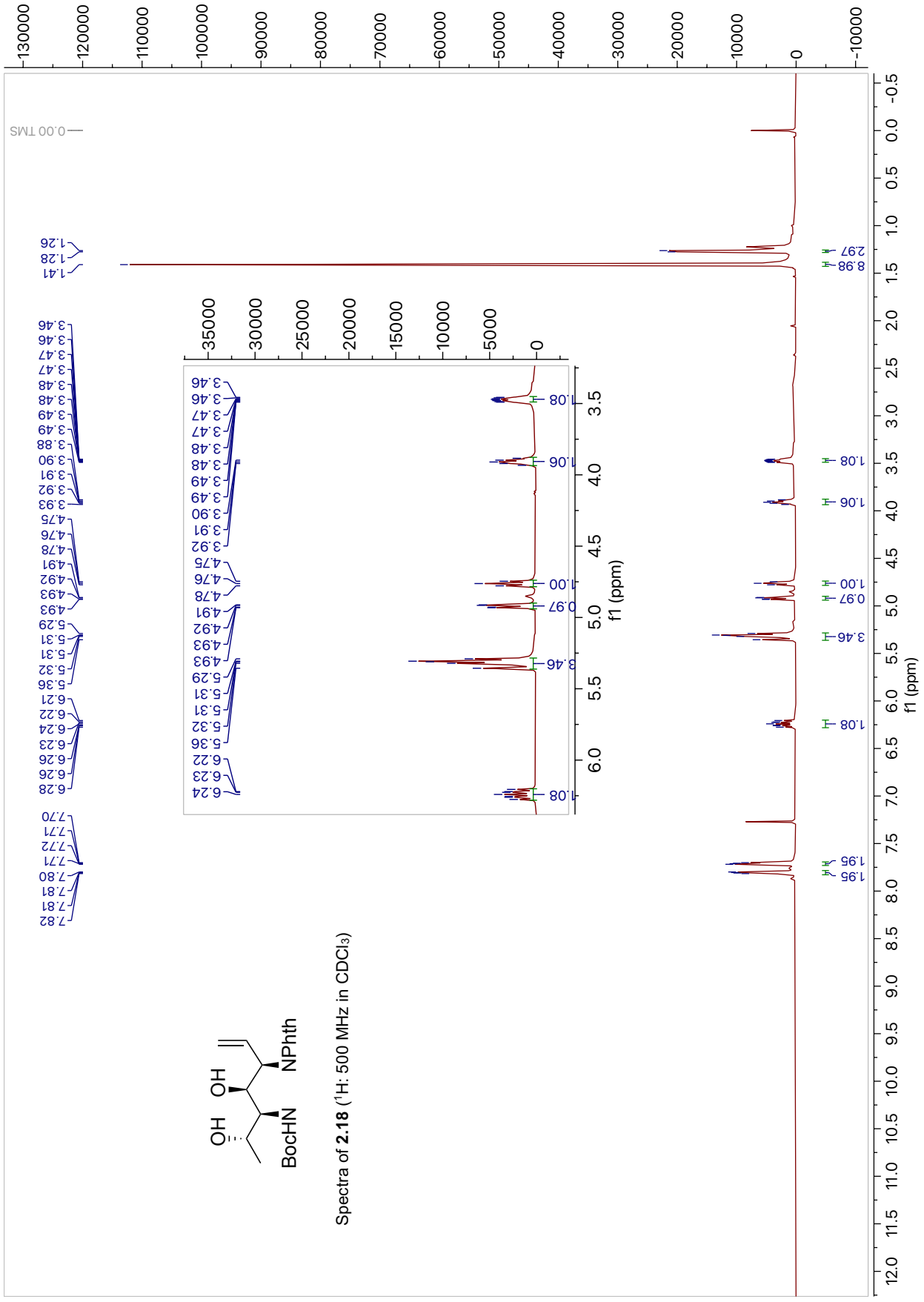
OH
OH
BocHN
NPhth
Spectra of 2.18 (¹H: 500 MHz in CDCl₃)
f1 (ppm)

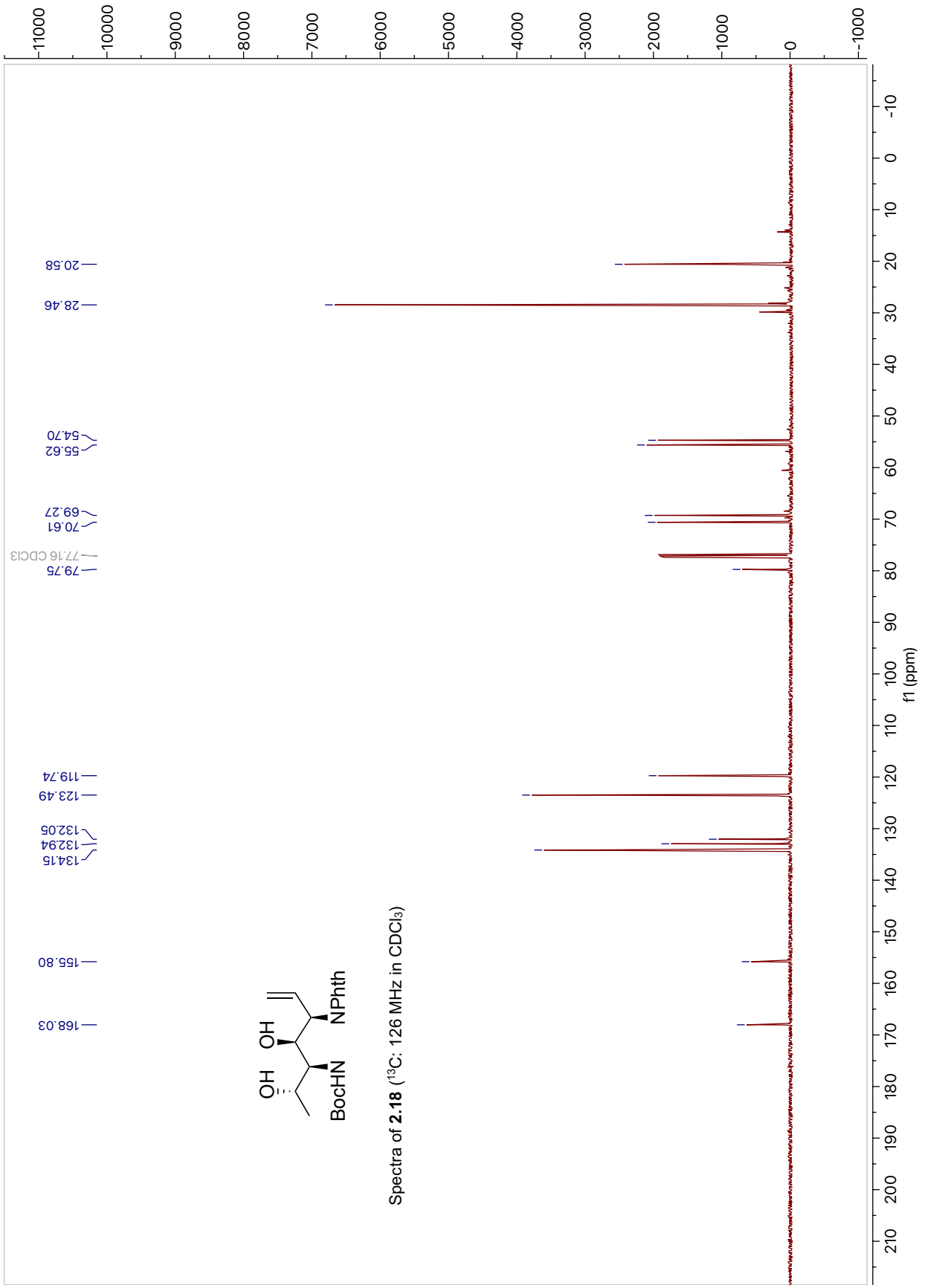
Spectra of 2.18 (13C: 126 MHz in CDCl3)
OH
OH
BocHN
NPhth
168.03
155.80
134.15
132.94
132.05
123.49
119.74
79.75
77.16 CDCl3
70.61
69.27
55.62
54.70
28.46
20.58
f1 (ppm)

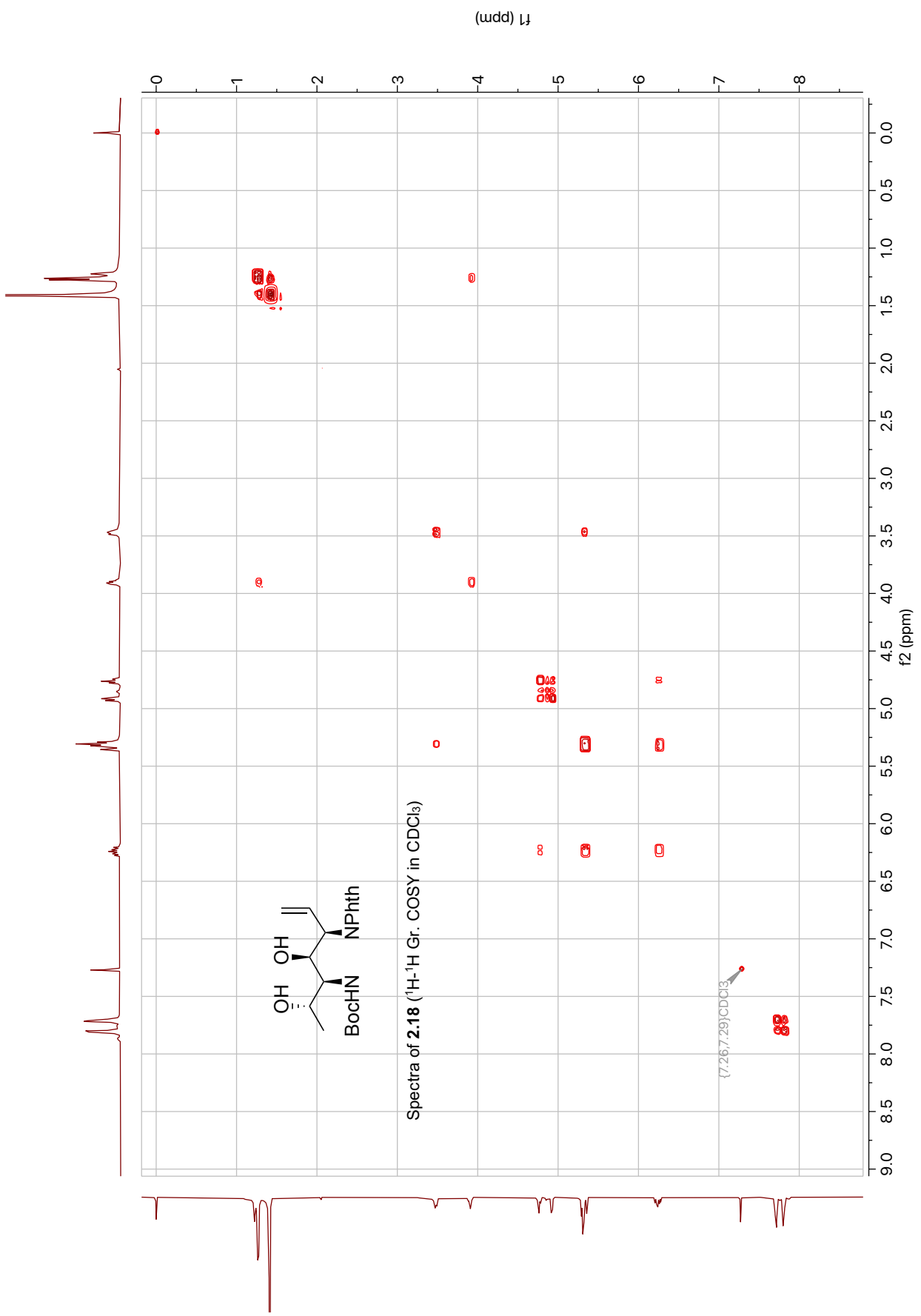
Spectra of 2.18 (1H-1H Gr. COSY in CDCl3)
OH
OH
BocHN
NPhth
{7.26,7.29}CDCl3
f2 (ppm)
f1 (ppm)

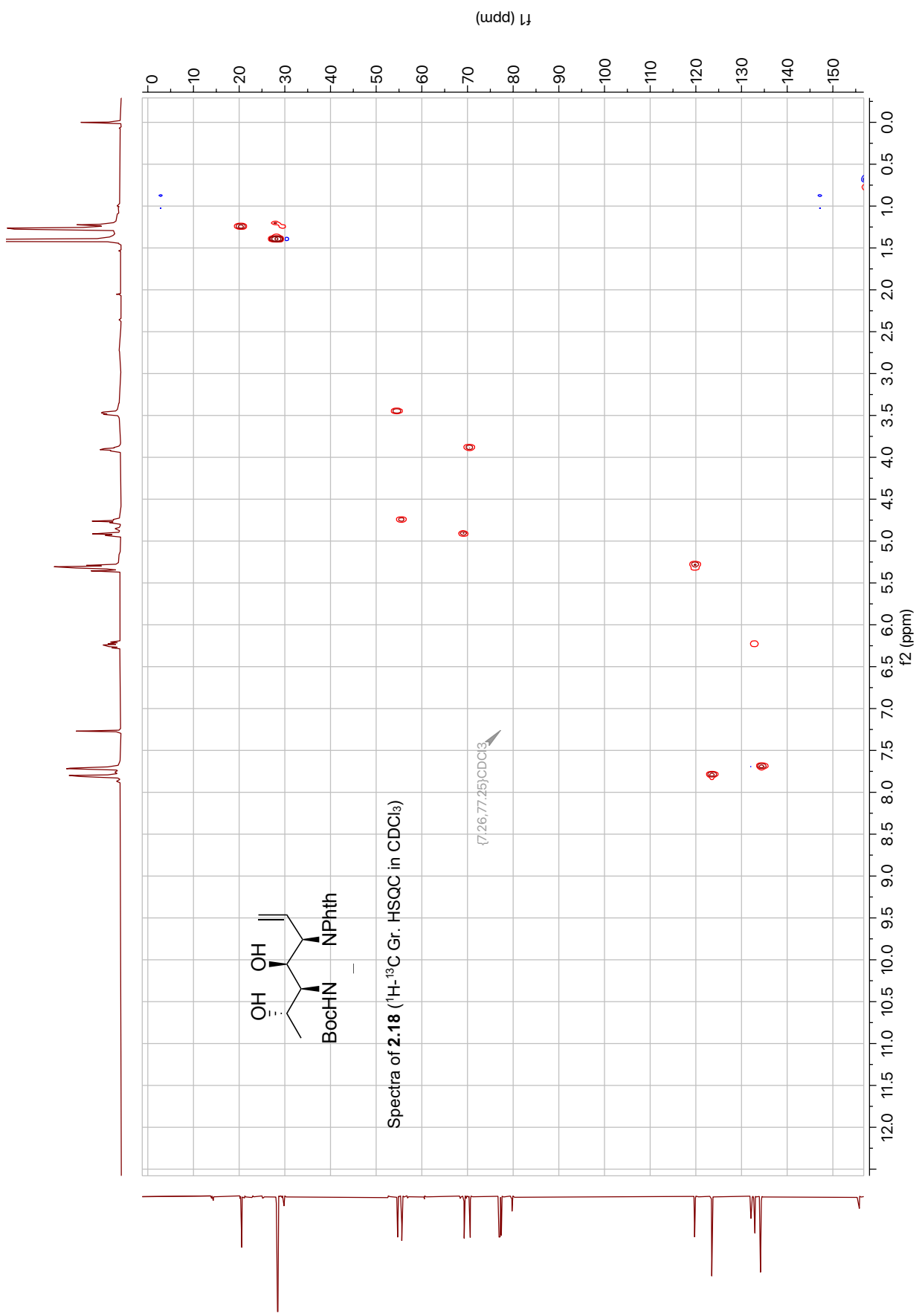
Spectra of 2.18 (1H-13C Gr. HSQC in CDCl3)
{7.26,77.25}CDCl3
f2 (ppm)
f1 (ppm)
OH
OH
BocHN
NPhth

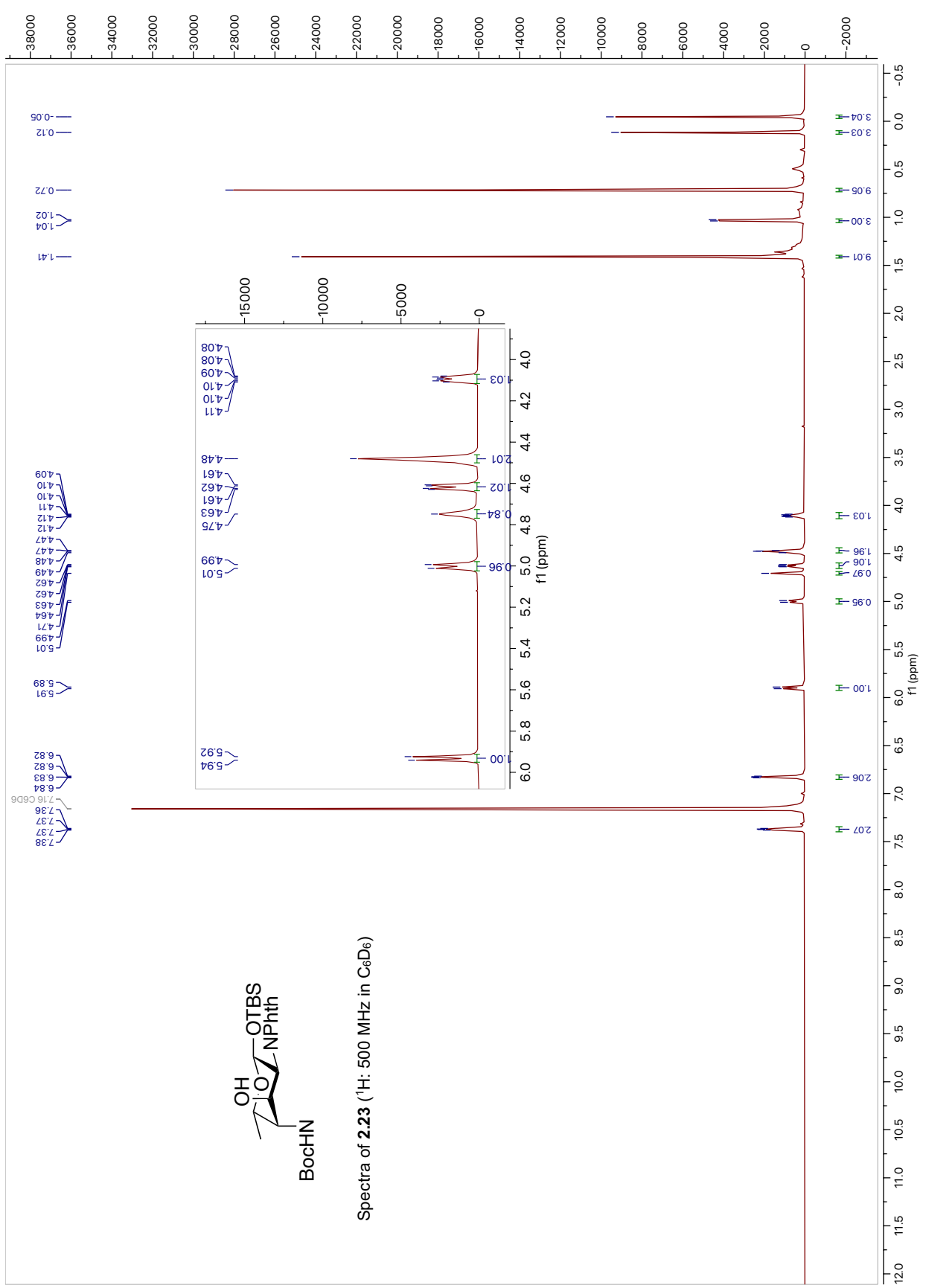


Spectra of **2.23** ($^1$H: 500 MHz in $C_6D_6$)

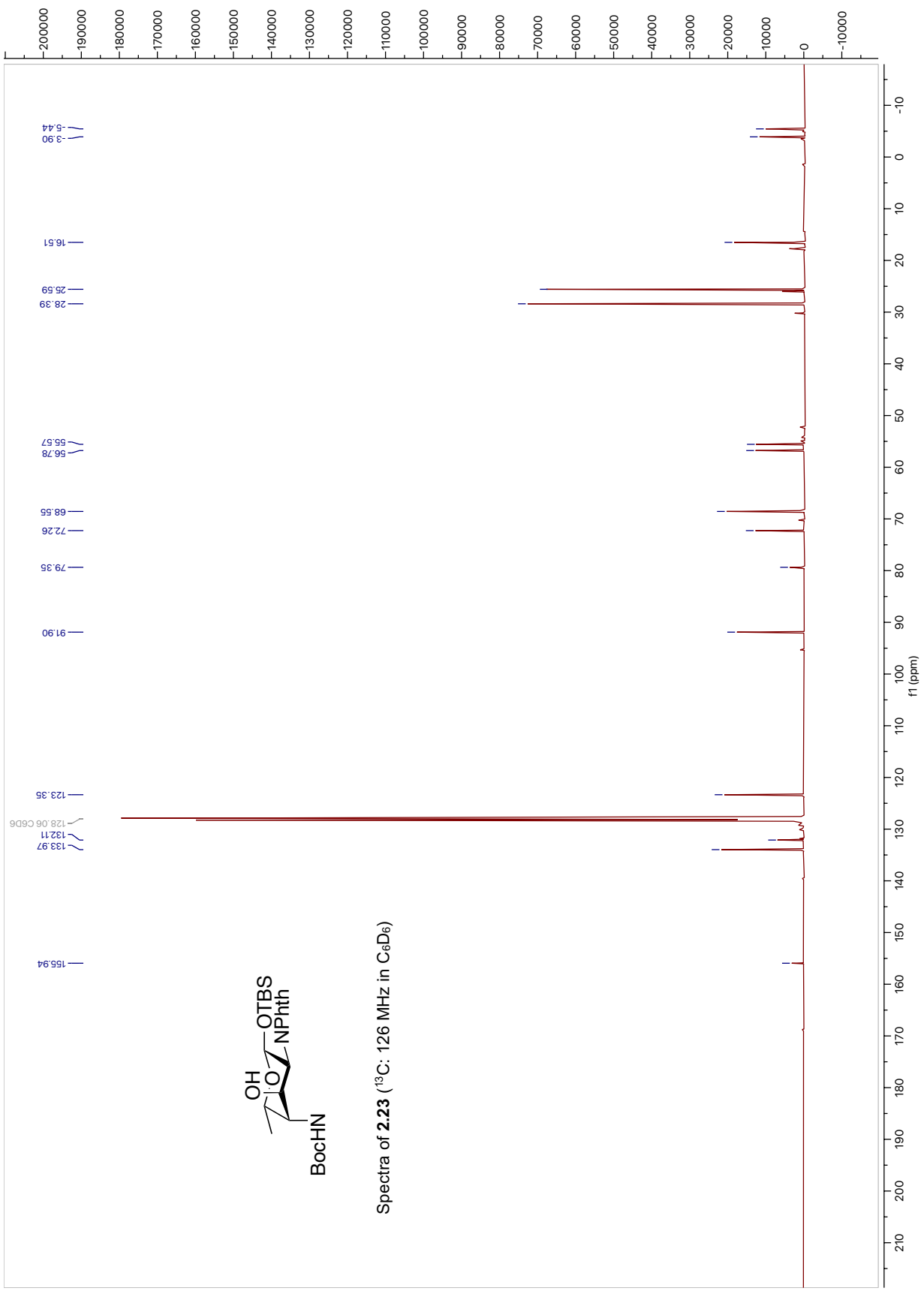
Spectra of 2.23 (13C: 126 MHz in C6D6)
OH
OTBS
NPhth
BocHN
155.94
133.97
132.11
128.06 C6D6
123.35
91.90
79.35
72.26
68.55
56.78
55.57
28.39
25.59
16.51
-3.90
-5.44
f1 (ppm)

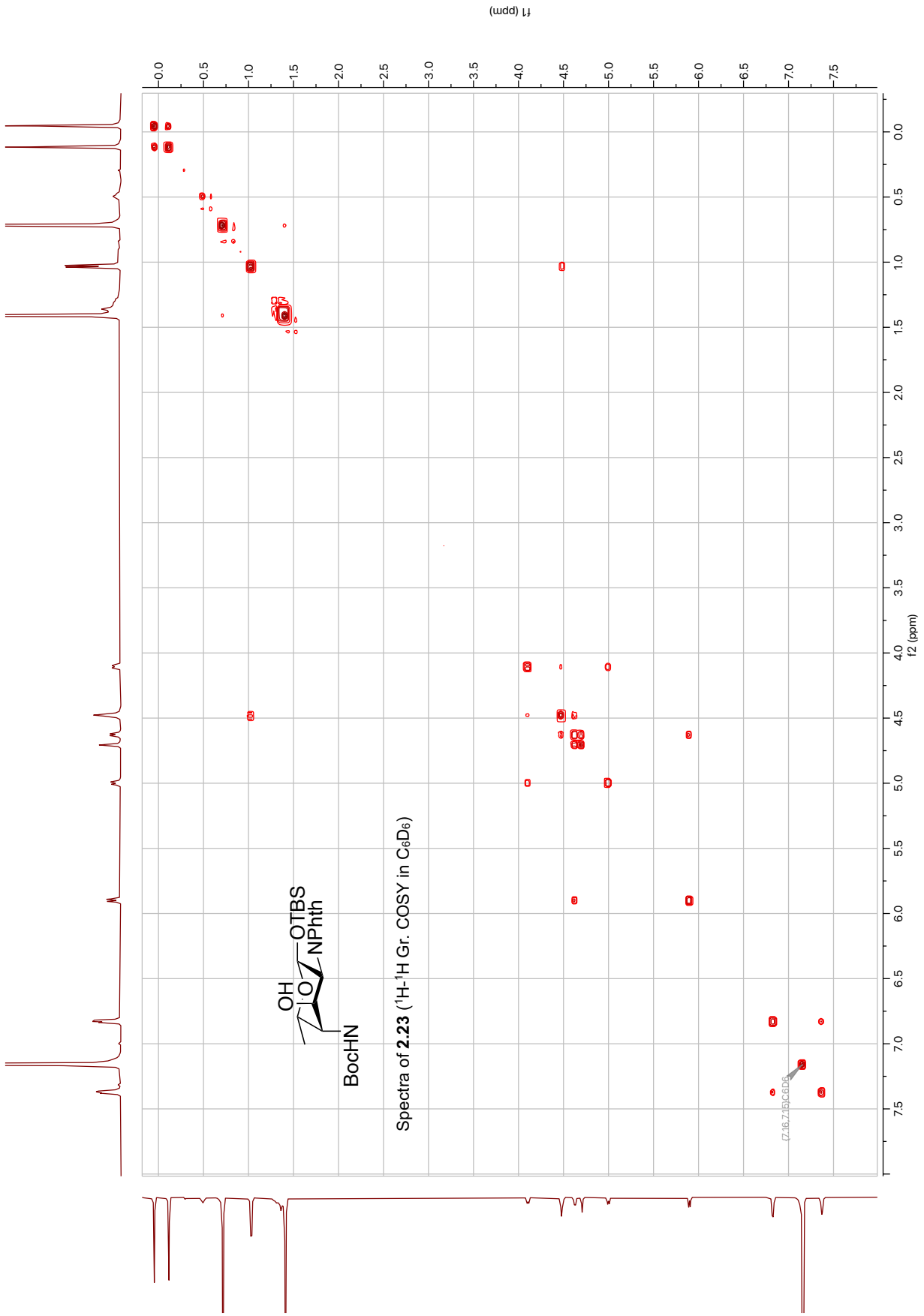
f1 (ppm)
f2 (ppm)
Spectra of 2.23 (1H-1H Gr. COSY in C6D6)
OH
O
OTBS
NPhth
BocHN
(7.16,7.16)C6D6

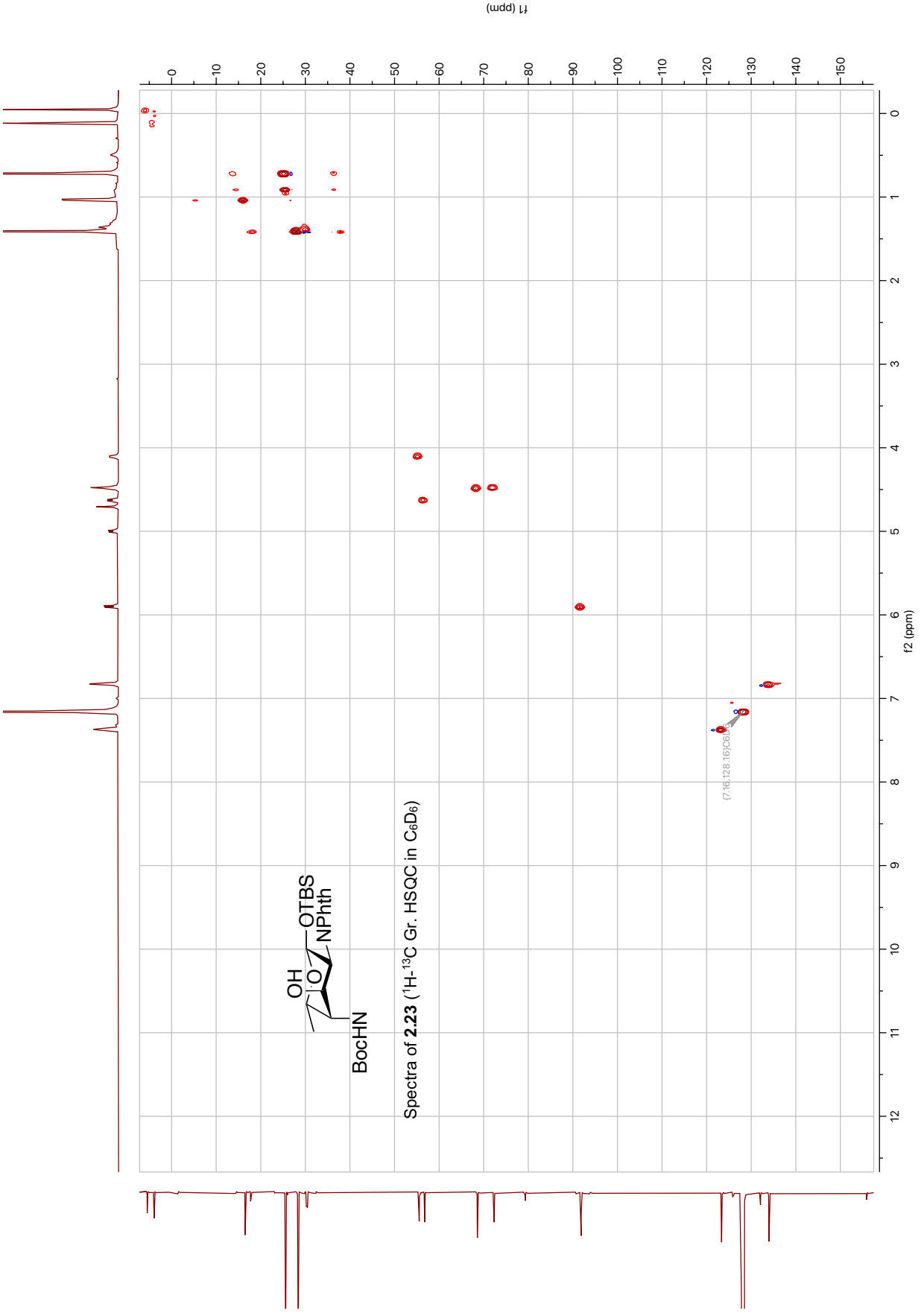
f1 (ppm)
f2 (ppm)
Spectra of 2.23 (1H-13C Gr. HSQC in C6D6)
OH
O
OTBS
NPhth
BocHN

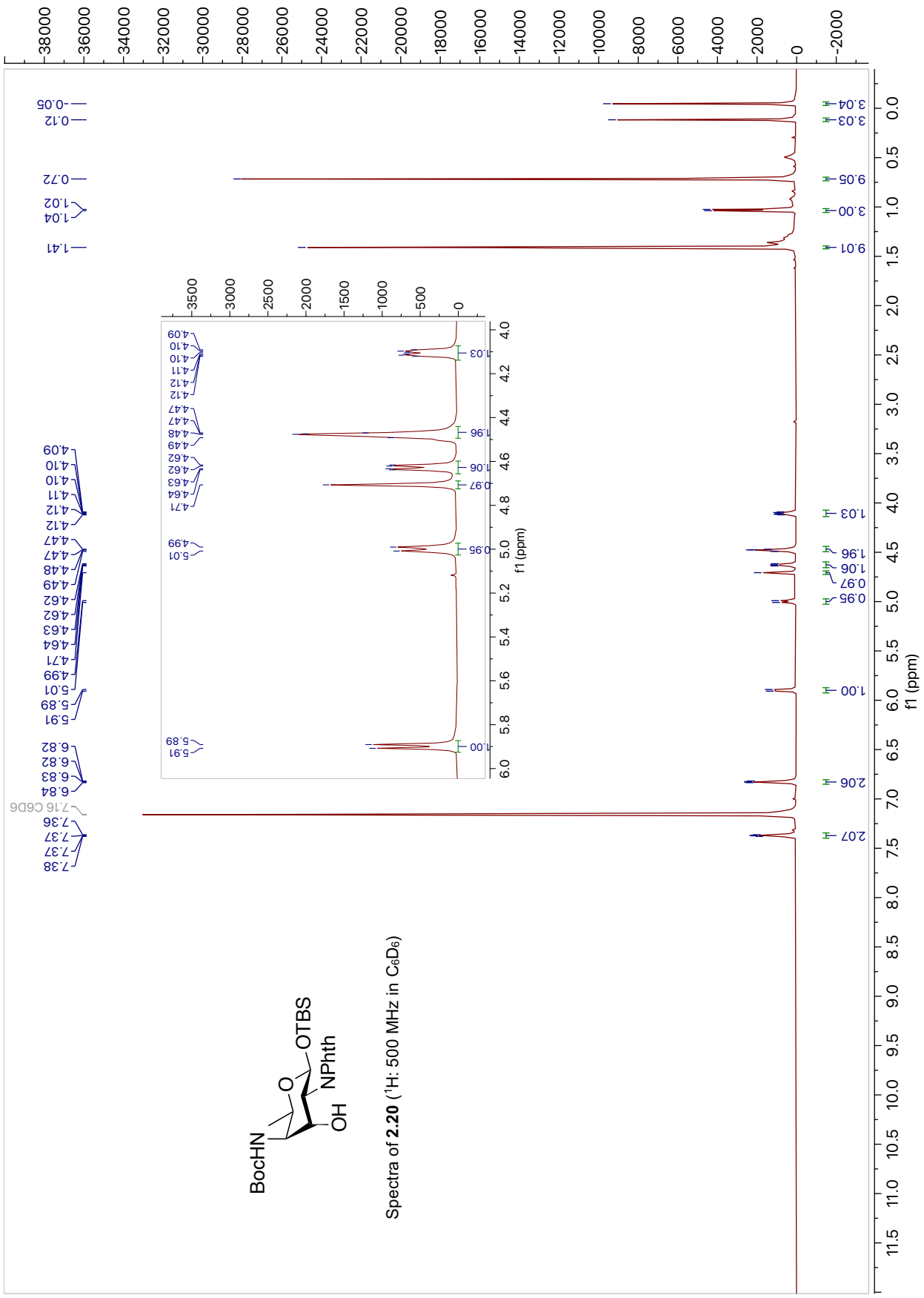
BocHN
O
OTBS
NPhth
OH
Spectra of 2.20 (1H: 500 MHz in C6D6)
f1 (ppm)

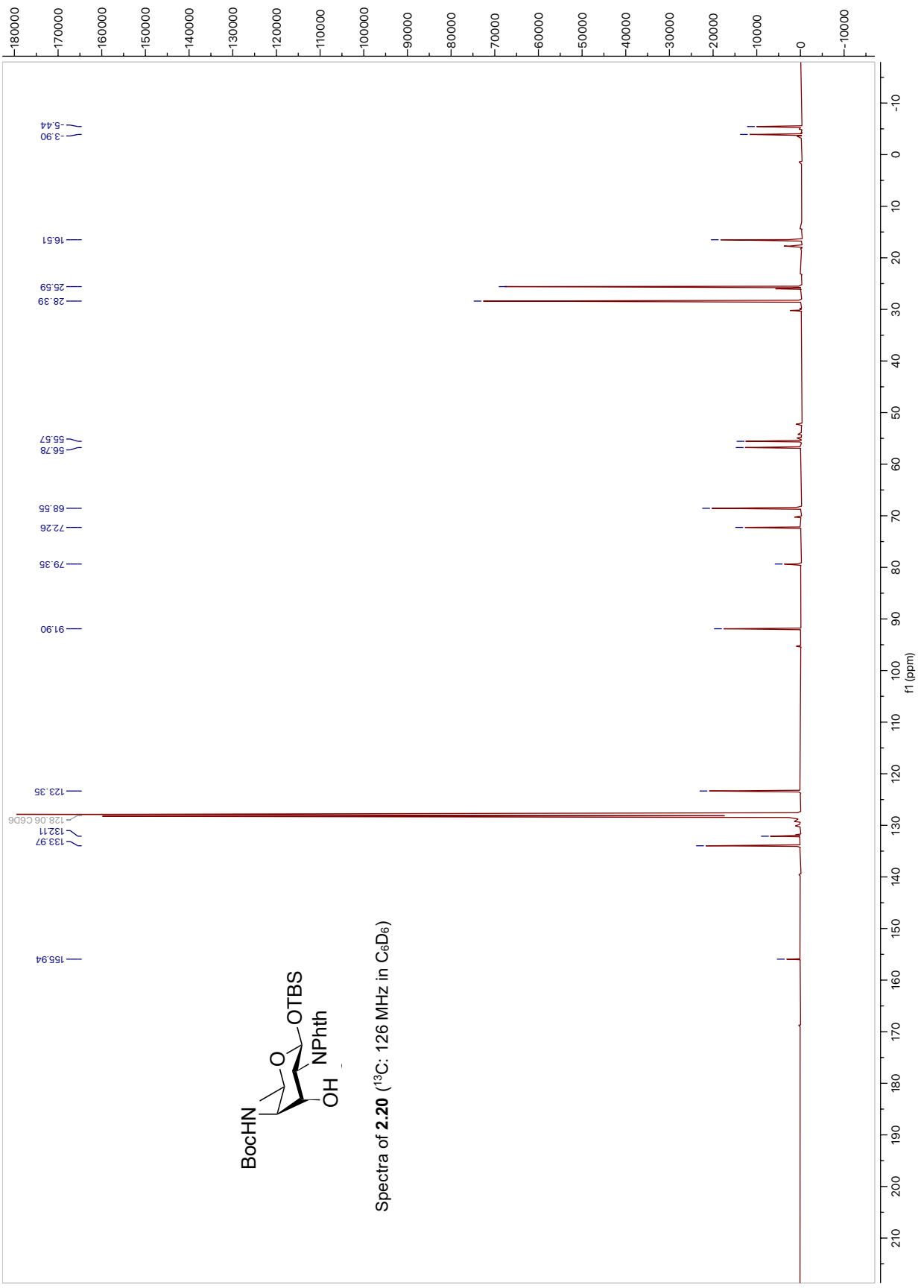
BocHN
O
OTBS
NPhth
OH
Spectra of 2.20 (13C: 126 MHz in C6D6)
f1 (ppm)

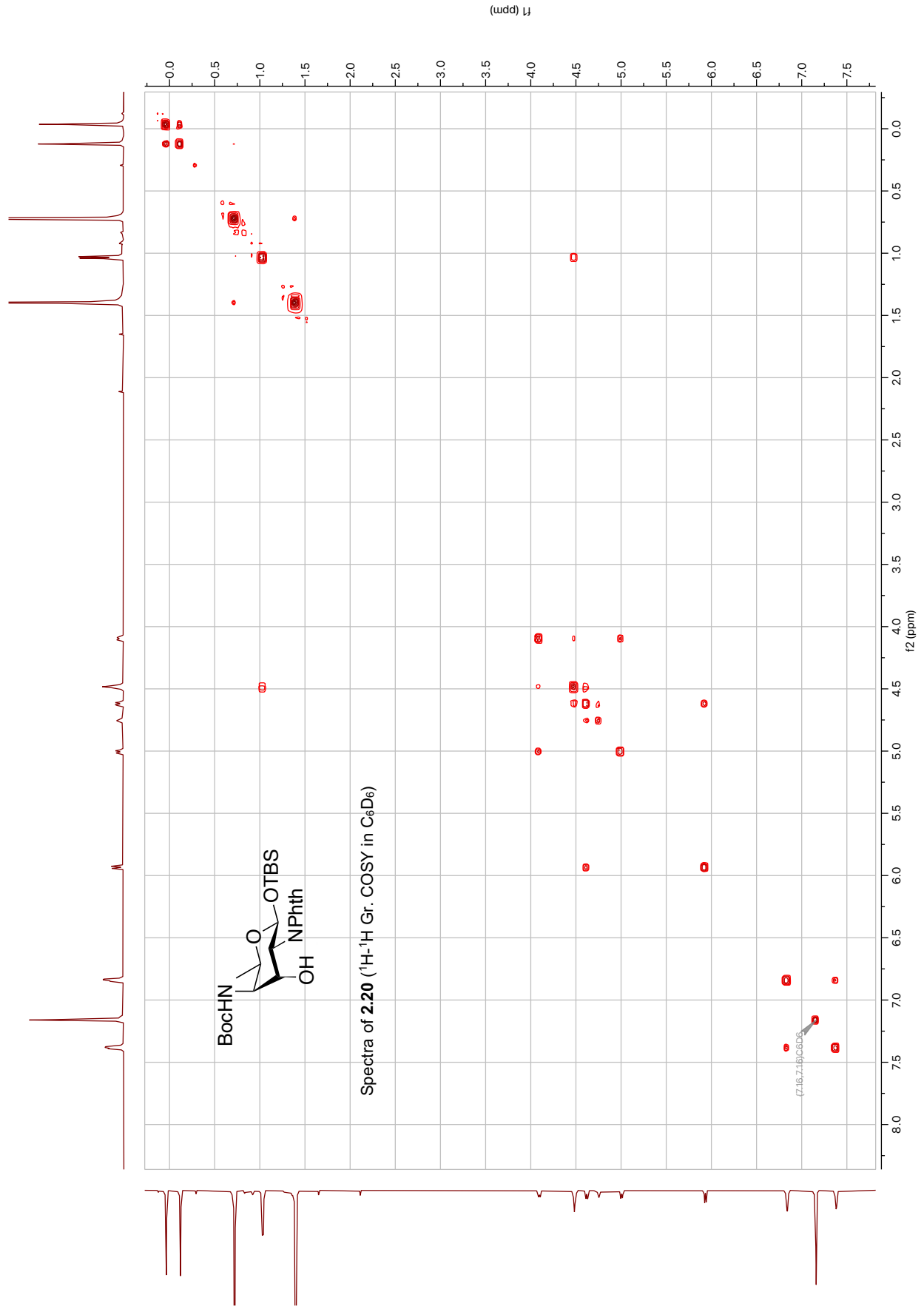
f1 (ppm)
f2 (ppm)
Spectra of 2.20 (¹H-¹H Gr. COSY in C6D6)
BocHN
O
OTBS
NPhth
OH
(7.16,7.16)C6D6

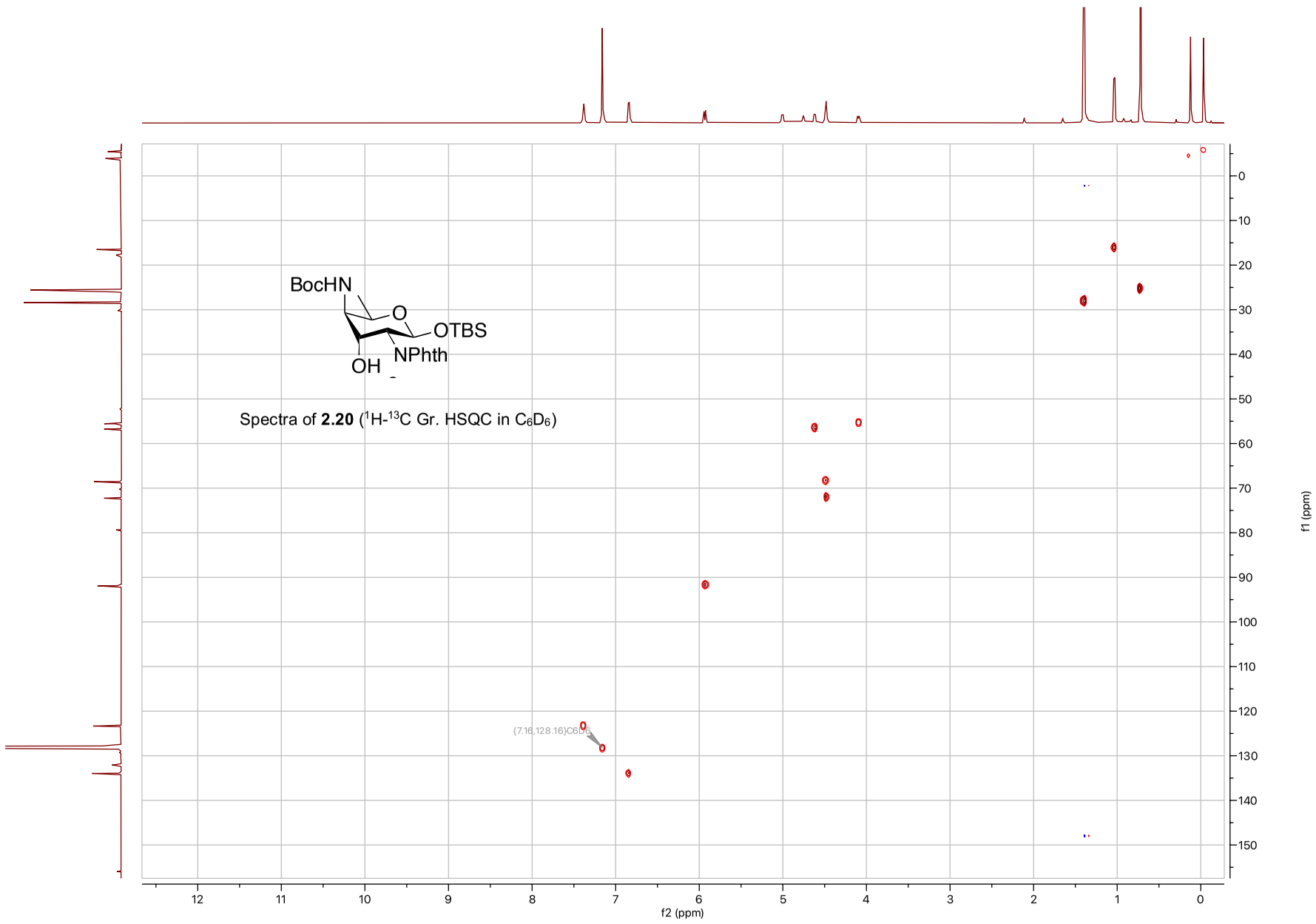
BocHN
O
OTBS
NPhth
OH
Spectra of **2.20** ($^{1}$H-$^{13}$C Gr. HSQC in $C_6D_6$)
{7.16,128.16}C6D6
f2 (ppm)
f1 (ppm)

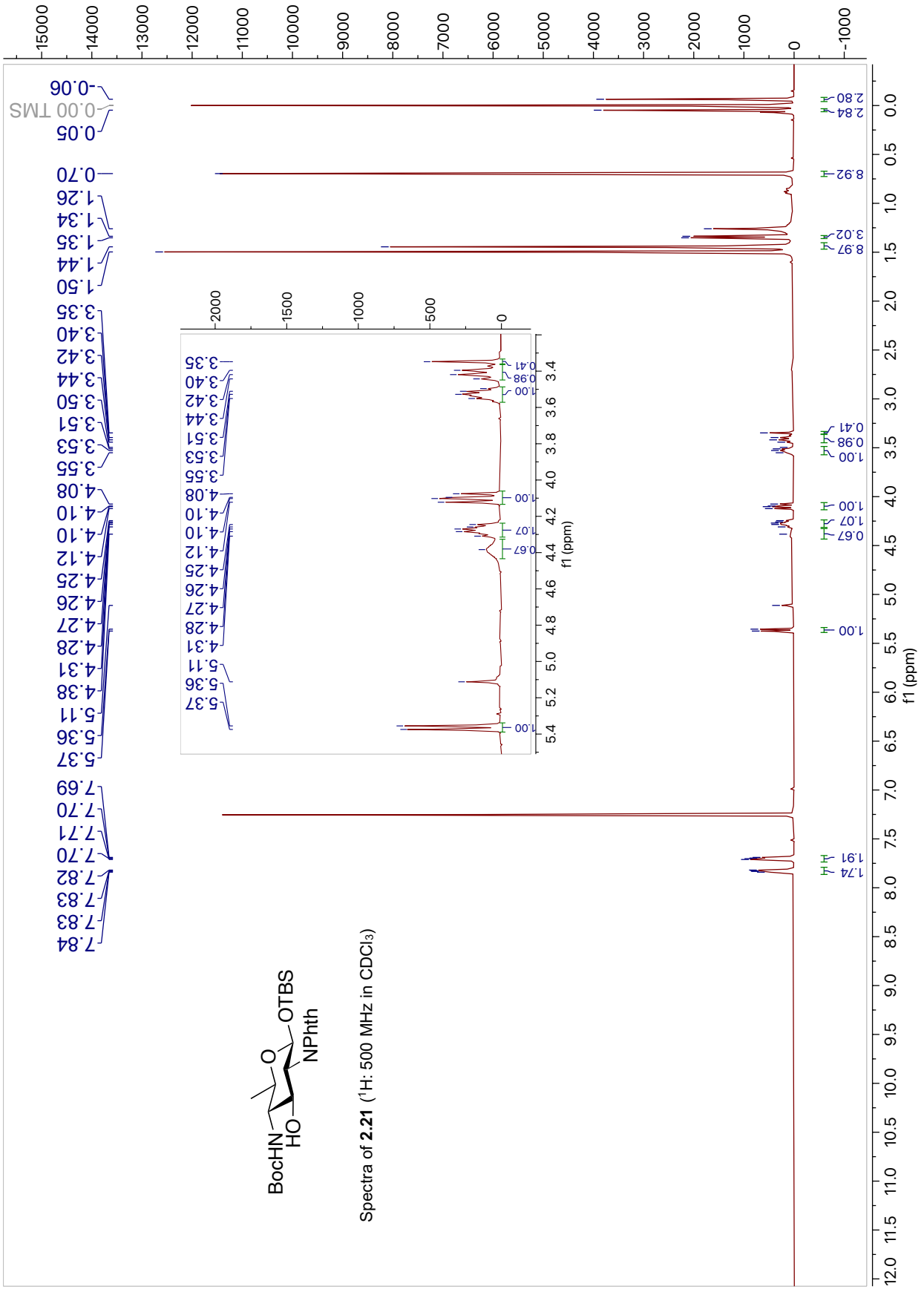
BocHN
HO
O
OTBS
NPhth
Spectra of **2.21** ($^1$H: 500 MHz in $CDCl_3$)
f1 (ppm)

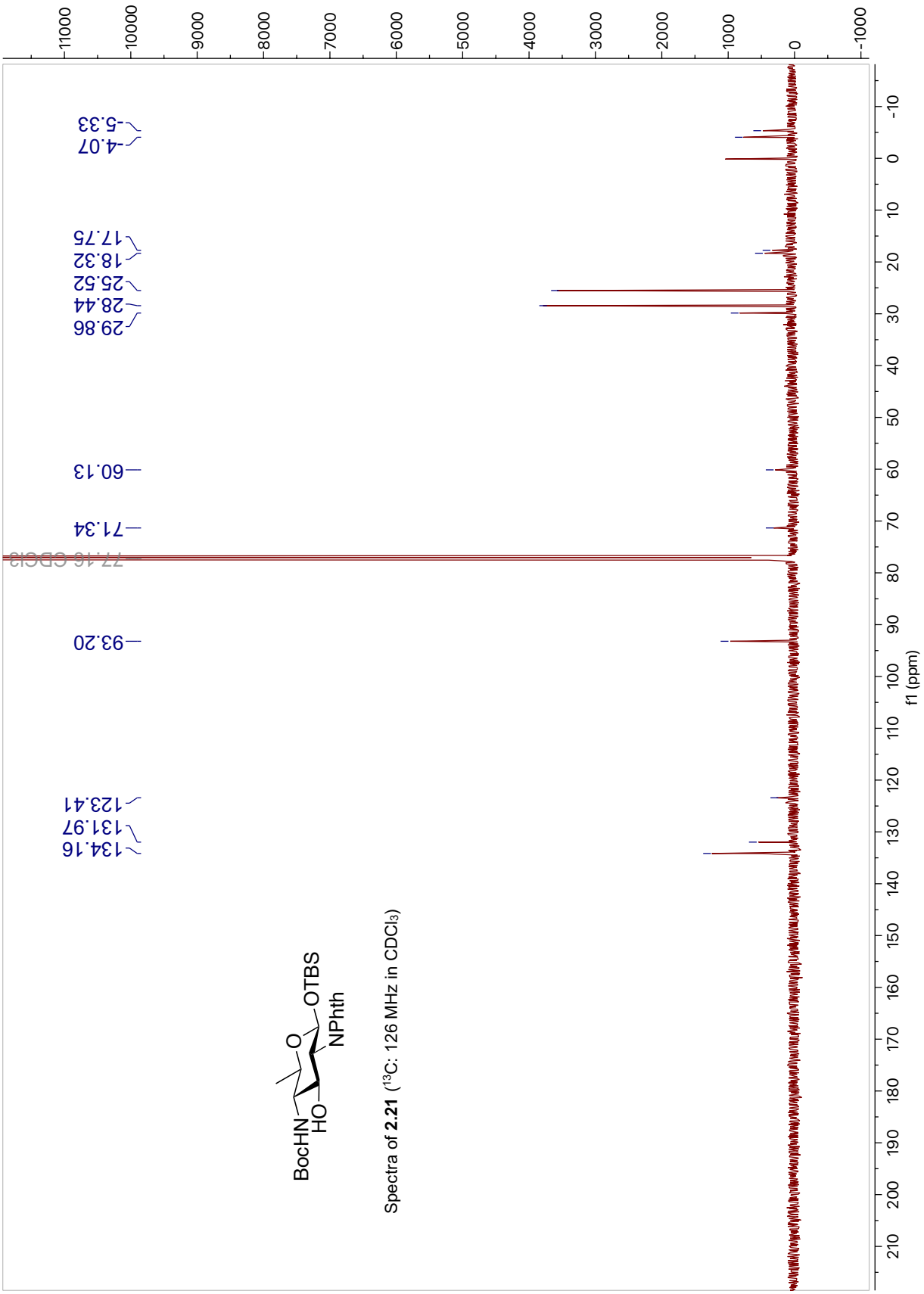
-5.33
-4.07
17.75
18.32
25.52
28.44
29.86
60.13
71.34
77.16 CDCl3
93.20
123.41
131.97
134.16
BocHN
HO
O
OTBS
NPhth
Spectra of 2.21 (13C: 126 MHz in CDCl3)
f1 (ppm)

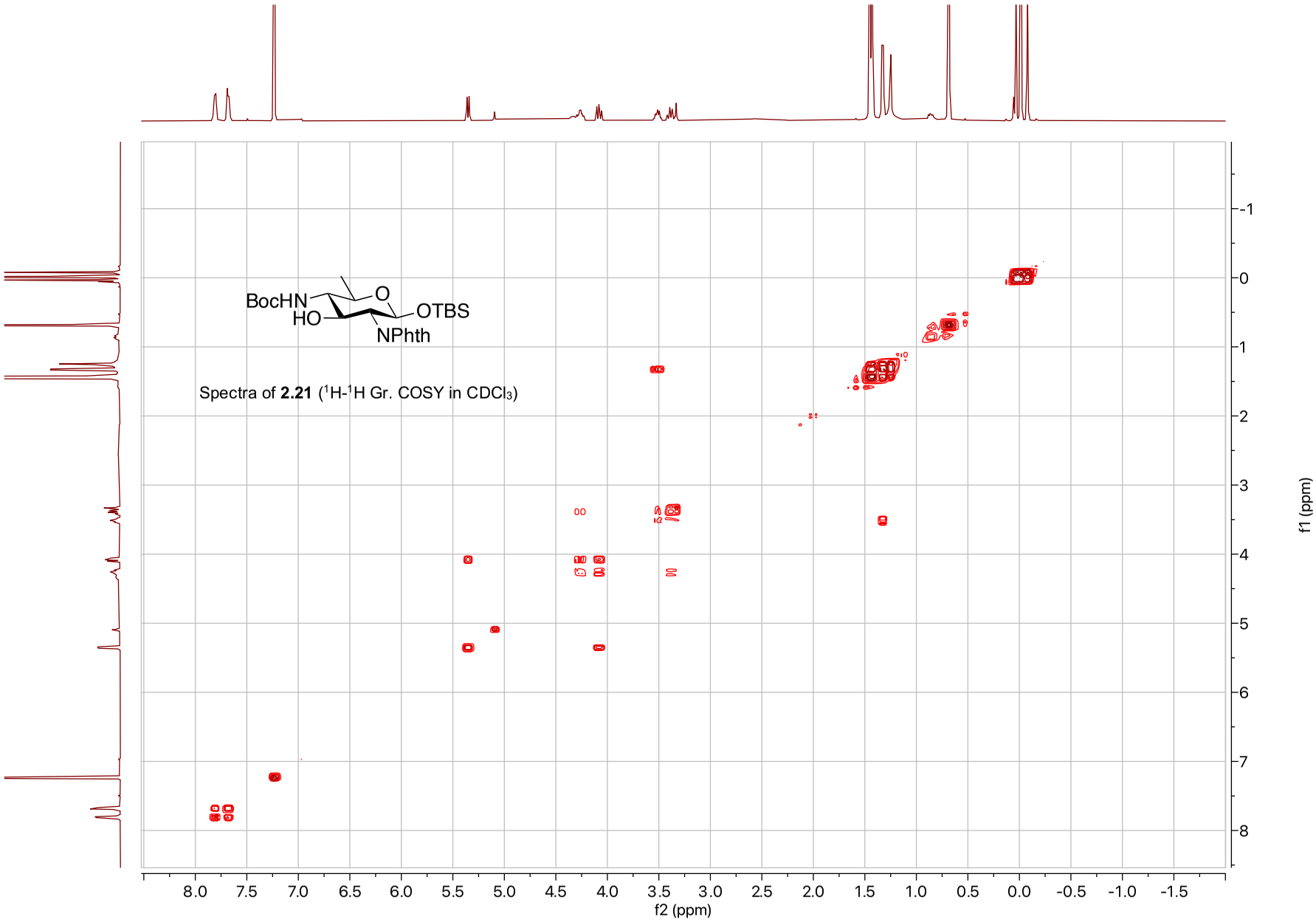
BocHN
HO
O
OTBS
NPhth
Spectra of **2.21** ($^1$H-$^1$H Gr. COSY in $CDCl_3$)
f2 (ppm)
f1 (ppm)

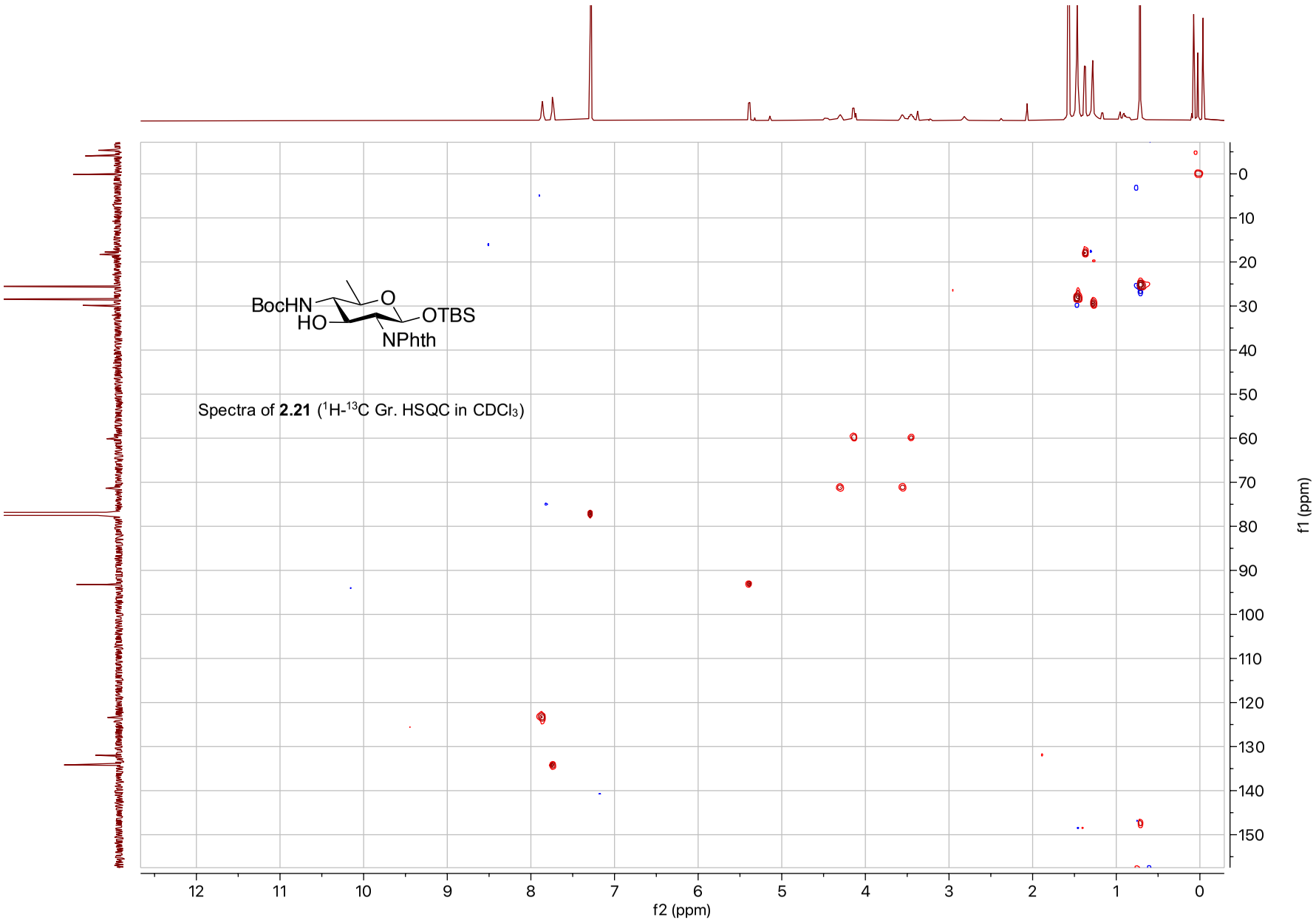
BocHN
HO
O
OTBS
NPhth
Spectra of 2.21 (1H-13C Gr. HSQC in CDCl3)
f2 (ppm)
f1 (ppm)

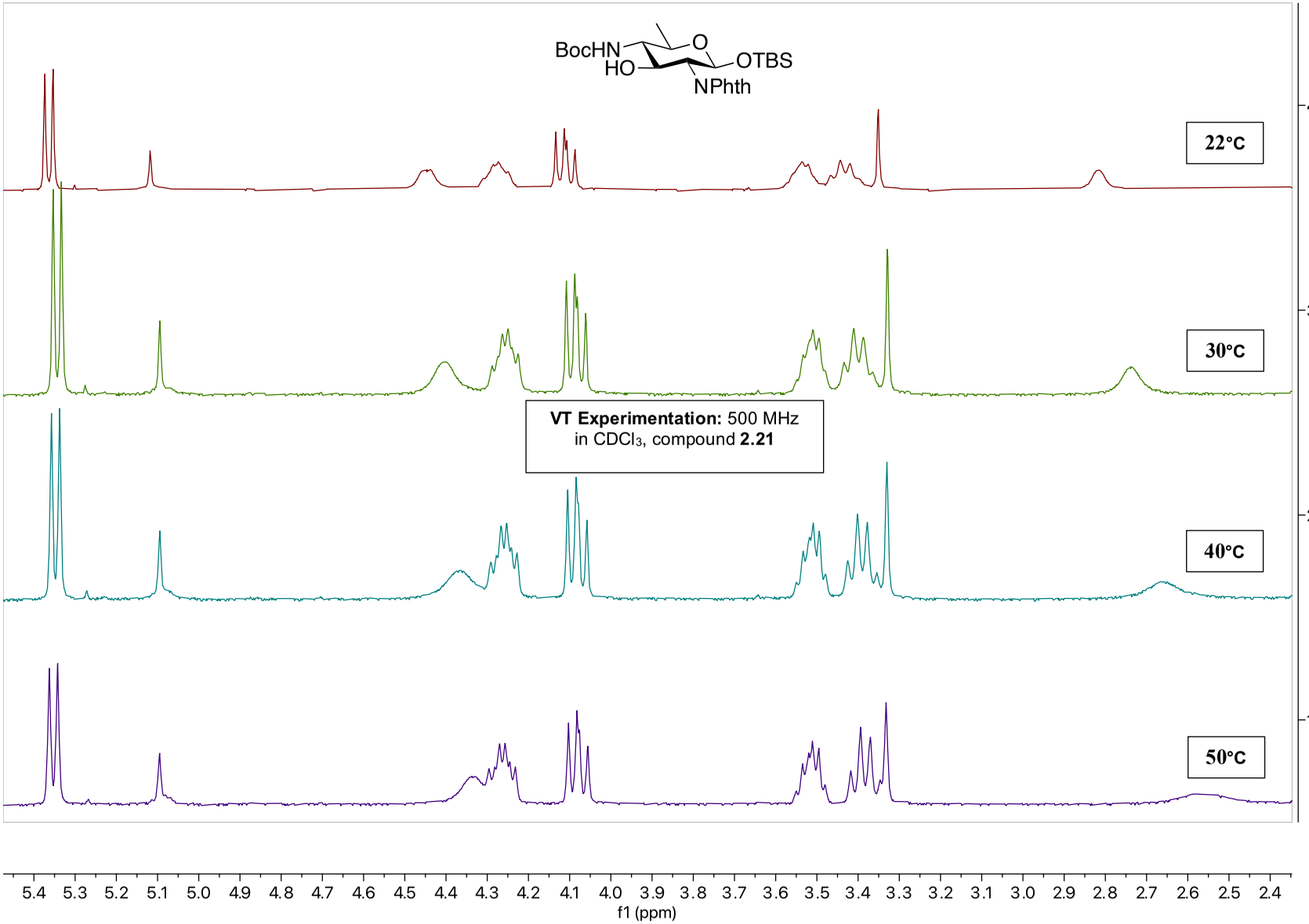
BocHN
HO
O
OTBS
NPhth
22°C
30°C
40°C
50°C
VT Experimentation: 500 MHz in CDCl3, compound 2.21
4
3
2
1
5.4 5.3 5.2 5.1 5.0 4.9 4.8 4.7 4.6 4.5 4.4 4.3 4.2 4.1 4.0 3.9 3.8 3.7 3.6 3.5 3.4 3.3 3.2 3.1 3.0 2.9 2.8 2.7 2.6 2.5 2.4
f1 (ppm)

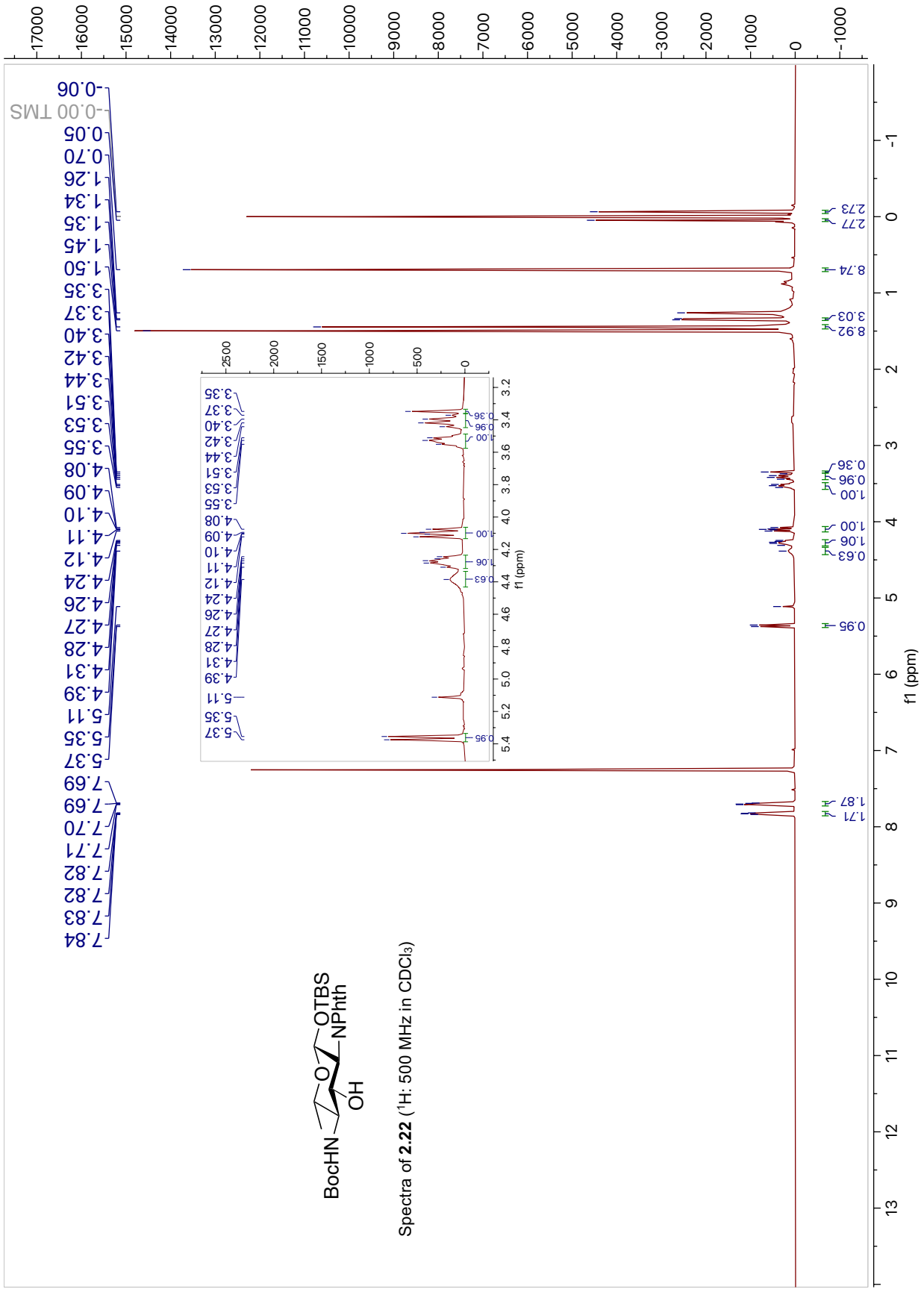
BocHN
O
OTBS
NPhth
OH
Spectra of 2.22 (1H: 500 MHz in CDCl3)
f1 (ppm)
TMS

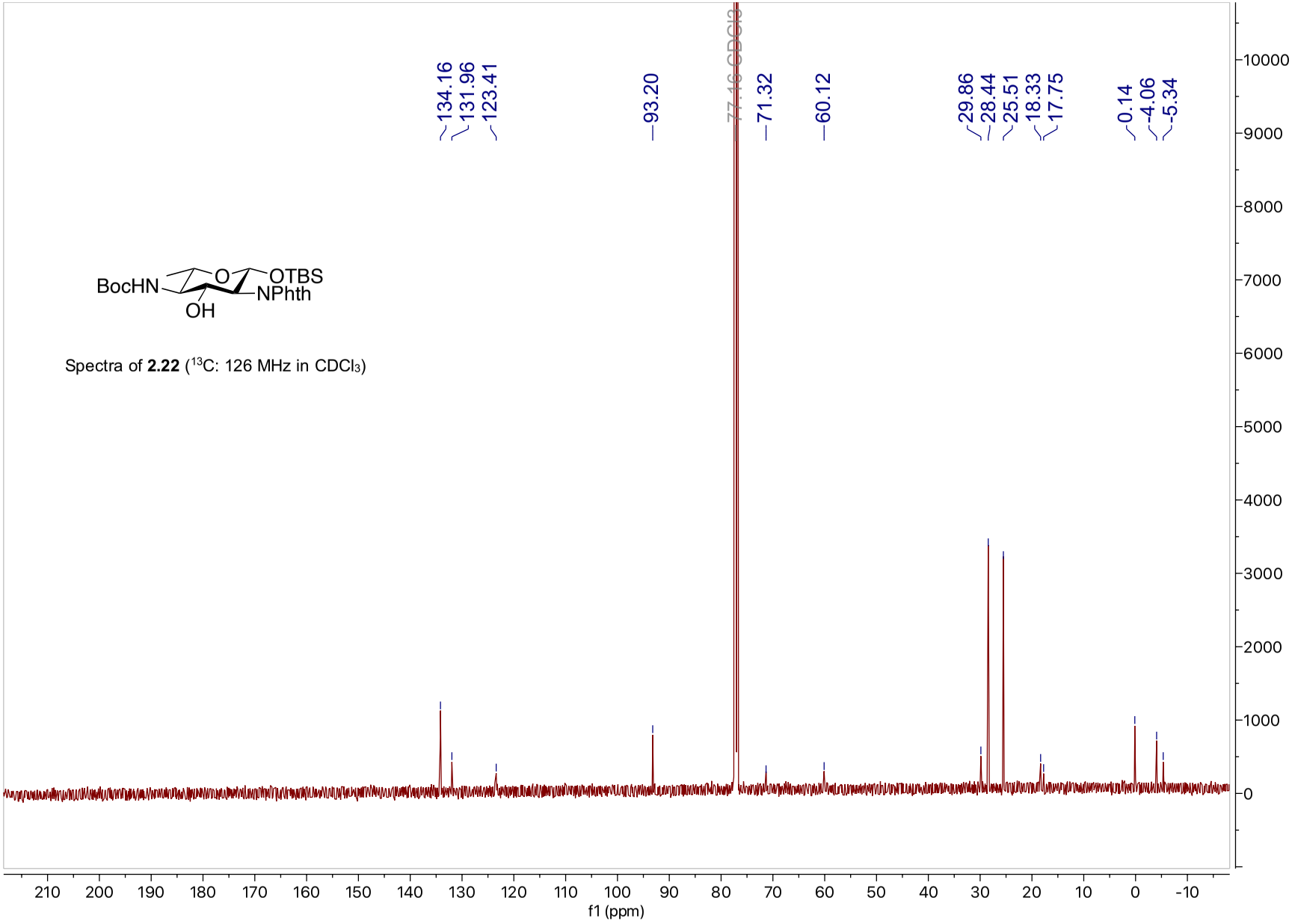
134.16
131.96
123.41
93.20
77.16 CDCl3
71.32
60.12
29.86
28.44
25.51
18.33
17.75
0.14
-4.06
-5.34
BocHN
O
OTBS
NPhth
OH
Spectra of 2.22 (13C: 126 MHz in CDCl3)
f1 (ppm)

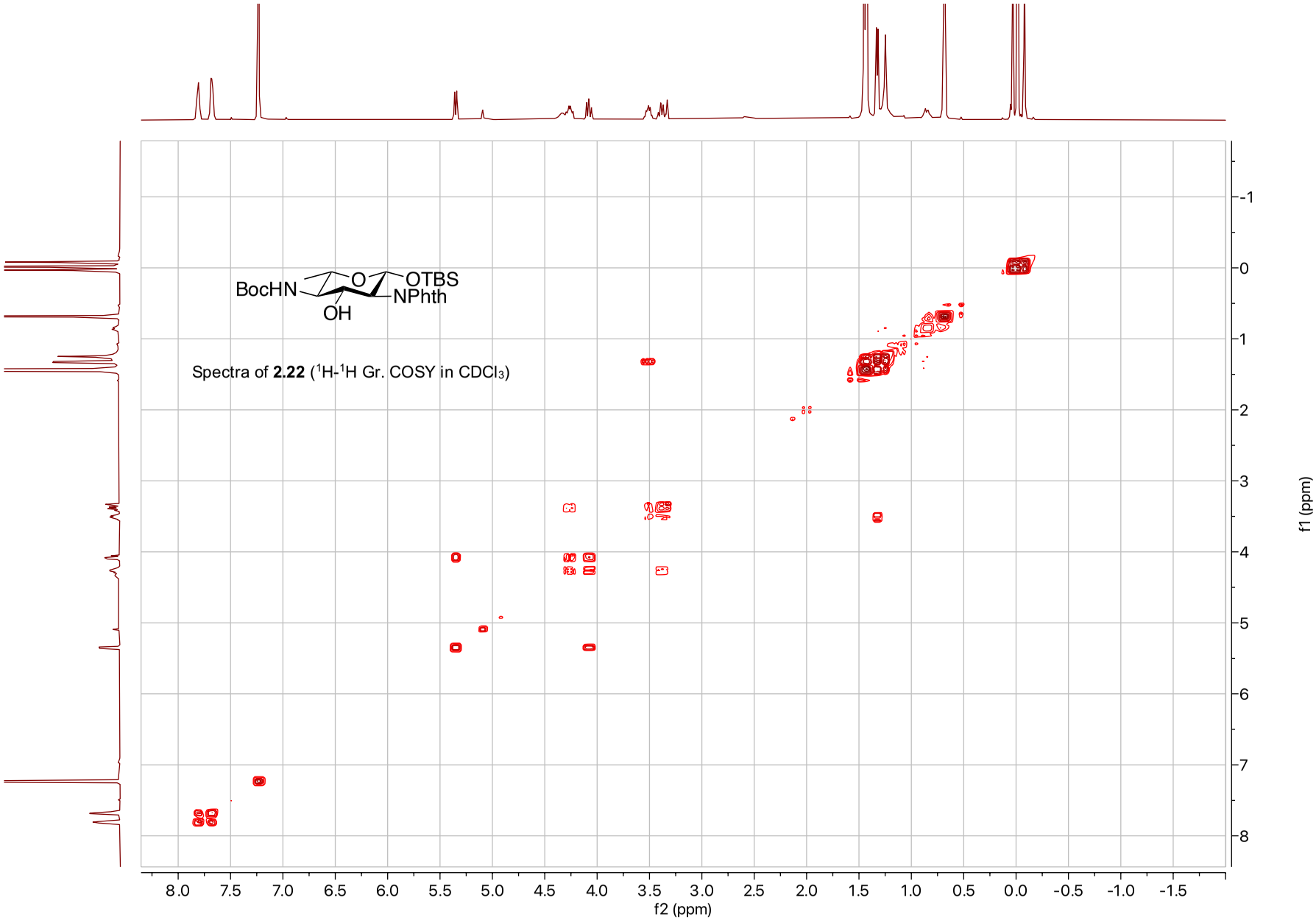
BocHN
O
OTBS
NPhth
OH
Spectra of 2.22 (1H-1H Gr. COSY in CDCl3)
f2 (ppm)
f1 (ppm)

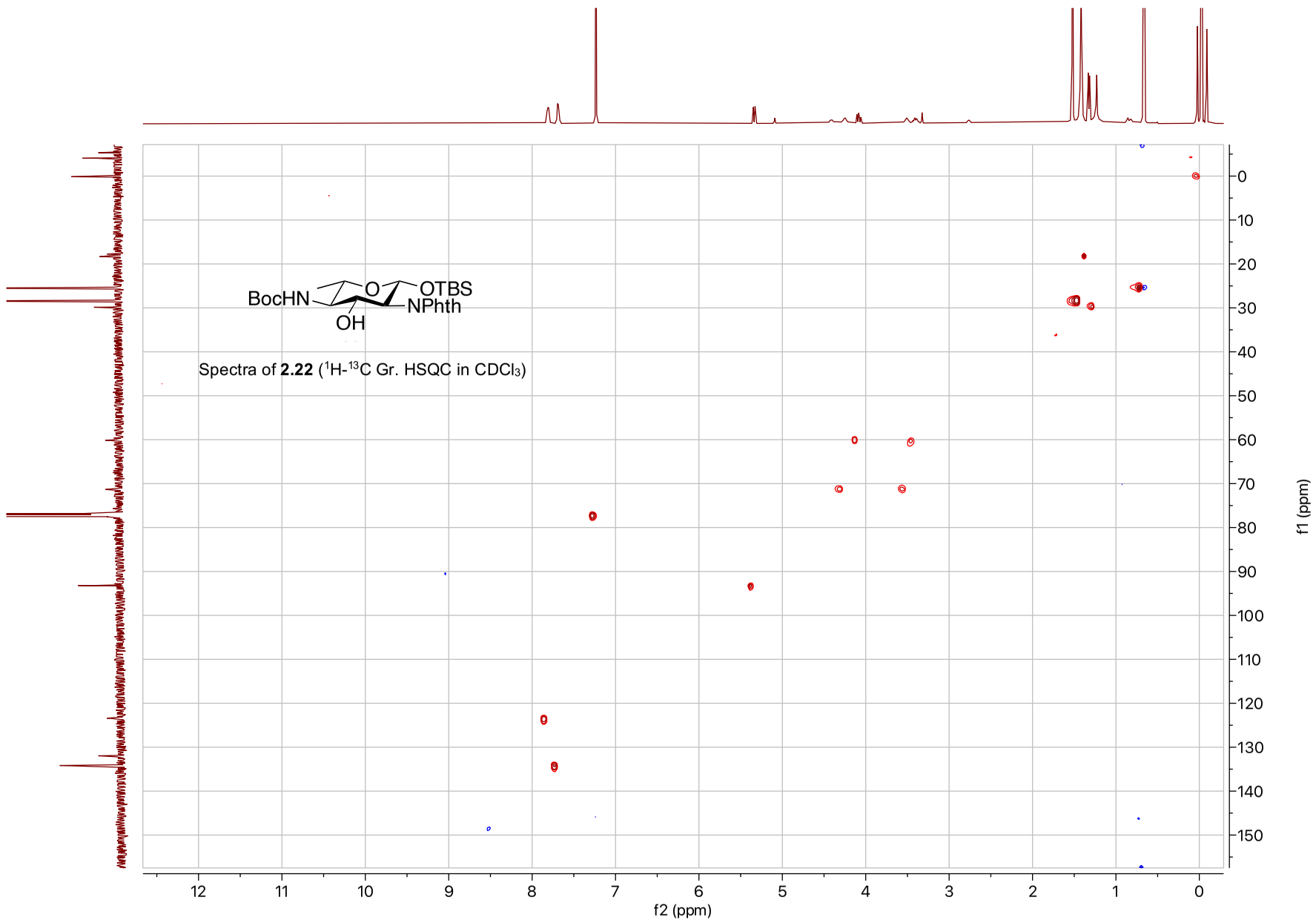
BocHN
O
OTBS
NPhth
OH
Spectra of **2.22** ($^{1}$H-$^{13}$C Gr. HSQC in $CDCl_3$)
f2 (ppm)
f1 (ppm)

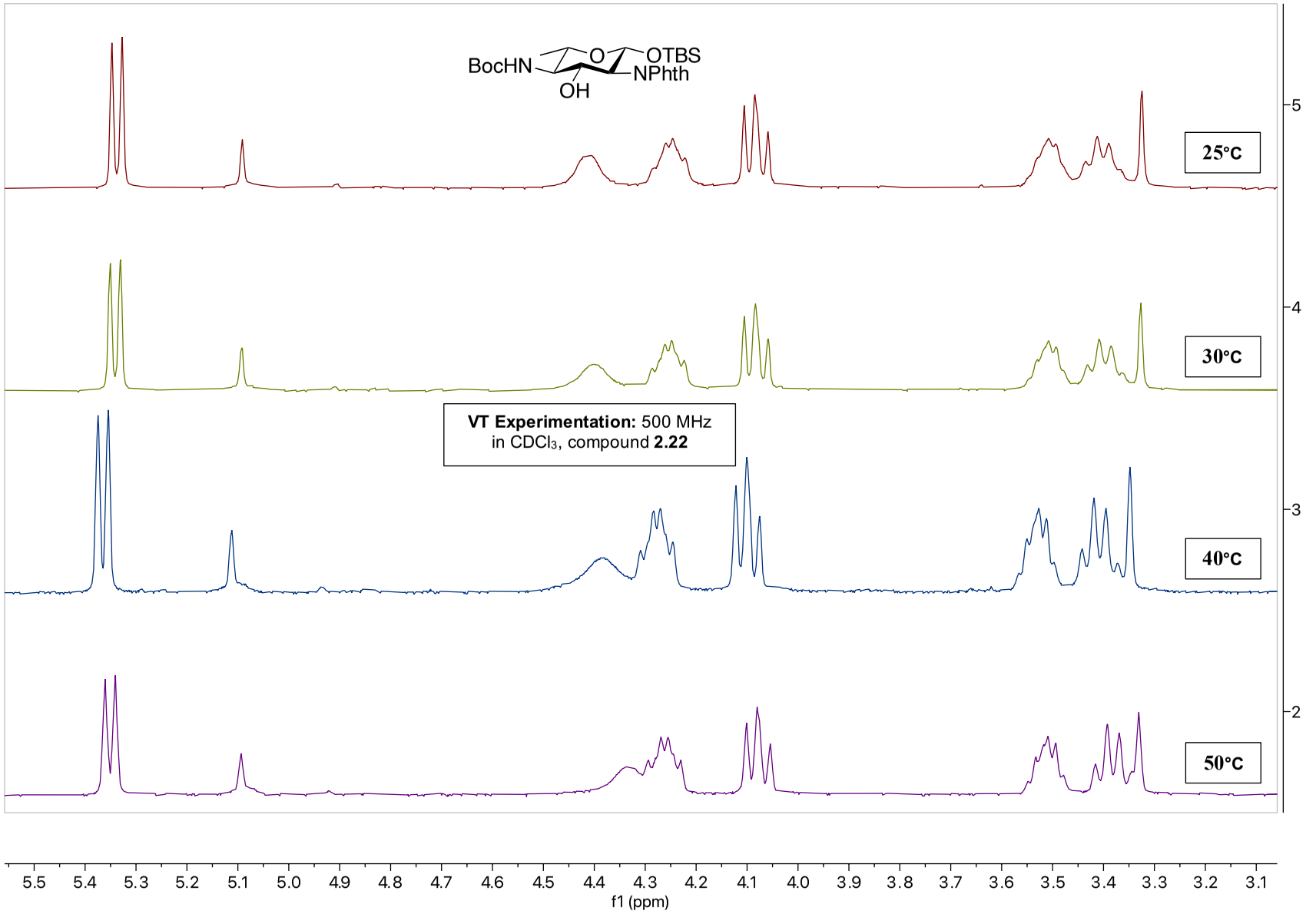
BocHN
O
OTBS
NPhth
OH
25°C
30°C
40°C
50°C
VT Experimentation: 500 MHz in CDCl3, compound 2.22
5
4
3
2
5.5 5.4 5.3 5.2 5.1 5.0 4.9 4.8 4.7 4.6 4.5 4.4 4.3 4.2 4.1 4.0 3.9 3.8 3.7 3.6 3.5 3.4 3.3 3.2 3.1
f1 (ppm)

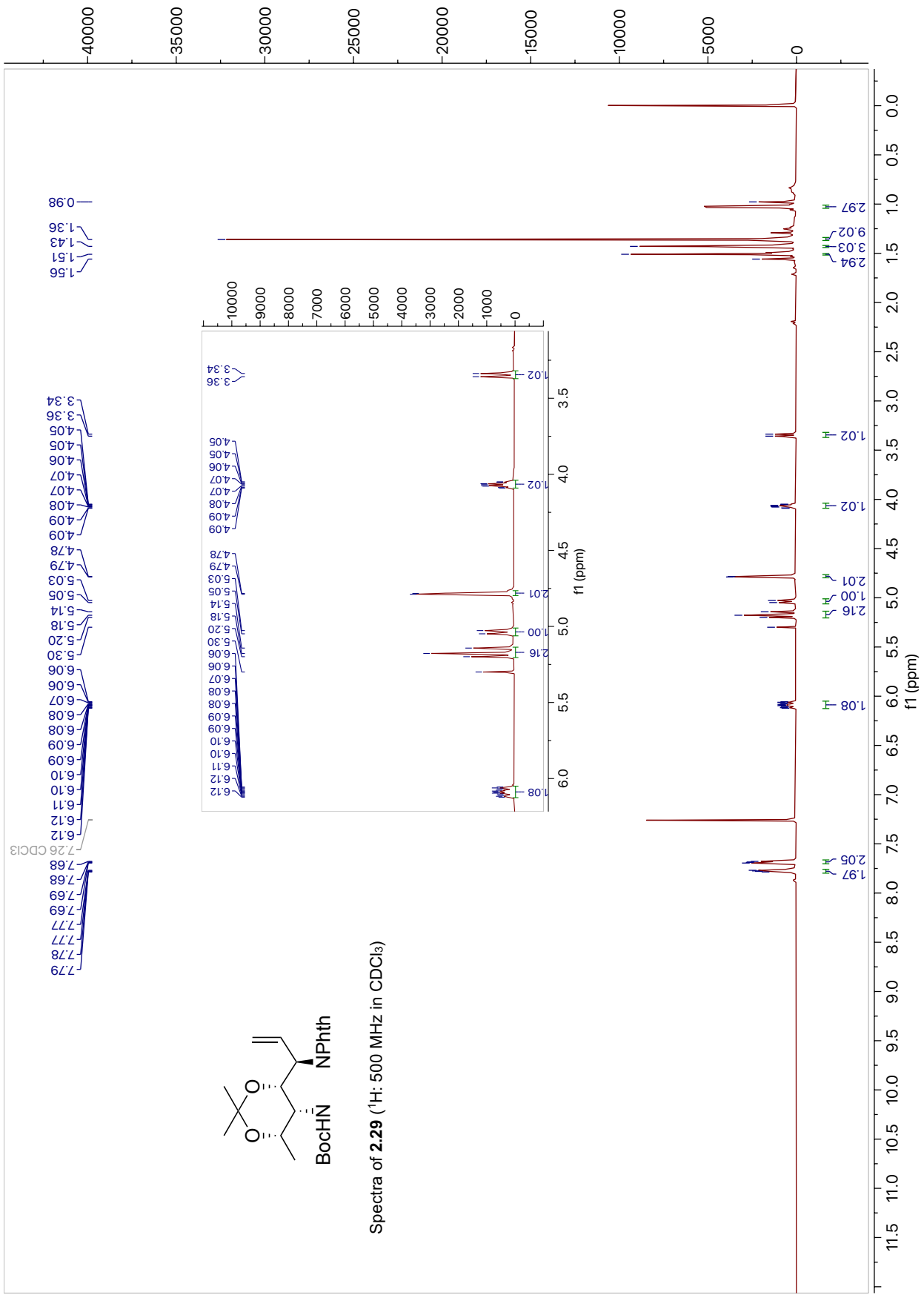


Spectra of **2.29** ($^1$H: 500 MHz in $CDCl_3$)

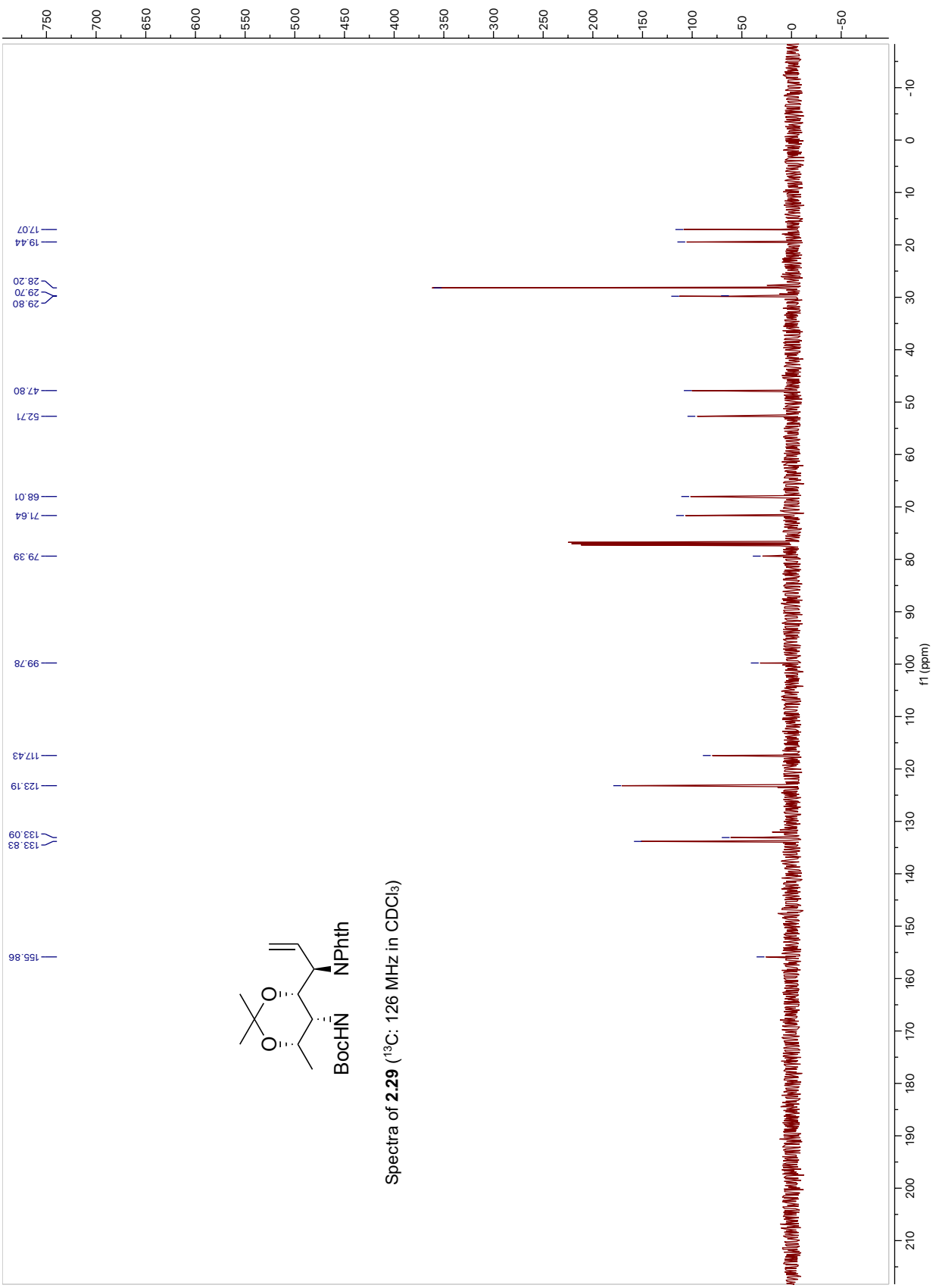
Spectra of 2.29 (13C: 126 MHz in CDCl3)
BocHN
NPhth
155.86
133.83
133.09
123.19
117.43
99.78
79.39
71.64
68.01
52.71
47.80
29.80
29.70
28.20
19.44
17.07
f1 (ppm)

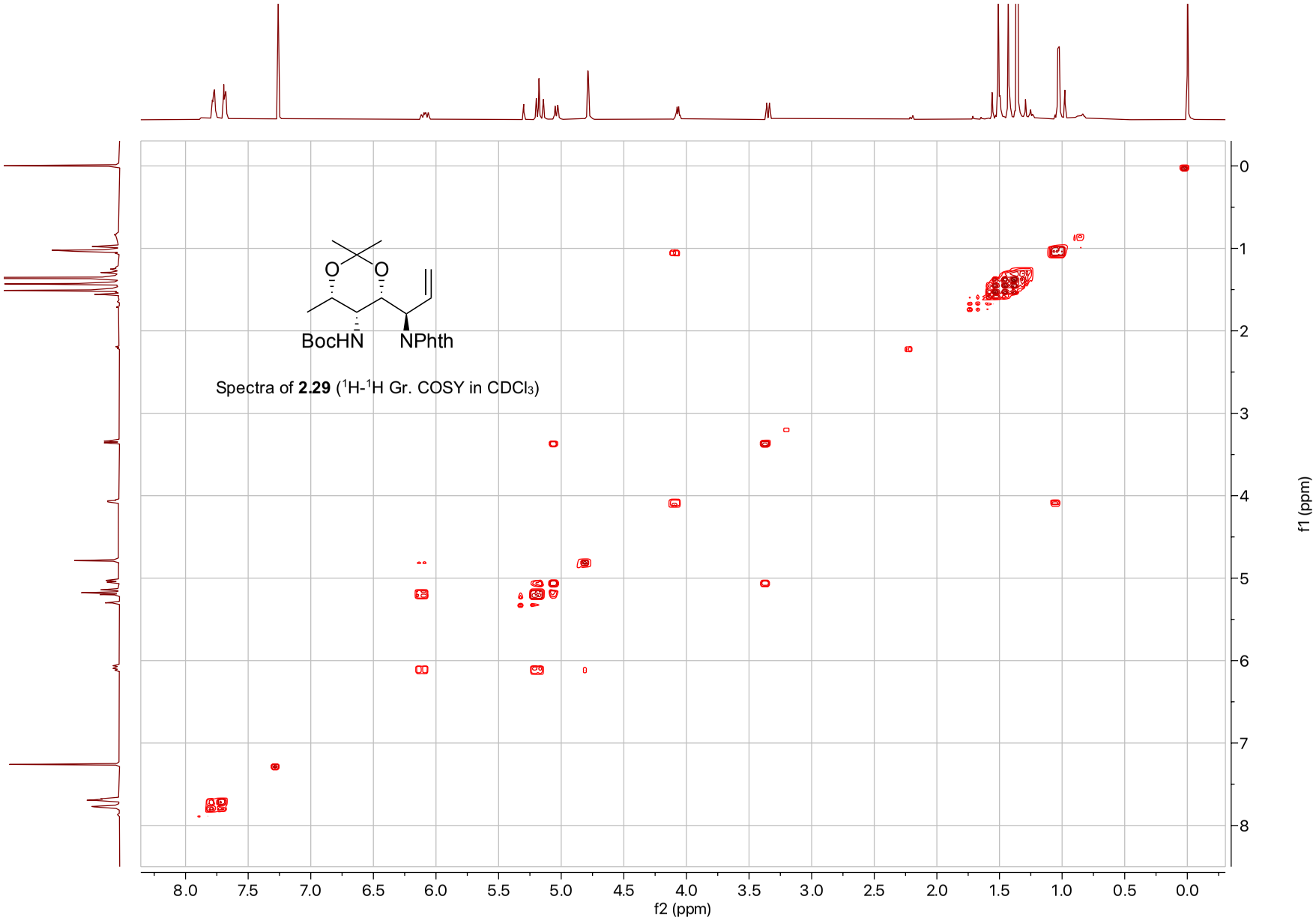
O
O
BocHN
NPhth
Spectra of **2.29** ($^1$H-$^1$H Gr. COSY in $CDCl_3$)
8.0
7.5
7.0
6.5
6.0
5.5
5.0
4.5
4.0
3.5
3.0
2.5
2.0
1.5
1.0
0.5
0.0
f2 (ppm)
0
1
2
3
4
5
6
7
8
f1 (ppm)

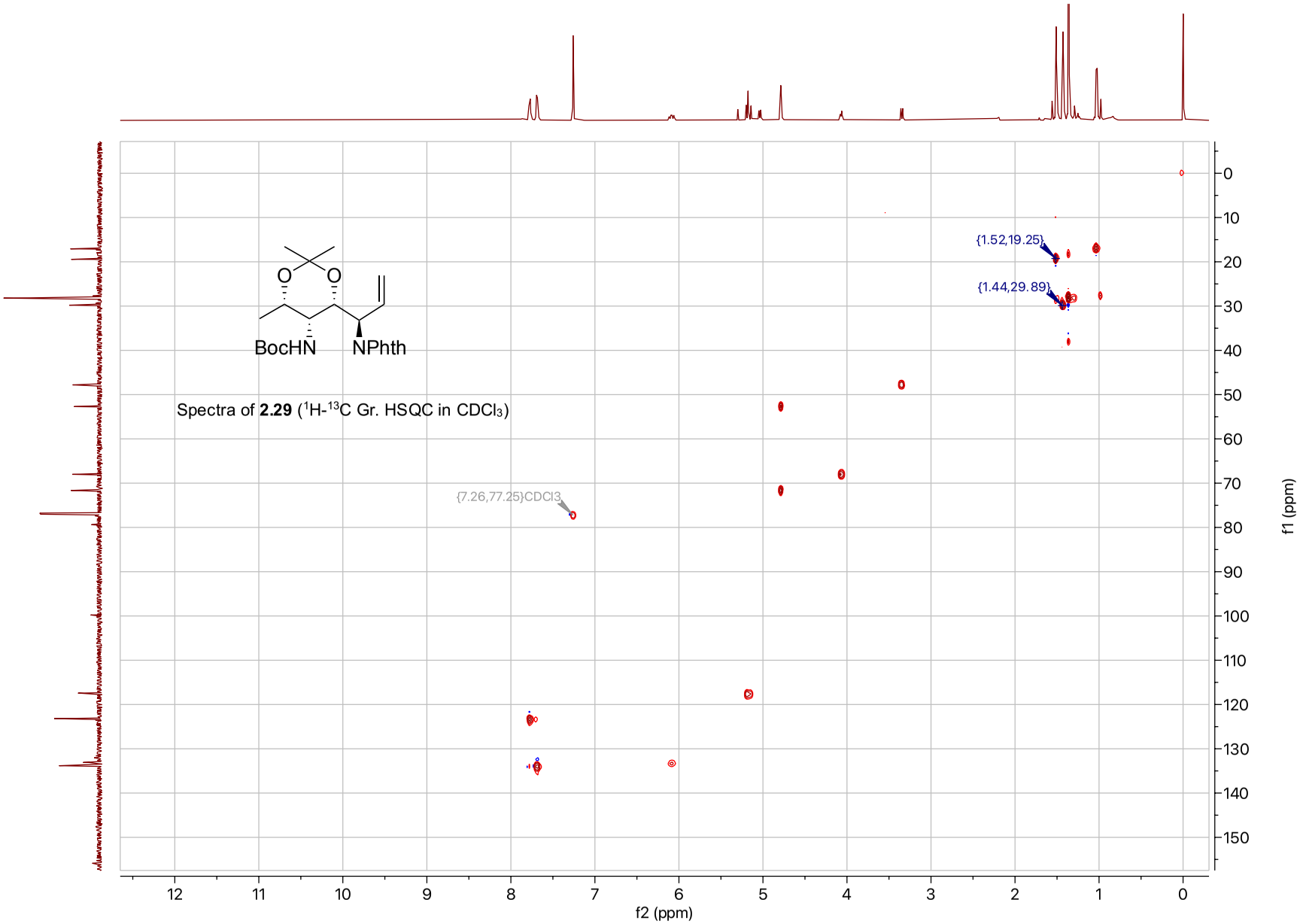
BocHN
NPhth
Spectra of 2.29 (1H-13C Gr. HSQC in CDCl3)
{7.26,77.25}CDCl3
{1.52,19.25}
{1.44,29.89}
f2 (ppm)
f1 (ppm)

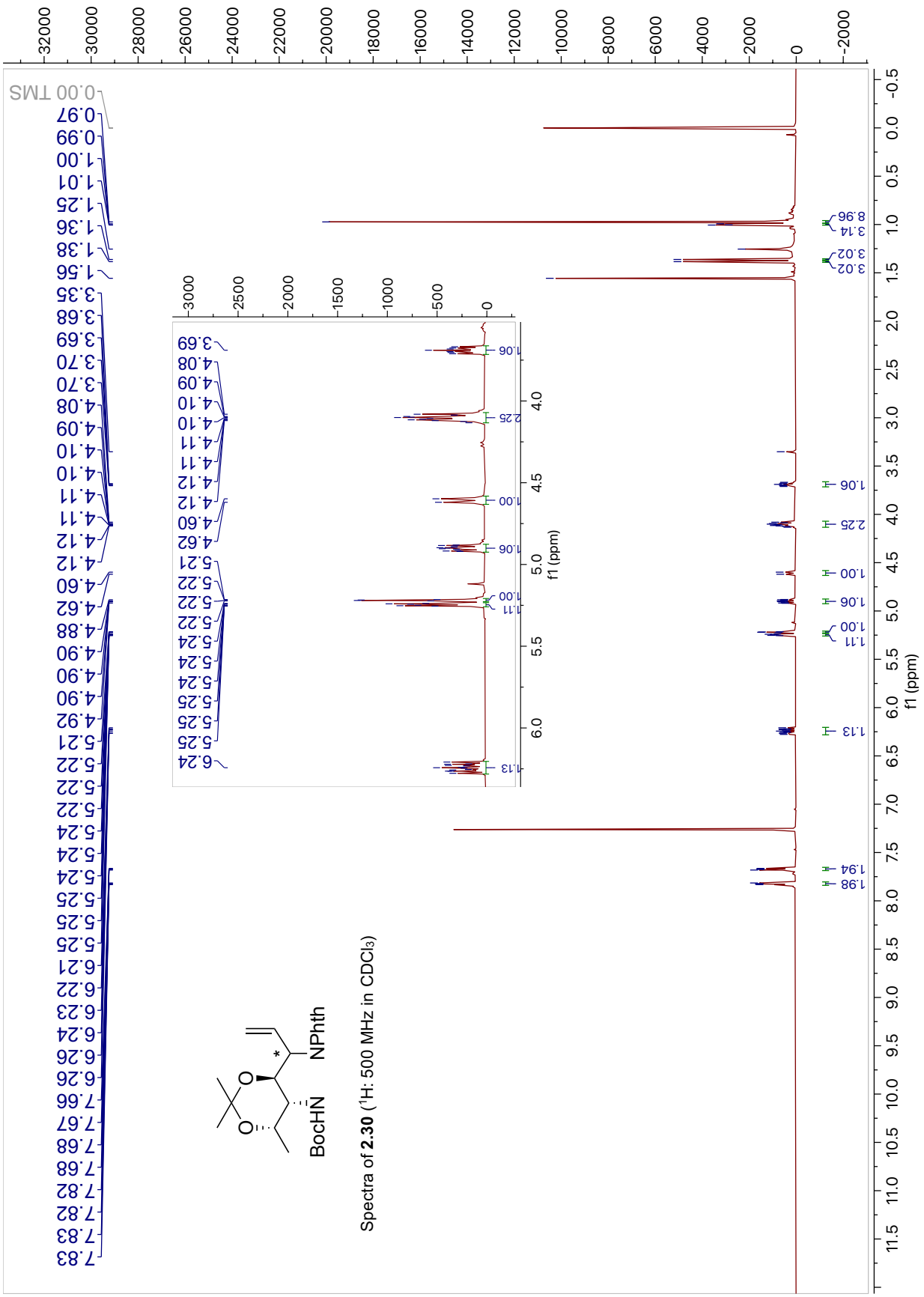
Spectra of 2.30 (1H: 500 MHz in CDCl3)
BocHN
NPhth
f1 (ppm)

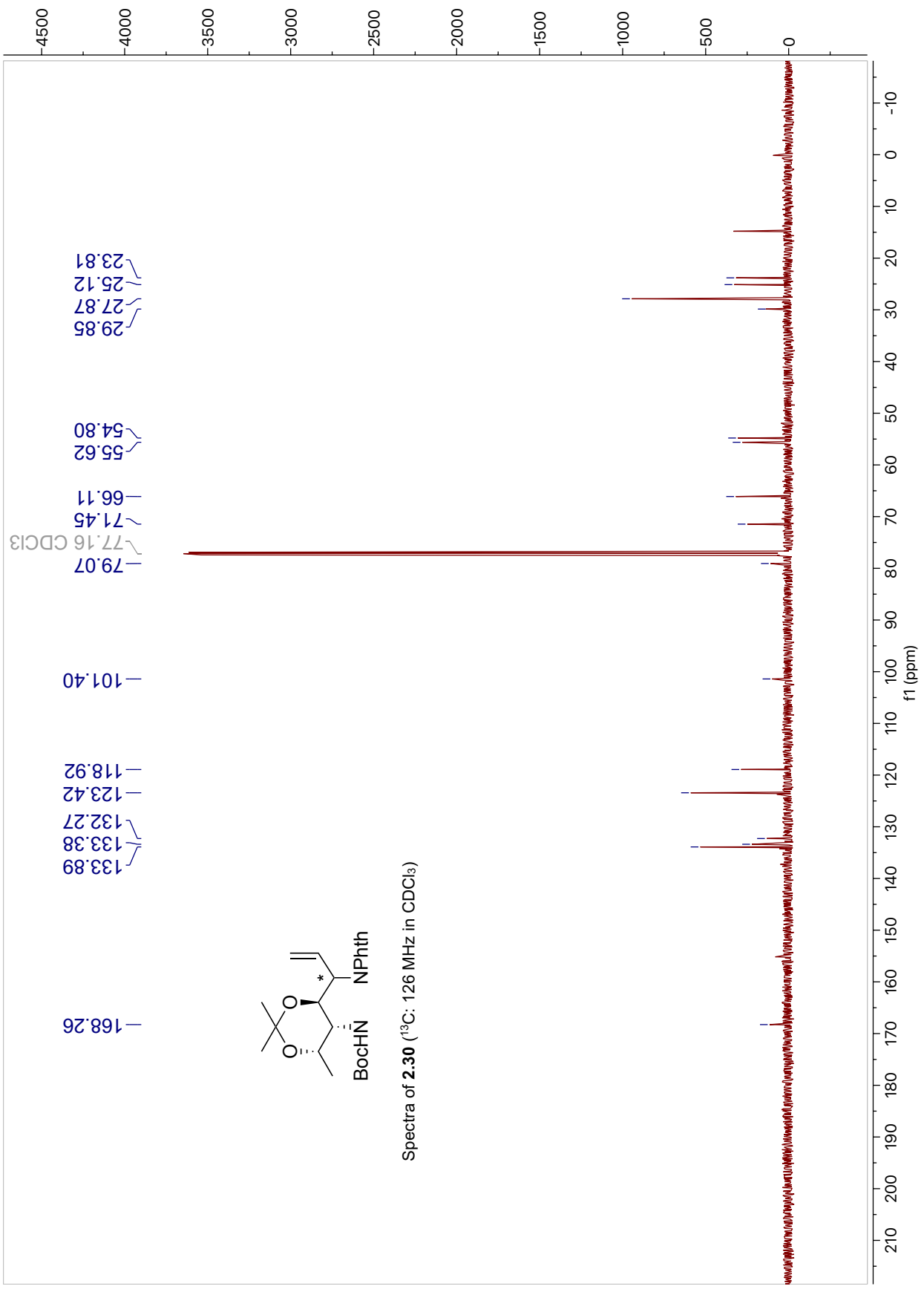
Spectra of 2.30 (13C: 126 MHz in CDCl3)
BocHN
NPhth
168.26
133.89
133.38
132.27
123.42
118.92
101.40
79.07
77.16 CDCl3
71.45
66.11
55.62
54.80
29.85
27.87
25.12
23.81
f1 (ppm)

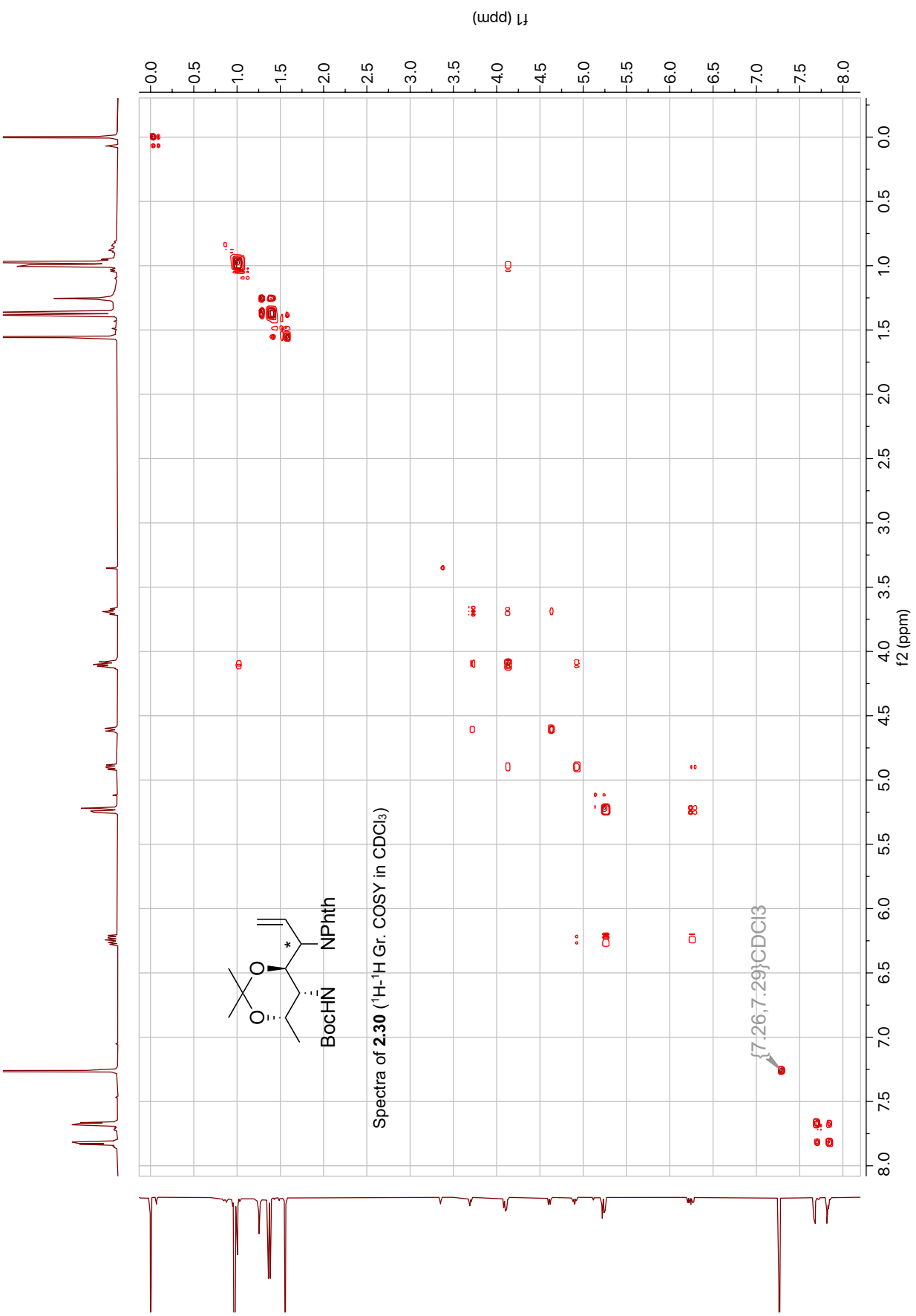
Spectra of **2.30** ($^1$H-$^1$H Gr. COSY in $CDCl_3$)
BocHN
NPhth
{7.26;7.29}CDCl3
f2 (ppm)
f1 (ppm)

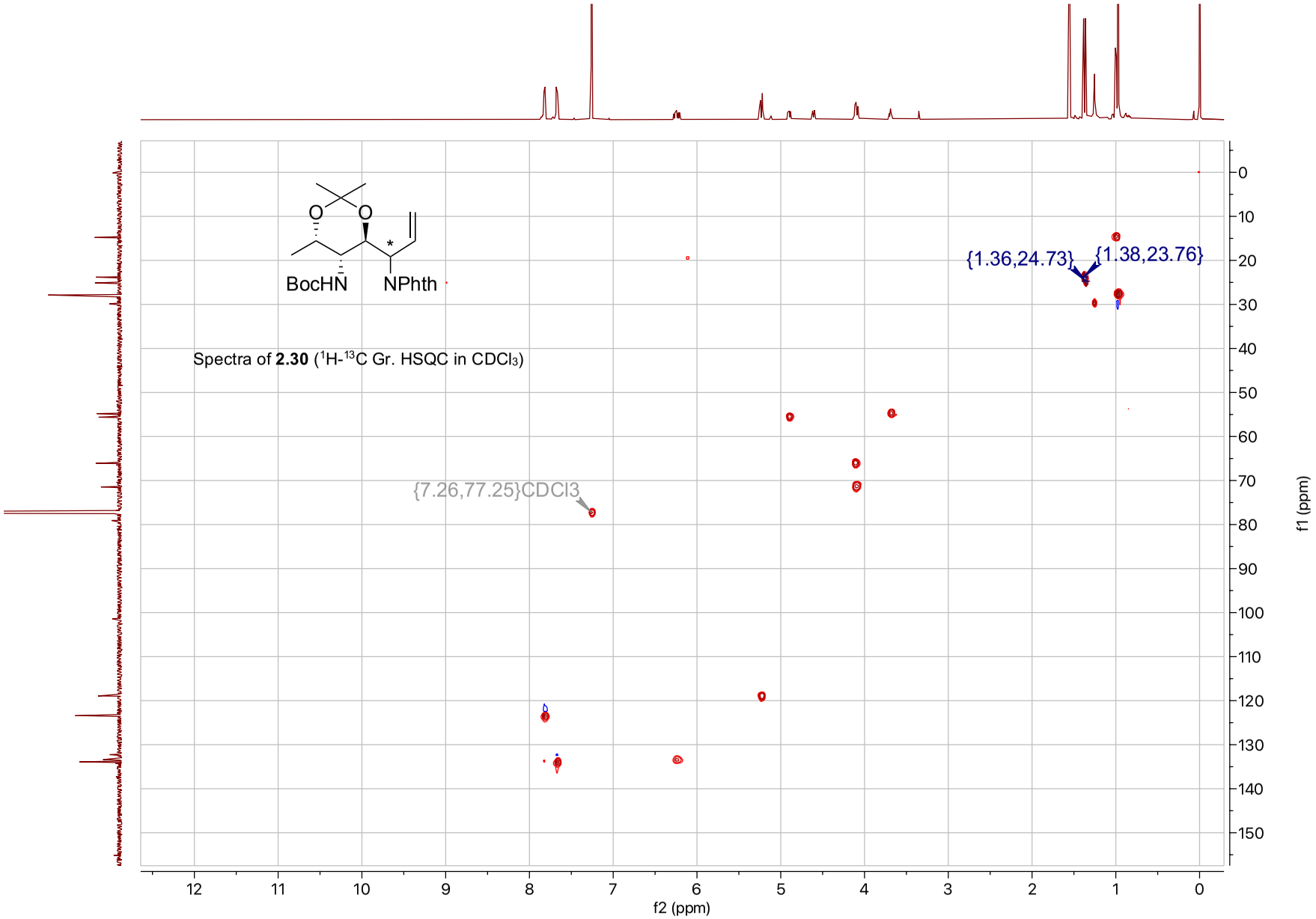
BocHN
NPhth
Spectra of **2.30** ($^{1}$H-$^{13}$C Gr. HSQC in CDCl$_3$)
{1.36,24.73}
{1.38,23.76}
{7.26,77.25}CDCl3
f2 (ppm)
f1 (ppm)

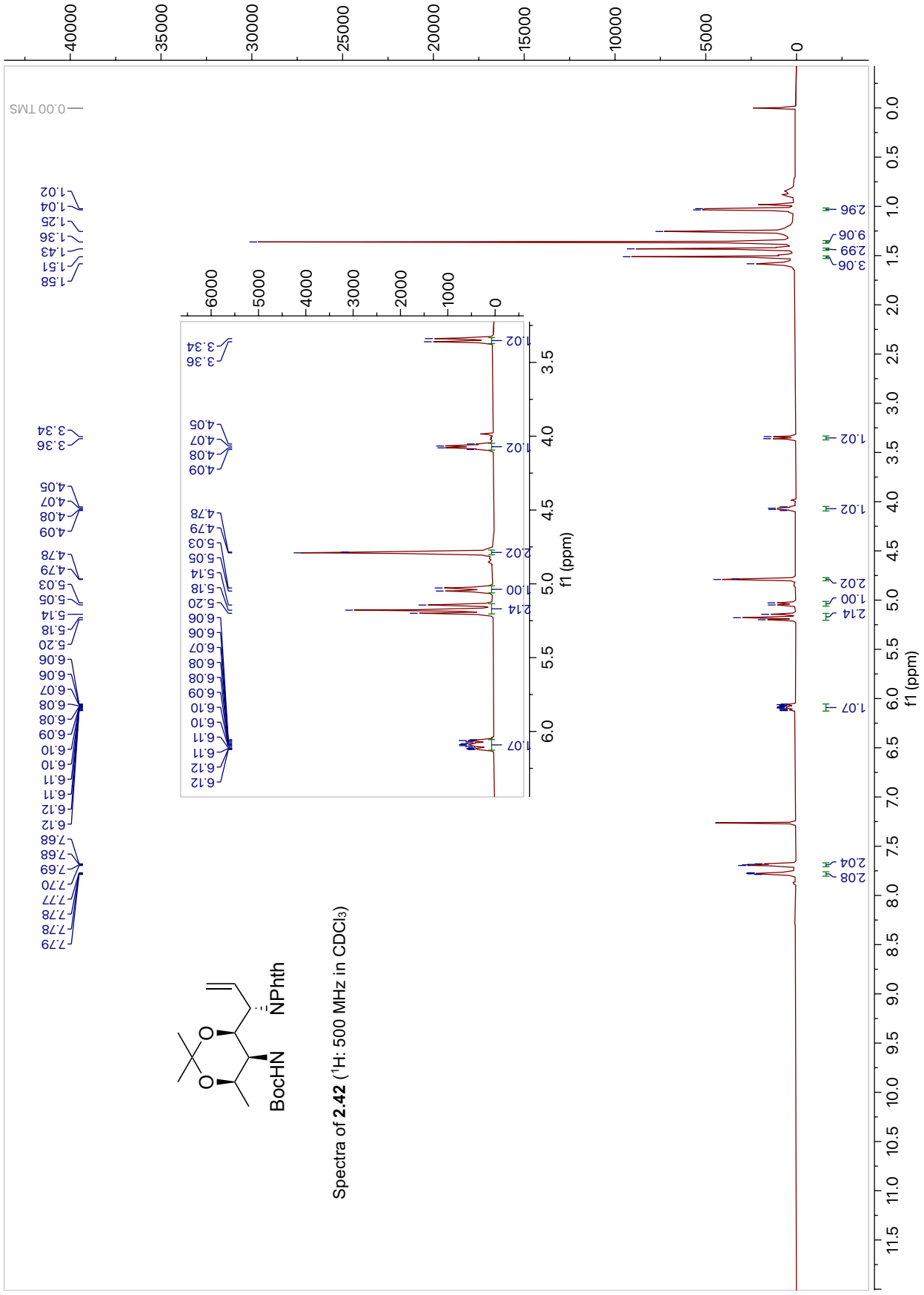
BocHN
NPhth
Spectra of 2.42 (1H: 500 MHz in CDCl3)
f1 (ppm)

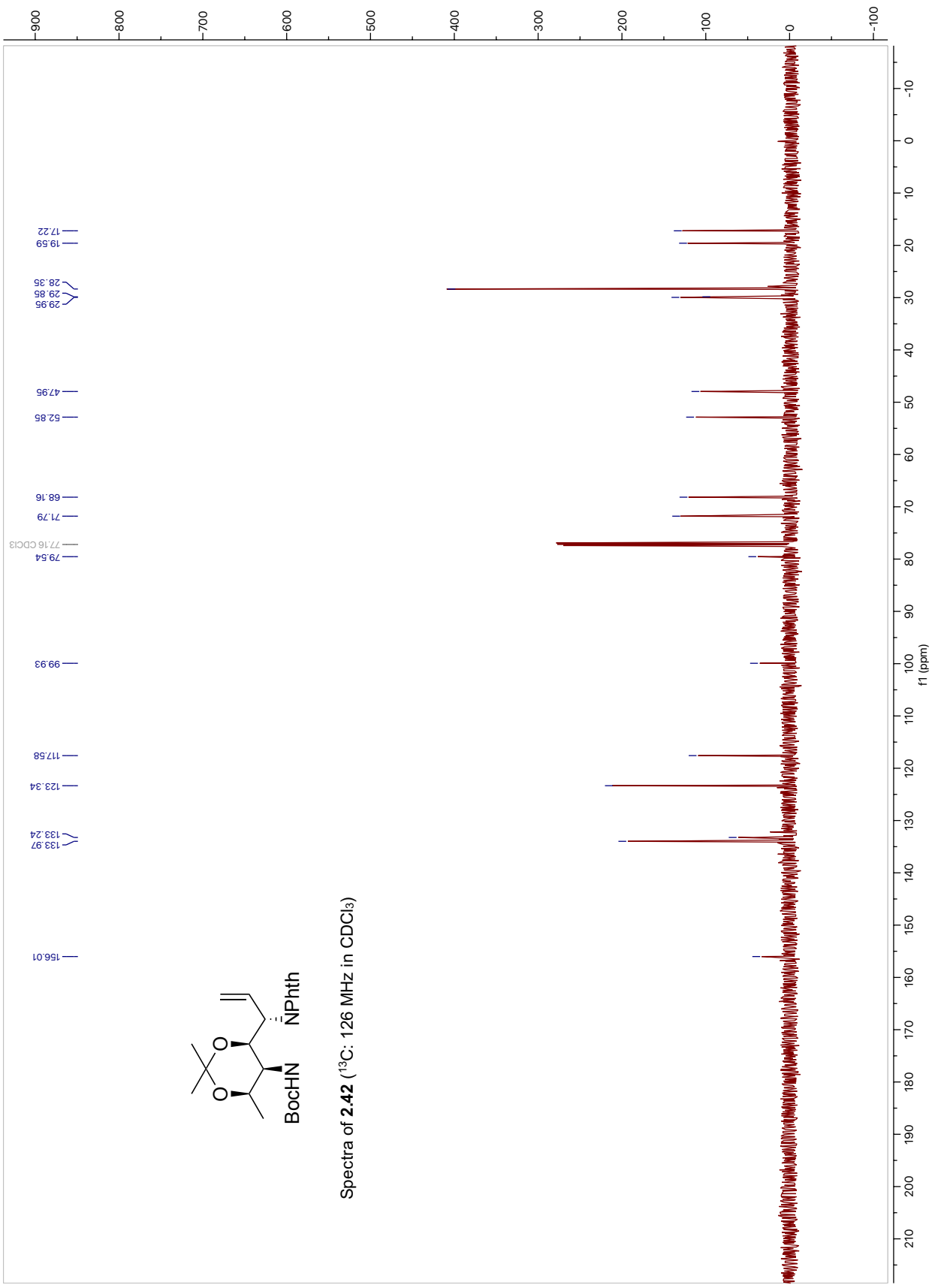
Spectra of 2.42 (13C: 126 MHz in CDCl3)
BocHN
NPhth
156.01
133.97
133.24
123.34
117.58
99.93
79.54
77.16 CDCl3
71.79
68.16
52.85
47.95
29.95
29.85
28.35
19.59
17.22
f1 (ppm)

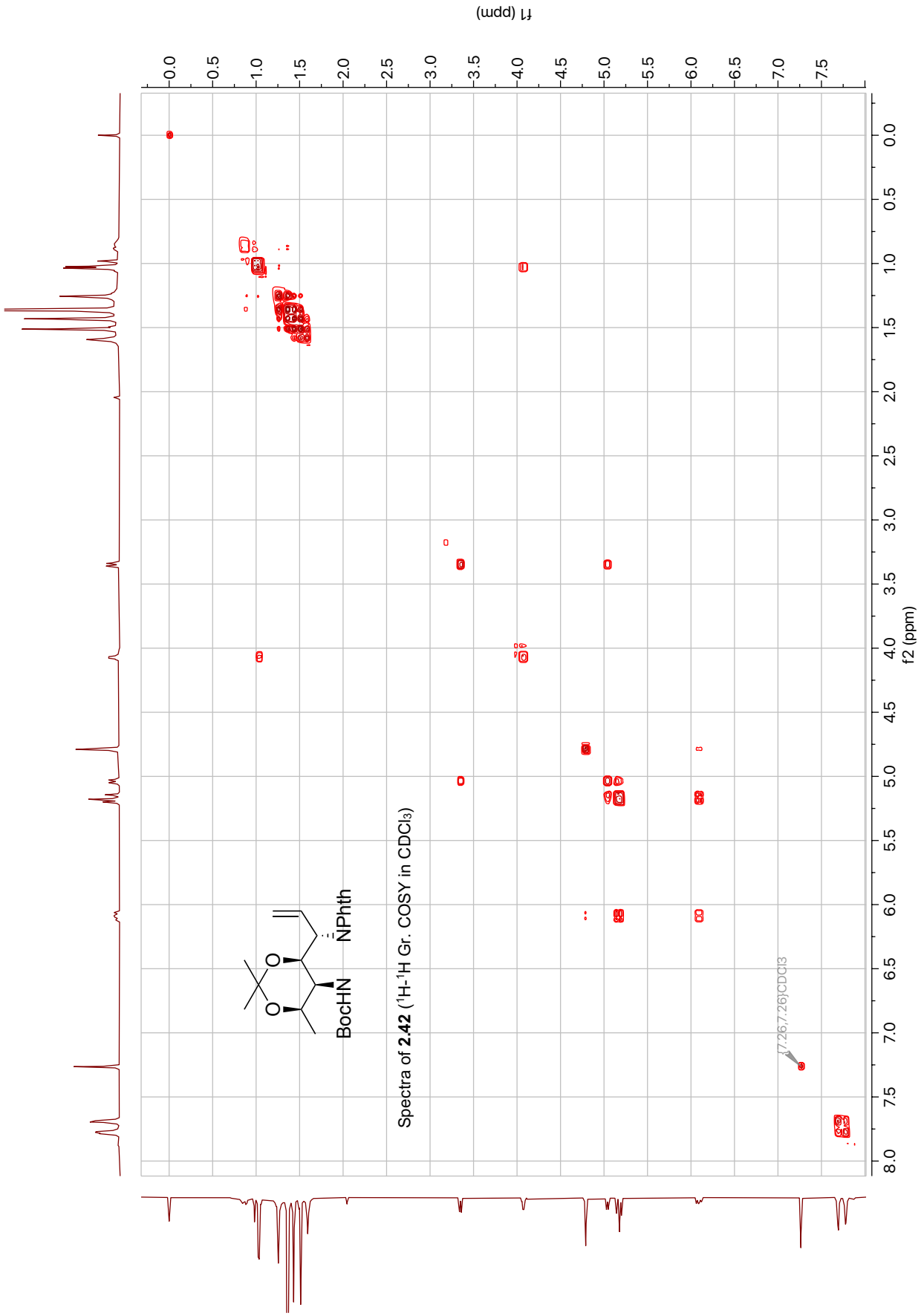
Spectra of 2.42 (1H-1H Gr. COSY in CDCl3)
BocHN
NPhth
f2 (ppm)
f1 (ppm)
7.26,7.26)CDCl3

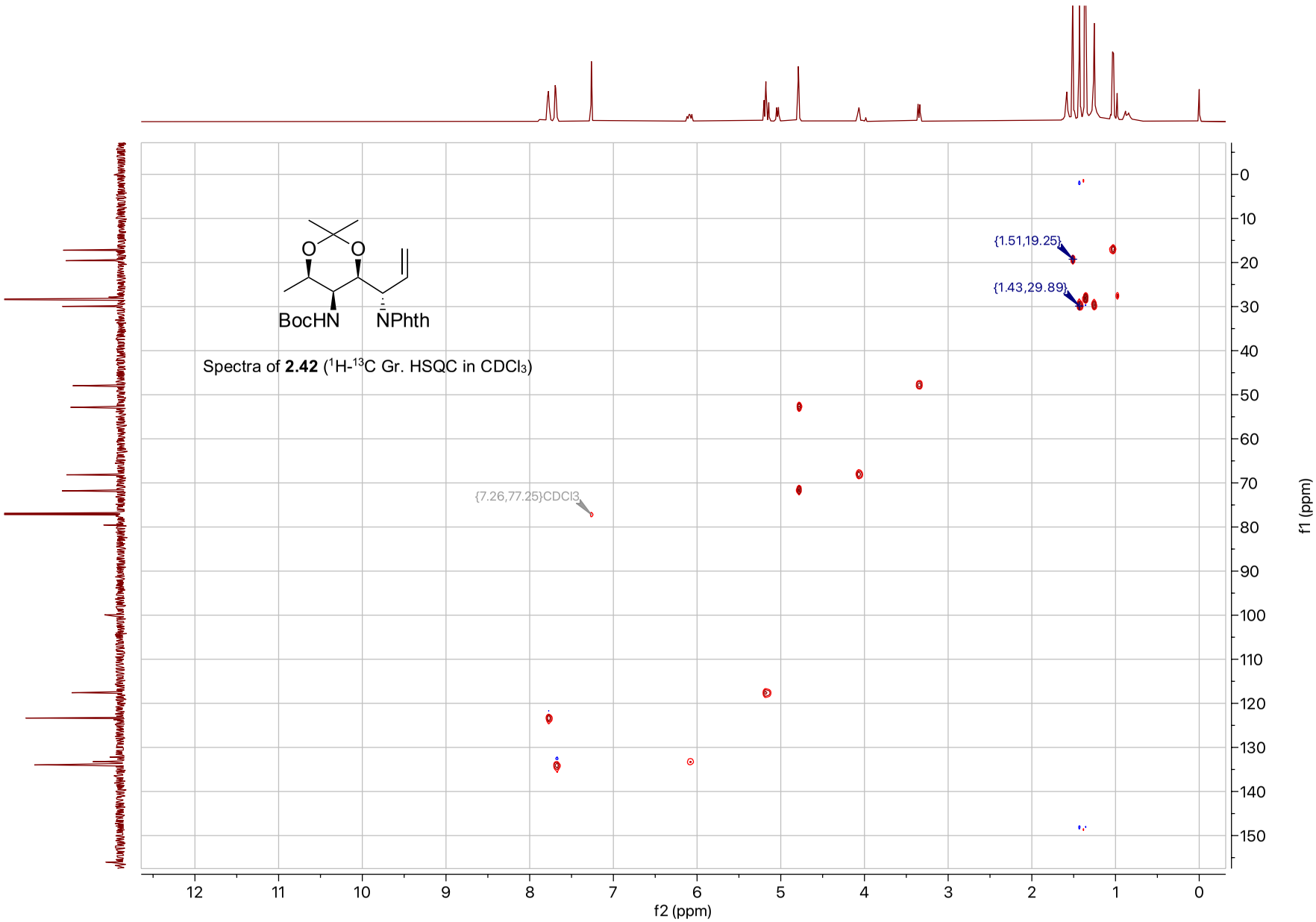
BocHN
NPhth
Spectra of **2.42** ($^{1}$H-$^{13}$C Gr. HSQC in $CDCl_3$)
{1.51,19.25}
{1.43,29.89}
{7.26,77.25}CDCl3
f2 (ppm)
f1 (ppm)

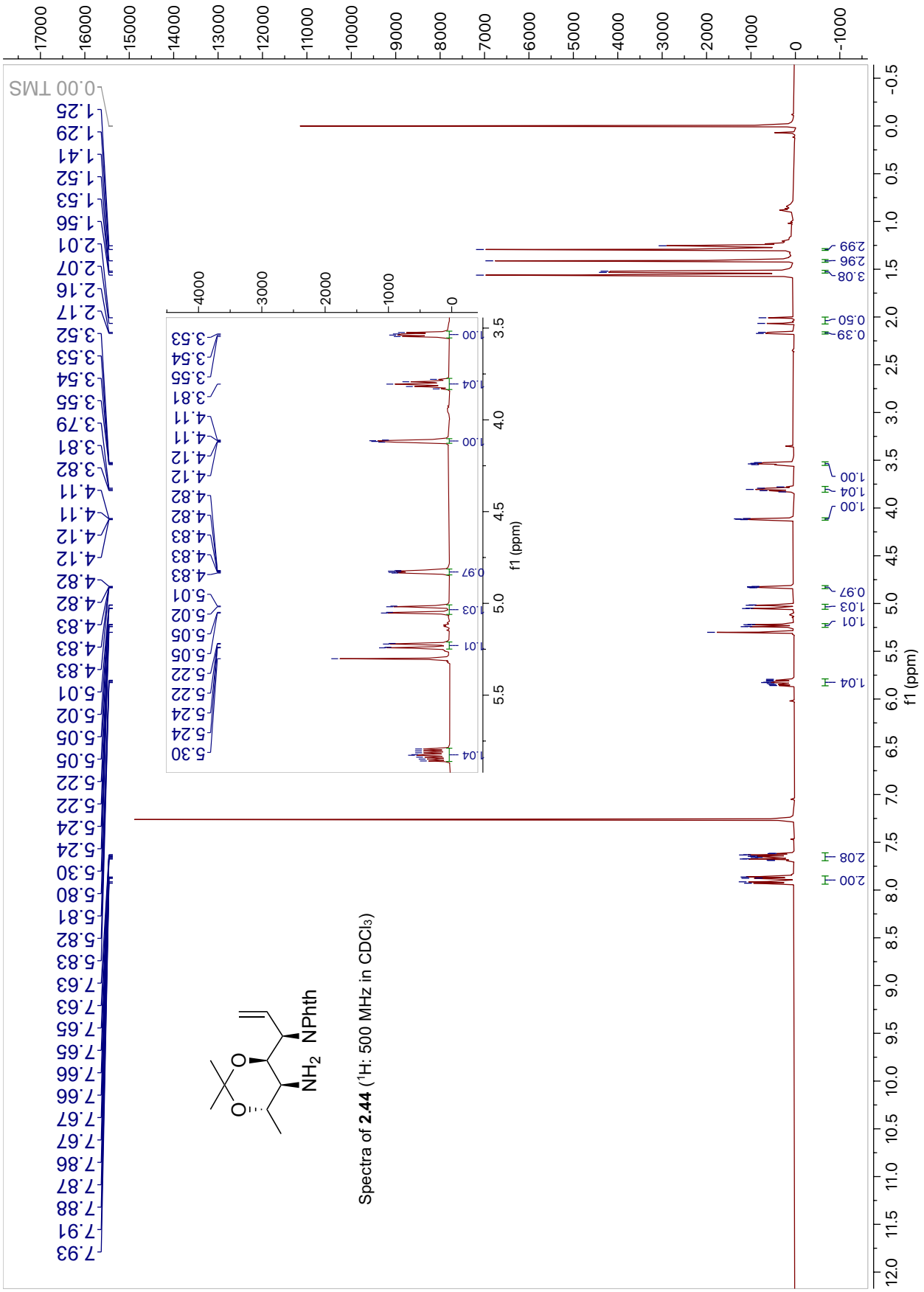
Spectra of 2.44 (1H: 500 MHz in CDCl3)
NPhth
NH2
O
O
f1 (ppm)
TMS
0.00
2.00
2.08
1.04
1.01
1.03
0.97
1.00
1.04
1.00
0.39
0.50
3.08
2.96
2.99

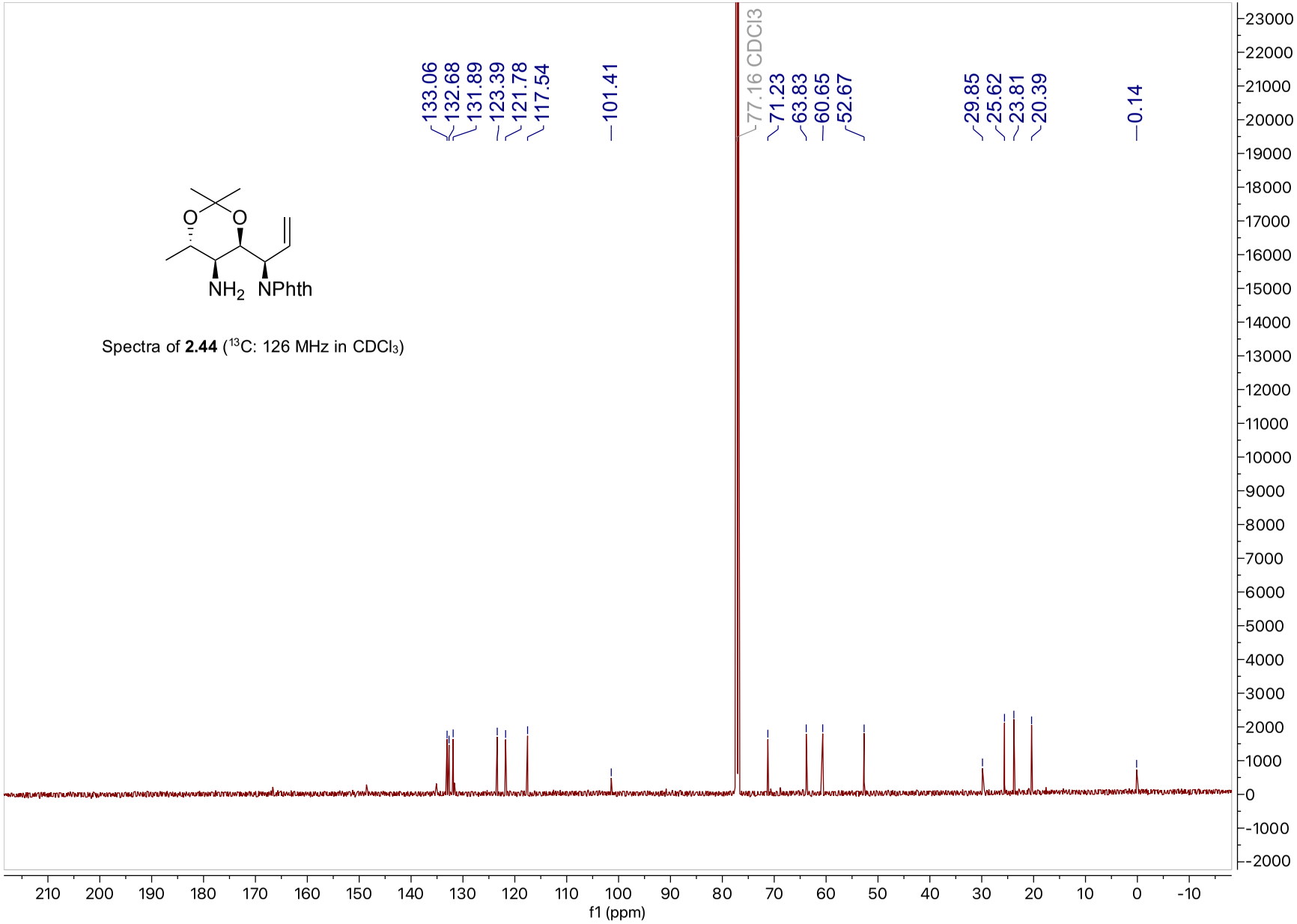
133.06
132.68
131.89
123.39
121.78
117.54
101.41
77.16 CDCl3
71.23
63.83
60.65
52.67
29.85
25.62
23.81
20.39
0.14
O
O
NH2
NPhth
Spectra of 2.44 (13C: 126 MHz in CDCl3)
f1 (ppm)

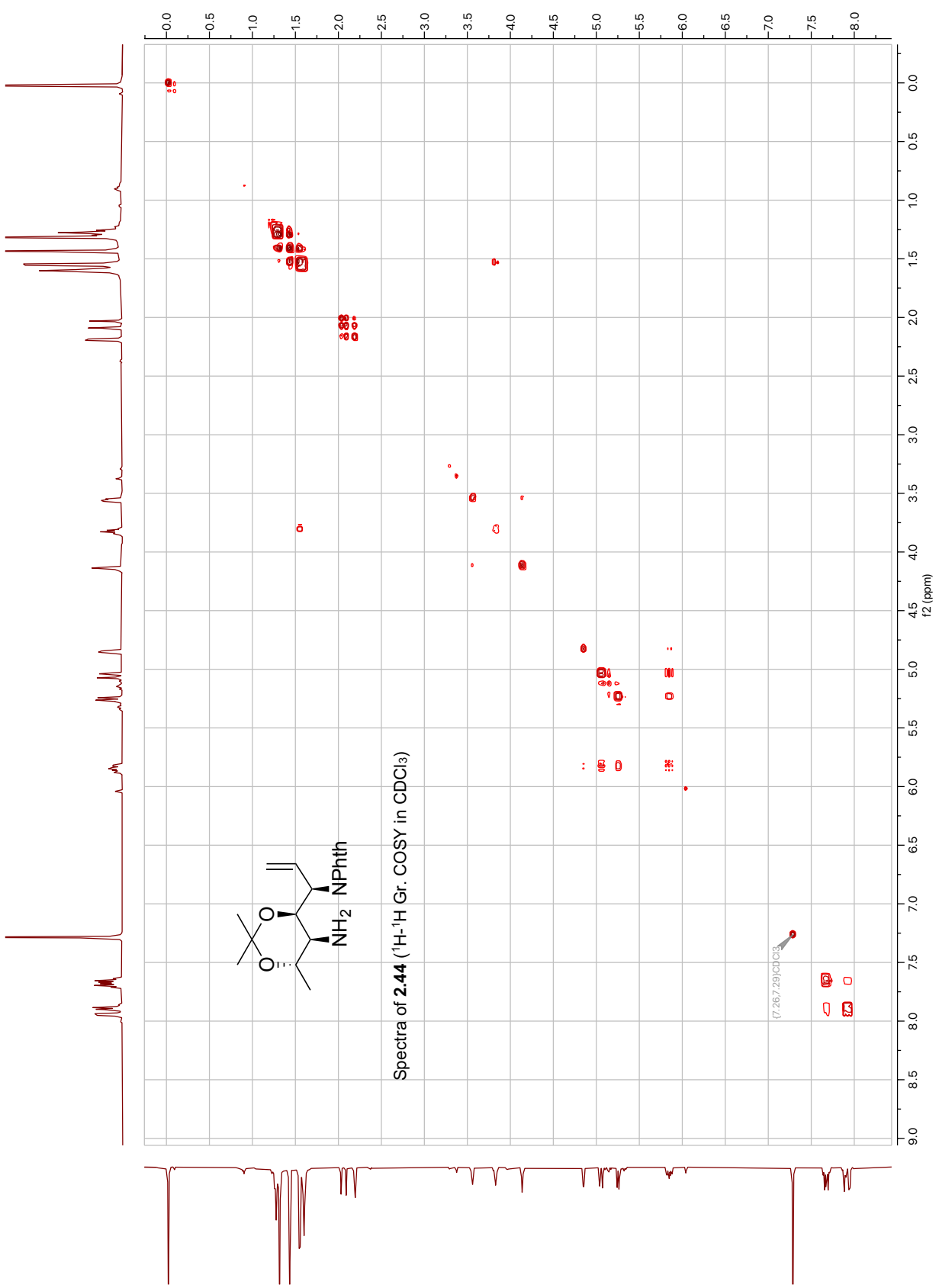
Spectra of 2.44 (¹H-¹H Gr. COSY in CDCl₃)
NH2
NPhth
f2 (ppm)
f1 (ppm)

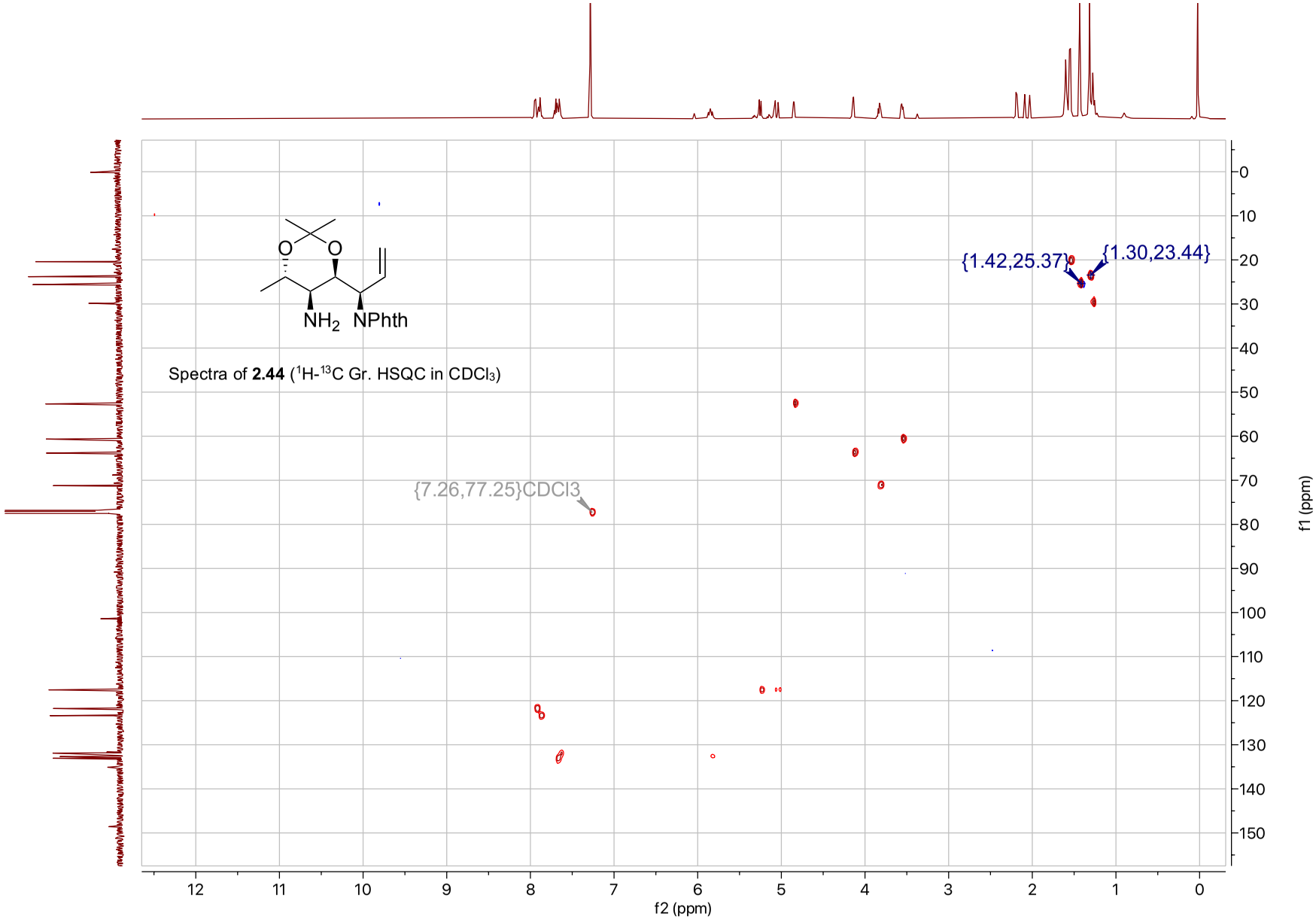
Spectra of **2.44** ($^{1}$H-$^{13}$C Gr. HSQC in $CDCl_3$)
{1.42,25.37}
{1.30,23.44}
{7.26,77.25}CDCl3
NH2
NPhth
f2 (ppm)
f1 (ppm)

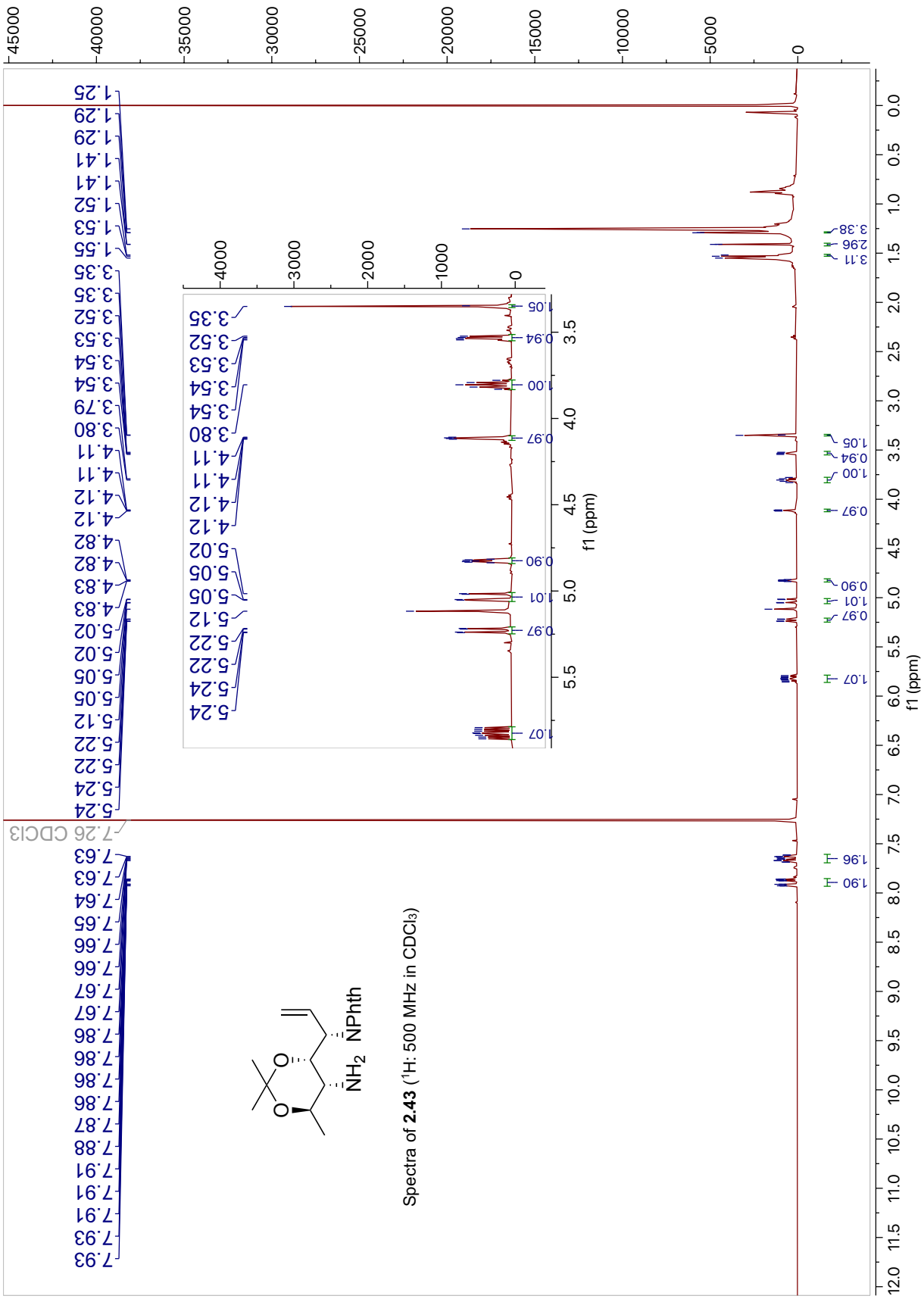
NH2 NPhth
Spectra of 2.43 (1H: 500 MHz in CDCl3)
f1 (ppm)

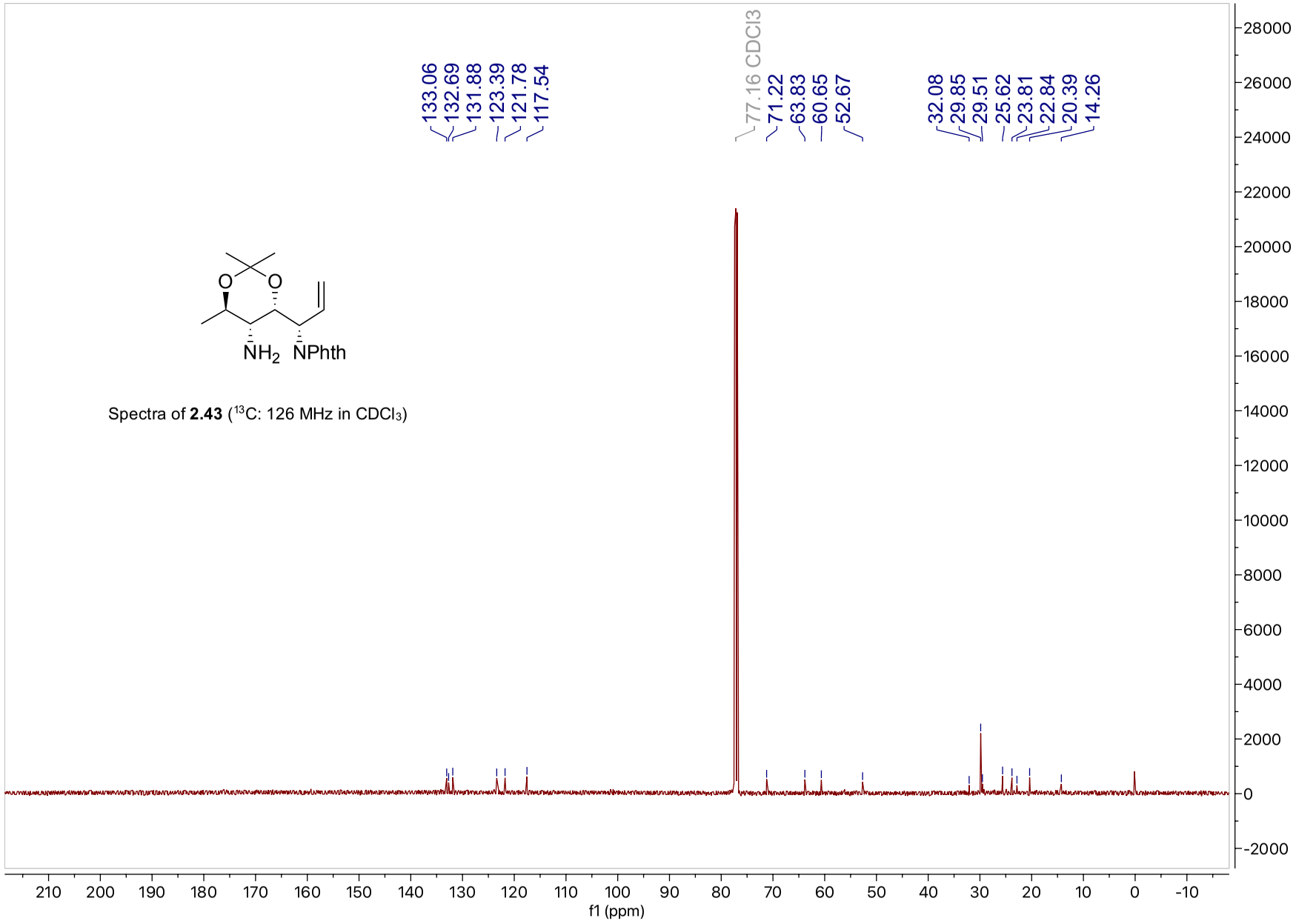
133.06
132.69
131.88
123.39
121.78
117.54
77.16 CDCl3
71.22
63.83
60.65
52.67
32.08
29.85
29.51
25.62
23.81
22.84
20.39
14.26
O
O
NH2
NPhth
Spectra of 2.43 (13C: 126 MHz in CDCl3)
28000
26000
24000
22000
20000
18000
16000
14000
12000
10000
8000
6000
4000
2000
0
-2000
210 200 190 180 170 160 150 140 130 120 110 100 90 80 70 60 50 40 30 20 10 0 -10
f1 (ppm)

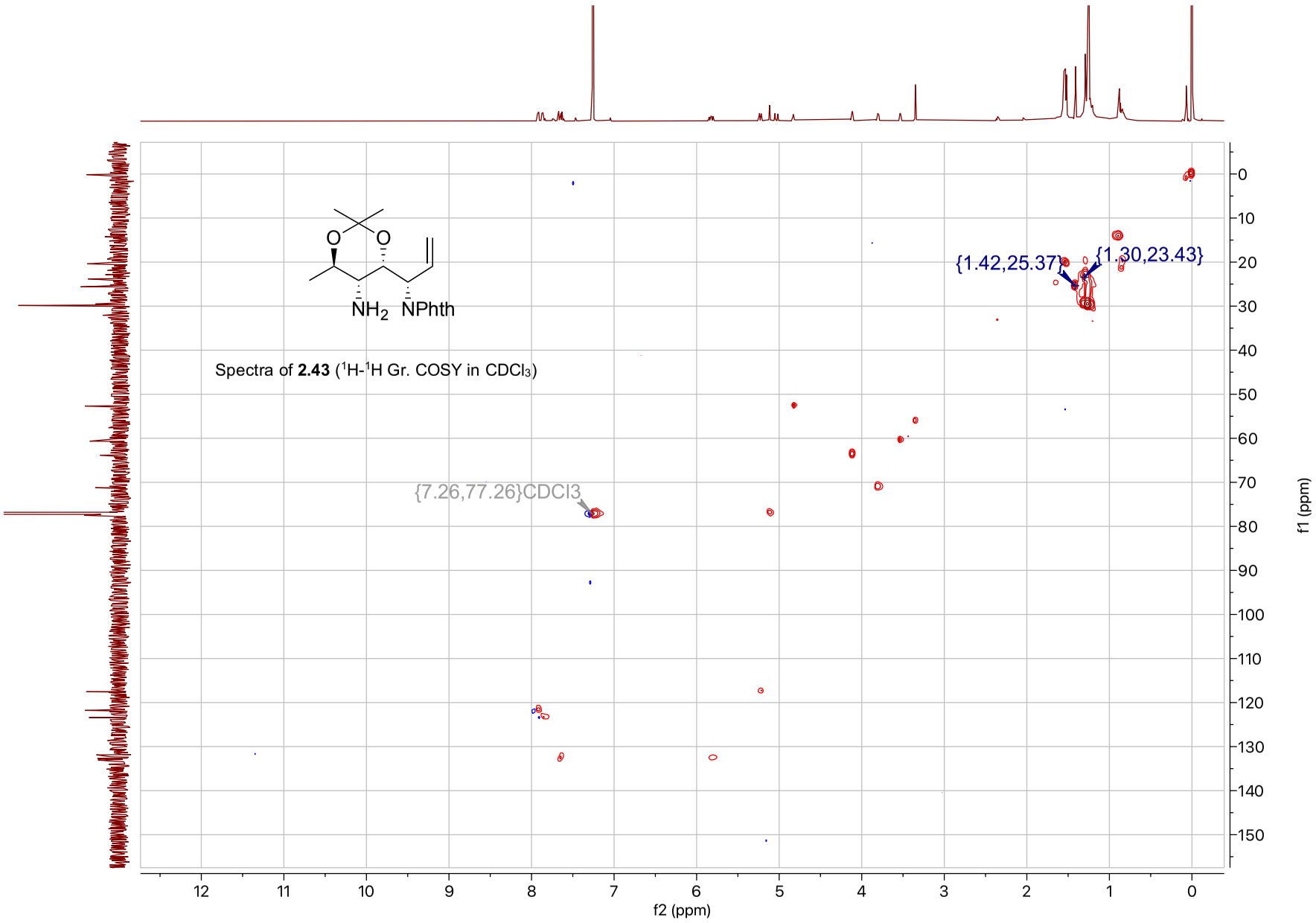
Spectra of **2.43** ($^1$H-$^1$H Gr. COSY in $CDCl_3$)
{7.26,77.26}CDCl3
{1.42,25.37}
{1.30,23.43}
NH2
NPhth
f2 (ppm)
f1 (ppm)

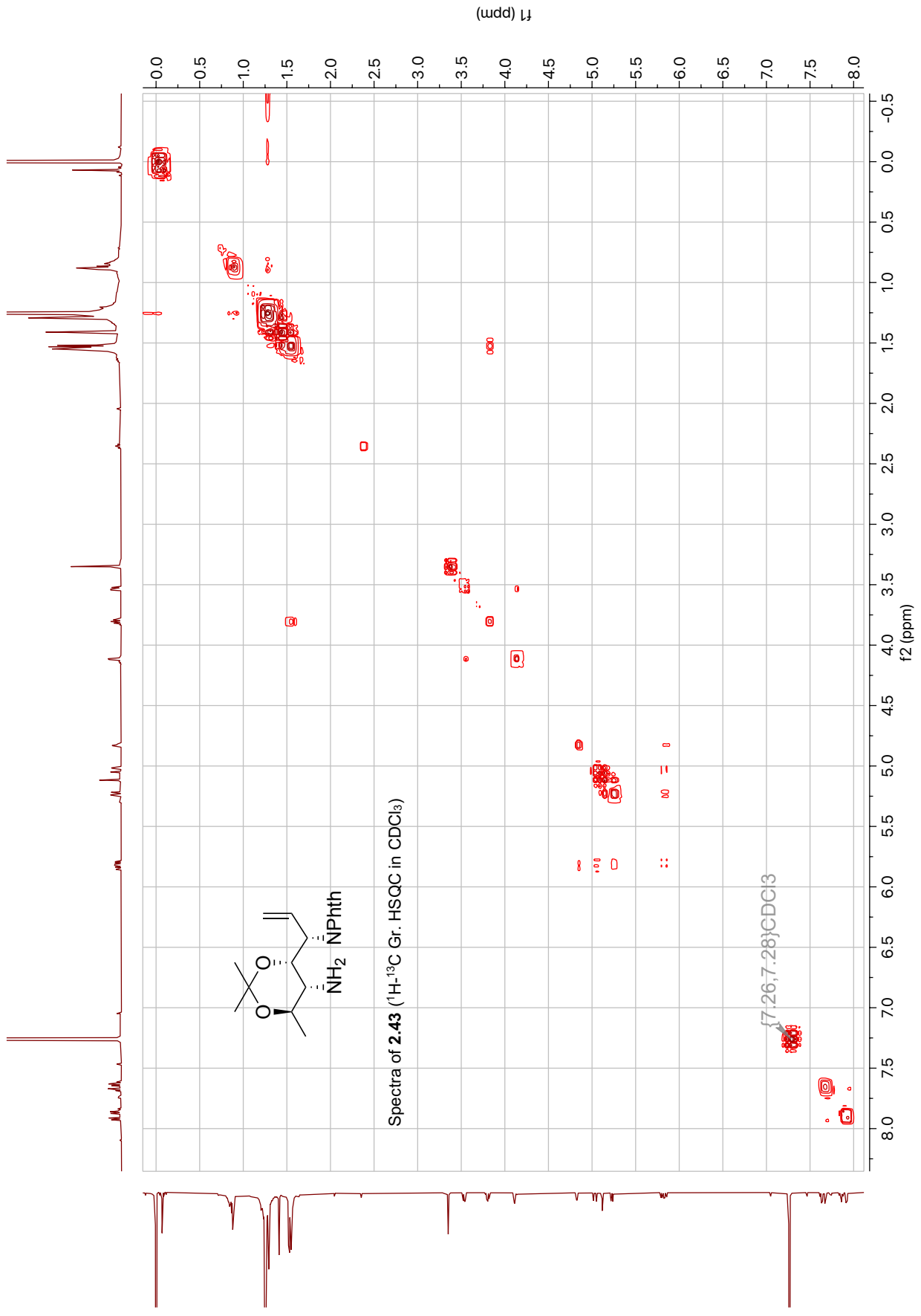
Spectra of **2.43** ($^{1}$H-$^{13}$C Gr. HSQC in $CDCl_3$)
$NH_2$
NPhth
{7.26,7.28}CDCl3
f2 (ppm)
f1 (ppm)

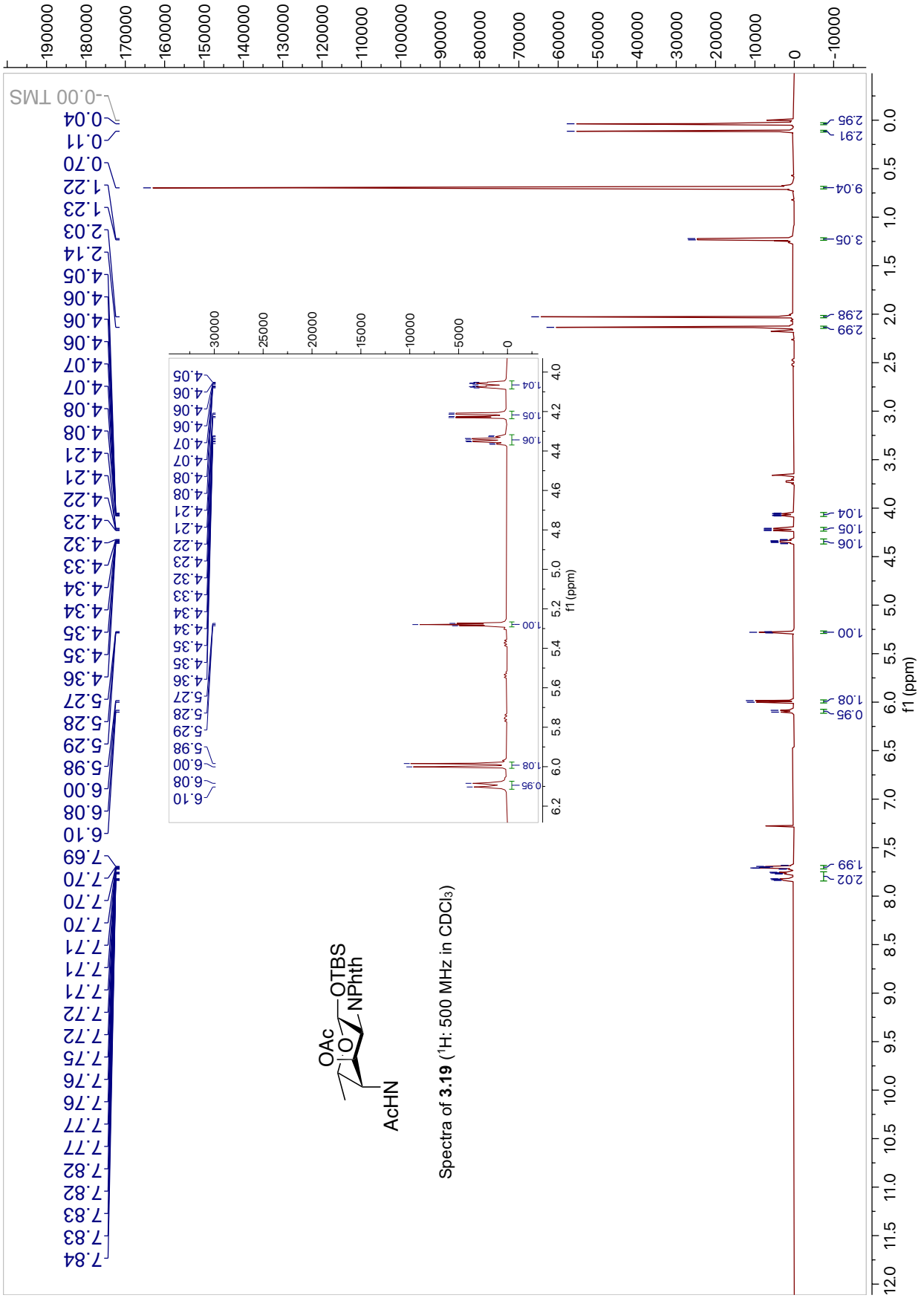


Spectra of **3.19** ($^1$H: 500 MHz in $CDCl_3$)

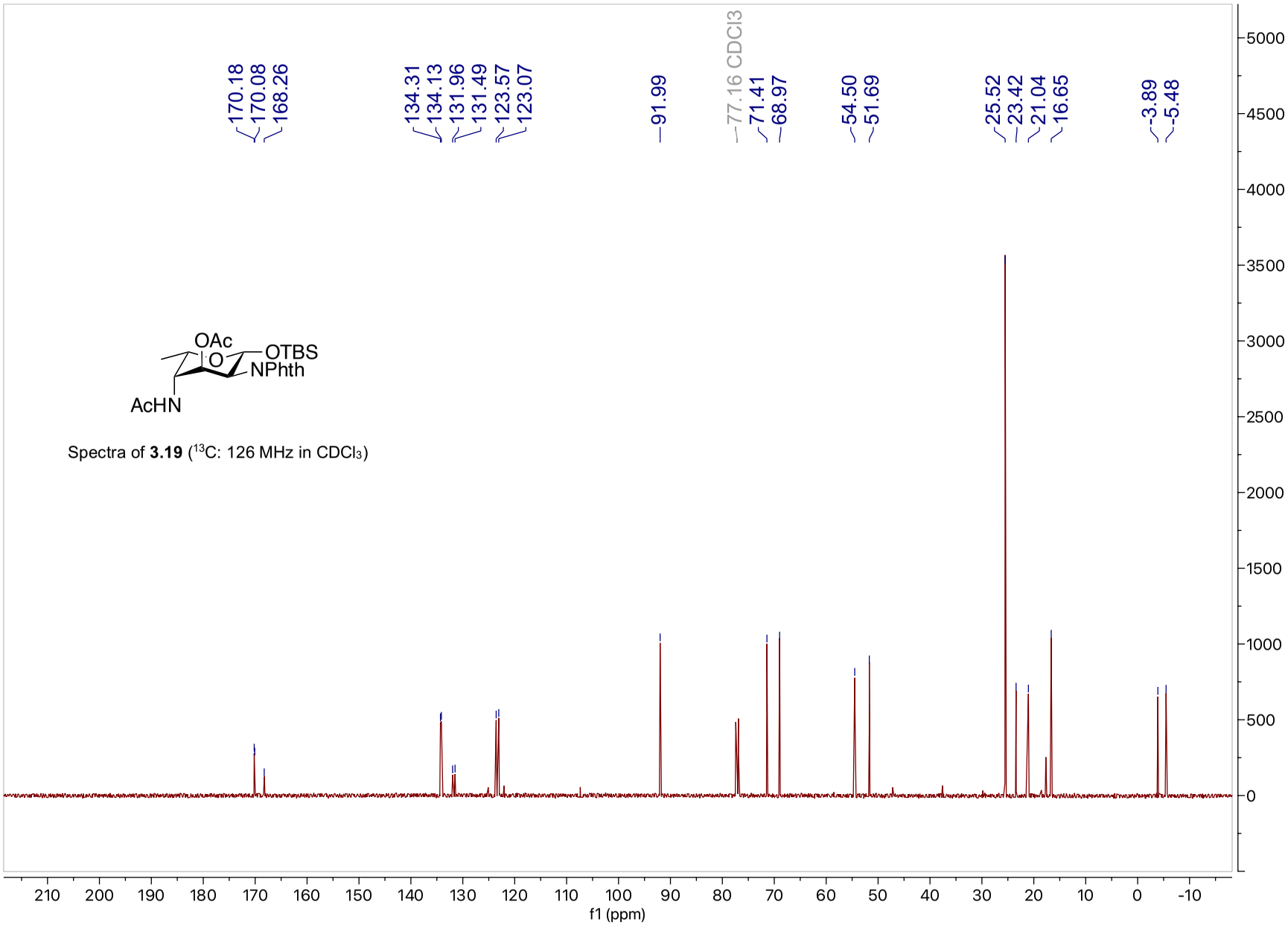


Spectra of **3.19** ($^{13}$C: 126 MHz in $CDCl_3$)

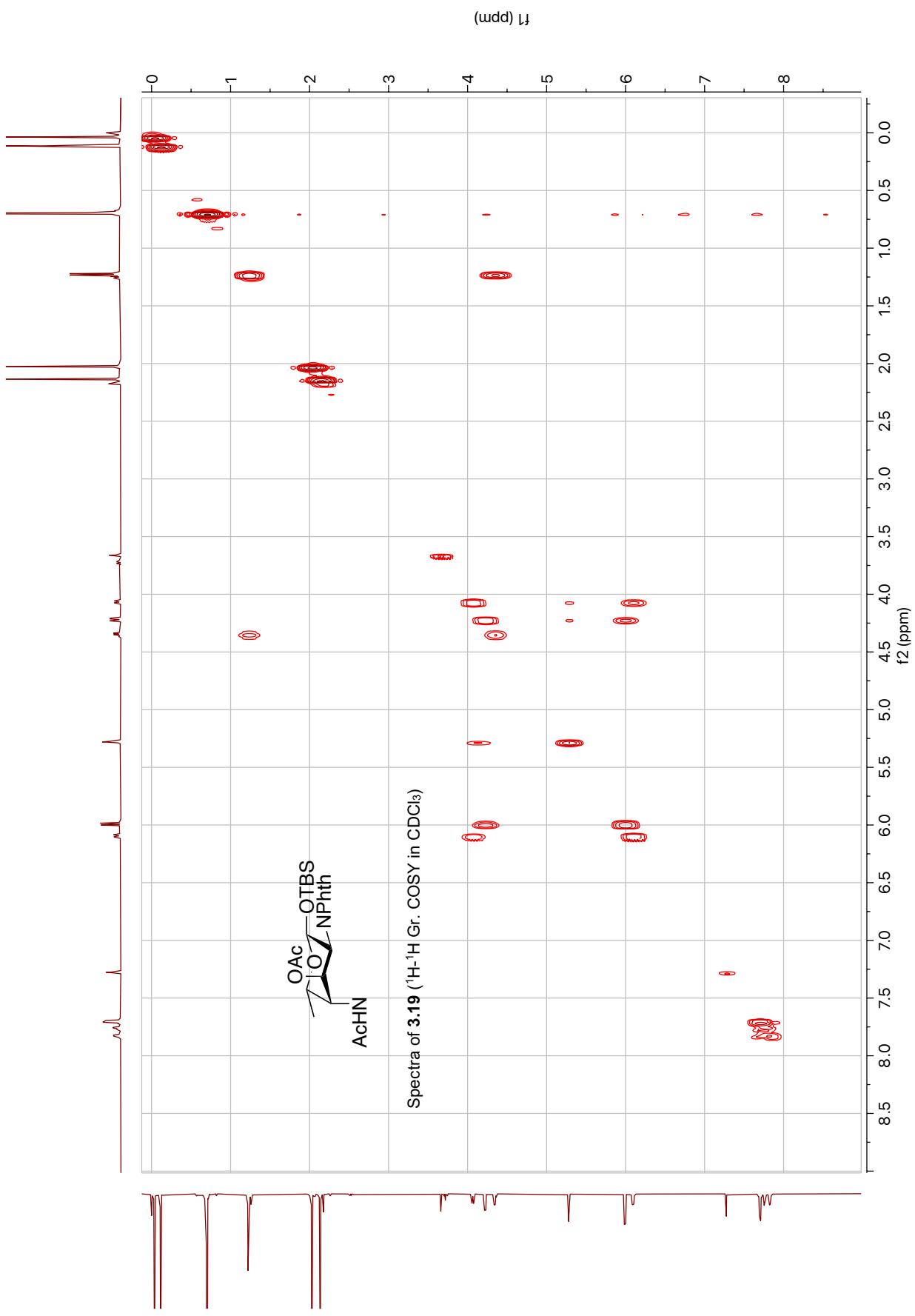
f1 (ppm)
f2 (ppm)
Spectra of 3.19 (1H-1H Gr. COSY in CDCl3)
OAc
OTBS
NPhth
AcHN

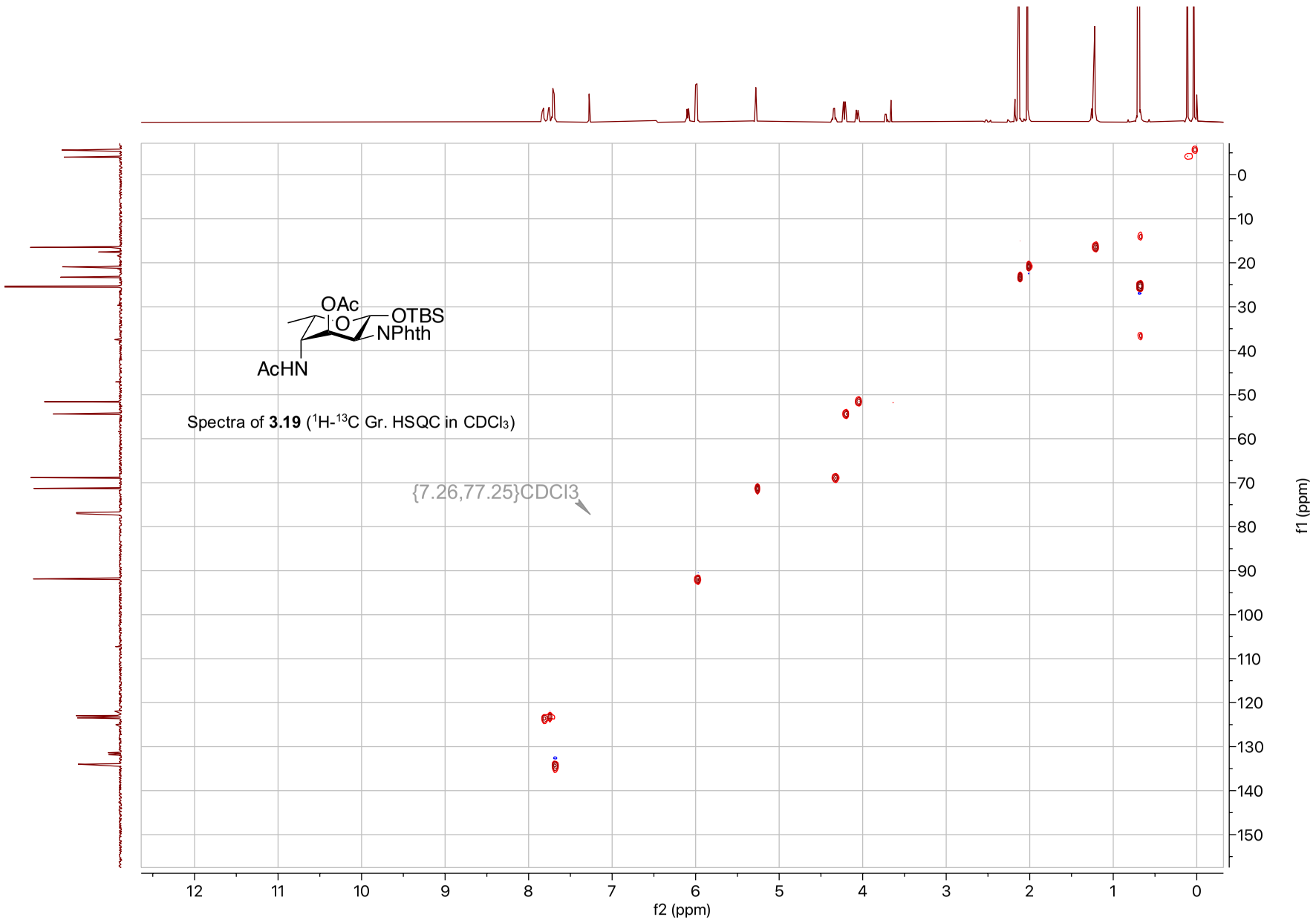
OAc
O
OTBS
NPhth
AcHN
Spectra of **3.19** ($^{1}$H-$^{13}$C Gr. HSQC in $CDCl_3$)
{7.26,77.25}CDCl3
f2 (ppm)
f1 (ppm)

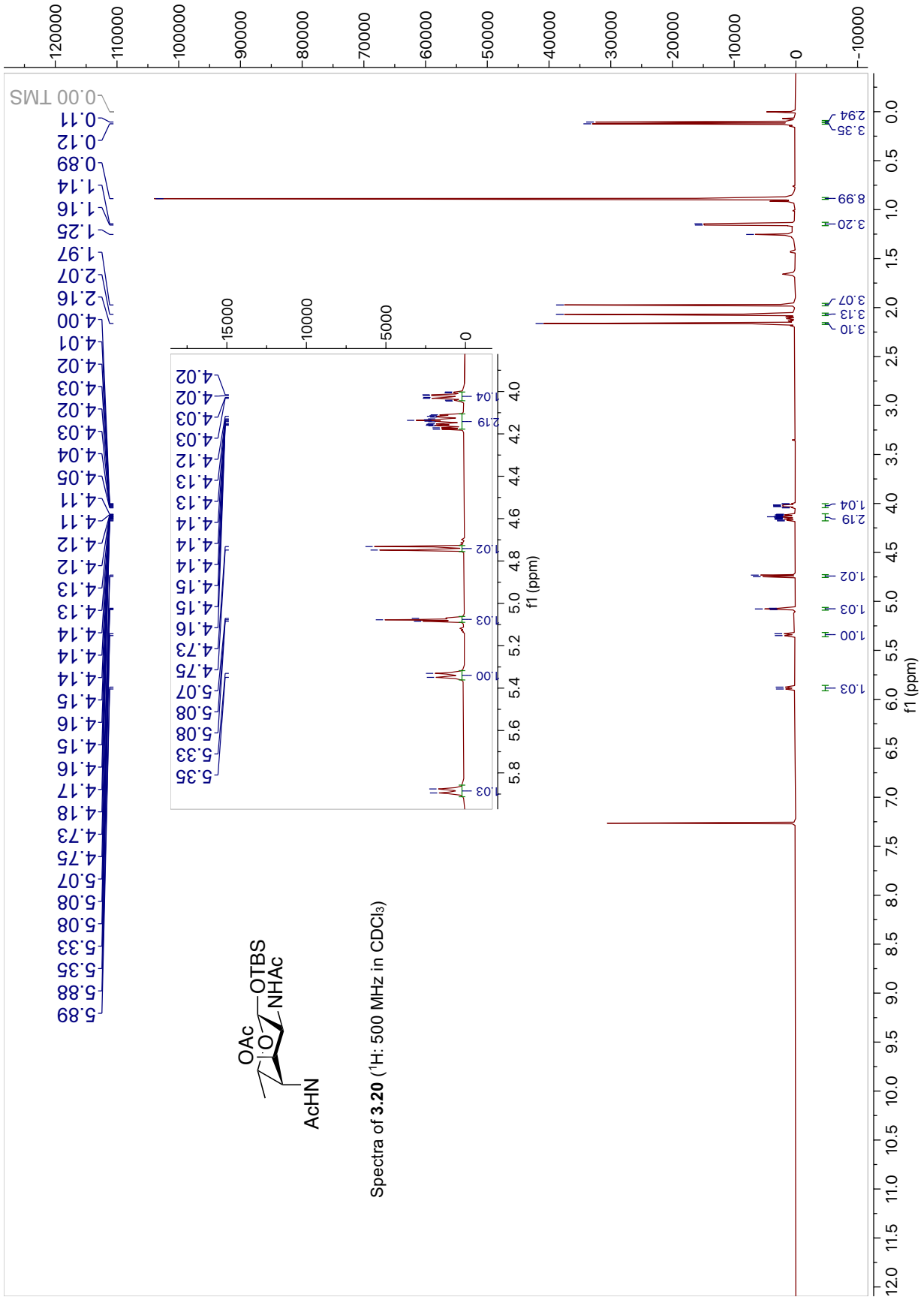
Spectra of 3.20 (1H: 500 MHz in CDCl3)
OAc
OTBS
NHAc
AcHN
f1 (ppm)

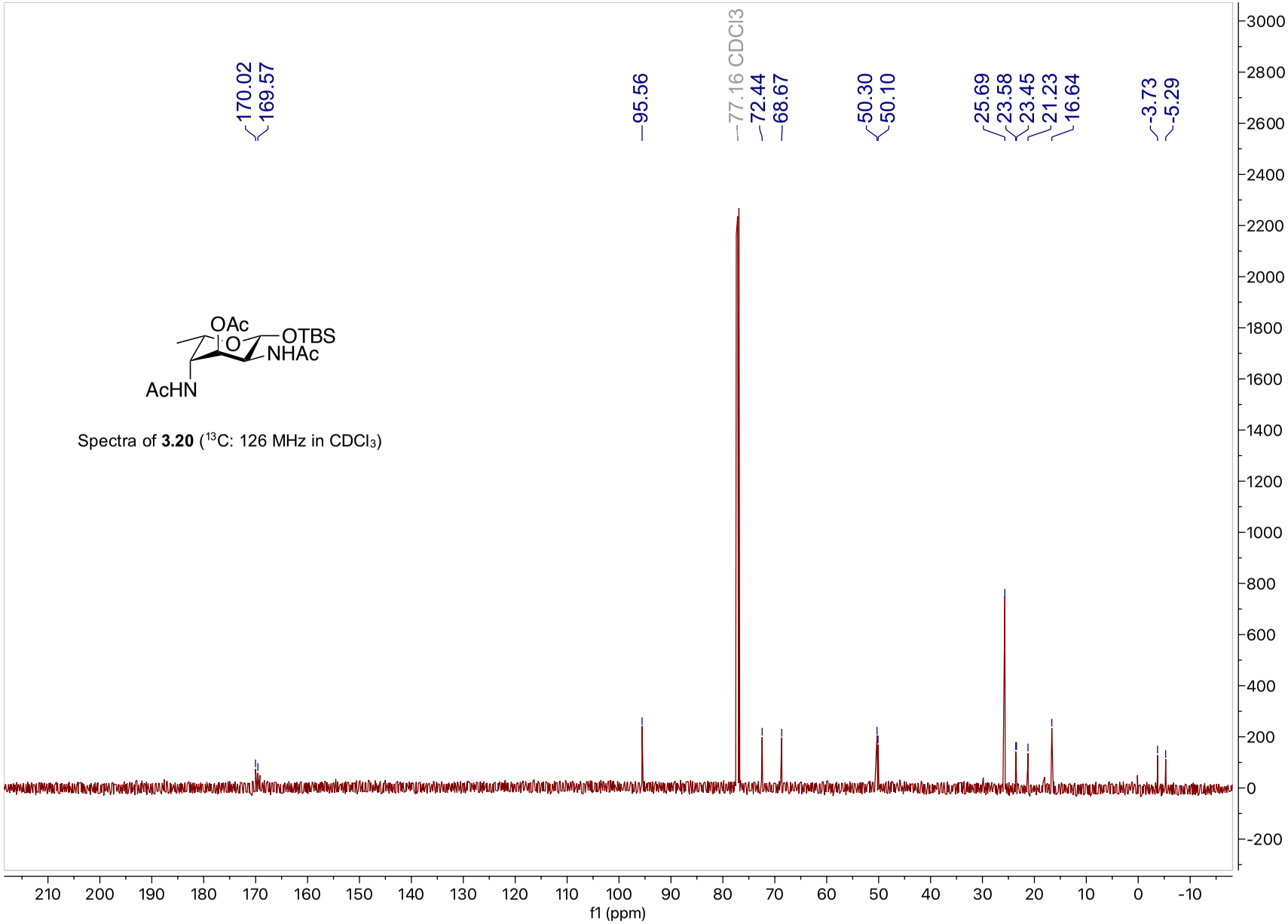


Spectra of **3.20** ($^{13}C$: 126 MHz in $CDCl_3$)

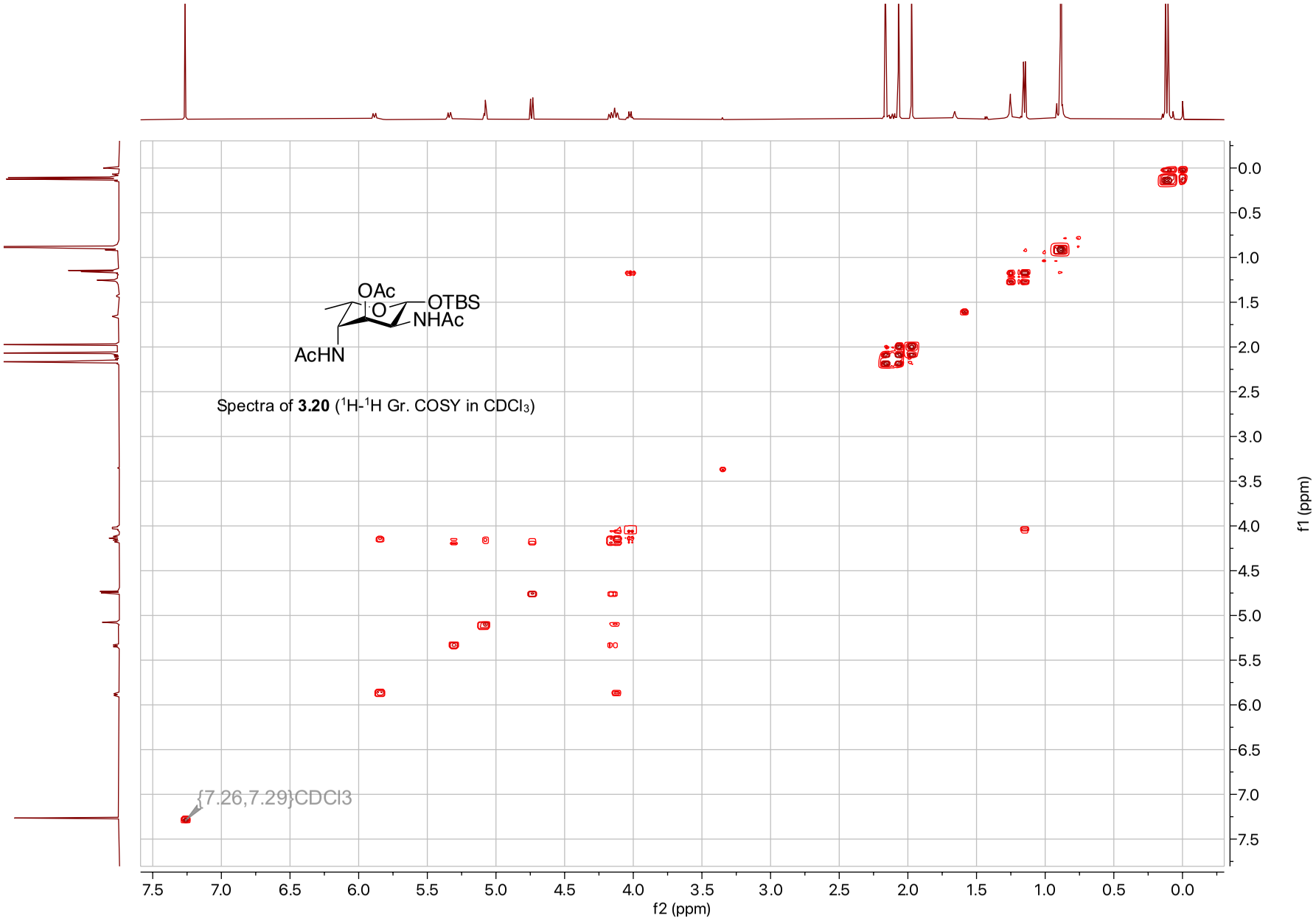
OAc
OTBS
NHAc
AcHN
Spectra of **3.20** ($^1$H-$^1$H Gr. COSY in $CDCl_3$)
{7.26,7.29}CDCl3
f2 (ppm)
f1 (ppm)

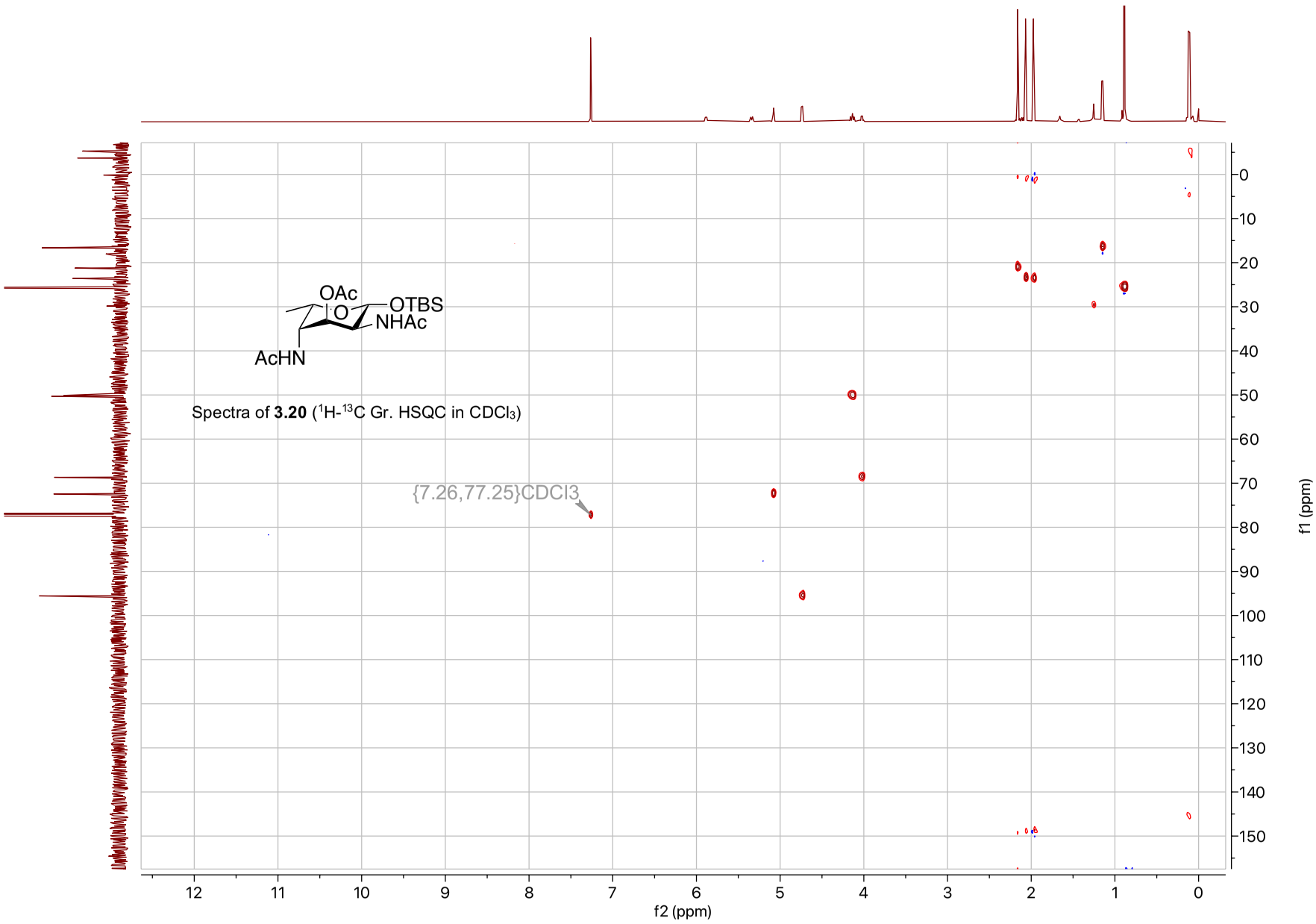
OAc
OTBS
NHAc
AcHN
Spectra of **3.20** ($^{1}$H-$^{13}$C Gr. HSQC in $CDCl_3$)
{7.26,77.25}CDCl3
f2 (ppm)
f1 (ppm)

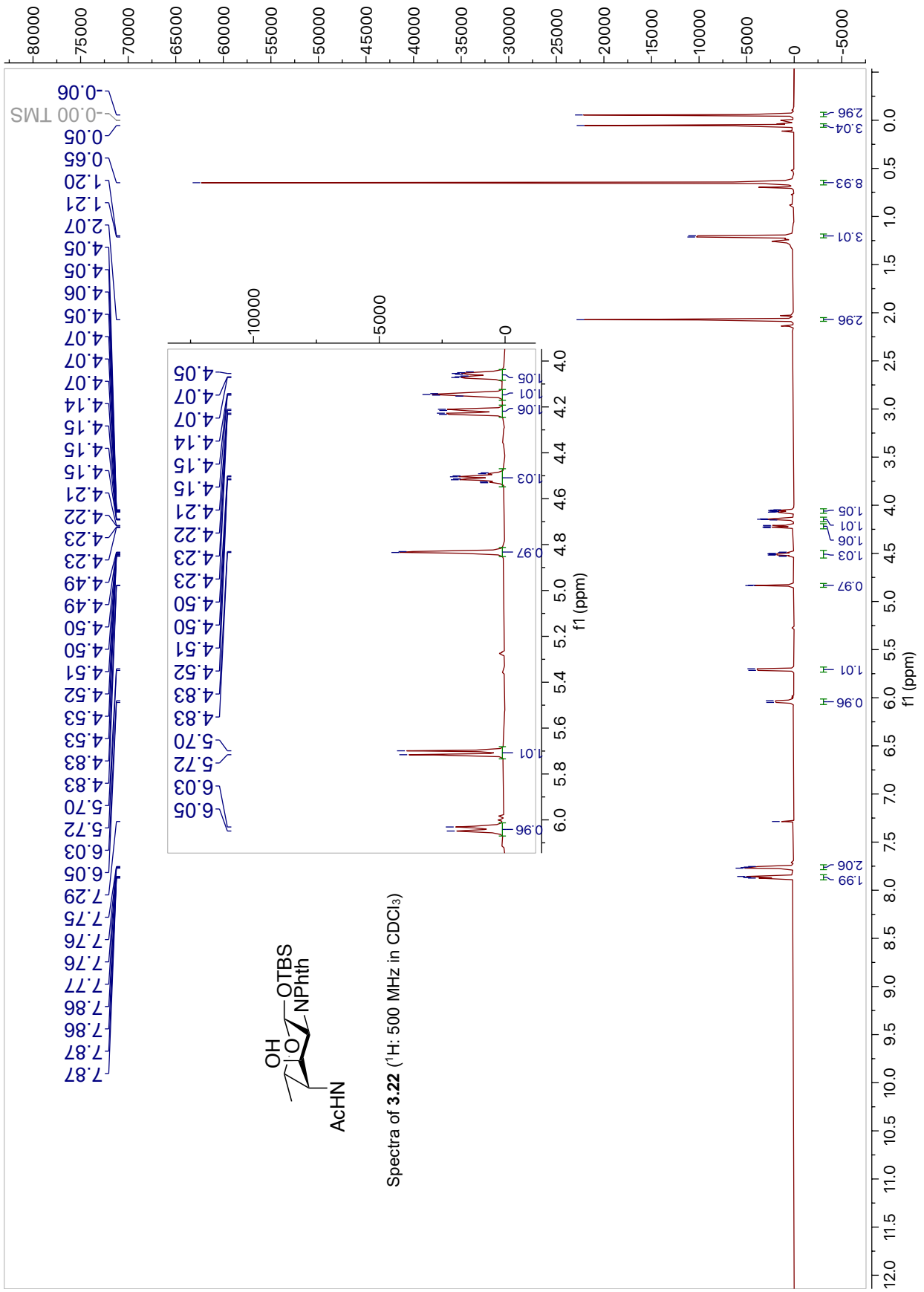
OH
O
OTBS
NPhth
AcHN
Spectra of 3.22 (1H: 500 MHz in CDCl3)
f1 (ppm)

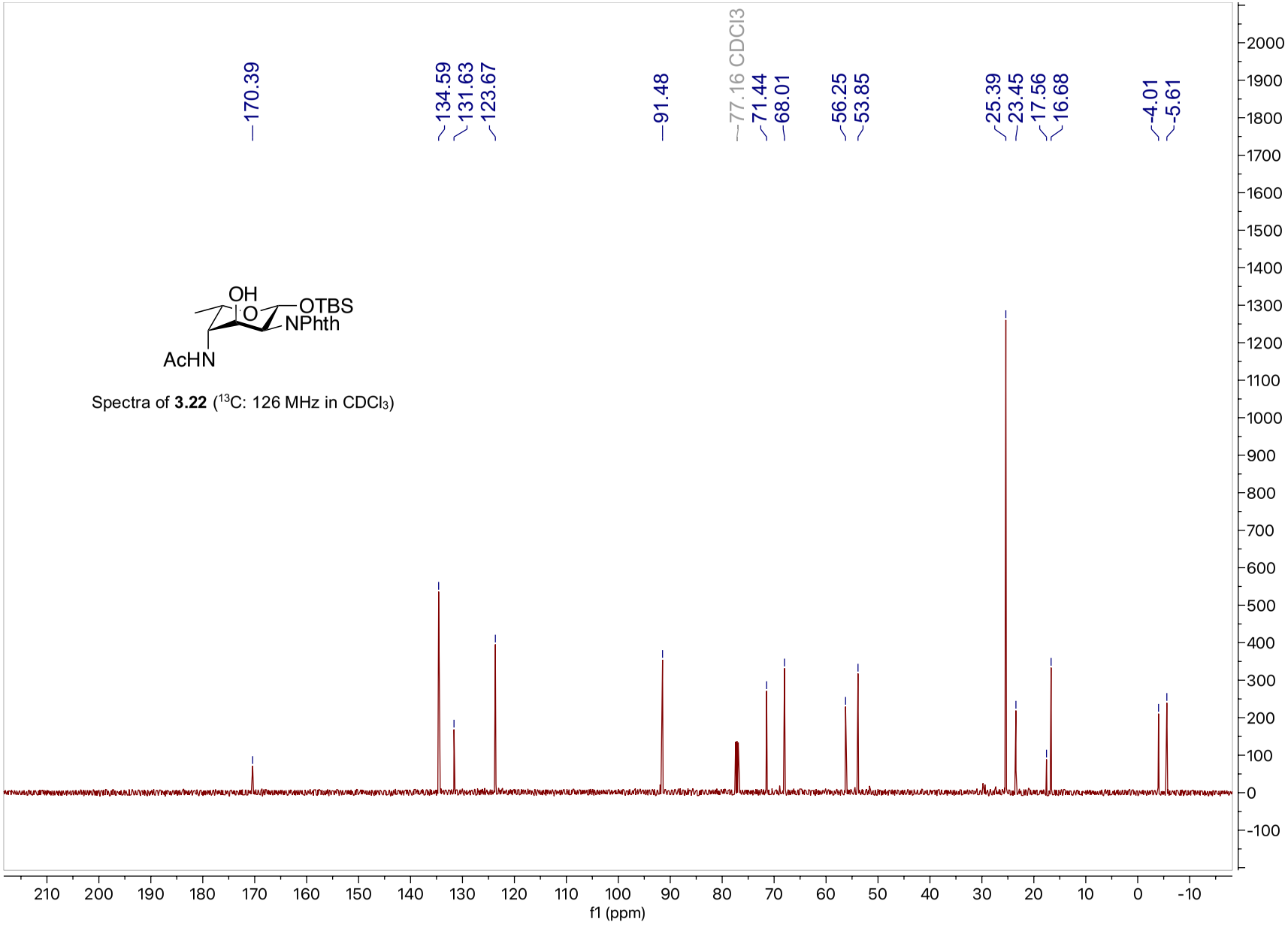


Spectra of **3.22** ($^{13}C$: 126 MHz in $CDCl_3$)

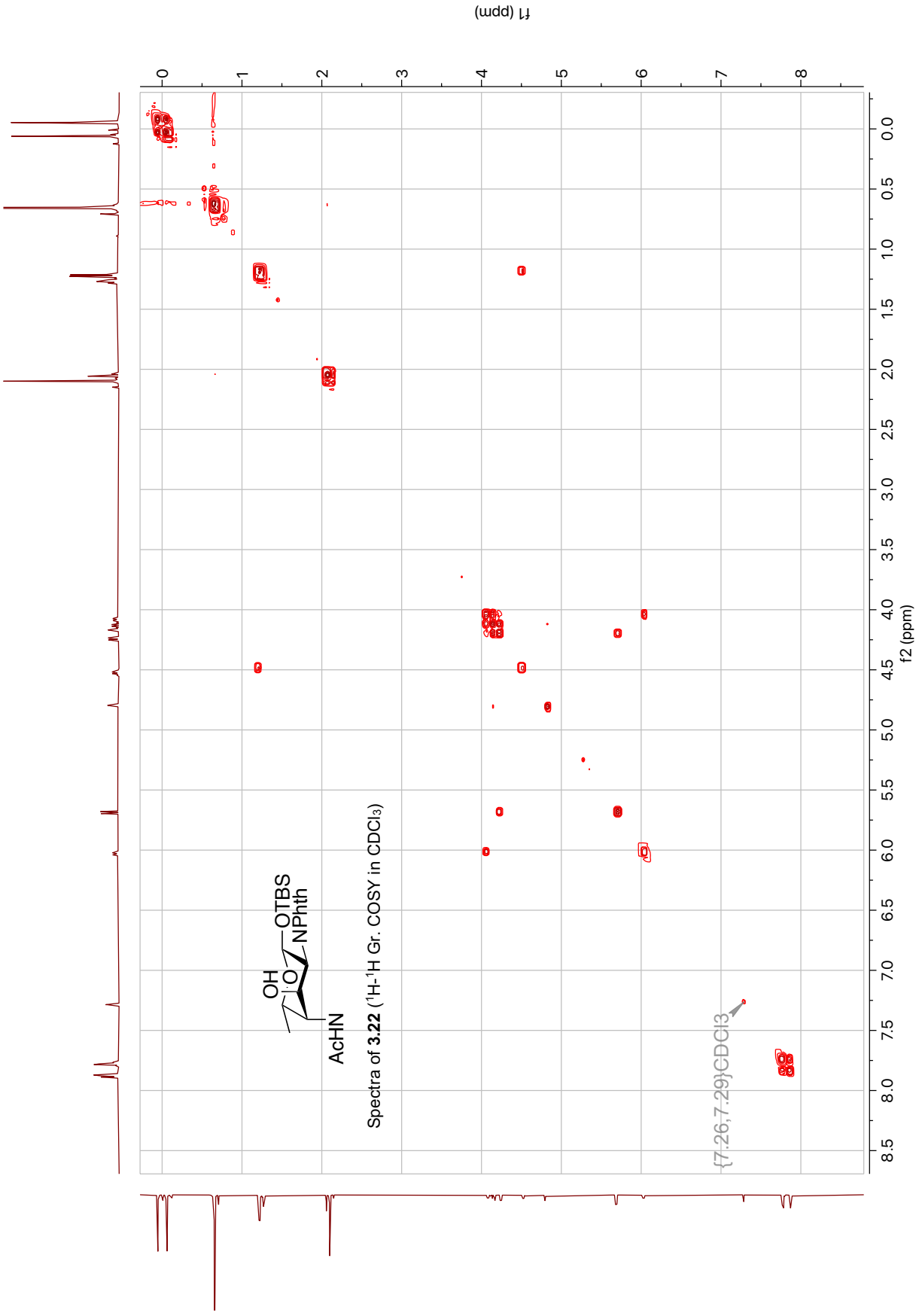
f1 (ppm)
f2 (ppm)
Spectra of 3.22 (1H-1H Gr. COSY in CDCl3)
OH
O
OTBS
NPhth
AcHN
{7.26,7.29}CDCl3

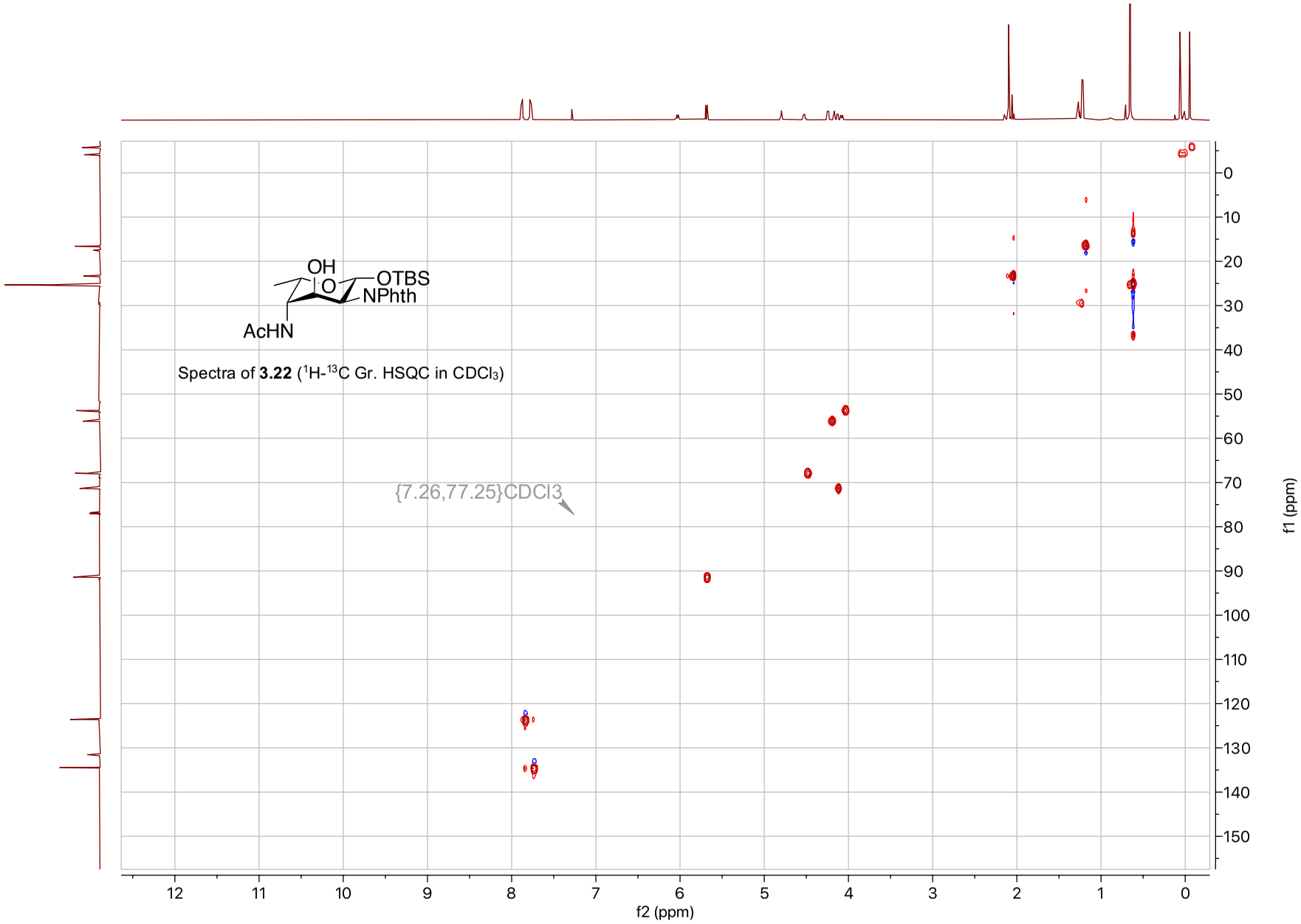
OH
O
OTBS
NPhth
AcHN
Spectra of 3.22 (1H-13C Gr. HSQC in CDCl3)
{7.26,77.25}CDCl3
f2 (ppm)
f1 (ppm)

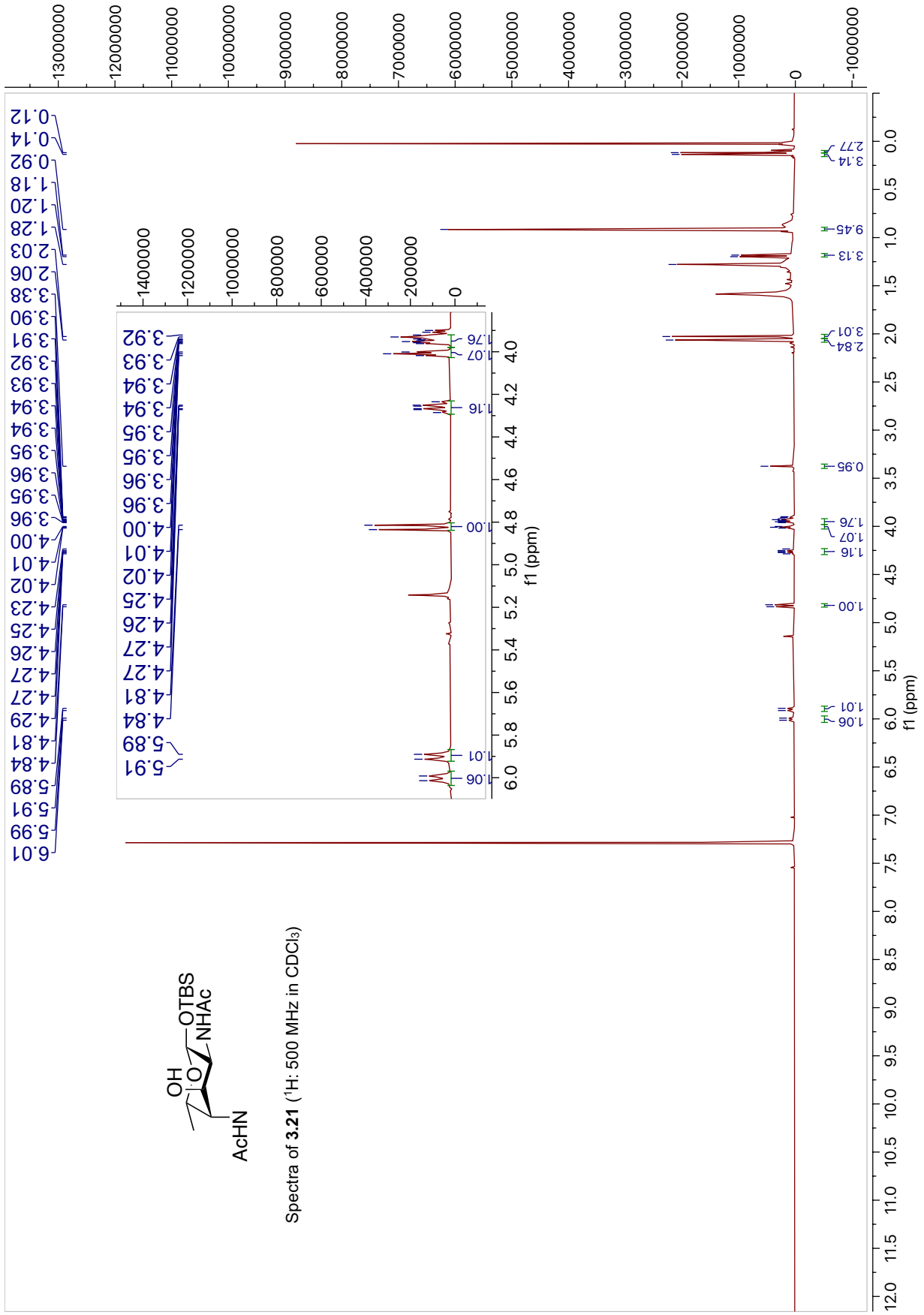
OH
OTBS
NHAc
AcHN
Spectra of **3.21** ($^1$H: 500 MHz in $CDCl_3$)
f1 (ppm)

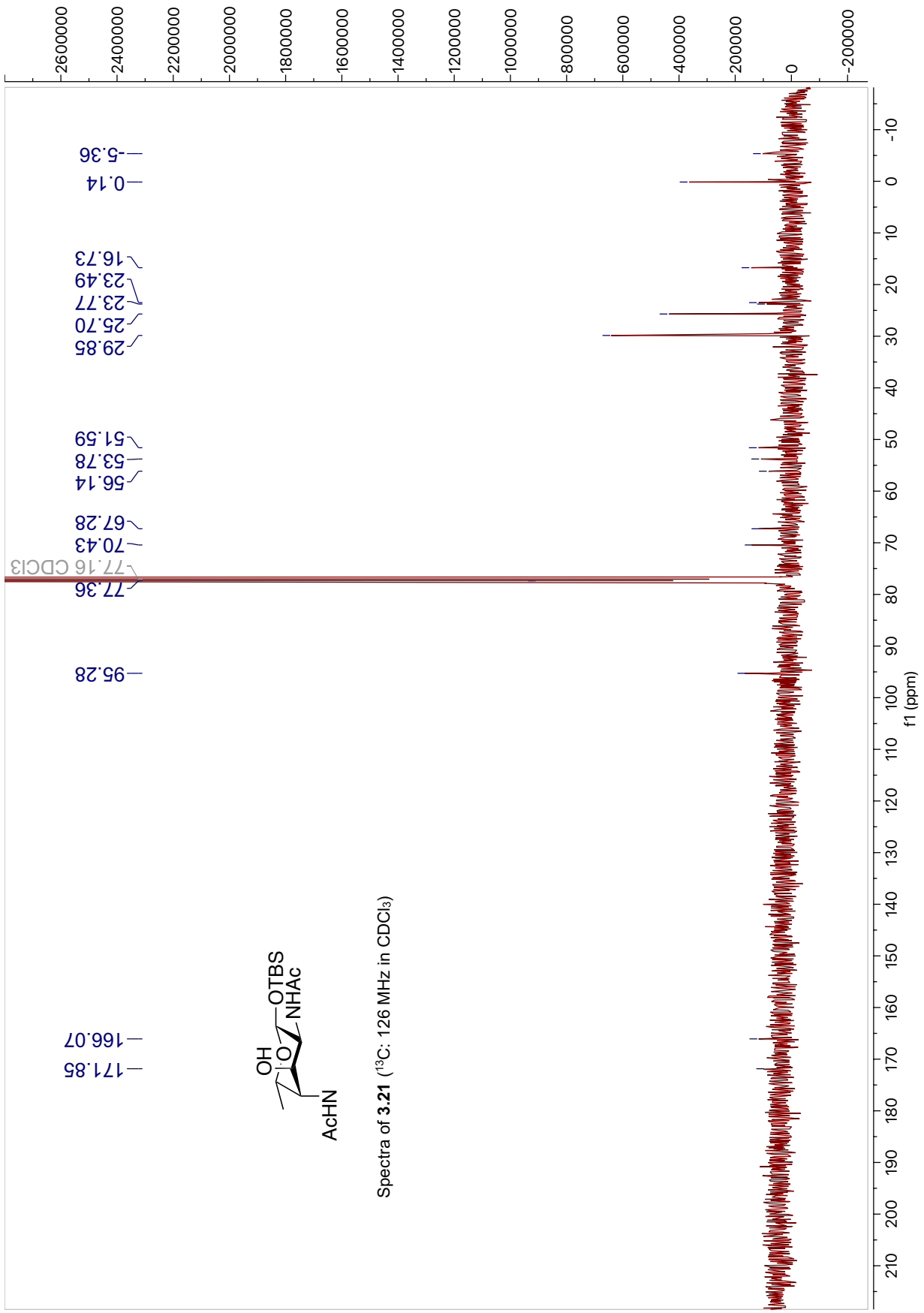
Spectra of 3.21 (13C: 126 MHz in CDCl3)
OH
O
OTBS
NHAc
AcHN
171.85
166.07
95.28
77.36
77.16 CDCl3
70.43
67.28
56.14
53.78
51.59
29.85
25.70
23.77
23.49
16.73
0.14
-5.36
f1 (ppm)


OH
O
OTBS
NHAc
AcHN
Spectra of 3.21 (1H-1H Gr. COSY in CDCl3)
{7.26,7.29}CDCl3
f2 (ppm)
f1 (ppm)

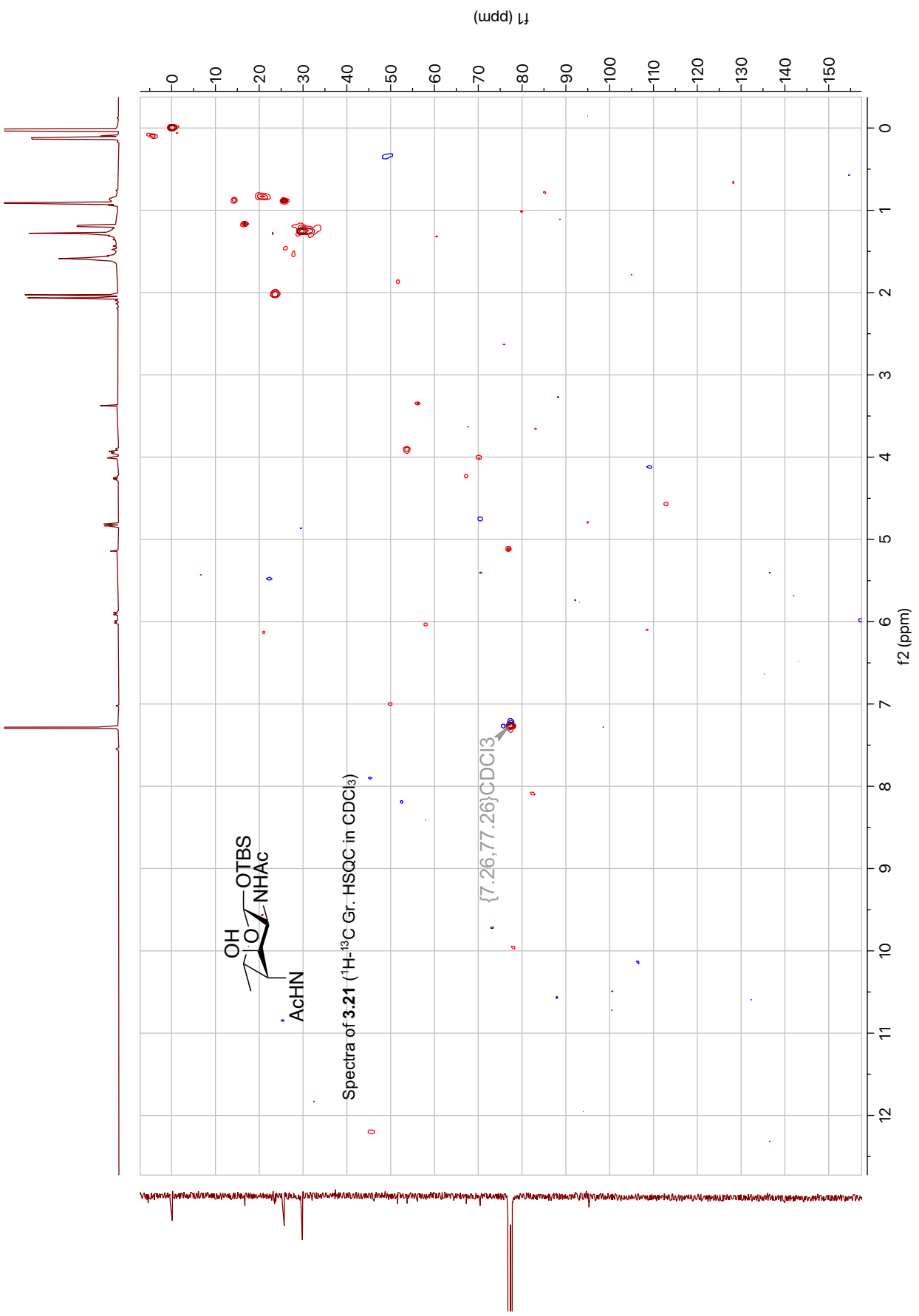
Spectra of 3.21 ($^{1}$H-$^{13}$C Gr. HSQC in $CDCl_3$)
{7.26,77.26}CDCl3
OH
O
OTBS
NHAc
AcHN
f2 (ppm)
f1 (ppm)

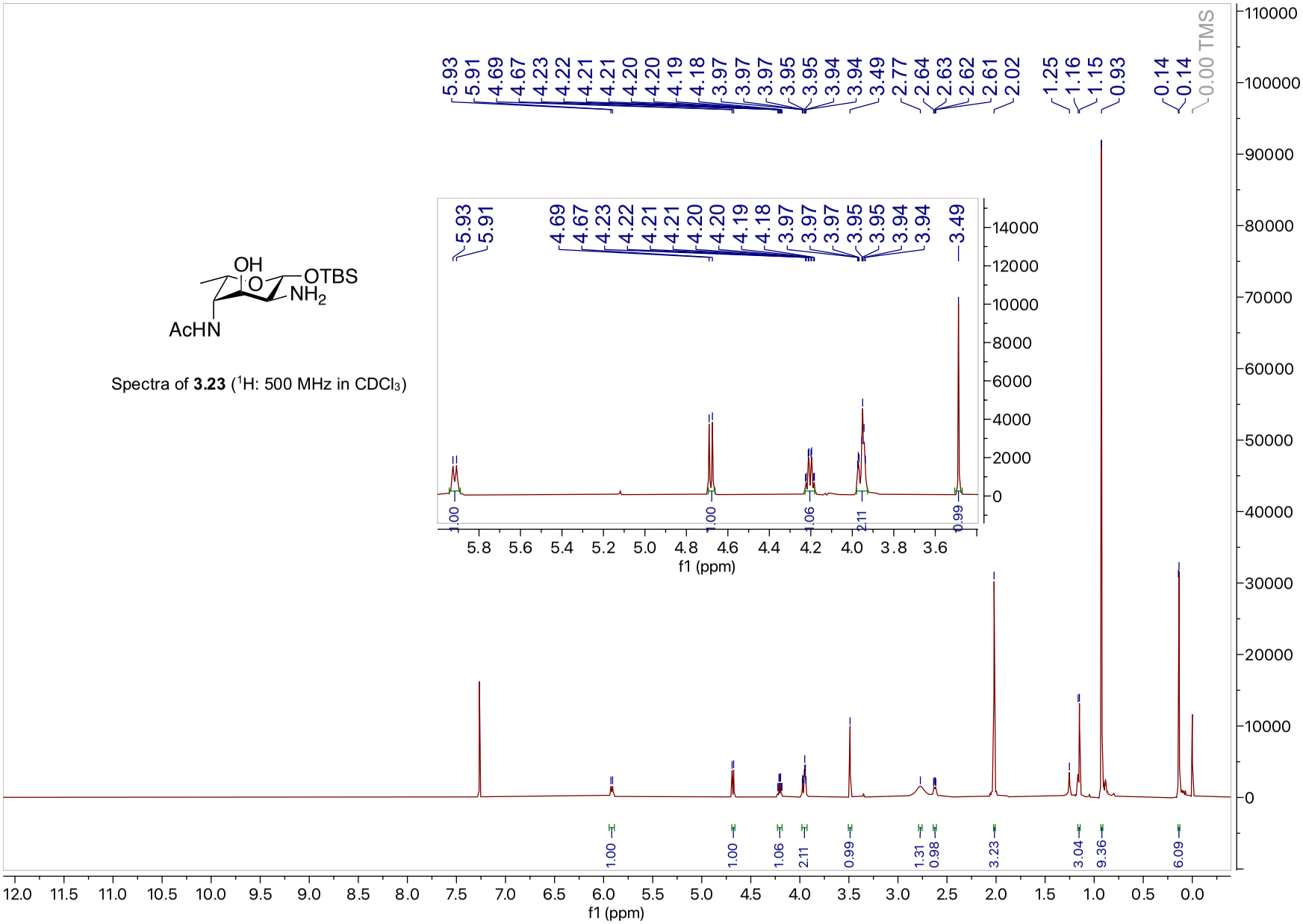
OH
OTBS
O
NH2
AcHN
Spectra of 3.23 (1H: 500 MHz in CDCl3)
5.93
5.91
4.69
4.67
4.23
4.22
4.21
4.21
4.20
4.20
4.19
4.18
3.97
3.97
3.97
3.95
3.95
3.94
3.94
3.49
2.77
2.64
2.63
2.62
2.61
2.02
1.25
1.16
1.15
0.93
0.14
0.14
0.00 TMS
f1 (ppm)
1.00
1.00
1.06
2.11
0.99
1.31
0.98
3.23
3.04
9.36
6.09

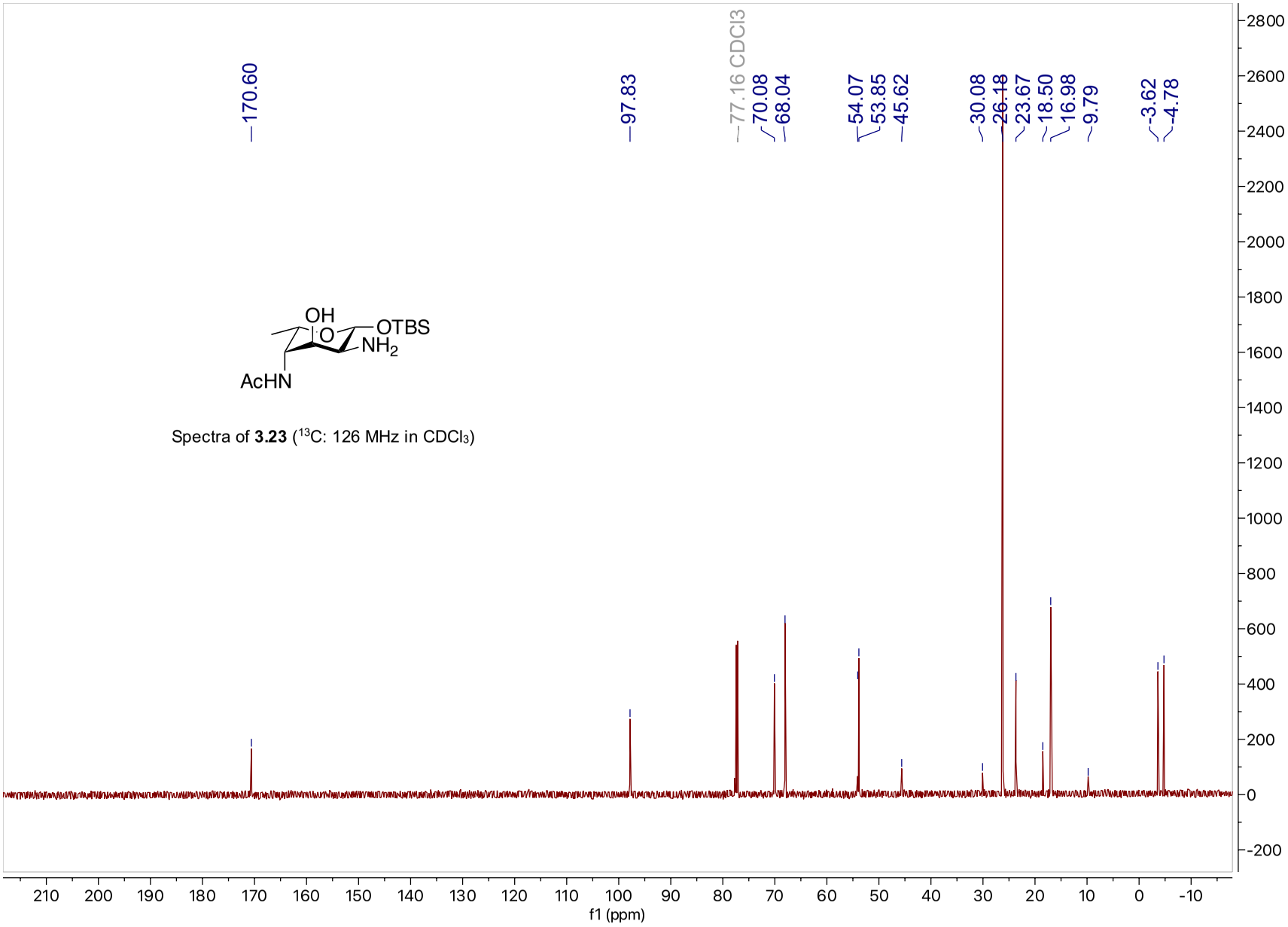


Spectra of **3.23** ($^{13}C$: 126 MHz in $CDCl_3$)

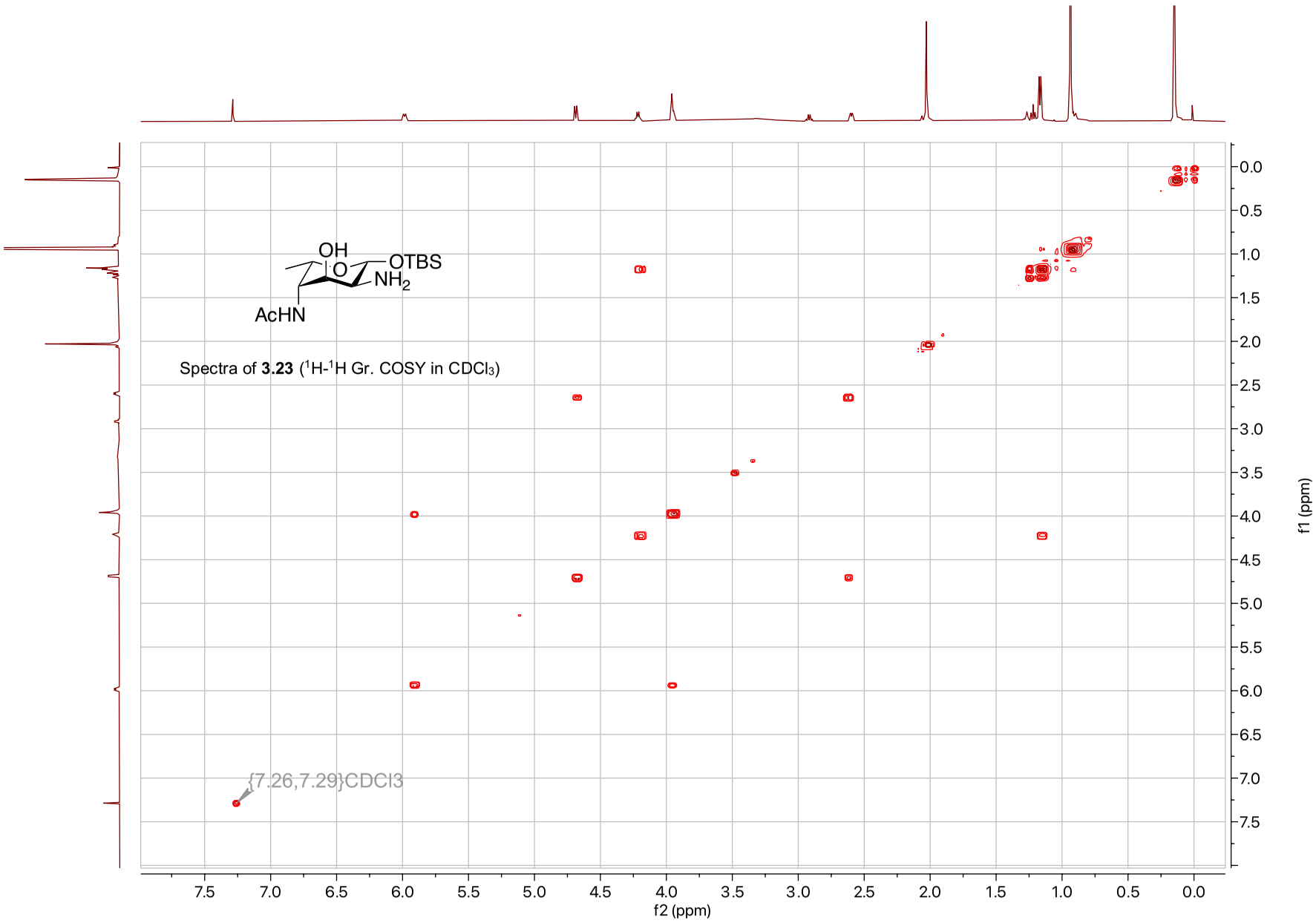
OH
O
OTBS
NH2
AcHN
Spectra of 3.23 (1H-1H Gr. COSY in CDCl3)
{7.26,7.29}CDCl3
f2 (ppm)
f1 (ppm)

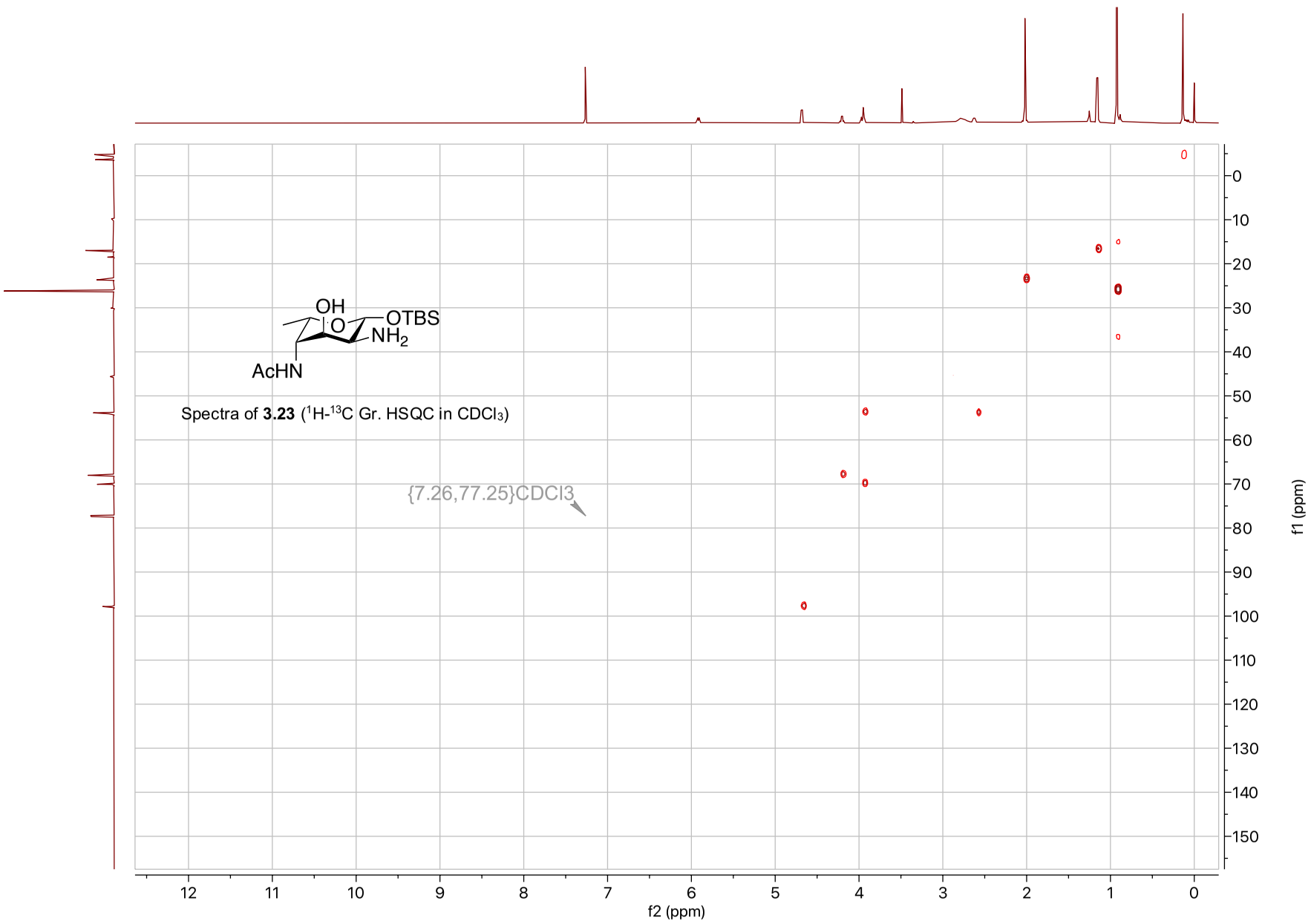
OH
O
OTBS
NH2
AcHN
Spectra of 3.23 (1H-13C Gr. HSQC in CDCl3)
{7.26,77.25}CDCl3
f2 (ppm)
f1 (ppm)

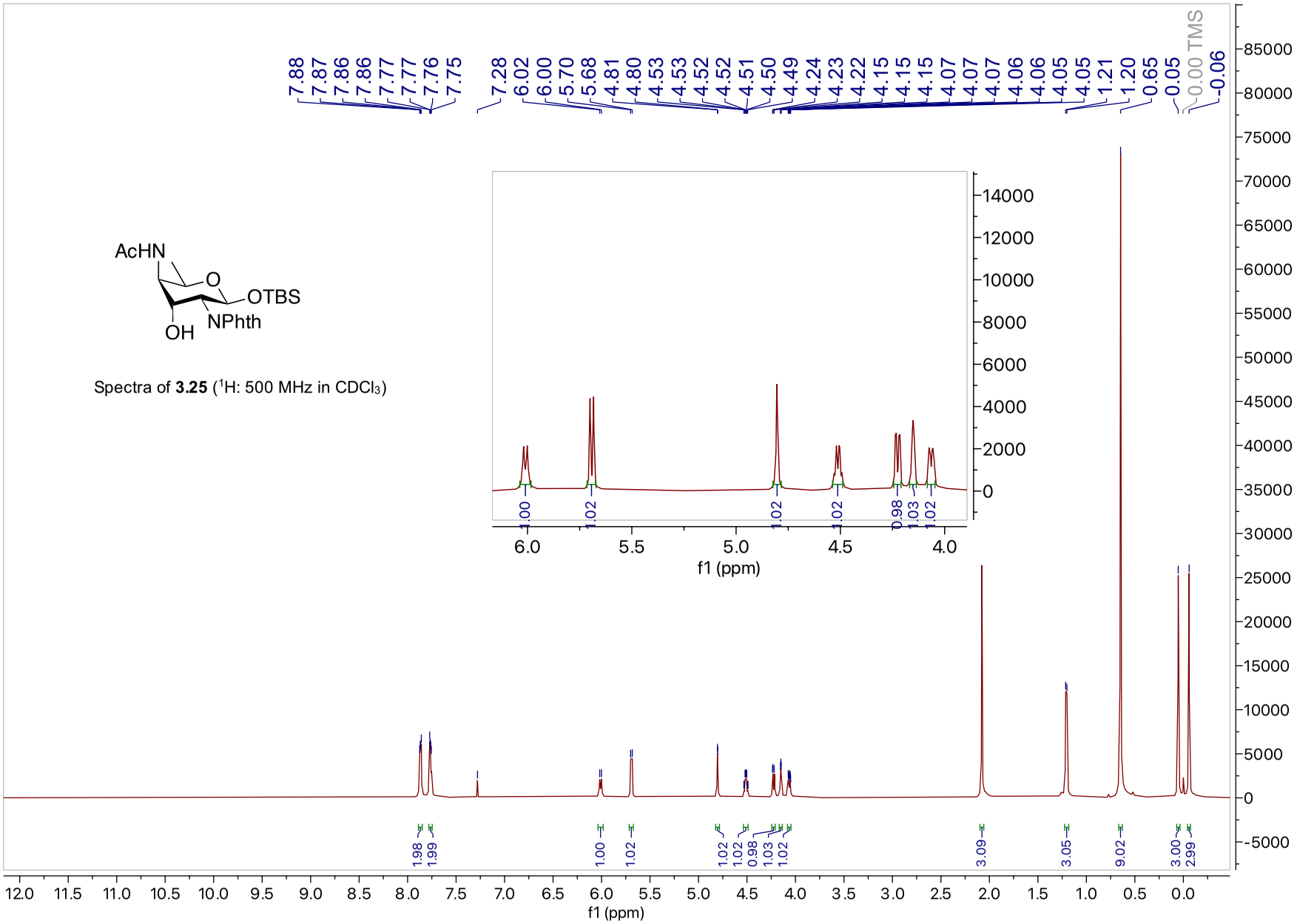
AcHN
O
OTBS
NPhth
OH
Spectra of **3.25** ($^1$H: 500 MHz in $CDCl_3$)
7.88 7.87 7.86 7.86 7.77 7.77 7.76 7.75 7.28 6.02 6.00 5.70 5.68 4.81 4.80 4.53 4.53 4.52 4.52 4.51 4.50 4.49 4.24 4.23 4.22 4.15 4.15 4.15 4.07 4.07 4.07 4.06 4.06 4.05 4.05 1.21 1.20 0.65 0.05 0.00 TMS -0.06
1.98 1.99 1.00 1.02 1.02 1.02 0.98 1.03 1.02 3.09 3.05 9.02 3.00 2.99
f1 (ppm)
1.00 1.02 1.02 1.02 0.98 1.03 1.02
f1 (ppm)

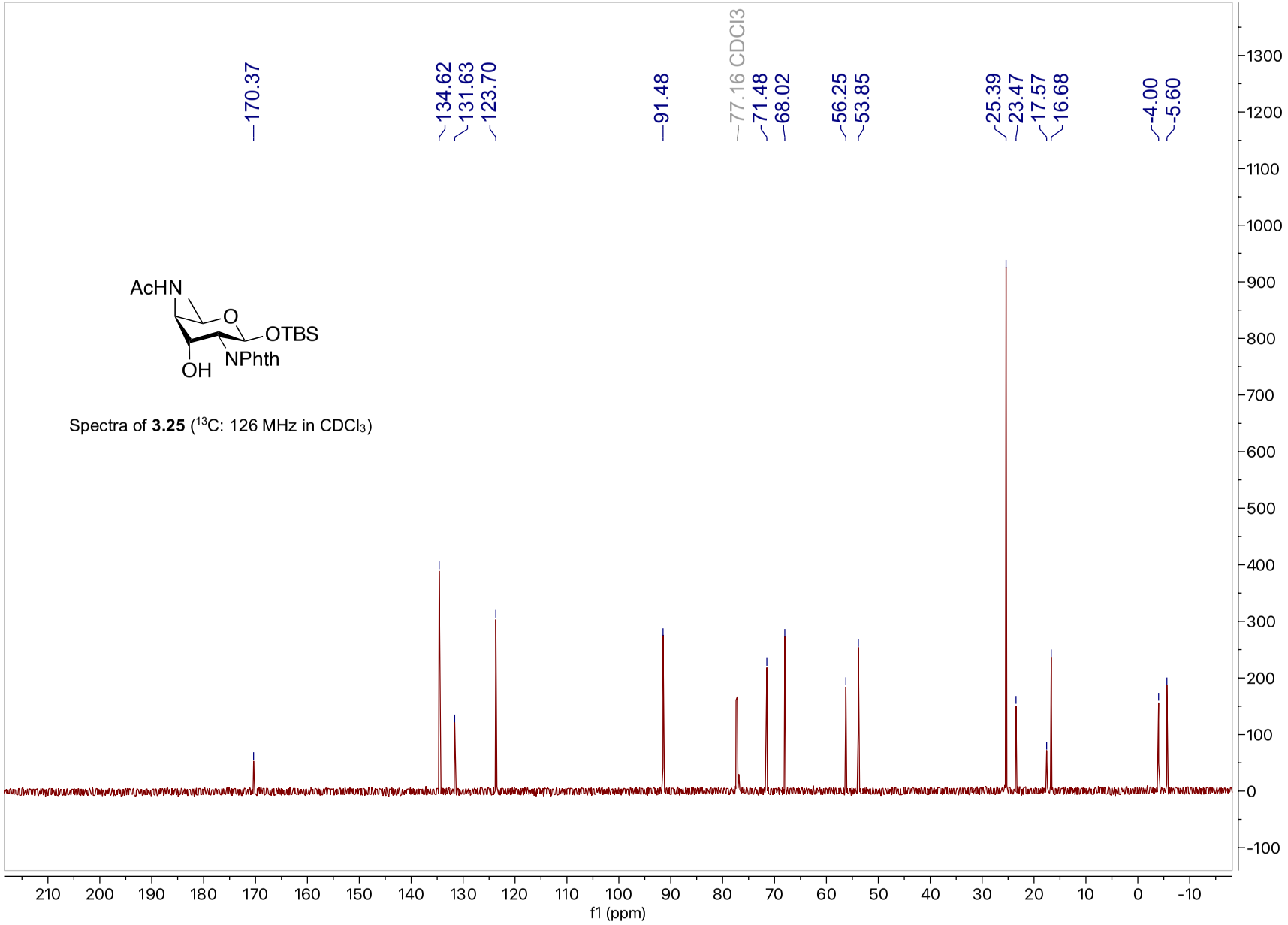


Spectra of **3.25** ($^{13}C$: 126 MHz in $CDCl_3$)

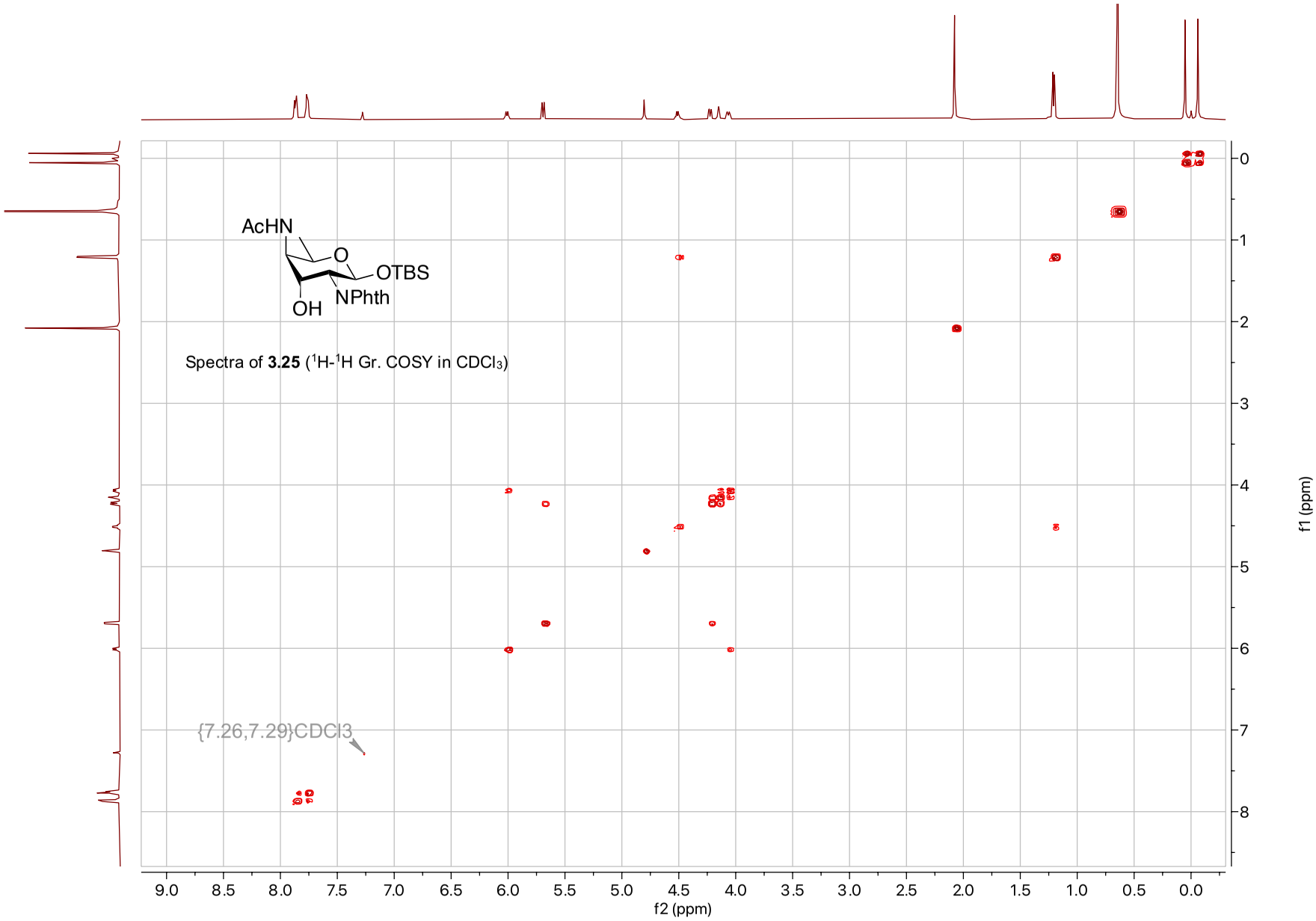
AcHN
O
OTBS
NPhth
OH
Spectra of 3.25 (1H-1H Gr. COSY in CDCl3)
{7.26,7.29}CDCl3
f2 (ppm)
f1 (ppm)

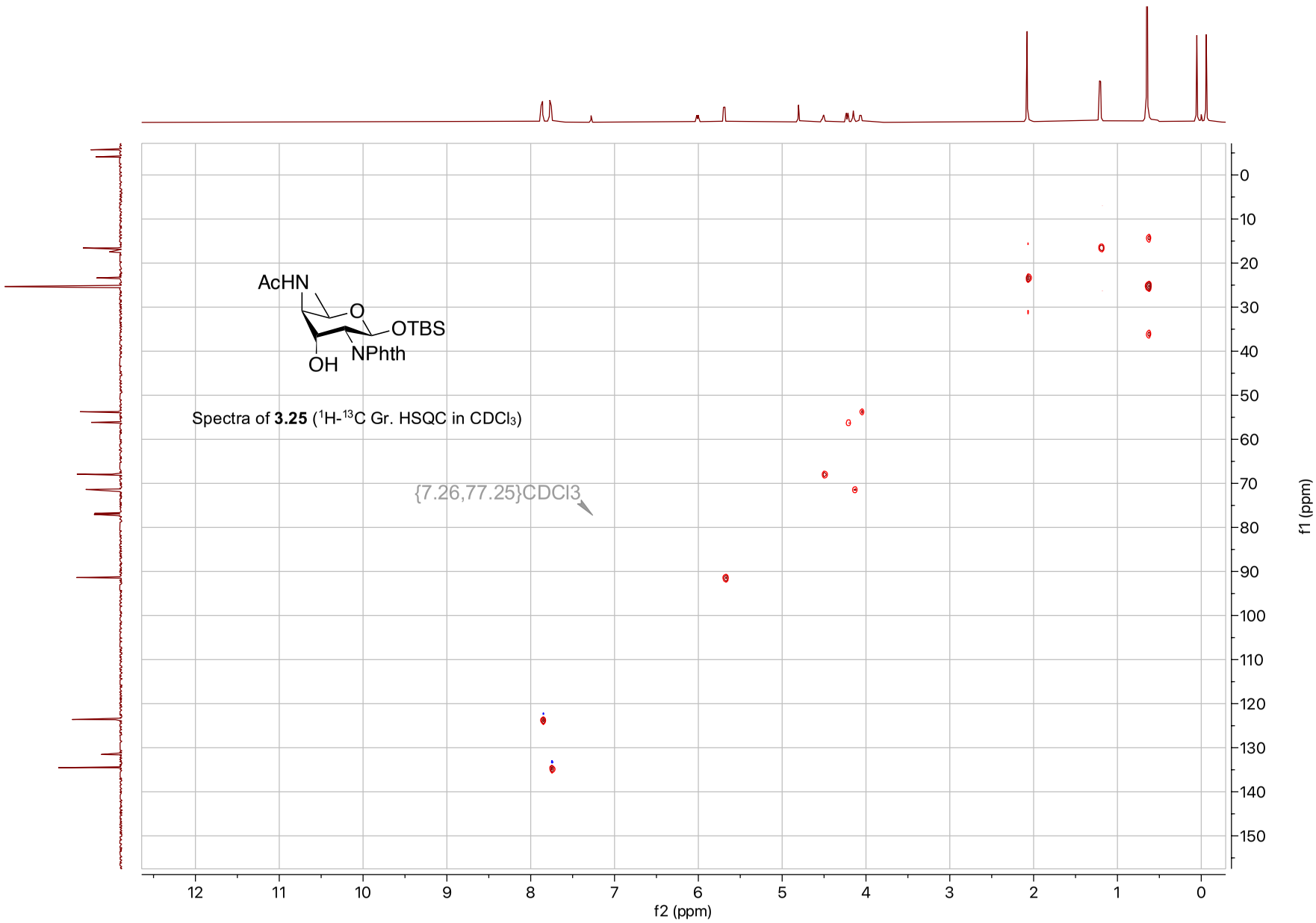
AcHN
O
OTBS
NPhth
OH
Spectra of **3.25** ($^{1}$H-$^{13}$C Gr. HSQC in $CDCl_3$)
{7.26,77.25}CDCl3
f2 (ppm)
f1 (ppm)

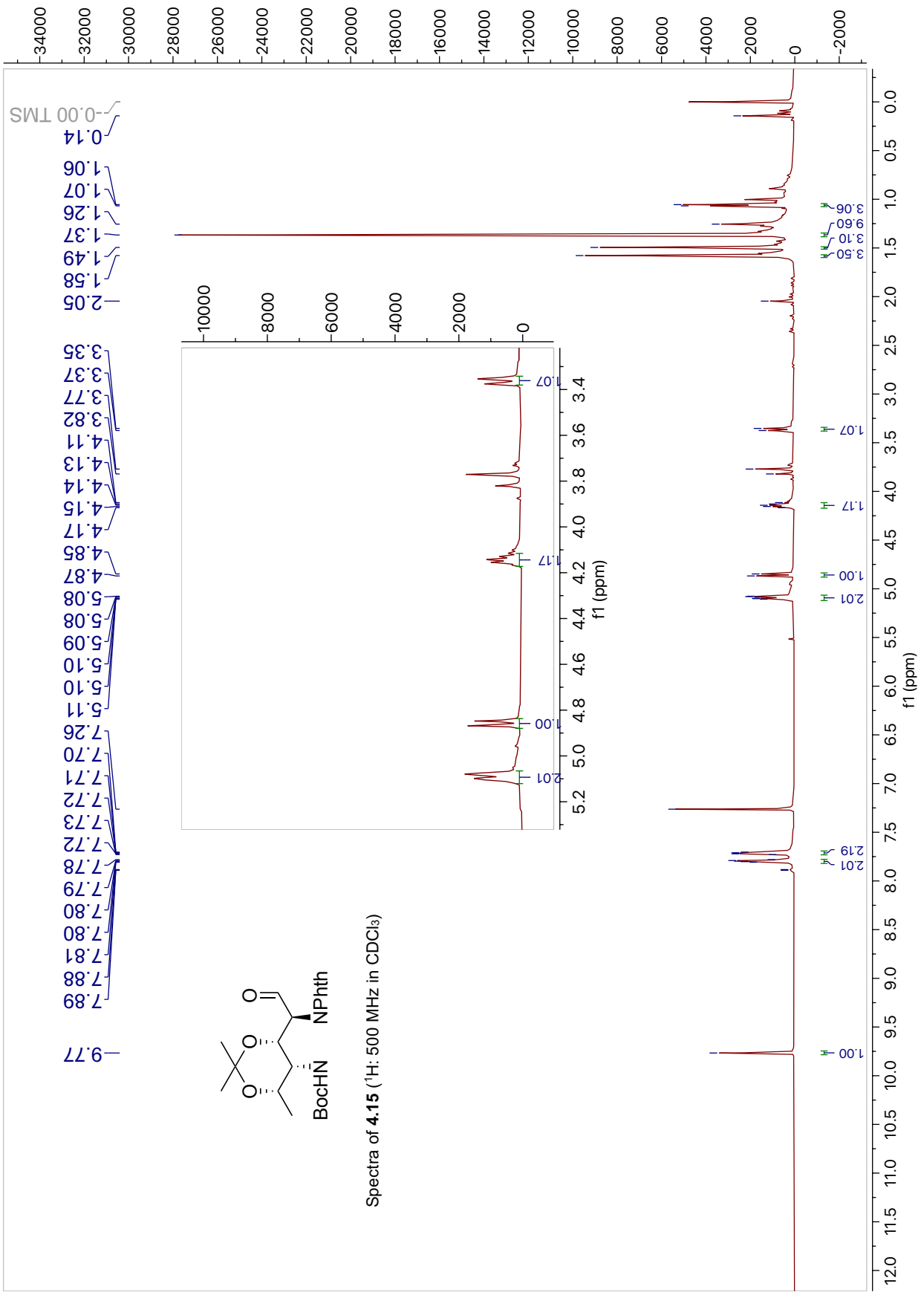
BocHN
NPhth
Spectra of 4.15 (1H: 500 MHz in CDCl3)
f1 (ppm)
TMS
0.14
1.06
1.07
1.26
1.37
1.49
1.58
2.05
3.35
3.37
3.77
3.82
4.11
4.13
4.14
4.15
4.17
4.85
4.87
5.08
5.08
5.09
5.10
5.10
5.11
7.26
7.70
7.71
7.72
7.73
7.72
7.78
7.79
7.80
7.80
7.81
7.88
7.89
9.77
3.50
9.60
3.10
3.06
1.07
1.17
1.00
2.01
2.19
2.01
1.00

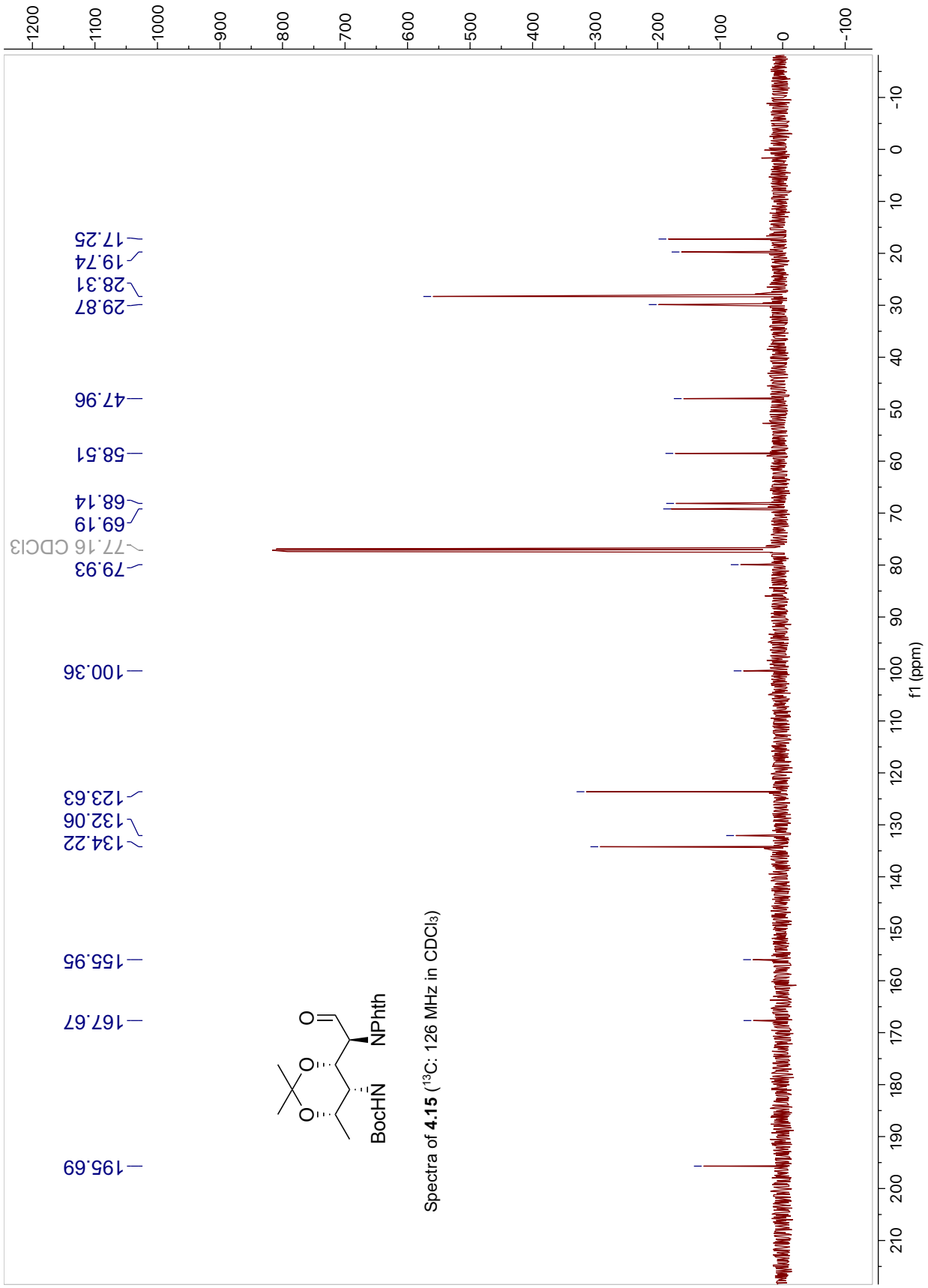
Spectra of 4.15 (13C: 126 MHz in CDCl3)
BocHN
NPhth
195.69
167.67
155.95
134.22
132.06
123.63
100.36
79.93
77.16 CDCl3
69.19
68.14
58.51
47.96
29.87
28.31
19.74
17.25
f1 (ppm)

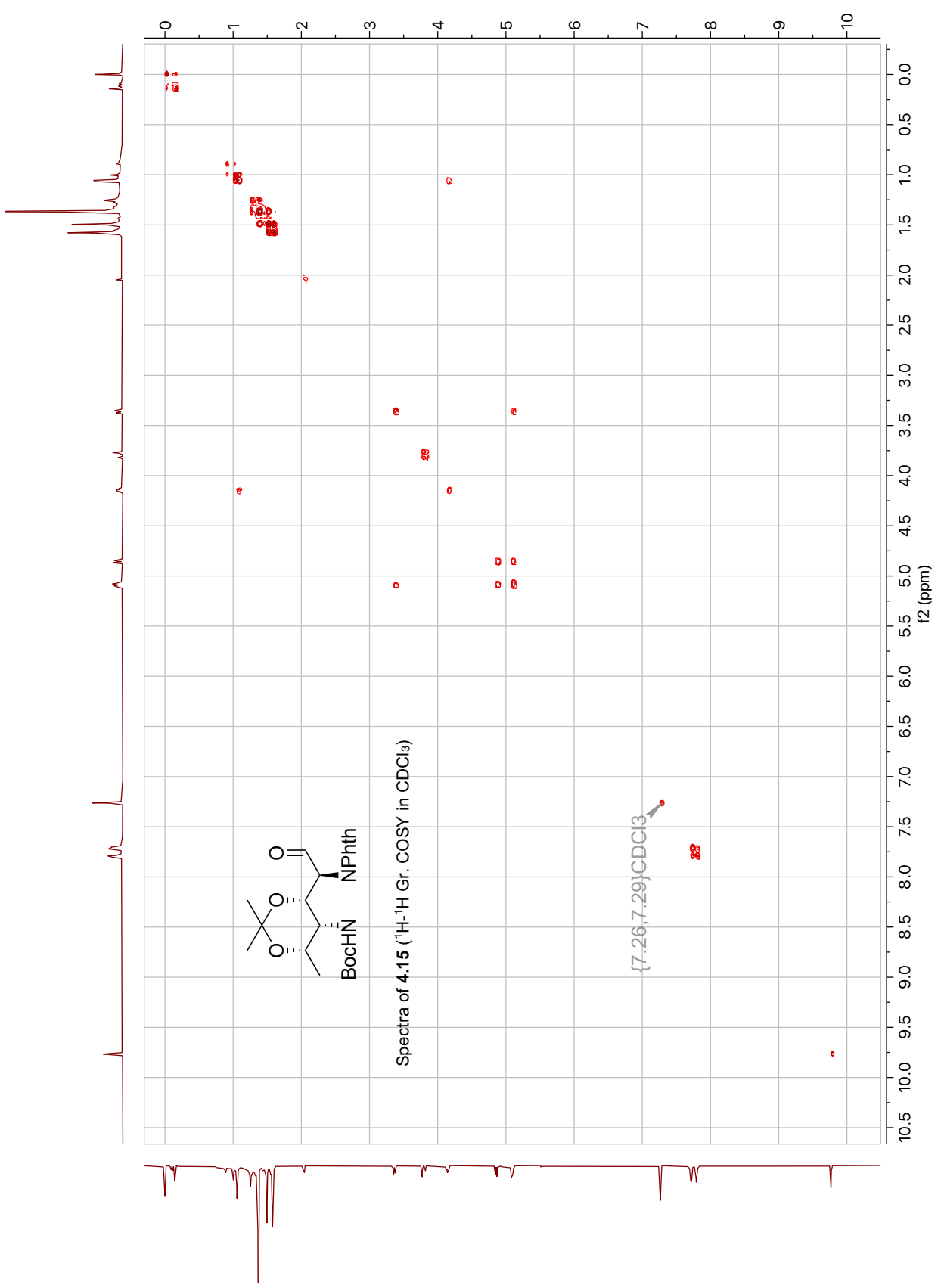
Spectra of 4.15 (1H-1H Gr. COSY in CDCl3)
BocHN
NPhth
{7.26,7.29}CDCl3
f2 (ppm)
f1 (ppm)

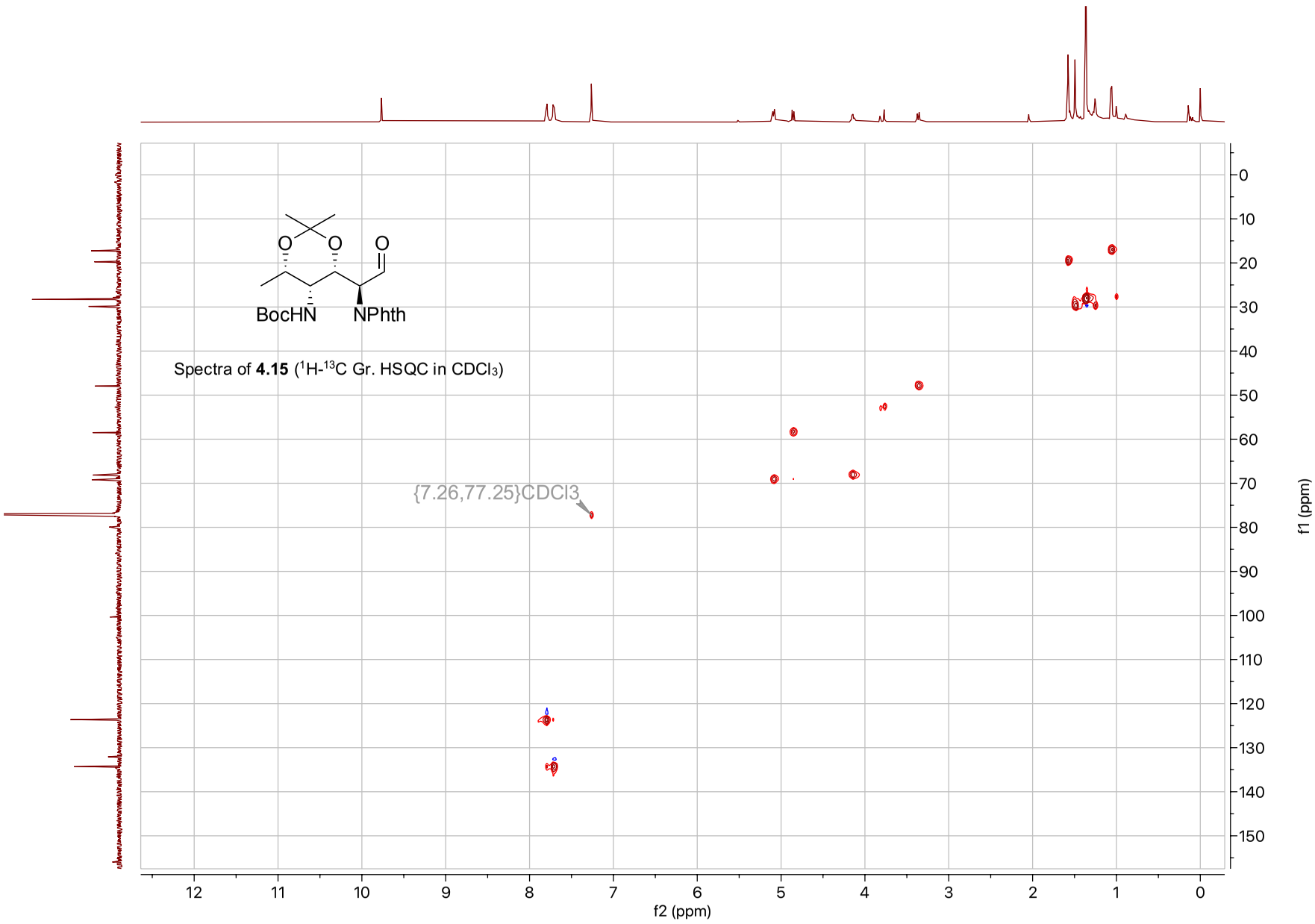
BocHN
NPhth
Spectra of 4.15 (1H-13C Gr. HSQC in CDCl3)
{7.26,77.25}CDCl3
f2 (ppm)
f1 (ppm)

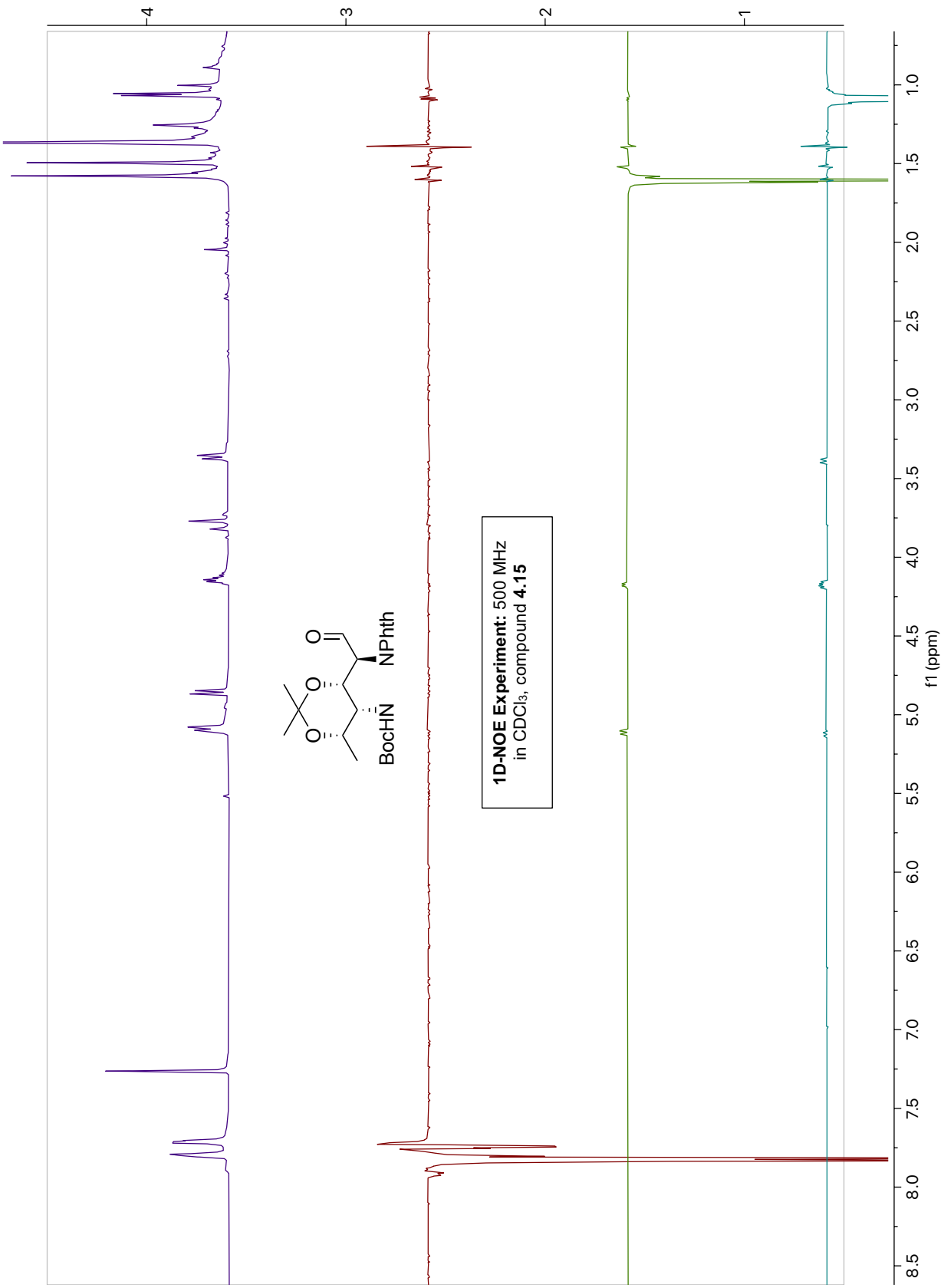
4
3
2
1
BocHN
NPhth
1D-NOE Experiment: 500 MHz
in CDCl3, compound 4.15
8.5
8.0
7.5
7.0
6.5
6.0
5.5
5.0
4.5
4.0
3.5
3.0
2.5
2.0
1.5
1.0
f1 (ppm)

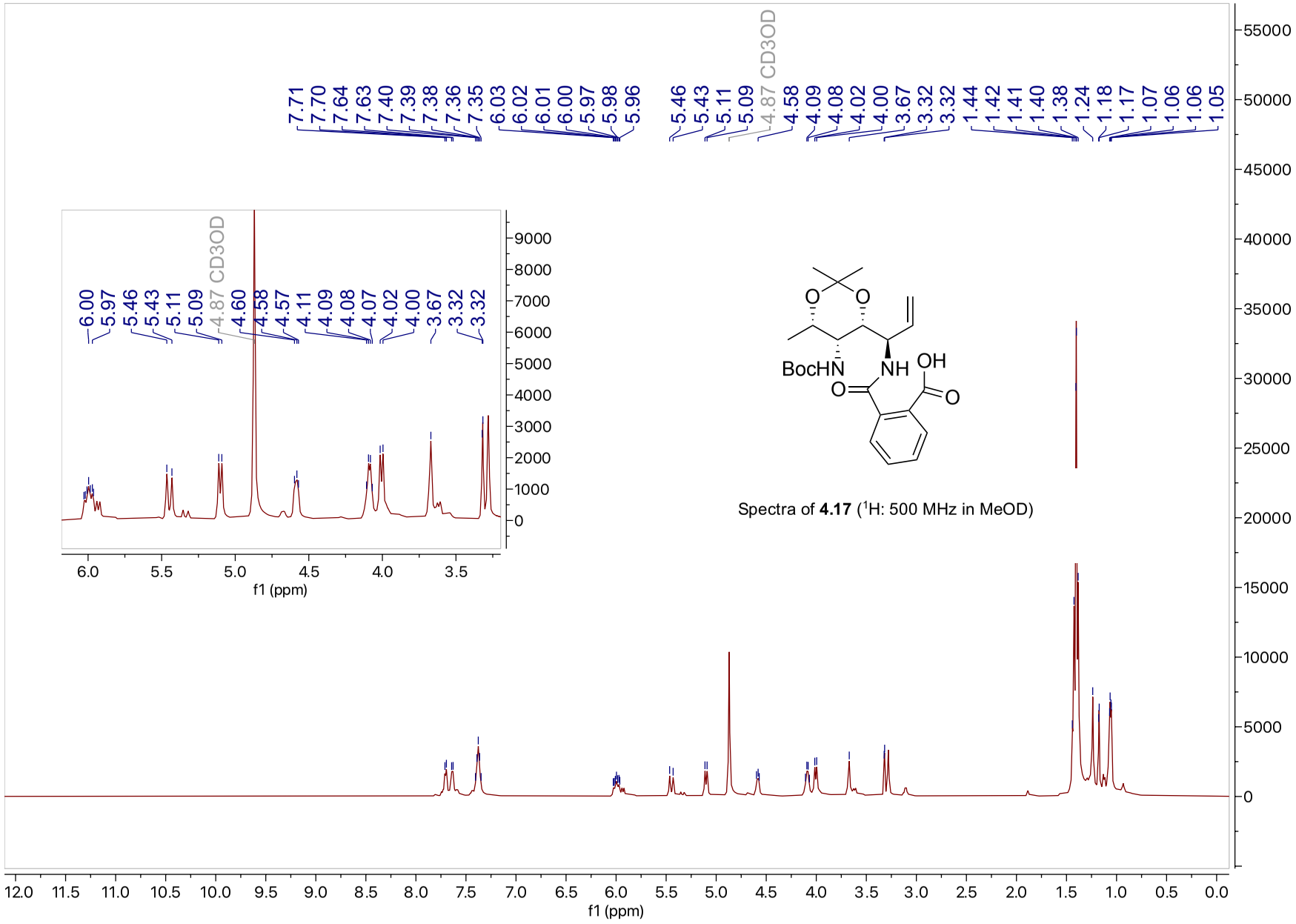
7.71
7.70
7.64
7.63
7.40
7.39
7.38
7.36
7.35
6.03
6.02
6.01
6.00
5.97
5.98
5.96
5.46
5.43
5.11
5.09
4.87 CD3OD
4.58
4.09
4.08
4.02
4.00
3.67
3.32
3.32
1.44
1.42
1.41
1.40
1.38
1.24
1.18
1.17
1.07
1.06
1.06
1.05
BocHN
NH
OH
O
O
O
O
O
Spectra of 4.17 (1H: 500 MHz in MeOD)
f1 (ppm)

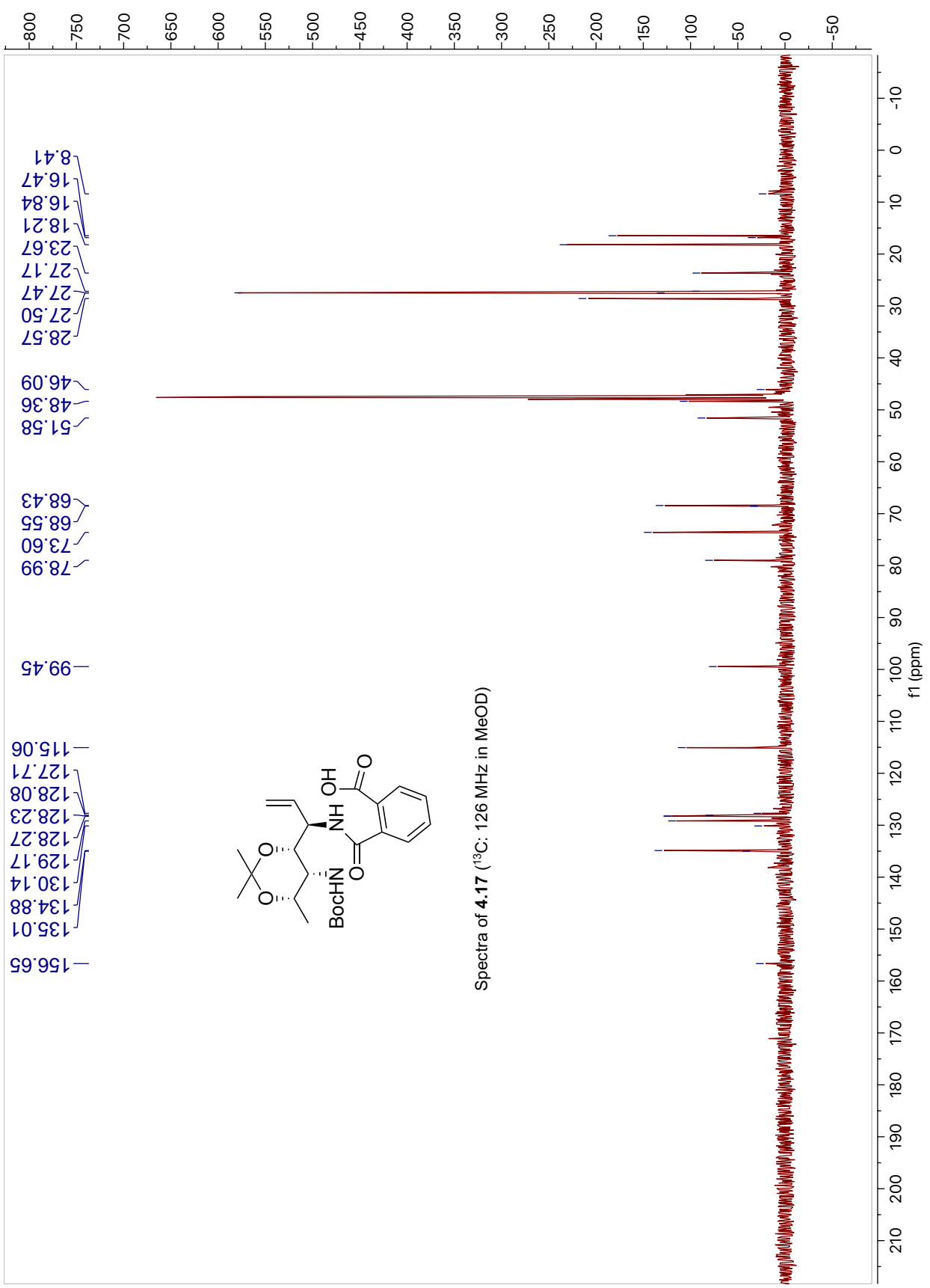
8.41
16.47
16.84
18.21
23.67
27.17
27.47
27.50
28.57
46.09
48.36
51.58
68.43
68.55
73.60
78.99
99.45
115.06
127.71
128.08
128.23
128.27
129.17
130.14
134.88
135.01
156.65
BocHN
NH
OH
O
O
O
O
Spectra of 4.17 (13C: 126 MHz in MeOD)
f1 (ppm)

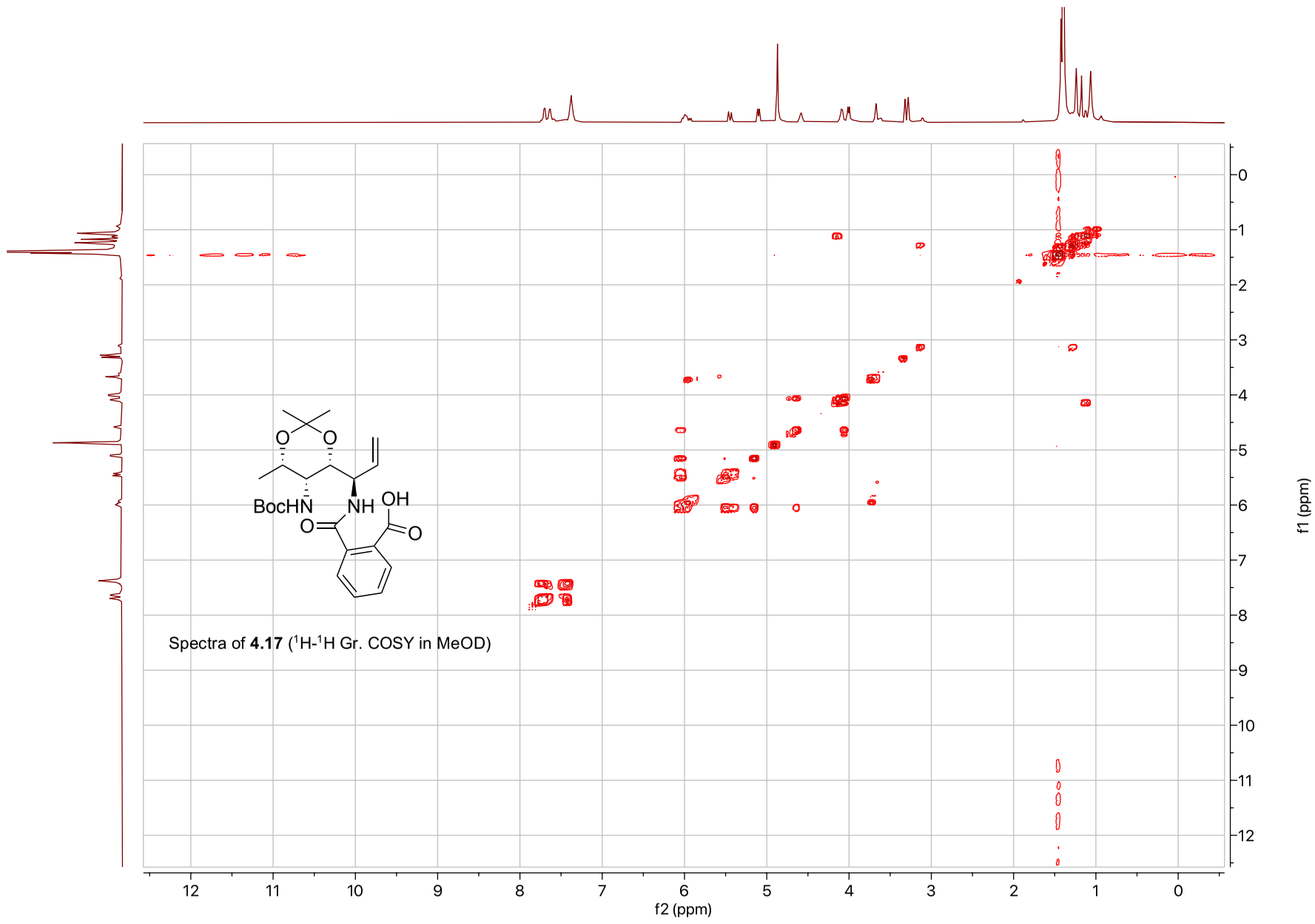
BocHN
NH
OH
O
O
O
O
Spectra of **4.17** ($^{1}$H-$^{1}$H Gr. COSY in MeOD)
f2 (ppm)
f1 (ppm)
12
11
10
9
8
7
6
5
4
3
2
1
0

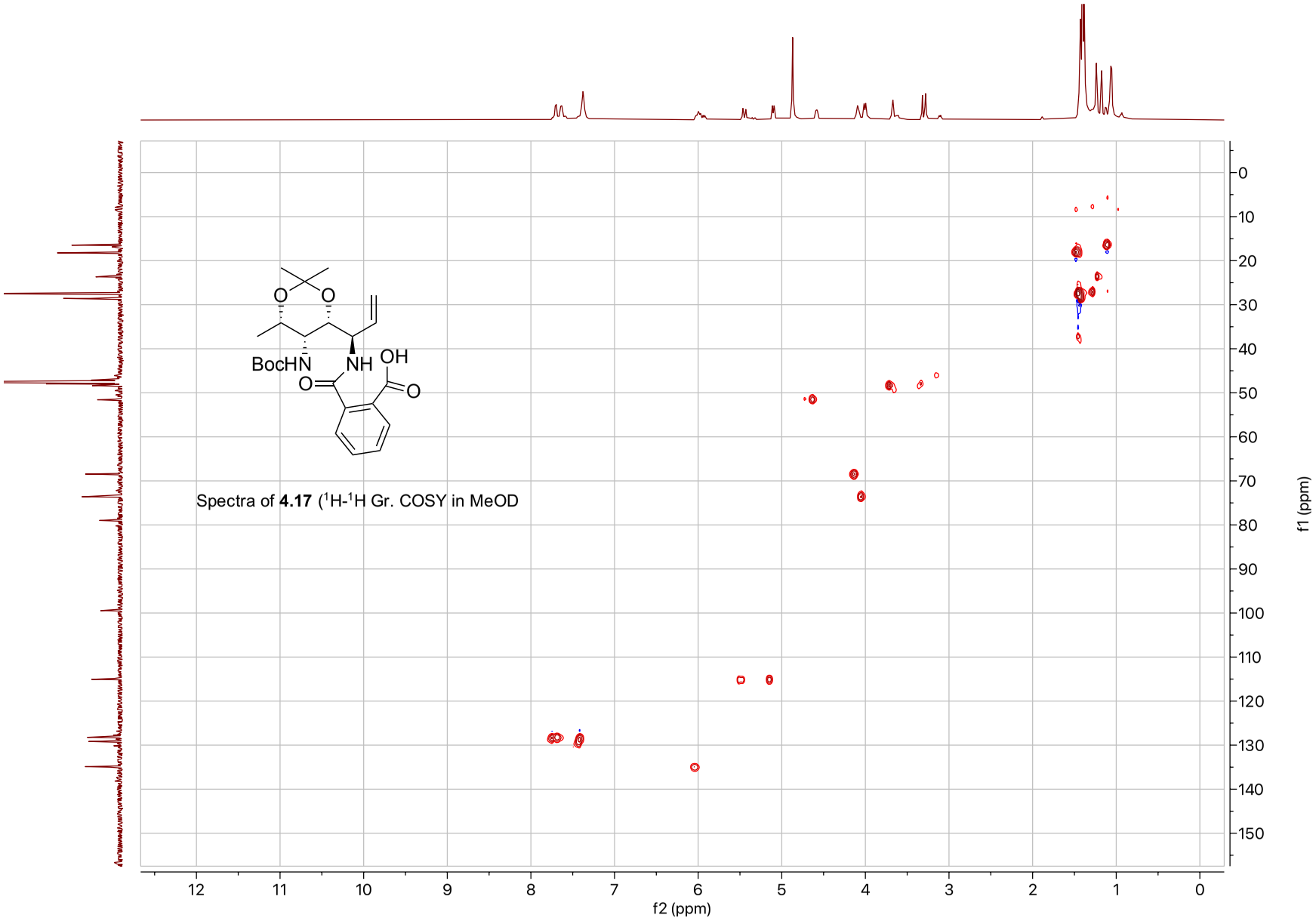
BocHN
NH
OH
O
O
O
O
Spectra of **4.17** ($^1$H-$^1$H Gr. COSY in MeOD
f2 (ppm)
f1 (ppm)

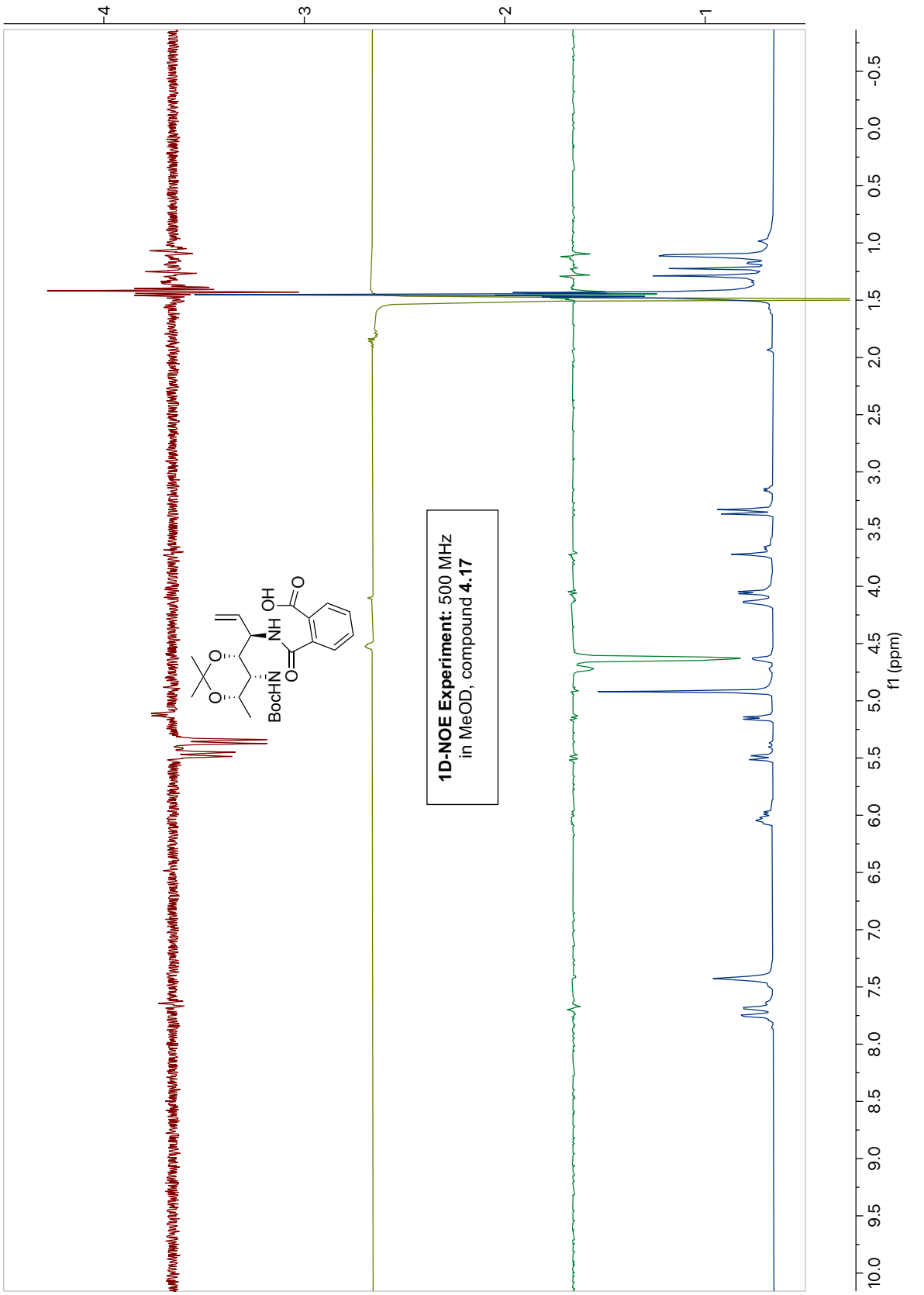
4
3
2
1
BocHN
NH
OH
O
O
O
O
O
1D-NOE Experiment: 500 MHz
in MeOD, compound 4.17
10.0
9.5
9.0
8.5
8.0
7.5
7.0
6.5
6.0
5.5
5.0
4.5
4.0
3.5
3.0
2.5
2.0
1.5
1.0
0.5
0.0
-0.5
f1 (ppm)